Australian Government
Geoscience Australia

The major rare-earth-element deposits of Australia: geological setting, exploration, and resources

Dean M. Hoatson, Subhash Jaireth & Yanis Miezitis

DEPARTMENT OF RESOURCES, ENERGY AND TOURISM

Minister for Resources and Energy: The Hon. Martin Ferguson, AM MP
Secretary: Mr Drew Clarke PSM

GEOSCIENCE AUSTRALIA

Chief Executive Officer: Dr Chris Pigram

ISBN 978–1–921954–01–6 (hardcopy)

ISBN 978–1–921954–02–3 (webcopy)

GeoCat 71820

Bibliographic Reference

Hoatson, D.M., Jaireth, S. and Miezitis, Y., 2011. The major rare-earth-element deposits of Australia: geological setting, exploration, and resources. Geoscience Australia, 204 pp.

Cover Photograph and Illustrations

Front cover: Mount Weld in Western Australia is one of the richest rare-earth-element deposits in the world, with significant additional resources of niobium, tantalum, and phosphate. This aerial view shows the mine workings, in laterite developed above a ~2025 million year carbonatite intrusion. Lynas Corporation Limited (http://www.lynascorp.com/index.asp) is acknowledged for providing the aerial photograph.

Back cover: geological map and cross-section of the Mount Weld rare-earth-element deposit.

Australian Government
Geoscience Australia

THE MAJOR RARE-EARTH-ELEMENT DEPOSITS OF AUSTRALIA: GEOLOGICAL SETTING, EXPLORATION, AND RESOURCES

Dean M. Hoatson[1], Subhash Jaireth[1] & Yanis Miezitis[1]

[1.] Onshore Energy and Minerals Division, Geoscience Australia, GPO Box 378, Canberra, ACT 2601

SCOPE AND OBJECTIVES

The rare-earth elements (REE) have unique and diverse chemical, magnetic, and luminescent properties that make them strategically important in a number of high-technology industries. Traditionally they have been used for car engine exhausts, magnets, catalysts, metallic alloys in metallurgy, and for colouring and polishing glass. However, their applications in many emerging technologies associated with the transport, information, environment, energy, defence, nuclear, and aerospace industries have gained rapid momentum in recent years. Dramatically increasing prices for the REE reflect this expanding range of applications and the narrow global supply base. Consequently, the REE are increasingly becoming more attractive commodity targets for the minerals industry.

This report produced by Geoscience Australia[1] reviews the distribution, geological characteristics, resources, and potential of Australia's major REE deposits. With the exception of Barrie (1965), Towner et al. (1996), Cassidy et al. (1997), and Miezitis (2010), very few publications have described these deposits and compiled their resources at a national scale. In addition, there is a paucity of published documentation describing the geological features of key REE deposits in Australia similar to Lottermoser's (1988, 1990, 1991, 1994) comprehensive mineralogical-geochemical investigations on carbonatite-associated deposits. This report provides an up-to-date review of such deposits as a stimulus for future research into the geological characteristics of REE in Australia. In a mineral-systems framework, we examine the elements considered important for the formation of REE deposits and provide suggested exploration guidelines relevant to Australia. Also included is a compilation of recent products and national databases produced by Geoscience Australia that have potential applications in the exploration for REE deposits. The information and main messages presented in this review are intended to inform the public, students, and professionals.

The review comprises five chapters that are structured as follows:

Chapter 1 is a general overview of the REE, and provides background information on the discovery, major properties, applications, and production and resource status of the REE from a global and Australian perspective. A brief summary of the major events relating to REE exploration in Australia concludes the chapter.

Chapter 2 is focused on the geochemical behaviour of the REE. Metal abundances in mantle-crustal environments, various host rock types and hydrothermal fluids, partitioning into magmas of different composition, and behaviours in hydrothermal fluids are discussed within a evolutionary geochemical cycle framework.

Chapter 3 summarises the geological settings and main features of the major REE deposits in Australia, including stratigraphy, age and source of REE, resources, economic significance, and the genesis of fourteen type deposits. This information is used to compile a classification scheme for all Australian deposits.

Chapter 4 incorporates the information provided by the type examples described in Chapter 3 and assesses those criteria considered critical for the formation of each particular deposit type. This mineral-system approach differs from description-based classifications in that it can predict potential new areas and types of REE mineralisation.

Chapter 5 summarises exploration techniques for REE in Australia. It also provides information on some recent innovative digital national maps and databases produced by Geoscience Australia that could facilitate exploration.

Appendices 1 to 10 provide national and global REE data, exploration history, useful www links, and glossaries of resource and scientific terms.

The REE resource data used in this review for Australia's deposits are from OZMIN (2011: Ewers and Ryburn, 1997)—Geoscience Australia's national database of mineral deposits and resources.

[1] Geoscience Australia (http://www.ga.gov.au/; formerly the Bureau of Mineral Resources, Geology and Geophysics; and the Australian Geological Survey Organisation) is the Australian Government's geoscience agency which provides geoscientific information and knowledge to enable government and the community to make informed decisions about the exploitation of resources, the management of the environment, and the safety of critical infrastructure.

ACKNOWLEDGEMENTS

This report of the major REE deposits in Australia was undertaken as part of the Mineral Exploration Promotion Project (leaders: Mike Huleatt and Paul Henson) within the Onshore Energy and Minerals Division (OEMD) of Geoscience Australia. The review has compiled public information and data from a range of domestic and international sources, in addition to the latest information held by Geoscience Australia and the State/Territory geological surveys. An important component of this information was derived from various mining companies operating in Australia and elsewhere.

Lynas Corporation Limited (http://www.lynascorp.com/) is acknowledged for the use of the Mount Weld photographs that feature on the cover and in Chapter 3 of this publication. In particular, Georgia Bunn (Communications Manager) is thanked for her assistance. Richard Brescianini (General Manager of Exploration and Development) of Arafura Resources Limited (http://www.arafuraresources.com.au/) is also thanked for providing the images of the Nolans Bore deposit in central Australia. Jim Mason (previously GA) provided some of the landscape photographs.

The following people and organisations are thanked for granting permission for information and photographs relating to the discovery and applications of the REE used in Chapter 1: Stephen Gagnon (Thomas Jefferson National Accelerator Facility, Virginia, USA: http://www.jlab.org/); Dr. Norman Holden (National Nuclear Data Center, Brookhaven National Laboratory, Upton, New York: http://www.nndc.bnl.gov/); Mark Saxon (President and CEO of Tasman Metals Limited: http://www.tasmanmetals.com/s/OresMinerals.asp); Dr. Peter van der Krogt (Elementymology & Elements Multidict: http://elements.vanderkrogt.net/); Tantalus Rare Earths AG (http://tre-ag.com/en/rare-earths_applications.php); Peggy Greb, United States Department of Agriculture, Agricultural Research Service: http://www.ars.usda.gov/is/graphics/photos/jun05/d115-1.htm); and John Veevaert (http://trinityminerals.com/ms2003/day3.shtml). Photographs of chemists used in Chapter 1 have expired copyright status (i.e., in the public domain) and are reproduced from Wikimedia Commons (http://commons.wikimedia.org/wiki/Main_Page).

The following geoscientists from Geoscience Australia (GA) provided summaries in Chapter 5 of how GA's National datasets can be used for the exploration of REE: Patrice de Caritat (National Geochemical Survey of Australia); David Champion (Felsic Igneous Rocks); Lynton Jaques (Kimberlite Map of Australia); Peter Milligan (Gravity and Magnetic Maps of Australia); Oliver Raymond (Surface Geology of Australia Map); Murray Richardson and Brian Minty (Radiometric Map of Australia); and Ian Roach and Marina Costelloe (Airborne Electromagnetic Surveys).

The report was improved from comments received from Leesa Carson, Paul Henson, David Huston, Terry Mernagh (GA), and Lynton Jaques and Alastair Stewart (previously GA). The visual impact of the figures owes much to the cartographic skills of Silvio Mezzomo and Chris Evenden (GA), the two fold-out maps were drawn by Gayle Young (GA), and Alissa Harding and Maria Bentley (GA) were responsible for the design and production of the report.

EXECUTIVE SUMMARY

The rare-earth elements (REE) are a group of seventeen speciality metals that comprise the lanthanide series of elements: lanthanum (La), cerium (Ce), praseodymium (Pr), neodymium (Nd), promethium (Pm), samarium (Sm), europium (Eu), gadolinium (Gd), terbium (Tb), dysprosium (Dy), holmium (Ho), erbium (Er), thulium (Tm), ytterbium (Yb), lutetium (Lu), in addition to scandium (Sc) and yttrium (Y), which show similar physical and chemical properties to the lanthanides. The REE have unique catalytic, metallurgical, nuclear, electrical, magnetic, and luminescent properties. Their strategic importance is indicated by their use in a number of emerging and diverse technologies that are becoming increasingly significant in today's society. Applications range from routine (e.g., lighter flints, glass polishing mediums, car alternators), to high-technology (lasers, magnets, batteries, fibre-optic telecommunication cables), to those that have futuristic purposes (high-temperature superconductivity, safe storage and transport of hydrogen for a post-hydrocarbon economy, environmental global warming and energy efficiency issues). Over the last two decades, the global demands of REE have significantly increased sympathetically with their dramatic expansion into high-technological, environmental, and economical environments.

REE are relatively abundant in the Earth's crust, but known minable concentrations are less common than for most other exploited metals. Past demand for REE has been met by a small number of producers and mines. Since the mid-1990s, China has dominated the global supply of REE, with most production derived from the very large Bayan Obo iron-niobium-REE deposit (Inner Mongolia, China) and from lateritic clays (southern China). In 1992, China surpassed the United States of America (USA) as the world's largest producer of rare-earth oxides (REO); being responsible for 95.5% of the world's output in 2009. At the end of 2010, China held 55 million tonnes (48.3%) of the world's economic resources of REO, followed by the Commonwealth of Independent States (former members of the Soviet Union) with 19 million tonnes (16.7%) and the USA with 13 million tonnes (11.4%). Australia's global REE impact in 2009 amounted to no recorded production and total Economic Demonstrated Resources in 2010 were 1.65 million tonnes of REO (1.45% of the global inventory).

Small-scale production of REE has taken place in Australia in the past with yttrium-rich minerals (gadolinite) first mined in 1913 from a pegmatite vein in the Cooglegong region near Marble Bar, Western Australia. Australia's REE industry attained an international profile when REE-bearing heavy minerals (monazite and xenotime) were obtained as by-products from beach sand mining activities in Western Australia, New South Wales, and Queensland. During the 1970s and 1980s, Australia's annual production was about 12 000 tonnes of monazite and 50 tonnes of xenotime. Australia became the world's largest producer of monazite when production peaked in 1985 with 18 735 tonnes of monazite. Between 1952 and the 'temporary closure' of the industry in 1995, Australia exported some 265 000 tonnes of monazite with an export value of $284 million (in 2008 dollars). Some beach sand mining projects are currently still operating in Western Australia (e.g., Cooljarloo) and Queensland (North Stradbroke Island). During the past decade there has been increasing industry interest in hard-rock REE deposits as the demand and global prices for these strategic metals have significantly increased. A number of deposits with significant resources (e.g., Mount Weld, WA; Nolans Bore, NT; Toongi, NSW) in different geological settings are now at advanced stages of development. Their planned production contributions (e.g., starting dates of 2011 for Mount Weld, ~2013 for Nolans Bore) are likely to have a discernible impact on the global supply of REE.

REE in Australia are associated with igneous, sedimentary, and metamorphic rocks in a wide range of geological environments. Elevated concentrations of these elements have been documented in various heavy-

mineral sand deposits (beach, dune, offshore marine, and channel), carbonatite intrusions, (per)alkaline igneous rocks, iron-oxide breccia complexes, calc-silicate rocks (skarns), fluorapatite veins, pegmatites, phosphorites, fluviatile sandstones, unconformity-related uranium deposits, and lignites. The distribution and concentration of REE in these deposits are influenced by various rock-forming processes, including enrichment in magmatic or hydrothermal fluids, separation into mineral species and precipitation, and subsequent redistribution and concentration through weathering and other surface processes. The lanthanide series of REE (lanthanum to lutetium) and yttrium show a close genetic and spatial association with alkaline felsic igneous rocks, but scandium in laterite is associated with ultramafic-mafic igneous rocks.

A mineral-systems approach has been used in this review to classify the major Australian REE deposits according to various mineralising criteria and/or associated geological events. This hierarchical classification framework has the advantage over more traditional descriptive classifications in that it attemps to understand the geological processes considered critical to the formation of a particular deposit type. It also has a more predictive capacity for identifying potential new areas and types of REE mineralisation. The highest level of the classification comprises four general '*Mineral-system association*' categories—Regolith, Basinal, Metamorphic, and Magmatic—and their sixteen '*Deposit Type*' members, namely:

1. Regolith—carbonatite-associated; ultramafic/mafic rock-associated;
2. Basinal—heavy-mineral sand deposits in beach, high dune, offshore shallow marine tidal, and tidal environments; phosphorite; lignite; unconformity-related;
3. Metamorphic—calc-silicate; and
4. Magmatic—(per)alkaline rocks; carbonatite; pegmatite; skarn; apatite and/or fluorite veins; and iron-oxide breccia complex.

The most commercially important REE deposits in Australia are related to magmatic and weathering processes associated with carbonatites and alkaline igneous rocks, and secondary placer deposits, such as heavy-mineral sand deposits. There is considerable potential for the discovery of high-grade, large tonnage polymetallic REE deposits in residual lateritic profiles of carbonatites and within alkaline igneous rocks in the Precambrian terranes of Australia. Residual laterite deposits associated with carbonatites are typically enriched in other metals, such as zirconium, niobium, and tantalum. They also have the advantage of being easily mined by open-pit methods and they do not require extensive crushing and milling. Mesozoic alkaline volcanic provinces of eastern Australia provide scope for lower-grade, polymetallic deposits in the primary zones of trachytic and associated alkaline rock complexes. The discovery of scandium-bearing nickel-cobalt laterites associated with Phanerozoic ultramafic-mafic rocks, and REE-bearing phosphorites in Cambrian basinal successions have recently created exploration interest throughout eastern Australia. Large iron-oxide breccia complexes (e.g., Olympic Dam, SA) may be an important source of by-product REE that could be exploited in the future. The economic significance of less conventional exploration targets where the REE are hosted by lignite and bauxite accumulations is yet to be established. In addition, ionic-adsorption clay deposits that are mined in southeastern China represent a potential exploration target in Australia.

The complex spatial distribution and concentration of REE in many Australian deposits reflect the subtle differences in physical and chemical behaviours of many elements (17 REE and associated metals) in the primary host rock and in the secondary weathering profile. Each orebody is 'unique' with different geological and metallurgical challenges. The pathway to production is project specific, and involves many intricate processing stages that often need to adapt during the life of the project. Some REE-bearing ores have associated abundances of uranium and thorium, thus environmental and competing land-use issues (e.g., heavy-mineral sand deposits along the coastal zone and National Parks) may also have to be considered. The development of a REE deposit from discovery to production may therefore be a protracted process involving many technical challenges and expensive commitments. Ideally, mining companies need a REE orebody with favourable geological-geochemical-processing parameters, a careful approach to environmental considerations, high levels of different skills, and access to processing technologies and significant amounts of capital.

CONTENTS

Chapter 3:

TABLES

CHAPTER ONE

WHAT ARE RARE-EARTH ELEMENTS?

1.1. INTRODUCTION

The rare-earth elements (REE) are a group of seventeen speciality metals that form the largest chemically coherent group in the Periodic Table of the Elements[1] (Haxel et al., 2005). The lanthanide series of inner-transition metals with atomic numbers ranging from 57 to 71 is located on the second bottom row of the periodic table (Fig. 1.1). The lanthanide series of elements are often displayed in an expanded field at the base of the table directly above the actinide series of elements. In order of increasing atomic number the REE are: lanthanum (La), cerium (Ce), praseodymium (Pr), neodymium (Nd), promethium (Pm), samarium (Sm), europium (Eu), gadolinium (Gd), terbium (Tb), dysprosium (Dy), holmium (Ho), erbium (Er), thulium (Tm), ytterbium (Yb), and lutetium (Lu). Scandium (Sc) and yttrium (Y), which have properties similar to the lanthanide series of elements, have atomic numbers of 21 and 39, respectively, and occur above the lanthanides in the Periodic Table of Elements (Fig. 1.1; Appendix 2).

REE are variously referred to as 'rare-earth metals' (REM), 'rare earths' (RE), 'rare-earth oxides' (REO), and 'total rare-earth oxides' (TREO). Such phrases as 'vitamins for industry', 'elements of the future', and '21st century gold' that are often used in the media today reflect their increasing strategic importance for many industrial applications. During recent times there has been much controversy about the actual number of elements included in the REE group. This has ranged from fifteen to eighteen elements. One of the world's leading authorities on chemical nomenclature and terminology, the International Union of Pure and Applied Chemistry (IUPAC: http://old.iupac.org/dhtml_home.html), has defined the REE as a group of seventeen chemically similar metallic elements that comprise the fifteen lanthanide elements (lanthanum to lutetium), scandium (Sc), and yttrium (Y). The latter two elements are classified as REE because of their similar physical and chemical properties to the lanthanides, and they are commonly associated with these elements in many ore deposits. Chemically, yttrium resembles the lanthanide metals more closely than its neighbor in the periodic table, scandium, and if its physical properties were plotted against atomic number then it would have an apparent number of 64.5 to 67.5, placing it between the lanthanides gadolinium and erbium. Some investigators who want to emphasise the lanthanide connection of the REE group, use the prefix 'lanthanide' (e.g., lanthanide REE: see Chapter 2). In some classifications, the second element of the actinide series, thorium (Th: Mernagh and Miezitis, 2008), is also included in the REE group, while promethium (Pm), which is a radioactive element not found in nature, is sometimes excluded. This particular review will follow the general guidelines recommended by the IUPAC with the REE defined by the fifteen lanthanide elements and the two closely related elements, scandium and yttrium. Thorium is excluded from, and promethium is included in, the final group of seventeen REE described in this report.

The fifteen lanthanide elements have been further subdivided by the British Geological Survey (Walters et al., 2010) into the:

1. light-rare-earth elements (LREE)—lanthanum, cerium, praseodymium, neodymium, promethium, samarium, and europium; and
2. heavy-rare-earth elements (HREE)—gadolinium, terbium, dysprosium, holmium, erbium, thulium, ytterbium, and lutetium.

In some classifications the more transitional elements samarium and europium may occur in either the LREE or the HREE subgroups. Despite its low atomic weight, yttrium (and scandium) is included with the HREE subgroup because its occurrence, ionic radius, and behavioural properties are closer to the HREE than

[1] Technical terms are explained in Appendix 1.

to the LREE (Cooper, 1990). The LREE are generally more abundant, and less valuable than the HREE. Furthermore, REE with even atomic numbers are more abundant than their neighbours of odd atomic numbers because of their greater relative stabilities of atomic nuclei. Consequently, abundance plots for the REE show zig-zag distribution trends (Fig. 1.2).

Other classifications further divide the REE into Middle REE (MREE) comprising Sm, Eu, Gd, Tb, and Dy, with the remainder of the elements from Ho to Lu, referred to as the HREE. This more detailed subdivision is generally not universally accepted, and in this report they are briefly described in Chapter 2.

The REE share many common physical and chemical properties that make them difficult to distinguish from each other or chemically separate. Such common properties include: silver, silvery-white, and grey metallic colours; soft, malleable, and ductile behaviours; high lustres, which readily tarnish in air; high electrical conductivities; reactive states (to form REO) especially at high temperatures; very small differences in solubility and complex formation between the REE; and dominant oxidation valence state of +3 when the REE are associated with non-metals (although europium has a valence state of +2 and cerium +4). The major physical and chemical properties of the REE are summarised in Table 1.1.

Table 1.1. Major physical and chemical properties of the rare-earth elements (modified from Gupta and Krishnamurthy, 2005; and other sources).

Element	Symbol	Atomic number	Atomic weight	Density (gcm^{-3})[1]	Melting point (°C)[1]	Boiling point (°C)[1]	Crustal abundance (ppm)[2]	Vicker's hardness[3]	Crystal structure[1,4]
Scandium	Sc	21	44.95	2.989	1541	2832	8	85	Hex
Yttrium	Y	39	88.90	4.469	1522	3337	30	38	Hex
Light-rare-earth elements									
Lanthanum	La	57	138.90	6.146	918	3469	30	37	Hex
Cerium	Ce	58	140.11	8.160	789	3257	60	24	Cub
Praseodymium	Pr	59	140.90	6.773	931	3127	7	37	Hex
Neodymium	Nd	60	144.24	7.008	1021	3127	25	35	Hex
Promethium[5]	Pm	61	145.00	7.264	1042	3000	4.5×10^{-20}	-	Hex
Samarium	Sm	62	150.36	7.520	1074	1900	5	45	Rho
Europium	Eu	63	151.96	5.244	822	1597	1	17	Cub
Heavy-rare-earth elements									
Gadolinium	Gd	64	157.25	7.901	1313	3233	4	57	Hex
Terbium	Tb	65	158.92	8.230	1356	3041	0.7	46	Hex
Dysprosium	Dy	66	162.50	8.551	1412	2562	3.5	42	Hex
Holmium	Ho	67	164.93	8.795	1474	2720	0.8	42	Hex
Erbium	Er	68	167.26	9.066	1529	2510	2.3	44	Hex
Thulium	Tm	69	168.93	9.321	1545	1727	0.32	48	Hex
Ytterbium	Yb	70	173.04	6.966	819	1466	2.2	21	Cub
Lutetium	Lu	71	174.97	9.841	1663	3315	0.4	77	Hex

[1] Source of data: Periodic Table of the Elements (http://www.chemicalelements.com/show/dateofdiscovery.html, and http://education.jlab.org/itselemental/).

[2] Crustal abundances in parts per million (ppm) from Christie et al. (1998).

[3] 10 kg load, kg/mm^2.

[4] Crystal structure abbreviations: Hex = hexagonal; Cub = cubic; Rho = rhombohedral.

[5] Rarest REE that is radioactive and has no long-lived or stable isotopes.

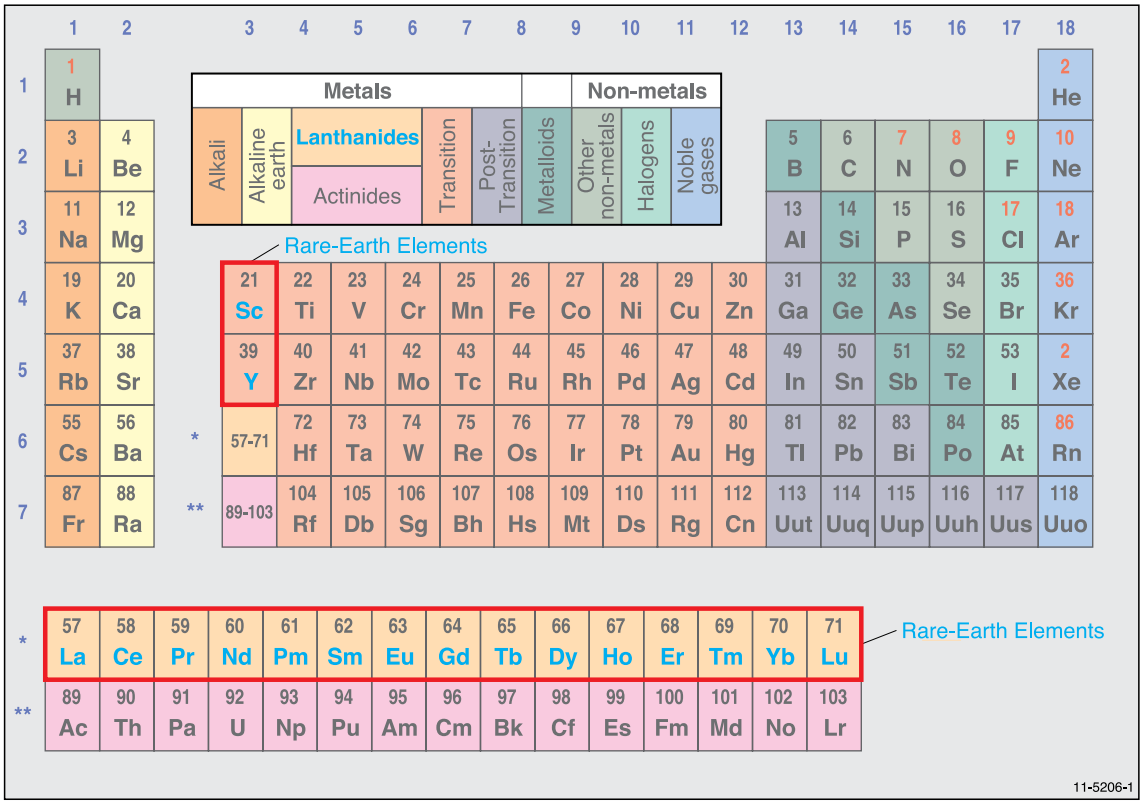

Figure 1.1. Periodic Table of Elements. The seventeen rare-earth elements as defined in this review are indicated in blue font and are contained within a red box. Modified from Dayah (1997).

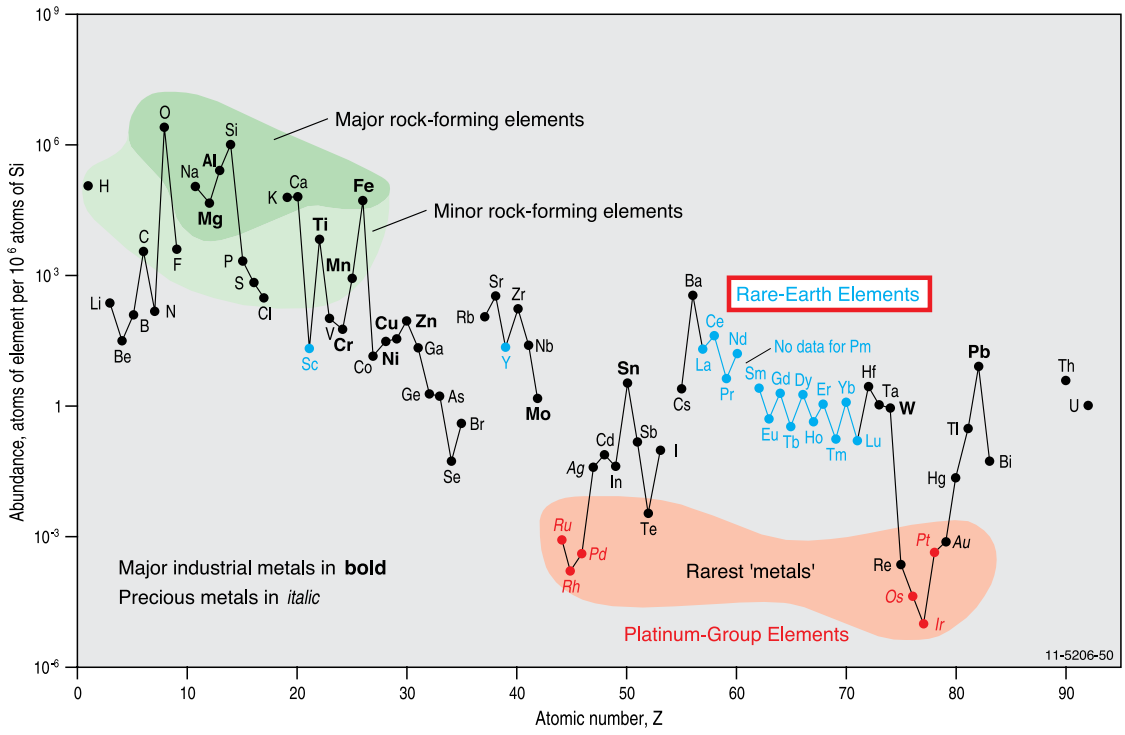

Figure 1.2. Abundances (atom fractions) of the chemical elements in Earth's upper continental crust in reference to atomic number. Many of the elements are grouped into: (1) Rare-Earth Elements (blue font); (2) Major and Minor rock-forming elements (dark and light green fields); (3) Rarest metals (orange field); and Platinum-Group Elements (red font). Modified from Haxel et al. (2005).

Rare-earth elements do not occur as free metals in the Earth's crust, such that all naturally occurring minerals consist of mixtures of various REE and non-metals. Bastnäsite [(Ce,La)(CO_3)F], monazite [(Ce,La,Nd,Th)PO_4], and xenotime (YPO_4) are the three most economically significant minerals of the 200 plus minerals known to contain essential or significant REE (Christie et al., 1998). The chemical compositions and discovery dates of some of the more common REE-bearing minerals are shown in Table 1.2[2].

Bastnäsite and monazite are principal sources of the LREE, which account for about 95% of the REE utilised (Cooper, 1990). Bastnäsite is named from the Swedish village of Bastnäs, where cerium ore was mined in the late 1800s. It is a fluoro-carbonate of cerium metals containing 60 to 70% REO including lanthanum and neodymium. Bastnäsite has been mined at the large Mountain Pass REE deposit in California, and China has vast bastnäsite deposits that exceed all the other known bastnäsite deposits. Monazite is a cerium, lanthanum, neodymium, and yttrium-bearing phosphate containing 50 to 78% REO. Monazite is also the principal ore of thorium, containing up to 30% thorium, which together with smaller quantities of uranium (up to 1%) imparts radioactive properties to the monazite. Xenotime is a yttrium-bearing phosphate hosting 54 to 65% REO, and comprising other REE such as erbium and cerium, and thorium. Xenotime and minerals such as allanite are common sources of the HREE and yttrium.

Bastnäsite occurs predominantly in calc-silicate rich rocks related to alkaline intrusive igneous complexes, in particular carbonatite, dolomitic breccia with syenite intrusives, pegmatite, and amphibolite skarn. Monazite and xenotime are more common as accessory minerals in low-calcium granitic rocks, gneisses, pegmatites, and aplites. Xenotime is commonly associated with zircon and can enclose that mineral. Following weathering of granites and pegmatites, monazite and xenotime are concentrated in heavy mineral placer deposits because of their resistance to chemical attack and high specific gravities.

Other commercial sources of REE are apatite and loparite (western Russia), REE-bearing clays ('Longnan clay' or 'southern ionic clay', Jiangxi Province, China), and various minerals, such as allanite that are produced as a by-product of uranium mining (Canada). Of lesser importance are zircon (Th, Y, and Ce) and euxenite. One of the major commercial sources of scandium is as a by-product from the processing of uranium and tungsten.

Some of the most common REE-bearing minerals are compiled in Table 1.2. The majority of these minerals were discovered in Europe (Russia, Norway, Sweden, Greenland, Germany), with some occurrences recorded from the USA, India, Brazil, Colombia, and Sri Lanka. Many other REE-bearing minerals that have been approved by the Commission on New Minerals and Mineral Names (CNMMN) of the International Mineralogical Association (IMA) can be found in Mandarino (1999). The minerals shown in Table 1.2 have been approved by the CNMMN.

Table 1.2. Rare-earth-element-bearing minerals.

Mineral	Mineral chemistry	wt % REO	Discovered[1]
Aeschynite	(Ce,Ca,Fe,Th)(Ti,$Nb)_2$($O,OH)_6$	36	Norway; Ural Mountains, Russia
Allanite (orthite)	$(Ce,Ca,Y)_2(Al,Fe)_3(SiO_4)_3(OH)$	3 to 51	1810: Aluk Island, Greenland
Anatase	$(Ti,REE)O_2$	3	1801: St Christophe-en-Oisans, France
Ancylite–(Ce)	$SrCe(CO_3)_2(OH)•H_2O$	46 to 53	1899: Narssârssuk, Narsaq, Greenland
Apatite	$Ca_5(PO_4,CO_3)_3(F,Cl,OH)$	19	Bronze Age (3300–1200 BC); widespread
Bastnäsite– (Ce)[2]	(Ce,La)(CO_3)F	70 to 74	1838: Bastnäs mine, Västmanland, Sweden
Brannerite	$(U,Ca,Y,Ce)(Ti,Fe)_2O_6$	6	1920: Kelly Gulch, Stanley, Idaho, USA
Britholite–(Ce)	$(Ce,Ca)_5(SiO_4,PO_4)_3(OH,F)$	56	1901: Naujakasik, Narsaq, Greenland
Brockite	$(Ca,Th,Ce)(PO_4)•H_2O$		1962: Bassick mine, Colorado, USA
Calcio–ancylite (Ce)	$(Ca,Sr)Ce_3(CO_3)_4(OH)_3•H_2O$	60	Kola Peninsula, Russia
Cerianite–(Ce)	$(Ce^{4+},Th)O_2$	81	1955: Firetown, Sudbury, Ontario, Canada
Cerite–(Ce)	$Ce_9^{3+}Fe^{3+}(SiO_4)_6[SiO_3(OH)](OH)_3$	60	1751: Bastnäs mine, Västmanland, Sweden
Cheralite–(Ce)	$(Ce,Ca,Th)(P,Si)O_4$	5	Chera, Travancore, India
Chevkinite	$(Ca,Ce,Th)_4(Fe^{2+},Mg)_2(Ti,Fe^{3+})_3Si_4O_{22}$		1839: Ural Mountains, Russia
Churchite–(Y)	$YPO_4•2H_2O$	44	1923: Maffei mine, Bavaria, Germany
Crandallite	$CaAl_3(PO_4)_2(OH)_5•H_2O$		1917: Brooklyn mine, Silver City, Utah, USA

[2] The reader should refer to Table 1.2 for the chemical compositions of REE-bearing minerals since they will not be repeated throughout this report.

Table 1.2. Rare-earth-element-bearing minerals (continued).

Mineral	Mineral chemistry	wt % REO	Discovered[1]
Doverite (synchysite–(Y)	$YCaF(CO_3)_2$		1951: Scrub Oak mine, New Jersey, USA
Eudialyte	$Na_4(Ca,Ce)_2(Fe^{2+},Mn^{2+},Y)ZrSi_8O_{22}(OH,Cl)_2$	1 to10	1819: Kangerdluarssuq Firth, Narsaq, Greenland
Euxenite–(Y)	$(Y,Ca,Ce,U,Th)(Nb,Ta,Ti)_2O_6$	<40	1840: Jølster, Sogn og Fjordane, Norway
Fergusonite–(Ce)	$(Ce,La,Y)NbO_4$	47	1806: Kikertaursak, Greenland; Ukraine
Fergusonite–(Y)	$YNbO_4$		1826: Kikertaursak, Greenland
Florencite–(Ce)	$CeAl_3(PO_4)_2(OH)_6$	32	pre-1951: Mata dos Criolos, Minas Gerais, Brazil
Florencite–(La)	$(La,Ce)Al_3(PO_4)_2(OH)_6$		pre-1980: Shituru mine, Congo (Zaire), Africa
Fluocerite–(Ce)	$(Ce,La)F_3$		1845: Broddbo and Finnbo, Dalarna, Sweden
Fluocerite–(La)	$(La,Ce)F_3$		1969: Zhanuzak, Kazakhstan
Fluorapatite–(Ce)	$(Ca,Ce)_5(PO_4)_3F$	0 to 21	1860: Greifenstein Rocks, Saxony, Germany
Fluorite	$(Ca,REE)F$		1530: England; Czech Republic; Germany
Gadolinite	$(Ce,La,Nd,Y)_2Fe^{2+}Be_2Si_2O_{10}$	40	1788: Ytterby mine, Resarö, Sweden
Gagarinite–(Y)	$NaCaY(F,Cl)_6$		pre-1961: Akzhaylyautas Mountains, Kazakhstan
Gerenite–(Y)	$(Ca,Na)_2(YREE)_3Si_6O_{18}•2H_2O$		1998: Strange Lake, Quebec–Labrador, Canada
Gorceixite	$(Ba,REE)Al_3(PO_4)(PO_3OH)(OH)_6$		1906: Ouro Preto, Minas Gerais, Brazil
Goyazite	$SrAl_3(PO_4)_2(OH)_5•H_2O$		1884: Diamantina, Minas Gerais, Brazil
Hingganite–(Y)	$(Y,Yb,Er)_2Be_2Si_2O_8(OH)_2$		1984: Greater Hinggan Mountains, China
Huanghoite–(Ce)	$BaCe(CO_3)_2F$	38	1960s: Bayan Obo deposit, Inner Mongolia
Hydroxylbastnäsite–(Ce)	$(Ce,La)(CO_3)(OH,F)$	75	Kola Peninsula and Ural Mountains, Russia
Iimoriite–(Y)	$Y_2(SiO_4)(CO_3)$		pre-1970: Honshu Island, Japan
Kainosite–(Y)	$Ca_2(Y,Ce)_2Si_4O_{12}(CO_3)•H_2O$	38	1885: Hidra, Vest-Agder, Norway
Loparite–(Ce)	$(Ce,Na,Ca)(Ti,Nb)O_3$	32 to 34	1925: Maly Mannepakhk, Kola Peninsula, Russia
Monazite–(Ce)	$(Ce,La,Nd,Th)PO_4$	35 to 71	1823: Ilmen Mountains, Ural Mountains, Russia
Mosandrite	$(Na,Ca,Ce)_3Ti(SiO_4)_2F$	<65	1841: Låven Island, Larvik, Norway
Parisite–(Ce)	$Ca(Ce,La)_2(CO_3)_3F_2$	59	Muzo mine, Colombia
Perovskite	$(Ca,REE)TiO_3$	≤37	1839: Achmatovsk mine, Ural Mountains, Russia
Pyrochlore	$(Ca,Na,REE)_2Nb_2O_6(OH,F)$		1826: Stavern, Larvik, Vestfold, Norway
Rhabdophane–(Ce)	$(Ce,La)PO_4•H_2O$		pre-1992: Fowey Consols, Cornwall, England
Rhabdophane–(La)	$(La,Ce)PO_4•H_2O$		1883: Salisbury Iron mines, Connecticut, USA
Rinkite	$(Ca,Ce)_4Na(Na,Ca)_2Ti(Si_2O_7)_2F_2(O,F)_2$		1884: Kangerdluarssuk, Narsaq, Greenland
Samarskite–(Y)	$(Y,Ce,U,Fe^{3+})_3(Nb,Ta,Ti)_5O_{16}$	12	1839: Blyumovskaya pit, Ural Mountains, Russia
Steenstrupine–(Ce)	$Na_{14}Ce_6Mn^{2+}Mn^{3+}Fe_2^{2+}(Zr,Th)(Si_6O_{18})_2(PO_4)_7•3H_2O$		1853–54: Kangerdluarssuk, Narsaq, Greenland
Synchysite–(Ce)	$Ca(Ce,La)(CO_3)_2F$	49 to 52	1953: Narsarsuk, Greenland
Thalénite–(Y)	$Y_3Si_3O_{10}(OH)$	63	Österby, Dalama, Sweden
Titanite (sphene)	$(Ca,REE)TiSiO_5$	≤3	1795: Hauzenberg, Bavaria,Germany
Uraninite	$(U,Th,Ce)O_2$		1772: Jáchymov, Bohemia, Czech Republic
Vitusite–(Ce)	$Na_3(Ce,La,Nd)(PO_4)_2$		1980: Kola Peninsula, Russia; Narsaq, Greenland
Xenotime–(Y)	YPO_4	52 to 67	1824: Ytterby mine, Sweden; Hidra, Norway
Yttrofluorite	$(Ca,Y)F_2$		1911: Hundholmen, Tysfjord, Norway
Yttrotantalite–(Y)	$(Y,U,Fe^{2+})(Ta,Nb)O_4$	<24	Ytterby mine, Resarö, Sweden
Zircon	$(Zr,REE)SiO_4$	<5	1783: Sri Lanka; 1789: Germany

Source of information: Habashi (1994); Long et al. (2010); mindat.org (http://www.mindat.org/index.php); and reproduced with permission, and modified, from Tasman Metals Limited (http://www.tasmanmetals.com/s/OresMinerals.asp).

[1] Estimated year of mineral discovery; discovery location, and/or type location of mineral occurrence.

[2] Minerals shown in bold have historically been processed to recover rare-earth elements.

Other minor REE-bearing minerals shown in this report, and not listed in this table, will have their chemical compositions shown in parenthesis in the text.

It is well established that REE are not rare, nor are they earth, as their name implies. The term 'rare earths' dates back to the 18th and 19th centuries, when many of the REE were considered 'rare' in the Earth's crust at the time they were first identified (mostly in Europe), and 'earths' because as oxides they have an earthy appearance and resemble such materials as lime, alumina, and magnesia. Despite their name, some of the REE are more common than gold, silver, and the platinum-group elements (PGEs), while cerium, yttrium, and lanthanum are more abundant than lead, tin, and uranium (Fig. 1.2). Chemically, the REE are so similar that over billions of years the individual elements (except scandium) have not been separated in nature (Cooper, 1990). The prominent 19th century British chemist and physicist, Sir William Crookes (1832–1919), stated that, *"rare earth elements perplex us in our researches, baffle us in our speculations and haunt us in our very dreams. They stretch like an unknown sea before us, mocking, mystifying and murmuring strange revelations and possibilities"*. The REE are not easy elements to isolate or to understand, and consequently there was often a very long lag time between the discovery of the individual REE and the determination of its chemical attributes and practical uses. For example, many REE were discovered in the ~1880s, but their detailed chemical attributes and applications were only defined many decades later. The fact that many REE occur together in the same mineral or rock provided further complications for their accurate identification. Such mineral hosts include monazite [$(Ce,La,Th,Nd,Y)PO_4$], loparite $(Na,Ce,Ca)_2(Ti,Nb)_2O_6$), bastnäsite [$(Ce,La,Y)CO_3F$], and lateritic ion-adsorption clays. Industries during these early times did not initially attempt to separate the individual REE, instead they used them in a blended hybrid metal alloy called 'misch' metal (German for mixed metal). In 1891, 'misch' metal provided one of the first commercial applications for REE, when it was used as an ingredient in lamp mantles. Such lamps were hung above open flames, where they burned and produced a bright white light. The industrial uses of the REE were not fully realised until the early 1960s when efficient separation techniques, such as ion exchange, fractional crystallisation, and liquid-liquid extraction, were developed.

1.2. DISCOVERY AND ETYMOLOGY

In 1751, the Swedish mineralogist and chemist, Baron Axel Fredrik Cronstedt (1722–1765) is credited with the first discovery of a mineral containing REE. Cronstedt, who also discovered nickel in the same year, described the heavy stone from the Bastnäs mine in Sweden, as 'Bastnäs tungsten'. It was not until 1803, that a group of Swedish and German chemists independently isolated and confirmed the rare-earth component of the heavy stone and called it cerium oxide, and the mineral they called cerite to honour the newly found small planet ceres (Habashi, 1994).

However, it was the discovery in 1787 of an unusually heavy greenish black rock in a small feldspar-bearing quarry near the village of Ytterby, on the island of Resarö near Stockholm in Sweden, that represents the seminal event in the identification record of the REE (Fig. 1.3A–E). This small quarry was originally mined in the 1500s for ironwork, and later in the 1700s feldspar was obtained for porcelain and the manufacture of glass. The unusual dark rock was found by amateur mineralogist Lieutenant Carl Axel Arrhenius (1757–1824), who named it ytterbite, after the local village. A few years later in 1794, the distinctive black rock was analysed by Johan Gadolin (1760–1852), a Finnish professor of chemistry at the University of Åbo in Finland. Gadolin determined that it contained a new element to be called yttrium. It was some fifty years later, that Swedish chemist Carl Gustav Mosander (1797–1858) found two other non-pure elements, terbium and erbium, were associated with the yttrium. The famous black rock from the dumps of the Ytterby quarry comprised 38% of new 'earth type' ('earths' are compounds of elements, usually oxides; hence the name rare-earth elements). After more than 100 years of research by many prominent European chemists, it was eventually shown that Arrhenius's original black rock sample contained at least ten new rare-earth elements that became known as dysprosium, erbium, gadolinium, holmium, lutetium, scandium, terbium, thulium, ytterbium, and yttrium. In recognition of John Gadolin's efforts of being the first person to isolate a REE, the unusual Ytterby mineral was renamed by German chemist Martin Klaproth (1743–1817) as gadolinite [$(Ce,La,Nd,Y)_2FeBe_2Si_2O_{10}$].

The seventeen members of the REE group were discovered between 1794 and 1945, with the majority (14) of the elements found in the nineteenth century. The four decades between 1870 and 1910 were the most productive period accounting for the reliable identification of eleven REE. The radioactive element promethium, which has no stable isotopes and is artificially produced, was the last REE to be 'found' in 1945. Most of the REE identified during the eighteenth and nineteenth centuries were named in recognition of the scientist who found them or defined their elemental properties. Several European chemists

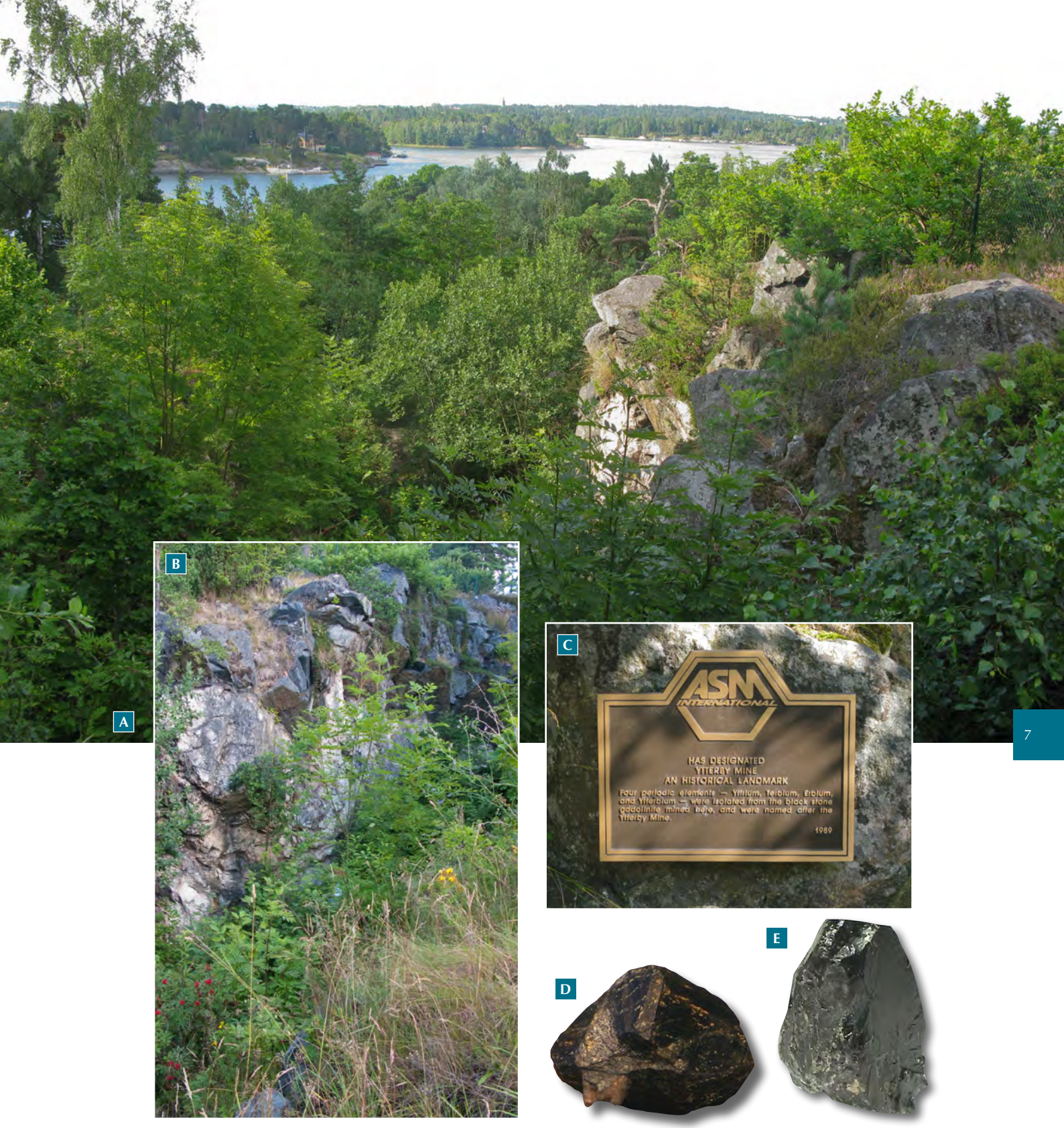

Figures 1.3A–E. The discovery in 1787 of the mineral gadolinite near the village of Ytterby in Sweden was a seminal event in the identification record of the rare-earth elements. The images in this figure are from this historic site.

A. Panoramic view from the Ytterby rare-earth-element mine, Resarö, Sweden. Rare-earth elements were first isolated from the mineral gadolinite found near the village of Ytterby.

B. Close-up of the Ytterby rare-earth-element-mine.

C. Plaque that denotes the significance of the Ytterby rare-earth-element occurrence.

D–E. Gadolinite specimens from the Ytterby mine, Sweden. The specimen shown in D is 2 cm across and has well-developed crystal faces, whereas the fractured sample shown in E is 1.8 cm in size and has a high lustre and vitreous appearance.

Images A to C are reproduced with permission from Peter van der Krogt, http://elements.vanderkrogt.net/Ytterby/index.html

Images D and E are reproduced with permission from John Veevaert, http://trinityminerals.com/ms2003/day3.shtml and http://www.rareterra.com/cgi-bin/rareminerals/specimen.cgi?Specimen_Code=RG808&Specimen_Name_Starts=

and mineralogists, in particular from France, Sweden, Switzerland, and Germany, were instrumental in successfully isolating and identifying the REE (Table 1.3 and Fig. 1.4). Some of the REE were also named from their geographical source location, from Greek or Latin references and their mythical context, and from the person finding the original REE-bearing mineral rather than the scientist who isolated the element.

The discovery history of the REE highlights one hundred and fifty years of scientific endeavours, elaborate and laborious experimental trials, and frustrating analytical confusion. This protracted evolutionary record commenced before the time of Dalton's determination of atomic weight values, the development of the Periodic Table of Elements, the advent of optical spectroscopy, Bohr's theory of the electronic structure of atoms, and Moseley's x-ray detection method for atomic number determinations (Holden, 2004). The similar chemical properties of the REE made them difficult to chemically isolate and consequently many mixtures of elements were mistaken for elemental species. Other factors that hindered the accurate identification of the REE were the lack of spectral analysis and reliable atomic weight data for the elements. The fifteen elements of the lanthanide group have a narrow range of atomic weights that sequentially increase from 138.90 for lanthanum to 174.97 for lutetium (Table 1.1). Only scandium (atomic weight of 44.95) and yttrium (88.90), have atomic weights significantly different from the lanthanide group. Consequently, during these early explorative years, many erroneous species were named, including: austrium, berzelium, carolinium, celtium, columbium, damarium, decipium, demonium, denebium, didymium, donarium, dubhium, eurosamarium, euxenium, glaucodymium, incognitium, ionium, junonium, kosmium, lucium, metacerium, monium, mosandium, moseleyum, mssrium, neokosmium, nipponium, philippium, rogerium, russium, sirium, thorine, vestium, victorium, wasmium, and welsium. Three important developments that assisted with the resolution of this confusion were the production of very pure REE samples, the discovery of spectroscopic analysis in 1859, and the introduction of the Periodic Table of Elements (Fig. 1.1) in 1869.

The following summary of the discovery and derivation of names relating to the REE is in part from: History of the Origin of the Chemical Elements and their Discoverers by Holden (2004: http://www.nndc.bnl.gov/content/elements.html); Elementymology & Elements Multidict by Krogt (2011: http://elements.vanderkrogt.net/); the Thomas Jefferson National Accelerator Facility (reproduced with permission)–Office of Science Education (http://www.jlab.org/ and http://education.jlab.org/itselemental/); The Lanthanides (http://www.angelo.edu/faculty/kboudrea/periodic/trans_lanthanides.htm); and Habashi (1994). The REE in the following section are discussed in order of increasing atomic number (Z), commencing with scandium (atomic number of 21) and ending with lutetium (71). Table 1.3 provides a chronological summary of the discovery record of the rare-earth elements.

Scandium (Sc; Atomic Number (Z) = 21): Scandium derives its name from the Latin *scandia* for 'Scandinavia' where scandium-bearing minerals were found. It is never found free in nature, with its direct commercial sources being unusual REE-bearing minerals. Scandium was the first element whose discovery was predicted using the Periodic Table of the Elements. The existence of scandium was predicted nearly ten years before it was actually discovered. The prediction was made by Russian chemist Dmitri Mendeleev (1834–1907), who developed the Periodic Table of Elements based on his periodic law. The table originally contained a number of empty boxes for elements that had not been discovered. Chemists were able to search for these elements based on the properties of the elements around the empty boxes. Scandium was eventually discovered in 1879 by Lars Fredrik Nilson (1840–1899), a Swedish chemist, while attempting to produce a sample of pure ytterbia from 10 kilograms of the mineral euxenite [(Y,Ca,Er,La,Ce,U,Th)$(Nb,Ta,Ti)_2O_6$] from Scandinavia. The substance discovered using spectral analysis by Nilson was not pure scandium metal, but scandium oxide (Sc_2O_3). It is difficult to produce pure scandium metal from scandium oxide. Metallic scandium was produced for the first time in 1937.

Yttrium (Y; Z = 39): Yttrium was the first of the so-called REE discovered. It was discovered by Finnish chemist Johan Gadolin in 1794, while analysing the mineral gadolinite [$(Ce,La,Nd,Y)_2FeBe_2Si_2O_{10}$] from the Swedish village of Ytterby. The name of this element originally given by Gadolin was ytterbium, named after its location, and it was later shortened to yttrium by Anders Gustav Eckberg. Later another element was given the name ytterbium that Gadolin had previously proposed. In 1843, Carl Gustav Mosander (1797–1858), a Swedish professor of chemistry and mineralogy at the Caroline Institute in Stockholm, successfully separated the element.

Lanthanum (La; Z = 57): Lanthanum was discovered in 1839 by Carl Gustaf Mosander. The name was derived from the Greek *lanthana*, that means 'to

lie hidden or to escape notice' because it was an obscure component of cerium ore and it was difficult to separate from that rare-earth material. In 1825, Mosander undertook some separation experiments to prepare cerium sulphide. He became convinced that the refined samples also contained earth oxides. Some ten years later, he carried out further separation procedures and he obtained two oxide samples. For one of these he assigned the name lanthanum and for the other he used the name didymium (or twin). Lanthanum was eventually isolated in relatively pure form in 1923. Today, lanthanum is primarily obtained through an ion exchange process from monazite sand [$(Ce,La,Th,Nd,Y)PO_4$], a material rich in REE that can contain as much as 25% lanthanum.

Cerium (Ce; Z = 58): Cerium was discovered in 1803 by Swedish chemist Jöns Jacob Berzelius (1779–1848) and Swedish mineralogist Wilhelm von Hisinger (1766–1852), and also independently by German chemist Martin Heinrich Klaproth (1743–1817). Cerium was originally named cererium, but was shortened to cerium, after the dwarf planet Ceres discovered by Italian astronomer Giuseppe Piazzi in 1801, and named for Ceres, the Roman goddess of agriculture. Klaproth called the new element ochroite because of its yellow colour. It was first chemically isolated in 1875 by the American mineralogist and chemist William Frances Hillebrand (1853–1925) and the American chemist Thomas Norton.

Praseodymium (Pr; Z = 59): The name was originally praseodidymium that was subsequently shortened to praseodymium, which is derived from the Greek *prasios* for 'green' and *didymos* for 'twin' because of its pale green salts and its resemblance to another closely related REE, lanthanum. Praseodymium was discovered in 1885 by Austrian chemist Carl Auer von Welsbach (1858–1929). He separated praseodymium, as well as the element neodymium, from a material known as didymium. The first enduring commercial use of 'purified' praseodymium, which was first investigated in the late 1920s and continues today, is in the form of a yellow-orange stain for ceramics, 'Praseodymium Yellow'.

Neodymium (Nd; Z = 60): The name was originally neodidymium and was later shortened to neodymium, which is derived from the Greek *neos* for 'new-one' and *didymos* for 'twin'. Neodymium was discovered in 1885 by Carl Auer von Welsbach during fractional crystallisation procedures that involved the separation of praseodymium from the material didymium. Its identification was confirmed by spectroscopic analysis. However, it was not isolated in relatively pure form until 1925, and the first large-scale commercial production of neodymium commenced in the 1950s. High purity (above 99%) neodymium was initially obtained through an ion-exchange process from monazite, but in more recent times most neodymium is extracted from bastnäsite and purified by solvent extraction.

Promethium (Pm; Z = 61): Promethium was the last of the seventeen REE discovered. Its existence was predicted by Czech chemist Bohuslav Brauner (1855–1935) in 1902, but it was not until 1947 that its discovery was confirmed. Promethium is a radioactive metal that has never been found on the Earth's surface; it has only been prepared artificially in particle accelerators and in other unusual reactions. The longest lived isotope of promethium has a short life of less than 20 years and it only exists in nature in negligible amounts (i.e., about 570 g in the entire Earth's crust). Brauner expanded Mendeleev's Periodic Table of the Elements by extending it past lanthanum, and he also predicted the existence of a new element located between neodymium and samarium. The name promethium is derived from the mythical Greek god figure 'Prometheus' who stole fire from heaven and gave it to mankind, and was subsequently punished. Several groups claimed to have produced the element, but they could not confirm their discoveries because of the difficulty of separating promethium from other elements. There were claims of discovery of such an element called Florentium in Italy in 1924, and at the University of Illinois, USA, in 1926, where the new element was named illinium. It was later found that these new 'elements' did not exist in nature and both claims were subsequently discarded. In 1941, neodymium and praseodymium were irradiated with neutrons, deuterons and alpha particles at the Ohio State University in the USA and new activities were recorded. It was determined some of these activities were associated with promethium. However, no chemical proof of promethium was available because the REE could not be separated from each other at that time. The break through came in the mid-1940s from a group of American chemists working on the Manhattan Project in Tennessee which was aimed at creating fuel for the atomic bomb. Promethium was first synthesised and identified in 1945 (confirmed in 1947) in fission products from the thermal neutron fission of U^{235} at the Clinton (later Oak Ridge National Laboratory, Oak Ridge, Tennessee) laboratory by Charles D. Coryell (1912–1971), Jacob A. Marinsky (b. 1918), and Lawrence E. Glendenin (1918–?). The fission products, Pm^{147} and Pm^{149} were also identified during the slow neutron activation of neodymium.

Samarium (Sm; Z = 62): Samarium derives its name from the mineral samarskite, in which it was found and which had been named after Vasili Samarsky-Bykhovets (1803–1870). Samarsky-Bykhovets was the Chief of Staff of the Russian Corps of Mining Engineers who granted access for German mineralogists to study mineral samples from the Ural Mountains. He became the first person to have a chemical element named after him, albeit indirectly. Detection of samarium and related elements was announced by several scientists in the second half of the 19th century; however, most sources grant this priority to the French chemist Paul Émile Lecoq de Boisbaudran (1838–1912). Samarium was observed spectroscopically by Swiss chemist Jean Charles Galissard de Marignac (1817–1894), professor of Chemistry at the University of Geneva, in the material dydimia in 1853. In 1879, Paul Émile Lecoq de Boisbaudran was the first to isolate samarium from the mineral samarskite [$(Y,Ce,U,Fe)_3(Nb,Ta,Ti)_5O_{16}$].

Europium (Eu; Z = 63): The element is named after the continent of Europe. According to mythology, the continent derives its name from the daughter of the Phoenician King Agenor, who was abducted by Zeus in the shape of a bull. Europium was first found by the French chemist Paul Émile Lecoq de Boisbaudran in 1890, who obtained spectral lines not accounted by the other REE samarium or gadolinium. However, the actual discovery of europium is generally credited to French chemist Eugène-Anatole Demarçay (1852–1904), who suspected samples of the recently discovered element samarium were contaminated with an unknown element in 1896 and who was able to isolate relatively pure europium from magnesium-samarium nitrate in 1901.

Gadolinium (Gd; Z = 64): Gadolinium derives its name from the mineral gadolinite, which in turn was named after the Finnish chemist, physicist, and mineralogist Johan Gadolin. Gadolinite was the first mineral discovered with confirmed concentrations of REE. Gadolinium has the distinction of being the only elemental name derived from Hebrew (*gadol* means 'great'). Spectroscopic evidence for the existence of gadolinium was first observed in 1880 by the Swiss chemist Jean Charles Galissard de Marignac while investigating gadolinite and didymia.

Terbium (Tb; Z = 65): The mineral gadolinite, discovered in a quarry near the village of Ytterby in Sweden has been the source of many REE. The element terbium was named after the Swedish village of Ytterby. In 1843, Carl Gustaf Mosander was able to separate gadolinite into three materials, which he named yttria, erbia, and terbia. As might be expected considering the similarities between their names and properties, scientists soon confused erbia and terbia and, by 1877, had reversed their names. What Mosander called erbia is now called terbia and visa versa. From these two substances, Mosander discovered two new elements, terbium and erbium. Pure forms of the metal were only isolated with the recent advent of ion exchange techniques.

Dysprosium (Tb; Z = 66): Dysprosium derives its name from the Greek *dysprositos* for 'hard to get at', in regard to the difficulty in separating this REE from an impure holmium oxide through a laborious sequence of dissolution in acid and ammonia. Discovery was first claimed in 1878 by the Swiss chemist Marc Delafontaine in the mineral samarskite and he called it philippia. However, philippia was subsequently found to be a mixture of terbium and erbium. Dysprosium was actually discovered by French chemist Paul Émile Lecoq de Boisbaudran (1838–1912) in 1886, as an impurity in erbia, the oxide of erbium. The grey-white metal was isolated in 1906 by Georges Urbain (1872–1938), another French chemist. Pure samples of dysprosium were first produced much later after the development of ion exchange analytical techniques in the 1950s.

Holmium (Ho; Z = 67): Holmium derives its name from the Latin *holmia* for 'Stockholm'. It was discovered in 1878 by the Swiss chemists Jacques-Louis Soret (1827–1890) and Marc Delafontaine (1837–1911), who noticed aberrant spectrographic absorption bands of a then-unknown element, which they called 'Element X'. Shortly later in 1879, it was independently described by the Swedish chemist Per Theodor Cleve (1840–1905). The three scientists are equally given credit for the element's discovery. It was first isolated in 1911 by chemist Holmberg, who proposed that the name holmium was either to recognise Cleve, who was from Stockholm, or perhaps to establish his own name in history. Cleve used the same chemical method that Carl Gustaf Mosander developed to discover lanthanum, erbium, and terbium, namely investigating the impurities of other REO. He started with erbia, the oxide of erbium (Er_2O_3), and removed all the known contaminants. After further processing, he obtained two new materials, one brown and the other green. Cleve named the brown material holmia, and the green material thulia. Holmia is the oxide of the element holmium and thulia is the oxide of the element thulium.

Erbium (Er; Z = 68): The mineral gadolinite discovered near Ytterby in Sweden has been the source of many REE, including erbium. In 1843, Swedish

chemist Carl Gustaf Mosander separated gadolinite into three materials, which he named yttria, erbia, and terbia. From these substances, Mosander discovered two new elements, terbium and erbium. However, during these early times erbia and terbia were confused. After 1860, terbia was renamed erbia, and after 1877, what had been known as erbia, was renamed terbia. Fairly pure Er_2O_3 was independently isolated in 1905 by chemists Georges Urbain (1872–1938) and Charles James, and pure erbium metal was not produced until 1934.

Thulium (Tm; Z = 69): Thulium derives its name from *Thule*, the earliest Latin name for the northern most part of the civilised world—'Scandinavia' (Norway, Sweden, and Iceland). However, to the ancient Greeks, Thule was simply the northernmost habitable region of the world. The chemical symbol for thulium was initially Tu, but his was changed by the International Commission on Atomic Weights to Tm, since the symbol Tu was at that time used for tungsten (symbol is now W). Thulium was discovered in 1879, when the Swedish chemist Per Theodor Cleve's was investigating the oxides of the REE. His analytical procedures were similar to the chemical separation methods previously developed by Carl Gustaf Mosander during his discovery of lanthanum, erbium, and terbium. He started with erbia, the oxide of erbium (Er_2O_3), and removed all of the known contaminants. After further processing, Cleve obtained a green product which he named thulia. Thulia is the oxide of the element thulium, which was first isolated in 1911 by the American chemist Charles James. High-purity thulium oxide was first produced commercially in the late 1950s, with the advent of more sophisticated ion-exchange separation technology.

Ytterbium (Yb; Z = 70): Many REE have been derived from the mineral gadolinite found in a quarry near Ytterby in Sweden. The element ytterbium was named after the Swedish village of Ytterby. It was the fourth element named after this village (also yttrium, erbium, and terbium). In 1843, Swedish chemist Carl Gustaf Mosander separated gadolinite into yttria, erbia, and terbia. Jean Charles Galissard de Marignac, French professor of Chemistry at the University of Geneva, discovered in 1878 that erbia consisted of two components. One component was named ytterbia by Marignac, while the other component retained the name erbia. Due to his original understanding of the composition of ytterbia, Marignac is credited with the discovery of ytterbium. Marignac believed that ytterbia was a compound of a new element, which he named ytterbium. Other chemists produced and experimented with ytterbium in an attempt to determine some of its properties. Unfortunately, the various scientists obtained different results from the same experiments. While some of them interpreted these inconsistent results to be due to poor procedures or faulty equipment, the French chemist Georges Urbain proposed that ytterbium wasn't an element at all, but a mixture of two elements. In 1907, Urbain was able to separate ytterbium into two elements. He named one of the elements neoytterbium and the other element lutecium. Auer von Welsbach independently isolated these elements from ytterbia at about the same time. Chemists eventually changed the name neoytterbium back to ytterbium, and similarly, the spelling of lutecium to lutetium. The chemical and physical properties of ytterbium could not be determined until 1953, when more purified samples of ytterbium sample were produced.

Lutetium (Lu; Z = 71): The name of this REE was originally 'lutecium' but in 1949, the IUPAC changed the 'c' to 't' since the name derives from *Lutetia*, the ancient Latin name for the city of 'Paris', rather than from its French equivalent *lutece*. Three scientists independently found lutetium as an impurity in the mineral 'ytterbia'. The discovery is credited to the French chemist Georges Urbain in 1907, although both Austrian chemist Carl Auer von Welsbach and American chemist Charles James declared similar findings. Auer von Welsbach named the element cassiopeium for the constellation 'Cassiopeia'. Although a scientific paper written by Auer von Welsbach's appeared prior to a similar discussion by Urbain, Urbain argued that he had submitted his paper to the editor first. The International Committee on Atomic Weights, where Urbain was one of the four members, adopted Urbain's name and his claim of priority. The German Atomic Weights' Committee accepted Auer von Welsbach's name of cassiopeia for the element for the next forty years. Urbain's name for the element was officially adopted by the IUPAC in 1949 based on consideration of prevailing usage, finally ending the controversy. Ironically, Charles James, who had avoided the public controversy, worked on a much larger scale than the others, and probably possessed the largest supply of lutetium at the time.

Table 1.3 and Figure 1.4 provide summaries of the eminent chemists responsible for the discovery and naming of the rare-earth elements.

Table 1.3. Chronological discovery record of the rare-earth elements.

Element (chemical symbol)	Atomic number	Year	Discoverer	Origin of name
Yttrium (Y)	39	1794	Johan Gadolin (Finnish)	Ytterby mine, Sweden
Cerium (Ce)	58	1803	Jöns Jacob Berzelius (Swedish); Wilhelm von Hisinger (Swedish); Martin Heinrich Klaproth (German)	Small planetoid Ceres
Lanthanum (La)	57	1839	Carl Gustaf Mosander (Swedish)	Greek: *lanthana* for 'to lie hidden or to escape notice' since it lay concealed in the earth
Terbium (Tb)	65	1843	Carl Gustaf Mosander (Swedish)	Ytterby mine, Sweden
Erbium (Er)	68	1843	Carl Gustaf Mosander (Swedish)	Ytterby mine, Sweden
Holmium (Ho)	67	1878	Jacques-Louis Soret (Swiss); Marc Delafontaine (Swiss); Per Theodor Cleve (Swedish)	Latin: *holmia* for 'Stockholm'
Ytterbium (Yb)	70	1878	Jean Charles Galissard de Marignac (French)	Ytterby mine, Sweden
Scandium (Sc)	21	1879	Lars Fredrik Nilson (Swedish)	Latin: *scandia* for 'Scandinavia'
Samarium (Sm)	62	1879	Paul Émile Lecoq de Boisbaudran (French)	The mineral samarskite and its its finder, the Russian mine official Colonel von Samarsky
Thulium (Tm)	69	1879	Per Theodor Cleve (Swedish)	Latin: *Thule* for ancient name for 'Scandinavia'
Gadolinium (Gd)	64	1880	Jean Charles Galissard de Marignac (Swiss)	Hebrew: *gadol* for 'great' and in honour of Finnish chemist Johan Gadolin
Praseodymium (Pr)	59	1885	Carl Auer von Welsbach (Austrian)	Greek: *prasios* for 'green' in reference to the colour of its salts, and *didymos* for 'twin', because of its resemblance to another closely related REE, lanthanum
Neodymium (Nd)	60	1885	Carl Auer von Welsbach (Austrian)	Greek: *neos* for 'new-one' and didymos for 'twin'
Dysprosium (Dy)	66	1886	Paul Émile Lecoq de Boisbaudran (French)	Greek: *dysprositos* for 'hard to get at' because of the difficult involved with its detection and isolation
Europium (Eu)	63	1896	Eugène-Anatole Demarçay (French)	After the continent Europe, which itself comes from *Europa* in Greek mythology
Lutetium (Lu)	71	1907	Georges Urbain (French)	Latin: *Lutetia* for the place where Paris was founded
Promethium (Pm)	61	1945	Charles D. Coryell; Jacob A. Marinsky; Lawrence E. Glendenin (all American)	Greek: Prometheus who brought fire to mankind in reference to harnessing of the energy of the nuclear fission and warning against its dangers

Figure 1.4. Famous European chemists responsible for the discovery and confirmation of the rare-earth elements (REE). Many of the REE identified during the eighteenth and nineteenth centuries were named in recognition of the scientist who found them or defined their elemental properties. Other elements were named after their geographical source location, or were derived from a Greek or Latin mythical heritage. All photographs are from Wikimedia Commons (http://commons.wikimedia.org/wiki/Main_Page).

1.3. MAJOR PROPERTIES AND APPLICATIONS

The REE have unique and diverse chemical, magnetic, and luminescent properties that make them strategically important in a number of high-technology industries. Traditionally they have been used for colouring and polishing glass, sintering aids in ceramics, car engine exhausts, magnets, catalysts, and metallic alloys in metallurgy. However, their applications in many emerging technologies associated with the transport, information, environment, energy, defence, nuclear, and aerospace industries have gained rapid momentum in recent years. The most significant increases in demand are the predicted expansion in hybrid car components (primarily batteries and magnets), compact fluorescent light bulbs, phosphors in computer and plasma screens, petroleum catalysts, superconductors, samarium-cobalt and neodymium-iron-boron high-flux supermagnets in electric motors for hybrid cars and wind turbine generators, glass manufacturing, electronic polishing, fuel-cell technology, and multi-level electronic components such as DVD drives. Oxides of the REE are now used in the environment as chemical tracers to monitor geological materials associated with river catchments and to determine erosion rates of drainage-watershed systems (Fig. 1.5).

Curtis (2011) has forecasted that the future demand for REE in most applications will increase with battery alloys and magnets being the most dominant growth drivers. For example, projected annual growth rates of REE are estimated for the following applications: battery alloys (15%); magnets (12%); polishing powder (10%); autocatalysts (8%); phosphors (8%); fluid cracking catalysts (4%); metallurgy (2%); and others (8%).

Figure 1.5. Rare-earth oxides that are used as chemical tracers to determine which parts of a watershed are eroding. Clockwise from top centre: praseodymium, cerium, lanthanum, neodymium, samarium, and gadolinium. Reproduced with permission (PD-USGOV-USDA-ARS) from the United States Department of Agriculture, Agricultural Research Service, at http://www.ars.usda.gov/is/graphics/photos/jun05/d115-1.htm Group Elements (red font). Modified from Haxel et al. (2005).

The REE are also becoming increasingly more important in many defence-related applications (http://www.molycorp.com/defense_applications.asp). The REE are used in many forms from low-purity concentrates and natural mixtures of metal ('mischmetal') to ultra high-purity compounds and metals.

The smallest commercial sector by volume, but largest by value, is europium and terbium, which are used in the production of phosphors for television media and energy efficient light globes (Miezitis, 2010). In 1967, europium was the first, high purity REE to enter the public marketplace as a source of the red colour in television sets. There had been colour monitors before the use of europium, but the colour quality was generally weak. The early televisions relied on phosphors—substances that glow when struck with electrons or other energised particles—to get their red, green, and blue colours, and the early red phosphors could not produce a very bright colour. Europium phosphors dramatically improved the quality of television pictures. Figure 1.6 summarises the distribution of REO applications according to value and volume.

1.3.1. Properties and applications of individual rare-earth elements

Scandium: A silvery-white metallic transition metal, scandium has historically been sometimes classified as a REE, together with yttrium and the lanthanides. Metallic scandium was first produced in 1937 and the first pound (0.45 kilograms) of pure scandium was produced in 1960. Scandium is rarely concentrated in nature because of its lack of affinity to combine with the common ore-forming anions. Its abundance is thought to be about 5 to 6 parts per million (ppm) in the Earth's crust. Interestingly, scandium is more common in the sun and certain stars than on Earth. Scandium is present in most of the REE and uranium deposits, but it is extracted from these ores in only a few mines worldwide. Its use is severely restricted by its scarcity of reliable supply as there are no primary scandium mines in production in the world. Scandium is found in common rock-forming minerals, such as biotite, hornblende, and pyroxene, and in trace amounts (5 to 100 ppm) in basalt and gabbro. Scandium also occurs in aluminium phosphate minerals, beryl, cassiterite, columbite, garnet, muscovite, REE minerals, and wolframite. Scandium can also be obtained from the rare minerals thortveitite

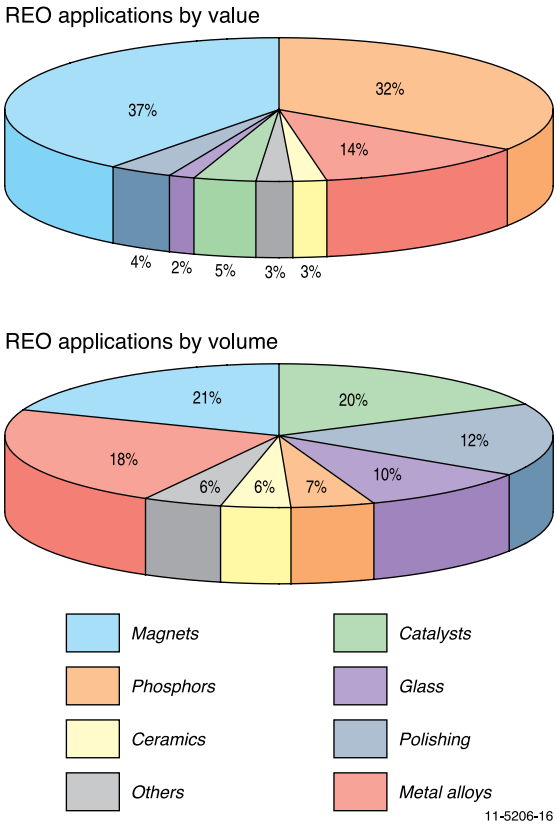

Figure 1.6. The major applications of the rare-earth oxides by value and volume. Modified from Kingsnorth (2010b).

$[(Sc,Y)_2Si_2O_7]$, which contains 44–48% scandium oxide Sc_2O_3, bazzite $(Be_3(Sc,Al)_2Si_6O_{18})$, wiikite (ill-defined mixture of REE), euxenite, and gadolinite, but it is usually obtained as a by-product of refining uranium and tantalum. Most scandium not obtained from uranium tailings is mined from Iceland, Madagascar, and the Scandinavian Peninsula.

Being a soft and light metal, scandium has alloy applications with aluminum in the aerospace industry. These alloys contain between 0.1 to 0.5% of scandium and are amongst the lightest and strongest alloys in the world. Companies that use scandium often buy the oxide rather than the pure metal. The oxide costs several thousand dollars per kilogram. By comparison, the pure metal costs a few hundred thousand dollars per kilogram therefore scandium is too expensive for widespread use. Due to its low availability and the difficulties in the preparation of metallic scandium, it took until the 1970s before applications for scandium were developed. Scandium's industrial applications include its ability to improve strength, ductility, and other properties when added to aluminum. Alloys of scandium and aluminum are also used in sporting equipment, such as aluminum baseball bats, bicycle frames, and lacrosse sticks. Scandium-stabilised zirconia as an electrolyte for Solid Oxide Fuel Cells (SOFC) significantly reduces the operating temperature of fuel cells, thereby providing a much longer life. SOFCs are expected to play a major role in the developing battery powered electric transportation industry. The enhanced application of SOFC has recently increased the global interest in scandium. Scientists have only studied a few compounds of scandium. About 20 kilograms (44 pounds) of scandium oxide (Sc_2O_3), also known as scandia, are used each year in the USA in the production of high-intensity discharge lamps, colour televisions, energy-saving lamps, glasses, and speciality welding wire. Scandium iodide (ScI_3) is added to mercury vapor lamps so that they will emit light that closely resembles sunlight. The radioactive isotope ^{46}Sc is used as a tracing agent in crude oil refinery crackers.

Yttrium: Yttrium is a soft, silver-metallic, lustrous and highly crystalline transition metal that generally forms inorganic compounds in the oxidation state of +3. It is chemically similar to the lanthanide elements, and it has traditionally been classified a REE. Yttrium is primarily obtained through an ion exchange process from monazite sand, a material rich in REE. It is a scarce metal that is also known as a blackish grey powder that never produces a spectrum.

Although metallic yttrium is not widely used, several of its compounds are currently utilised. Yttrium oxide (Y_2O_3) and yttrium orthovanadate (YVO_4) are both combined with europium to produce the red phosphor used in colour television picture tubes. Yttrium oxide is suitable for making superconductors, which are compounds that conduct electricity without any loss of energy. Yttrium metal is added to aluminium and magnesium to increase the strength of the alloy, and it is added to cast iron to enhance the workability of the metal. Metal alloys comprising yttrium, chromium, and aluminium are heat resistant and conduct heat. Yttrium oxide in glass and ceramics makes it heat- and shock-resistant, which has application in camera lenses. Garnets made from yttrium and iron ($Y_3Fe_5O_{12}$) are used as microwave filters in microwave communications equipment, resonators in frequency meters, magnetic field measurement devices, tunable transistors, and oscillators. Garnets made from yttrium and aluminum ($Y_3Al_5O_{12}$) are used in jewellery as simulated diamond. Yttrium is also used in the manufacturing of gas mantles for propane lanterns as a replacement for thorium, which is radioactive. Yttrium-based materials improve the efficiency of car engines and high-performance spark plugs. Radioactive isotopes of yttrium have medical applications for the treatment of cancers, nerve problems in the spinal chord, and rheumatoid arthritis.

Lanthanum: Lanthanum is a shiny grey, ductile, graphitic-like metal, and a dark lead-grey powder, soft to touch, and able to be pressed into a compact mass. It is found in some rare-earth minerals, usually in combination with cerium and other REE. Lanthanum is the first element of the lanthanide series, exhibits two oxidation states, +3 and +2, the former being much more stable, and it rapidly oxidises in air.

Important applications for lanthanum were not found for over one hundred years. The initial interest for lanthanum was largely scientific, being limited to investigators improving its separation techniques, purification, and defining its chemical spectrum. The first historical application of lanthanum was patented in 1885 for its use in gas lantern mantles. Its activity in catalysts for petroleum refining increases refinery yield by up to 10% while reducing overall power consumption. As most hybrid cars use nickel-metal hydride batteries, significant quantities of lanthanum are required for the production of hybrid automobiles. Typical hybrid automobile batteries require about 10 to 15 kg of lanthanum. Lanthanum is used to make carbon arc lights that are utilised in the motion picture industry for studio lighting and projector lights. Various compounds of lanthanum and other REE (oxides, chlorides, etc.) are components of various catalysis, such as petroleum cracking catalysts. Lanthanum also makes up about 25% of 'misch' metal, a material that is used to make flints for lighters. Lanthanum-bearing hydrogen sponge alloys are capable of storing up to 400 times their own volume of hydrogen gas in a reversible adsorption process. Lanthanum oxides (La_2O_3) improve the alkali resistance of glass, and are used in making special optical glasses (e.g., infrared-absorbing glass) and camera and telescope lenses because of the high refractive index and low dispersion of rare-earth glasses.

Cerium: Cerium is a soft, malleable, ductile, and shiny grey metal that readily oxidises to a green oxide, and reacts quickly in hot water. Pure cerium will ignite if it is scratched with a sharp object, but can be safely used if combined with other materials. The most common oxidation states are +3 and +4, followed by +8. Cerium is the most abundant of the REE with about 60 ppm occurring in the Earth's crust (Table 1.1). Important Ce-bearing minerals (Table 1.2) include allanite or orthite, rhabdophane, and synchysite, and its major sources are bastnäsite, hydroxylbastnäsite, and monazite.

Cerium is critical in the manufacture of environmental protection and pollution-control systems, from cars to refineries. It is used as a catalyst to refine petroleum and to oxidise unreacted hydrocarbons and reduce nitrogen oxides. As a diesel fuel additive for micro-filtration of pollutants, it promotes more complete fuel combustion for more energy efficiency. Cerium is used in carbon arc lights for studio lighting and projector lights, and is a component of 'misch' metal for flints in lighters and as an alloying agent to make special metals in permanent magnets and in tungsten electrodes for gas tungsten arc welding. Cerium oxide (Ce_2O_3 and CeO_2) is a component of the walls of self cleaning ovens and of incandescent lantern mantles. Cerium oxide (CeO_2) is used as an abrasive to polish glass surfaces in lenses and CRT displays, and to extend the life of the glass and improve its colour dispersion. Cerium sulphide (Ce_2S_3) in red pigments is increasingly being used in place of toxic cadmium salts. Ceric suphate ($Ce(SO_4)_2$) has applications in some chemical analysis processes. Other cerium compounds are used to make some types of glass as well as to remove colour from glass.

Praseodymium: Praseodymium is a soft, malleable, ductile, and reflective grey metal that reacts slowly in air to develop a green oxide coating, but it is very reactive in water. Its most common oxidation state is +3. Praseodymium is primarily sourced from bastnäsite and monazite.

The primary use of praseodymium is as an alloying agent with magnesium to create high-strength metals that are used in aircraft engines and in permanent magnet (neodymium-iron-boron) systems of small motors. It also makes up about 5% of 'misch' metal used in the making of flints for lighters. Praseodymium forms the core of high-intensity carbon arc lights used in the motion picture industry for studio lighting, projector lights, floodlights, and searchlights. Along with neodymium, it can filter certain wavelengths of light, such as in photographic filters, airport signal lenses, and tinted enamels and glass. For example, it forms a component of yellow didymium glass used in welder's and glass blower's goggles for protection against infrared radiation. Praseodymium is added to fiber optic cables as a doping agent where it is used as a signal amplifier. Praseodymium alloyed with nickel ($PrNi_5$) has such a strong magnetocaloric effect that it has allowed scientists to approach within one thousandth of a degree of absolute zero temperature.

Neodymium: Neodymium is a soft, malleable, ductile, reflective grey metal that easily oxidises in both air and water, and it is found in the +3, +2, and +4 oxidation states. Neodymium is not found naturally in metallic form or unaccompanied by other lanthanides. It is present in significant quantities in the ore minerals monazite and bastnäsite.

Neodymium compounds were first commercially used as a glass dye in 1927. Neodymium is an important component of metal alloys. When alloyed with iron and boron, it forms extremely strong permanent magnets (called rare-earth magnets or neodymium magnets), and it is used to strengthen alloys of magnesium. Cell phones, microphones, CD players, computer hard disks, and most sound systems use neodymium magnets. Neodymium-Iron-Boron (NdFeB) magnets maximise the power/cost ratios of various motors and mechanical systems. Neodymium makes up about 18% of 'misch' metal that is used to make flints for lighters. Neodymium is also a component of didymium glass, which is used to make certain types of welder's and glass blower's goggles. Neodymium is added to glass to remove the green colour caused by iron contaminants. It can also be added to glass to create violet, red, or grey colours. Some types of glass containing neodymium are used by astronomers to calibrate spectrometers and other types are used to create artificial rubies for lasers. Some neodymium salts are used to colour enamels and glazes.

Promethium: Promethium does not occur naturally on Earth, although it has been detected in the spectrum of a star in the constellation Andromeda. Promethium is an unstable radioactive element only found in trace amounts in uranium ores and recovered from the byproducts of uranium fission. Due to its instability, promethium does not accumulate above the concentration of about a picogram (10^{-12}) per tonne of ore. Promethium's most stable isotope, ^{145}Pm, has a half-life of 17.7 years. It decays into Nd^{145} through electron capture.

Promethium could be used to make a nuclear powered battery. This type of battery would use the beta particles emitted by the decay of promethium to make a phosphor give off light. This light would then be converted into electricity by a device similar to a solar cell. It is expected that this type of battery could provide power for five years. Due to its instability, promethium has few practical applications. Minor uses include beta radioactive sources for gauges that measure the thickness of sheets of steel and luminous blue and green paints on the face of watches. Potential applications include: portable X-ray sources in radioisotope thermoelectric generators that provide heat or power for space probes and satellites; miniature batteries in missiles and pacemakers; and in lasers that communicate with submerged submarines.

Samarium: Samarium is a high lustre, silvery, moderately hard metal obtained from monazite (which contains up to 2.8% samarium), bastnäsite, gadolinite, and samarskite. Stable in dry air, samarium oxidises in moist air and ignites when heated to 150°C. Within its compounds, it usually displays +2 and +3 oxidation states.

Samarium is used in carbon-arc lights for the motion picture industry, studio lighting, and projector lights. Its spectral absorption properties make it useful in filter glasses that surround neodymium laser rods and as a neutron absorber in nuclear reactors. It makes up about 1% of 'misch' metal, a material used in the manufacture of flints for lighters. Samarium forms a compound with cobalt ($SmCo_5$) in powerful permanent magnets that have the highest resistance to demagnetisation of any material known, and they can withstand high temperatures, above 700°C, without losing magnetic properties. These magnets are used in headphones, small motors, magnetic pickups for guitars, and in solar-powered aircraft. Radioactive samarium isotopes (^{153}Sm) kill cancer cells in the treatment of lung, prostrate, and breast cancer. Samarium oxide (Sm_2O_3) is added to glass to absorb infrared radiation and acts as a catalyst for the dehydration and dehydrogenation of ethanol (C_2H_6O). Other applications include catalysis of chemical reactions, radioactive dating, and an X-ray laser.

Europium: Europium is a moderately hard, silvery-grey metal that is the most reactive of the REE. It readily oxidises in air and water, and ignites when heated to 180°C. The dominant oxidation states of +2 and +3 are the same as samarium. Europium is never found in nature as a free element, however, it is hosted by many minerals, including monazite and bastnäsite.

There are no major commercial applications for europium metal, although it has been used to dope some types of plastics to make lasers. Europium has exceptional properties relating to photo emission. When it absorbs electrons or UV radiation, the europium atom changes energy levels to create a visible luminescent emission. Europium oxide (Eu_2O_3) is widely used as a red phosphor in the cathode-ray tubes of television sets and computer monitors, and as an activator for yttrium-based phosphors. Since it is a good absorber of neutrons, europium is being investigated for use in nuclear reactors. Europium has also been identified in the spectra of the sun and certain stars. Europium is added to fluorescent lighting to enhance a blue component for a more natural light, and to reduce up to 75% of the energy costs compared to incandescent lighting. Europium fluorescence is used to interrogate biomolecular interactions in drug-discovery screens, and in the anti-counterfeiting phosphors in Euro banknotes. Medical applications include tagging

complex biochemical agents for tracing materials during tissue research, and the screening of genetic diseases, such as Down's Syndrome. Geoscientists use depletion or enrichment concentrations of europium (called the europium anomaly) in minerals and rocks to understand geological processes.

Gadolinium: Gadolinium is a soft, ductile, silvery-white metal that is relatively stable in dry air, but oxidises in moist air and dissolves in water and acid. In the great majority of its compounds, gadolinium usually adopts the +3 oxidation state. The minerals monazite and bastnäsite are the primary sources.

Gadolinium has no large-scale applications, but it has a variety of specialised uses. It can be alloyed with iron, chromium, and other metals to improve their workability and their resistance to high temperatures and oxidation. With its unique magnetic behaviour, it is used in magnets for such electronic devices as disk drives, video recorders, compact disks, and in handling computer data and magneto-optic recording. Gadolinium can be combined with yttrium to form garnets that have applications in microwave technology, and gadolinium compounds are used to make green phosphors for colour televisions and compact disks. Gadolinium has the highest neutron cross-section of any stable nuclide and the greatest ability to capture thermal neutrons of all known elements. It is therefore used for shielding devices in neutron radiography, in magnetic resonance imaging for the detection of cancers, X-ray systems, and in control rods in nuclear reactors. Unfortunately, the two isotopes best suited for neutron capture, gadolinium-155 and gadolinium-157, are present in small amounts. As a result, gadolinium-based control rods quickly lose their effectiveness.

Terbium: Terbium is a soft, silvery-white metal that is not found in nature as a free element. Terbium occurs in the minerals cerite ($Ce_9^{3+}Fe^{3+}(SiO_4)_6[SiO_3(OH)](OH)_3$), xenotime ($YPO_4$), and euxenite, but is primarily obtained from monazite that typically contains up to 0.03% terbium. It oxidises very slowly in air, dissolves in water, and as typical of most other REE, it adopts the +3 oxidation state. As with its neighbour element dysprosium, it is very soft and can be cut by a knife.

Terbium is used in some types of solid-state devices and, along with zirconium dioxide (ZrO_2), as a crystal stabiliser that operate at high temperatures in fuel cells. Terbium has applications in magnetorestrictive alloys, which lengthen or shorten when exposed to a magnetic field. Terbium oxide is used as an activator for green phosphors (which fluoresce a brilliant lemon-yellow) in cathode-ray television tubes and energy-efficient fluorescent lamps. Terbium is also used in naval sonar systems, sensors, in the SoundBug device (its first commercial application), and other magnetomechanical devices. Terbium borate is used to make laser light.

Dysprosium: There are no major commercial applications for dysprosium, which is a silver, high-lustred metal that is so soft it can be cut with a knife. Dysprosium is not found in nature as a free element, and it is mainly obtained from monazite, xenotime, and bastnäsite. It is moderately reactive, oxidises in air, quickly dissolves in cold water, and has the dominant +3 oxidation state typical of the other REE.

Since it easily absorbs neutrons and has a high-melting point, dysprosium is alloyed with steel for use in nuclear reactors and in dosimeters for measuring exposure to radiation. When combined with vanadium and other REE, dysprosium is used in laser materials. Dysprosium oxide (Dy_2O_3) is combined with nickel and added to a special cement for cooling nuclear reactor rods. Its high magnetic susceptibility to magnetisation character is exploited in the manufacture of permanent magnets and data storage devices. Dysprosium has applications in high-precision liquid fuel injectors, transducers, wide-band mechanical resonators, and dysprosium iodide (DyI_3) is used in halogen lamps to enhance white light.

Holmium: Holmium is a soft, malleable, silvery-white metal that is stable in dry air at room temperature, but dissolves in acids. In its compounds, it is usually found in the +3 oxidation state. Some of holmium's compounds include holmium oxide (Ho_2O_3), holmium fluoride (HoF_3), and holmium iodide (HoI_3). It is primarily obtained from monazite, which can contain as much as 0.05% holmium.

Holmium is rare, expensive, and has no major commercial applications. Holmium has the highest magnetic strength of any element, and therefore is used to create the strongest artificially generated magnetic fields, when placed within high-strength magnets as a magnetic flux concentrator. Holmium is used in nuclear control rods where it has the ability to absorb nuclear fission-expelled neutrons. Holmium is an important REE component of microwave and laser equipment where the safety of human eyes is an issue during medical, dental, and fibre-optical procedures. Holmium also provides yellow and red colouring pigments for cubic zirconia and glass, and is used in calibration standards for optical spectrophotometers and gamma-ray spectrometers.

Erbium: Erbium is a soft, malleable, and grey-white metal that is stable in air, and does not oxidise as quickly as some of the other REE. It is largely obtained from the minerals xenotime, euxenite, monazite, and bastnäsite through an ion exchange process.

Erbium's everyday uses are varied. Erbium's principal uses involve its pink-colored Er^{3+} ions, which have optical fluorescent properties particularly useful in certain laser applications. The distinctive pink colour of erbium oxide is used to colour glass, cubic zirconia, porcelain, and glazes. Some of these tinted products are utilised in sunglasses and cheap jewellery. Erbium is commonly used as a photographic filter, and because of its resilience it is useful as a metallurgical additive. It can be alloyed with vanadium to make it softer and easier to shape. Erbium has remarkable optical properties and it is added to long-range fiber optic cables as a doping agent where it is used as a signal amplifier. High-power erbium–ytterbium fiber lasers are gradually replacing CO_2 lasers for metal welding and cutting applications. Erbium also has some uses as neutron-absorbing control rods in the nuclear power industry. Medical applications include dermatology, dentistry, and laser surgery. The erbium-nickel alloy Er_3Ni has an unusually high specific heat capacity at liquid-helium temperatures that is utilised in cryocoolers.

Thulium: Thulium is the least abundant of the naturally occurring REE. It is a soft and malleable, silvery grey metal that has only recently become available. Thulium is primarily obtained from monazite, which contains as much as 0.002% thulium, and bastnäsite, which contains as much as 0.0008% thulium. Thulium tarnishes in air very slowly, and it usually adopts the +3 oxidation state in its compounds. Its chemistry is similar to that of yttrium.

Rare and expensive, thulium has no major commercial applications. However, because of its unique photographic properties it is used in sensitive X-ray phosphors to reduce X-ray exposure, and one of its isotopes, ^{169}Tm, is used as a radiation source for portable X-ray machines. Such radiation sources have applications in medical and dental diagnosis, as well as detecting defects in mechanical and electronic components. Highly efficient thulium-based lasers are used in the military, medicine, meteorology, and surgery. Superficial ablation of skin tissue is carried out with thulium lasers that operate at wavelengths between 1930 and 2040 nm. As with yttrium, thulium is a REE component of high-temperature superconductors.

Ytterbium: Ytterbium is a malleable, ductile, and silvery metal that has few applications. It can be obtained from monazite, which has about 0.1% ytterbium, and from bastnäsite, which contains about 0.0006% ytterbium. Ytterbium oxidises slowly in air, but unlike other transition metals, the oxide does not flake off the surface, but forms a protective layer that inhibits further oxidation. It has similar chemical behaviour to yttrium, and as with most other REE, the dominant oxidation state is +3.

Ytterbium is alloyed with stainless steel to improve the strength and mechanical properties of dental tools, and it is also used as a doping agent in fiber optic cables for enhancement of amplification attributes. One of ytterbium's isotopes (^{169}Yb) is used as a radiation source substitute for portable X-ray machines. Such machines are useful for the radiography of small objects and when electricity is not available. Ytterbium is often used as a doping material (as Yb_3+) for high power and wavelength-tunable solid-state lasers. When subject to high stresses, the electrical resistance of ytterbium increases by an order of magnitude. Subsequently it is used in stress gauges to monitor ground movements and deformations initiated by earthquakes and underground explosions.

Lutetium: Lutetium is a silvery-white, hard, dense metal that is one of the most difficult elements to prepare. With thulium, lutetium is the least abundant of the naturally occurring REE, and because of the difficulty of separating it from other elements, it is very expensive—much more expensive than gold and platinum. It is obtained from monazite, which contains about 0.003% lutetium. In contrast to the other REE, it is resistant to oxidation in air, but it has the common oxidation state of +3.

Lutetium is an expensive and rare metal that has no large-scale commercial uses. It often occurs in association with yttrium and is sometimes used in metal alloys and as a catalyst in various chemical reactions. Some radioactive isotopes of lutetium are used as a catalyst in the cracking of petroleum products, in some hydrogenation and polymerisation processes, and in detectors for positron emission tomography. The radioactive isotope lutetium-177 (^{177}Lu) is used experimentally in targeted radionuclide therapy for tumors, and lutetium-176 (^{176}Lu) is used in nuclear technology to determine the age of meteorites.

Table 1.4 summarises the major applications of the REE that are gaining momentum in high-technical industries, and many of these applications are shown in Figures 1.6 and 1.7.

Table 1.4. Major applications of the rare-earth elements in emerging high-technology industries.

Heavy-rare-earth elements are shown in *italics* font; light-rare-earth elements are shown in normal font
(1) Catalysts: La, Ce, Nd, Pr, *Lu*, Y, Sm Automotive catalysts Petroleum refining, fuel catalytic cracking, ethane polymerisation Fuel and hybrids, diesel fuel additive Air pollution controls, water filtration, hydrogen storage, flints
(2) Permanent and ceramic magnets: Nd, Pr, Sm, *Dy*, *Tb*, *Tm*, La, Ce Cars—hybrids-plug-in and electric vehicles, window motors, screen wipers, starter motors, hybrid batteries, alternators, brakes Electronics—computer disc drives, data storage, iPods, DVDs, CDs, video recorders, consoles, video cameras, mobile phones Speakers, headphones, microphones, ceramic capacitors Wind-, hydro-, and tidal-power turbines Electrical motors, refrigeration, generators, cordless power tools Medical imaging Handheld wireless devices
(3) Phosphors: Y, Eu, *Tb*, *Gd*, Ce, La, *Dy*, Pr, Sc LCD televisions and monitors, plasma televisions and displays, mobile phone displays Energy efficient fluorescent lights, high-intensity lighting, LEDs, mercury-vapour lamps Phosphors—red (Eu), blue (Eu), and green (Tb)
(4) Polishing powders: Ce, La, Pr Television and computer screens—plasma, CRT Precision optical lenses and electronic components Silica wafers and chips, catalyst for self-cleaning ovens
(**5) Glass additives:** Ce, *Er*, *Gd*, *Tb*, La, Nd, *Yb*, Pm CRT screens to stabilise glass from cathode ray Glass—optical lenses, glass for digital cameras, tinted glass, UV-resistant glass, high-refractive index glass, fibre optics
(6) Ceramics: *Dy*, *Er*, Ce, Pr, Nd, *Gd*, *Ho*, La Colours in ceramics and glass —yellow (Ce), green (Pr), and violet (Nd)
(7) Energy storage: La, Ce, Pr, Nd, Pm Rechargeable NiMH batteries, battery electrodes, nuclear batteries
(8) Medical equipment: various REE MRI machines, X-ray imaging Surgical drills and tools, surgical lasers Electron beam tubes, computed tomography, neutron capture
(9) Other applications: Lasers—*Yb*, Y, *Dy*, *Tb*, Eu, Sm, Nd, Pr, *Gd*, *Ho*, *Er* Superconductors—*Gd*, Y Nuclear—Ce, *Er* Fertilisers—various REE High-technology alloys—*Yb*, Lu, *Er*, *Tb*, *Gd*, Eu, Sm, Nd, Pr, *Ho*, Sc

Ce = cerium, Dy = dysprosium, Er = erbium, Eu = europium, Gd = gadolinium, Ho = holmium, La = lanthanum, Lu = lutetium, Nd = neodymium, Pm = promethium, Pr = praseodymium, Sc = scandium, Sm = samarium, Tb = terbium, Tm = thulium, Y = yttrium, Yb = ytterbium.

Figure 1.7 (see opposite). Rare-earth elements are critical for many emerging technologies in a wide range of industries. Some of the major industries include: automobile, petroleum, glass, electronics, energy, solar, metallurgy, medical, space, defence, and entertainment.

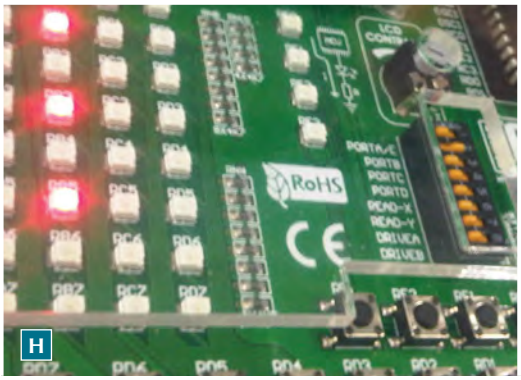

Source: A. Wikimedia Commons, photograph by Leaflet. **B.** Wikimedia Commons, photograph by David Monniaux. **C.** Wikimedia Commons, photograph by Aconcagua. **D.** and **E.** Courtesy of DOE/NREL. **F.** Wikimedia Commons, photograph by Rama. **G.** Australian Defence Force. **H.** Wikimedia Commons, photograph by Siegfried-A. Gevatter Pujals; LSIS Phillip Cullinan. **I.** Wikimedia Commons, photograph by Jan Ainali.

1.4. GLOBAL PRODUCTION AND RESOURCES

For thousands of years, the mining of metals has been an integral part of man's social and economic development. Mining was the second of man's major endeavours, agriculture being the first (Kennedy, 1990). Such metals as gold, silver, PGEs, nickel, copper, lead, zinc, iron, manganese, and cobalt were mined in Medieval Europe (~14th century), during ancient Roman (early AD) and Egyptian (~2500 BC) times, and there are examples of iron being used some 43 000 years ago during Prehistoric times (e.g., hematite was ground to red pigment ochres at the 'Lion Cave' in Swaziland: http://en.wikipedia.org/wiki/Mining#Prehistoric_mining:). Metals during the earliest phases of man's evolution were mainly used for decoration rather than for utility purposes because of their unique characteristics and rarity.

The commercial significance of the REE was not fully realised until the twentieth century with their global production gaining rapid momentum after the mid-1960s. The late evolution of the REE relative to other metals is attributed to the difficulty of isolating such metals with similar atomic structures and chemical properties, and separation analytical techniques that were critical to the accurate identification of the REE were only developed after the 1950s.

The mining of significant amounts of REE began in 1880 (Fig. 1.8). The REE were derived from monazite for the manufacture of incandescent mantles for the Welsbach gas light. Most of this period's production came from monazite in extensive beach sand deposits in Brazil, and from India when it entered the world market in 1911. Minor amounts of REE were also obtained from monazite-bearing alluvial placer deposits in Sri Lanka, and North America (Idaho and Carolina monazite belt), and later from Malaysia, Thailand, and Australia (described in Section 1.5). Both Brazil and India dominated the world REE market until the 1940s. Most of these deposits contained a high LREE component and were prone to high levels of radioactivity. Production from these small alluvial sources scaled down during the 1950s to 1960s (Fig. 1.8) at a similar time to when new 'hard-rock' sources of these elements were being found to be hosted with a number of minerals, including monazite, bastnäsite, and xenotime, and with ion-adsorption clays (Steinitz, 2010). Modest amounts of REE were produced from monazite veins, pegmatites, and carbonatite intrusions, and as by-products of uranium and niobium deposits. During the 1950s, REE-bearing veins in South Africa were an important source of REE, and China began recovering minor REE as a by-product of iron and steel production in Mongolia. In 1953, global demand of REO totalled just 1000 tonnes valued at $25 million compared to 2.7 million tonnes of copper worth $1.7 billion for that year. In the mid-1960s, the global production of REE changed dramatically with the introduction of the Mountain Pass deposit in the upper Mojave Desert of California. Discovered in 1949 and commencing production in 1952, the

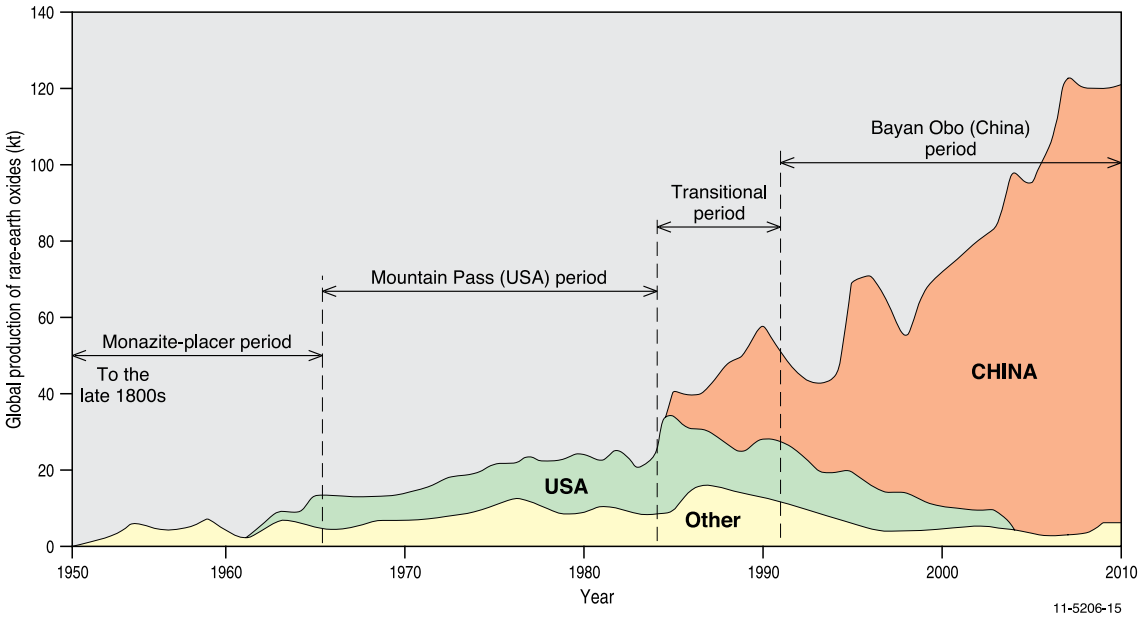

Figure 1.8. Global production of rare-earth oxides, 1950 to 2010. The relative minor production contribution from other countries is largely from monazite-bearing placers. Modified from Haxel et al. (2005).

world-class Mountain Pass deposit contains high concentrations of REE (8 to 12% REO) in a large carbonatite intrusion. The deposit is characterised by high levels of LREE along with much lower levels of radioactivity than the placer deposits. The carbonatite is a moderately dipping, tabular 1400 million years intrusive body associated with ultrapotassic alkaline plutons of similar age (Castor, 2008). From the mid-1960s to the 1990s, Mountain Pass was the world's largest source of REE. In the mid-1980s, it produced one third of the global supply of REO and 100% of the USA demand. Peak output was 20 000 tonnes of REO in 1990. Early development of the deposit was fast-tracked by the sudden demand for europium created by the commercialisation of colour televisions. By 1990, fourteen countries were mining REE with the USA the largest producer due to the contributions of the Mountain Pass deposit (Steinitz, 2010). During this period the USA was largely self sufficient in REE, but the USA soon became dependent on imports from other countries, and in particular China. After 1998, Mountain Pass REE sales declined substantially due to competition from China and to environmental constraints. Mountain Pass ceased mining in 2002. From 2000 onwards, more than 90% of REE required by the USA came from deposits in China. As of 2010, the Mountain Pass deposit had proven and probable reserves of 13 588 000 tonnes of 8.24% TREO, equating to 1 120 000 tonnes of contained metals. The Mountain Pass deposit is planned to resume production by 2012 (Long et al., 2010).

China's contribution to the global scene commenced in the mid-1980s when it actively supported research and development into the REE and it became a producer on the world stage. The industry initially grew rapidly in an unregulated fashion spawning businesses of all sizes from huge state-owned enterprises, through small businesses running REE processing plants to artisanal miners. By 1992, it had become the world's largest producer of LREE and HREE (Fig. 1.9; Appendices 3 and 4). The REE are mined very cheaply in China,

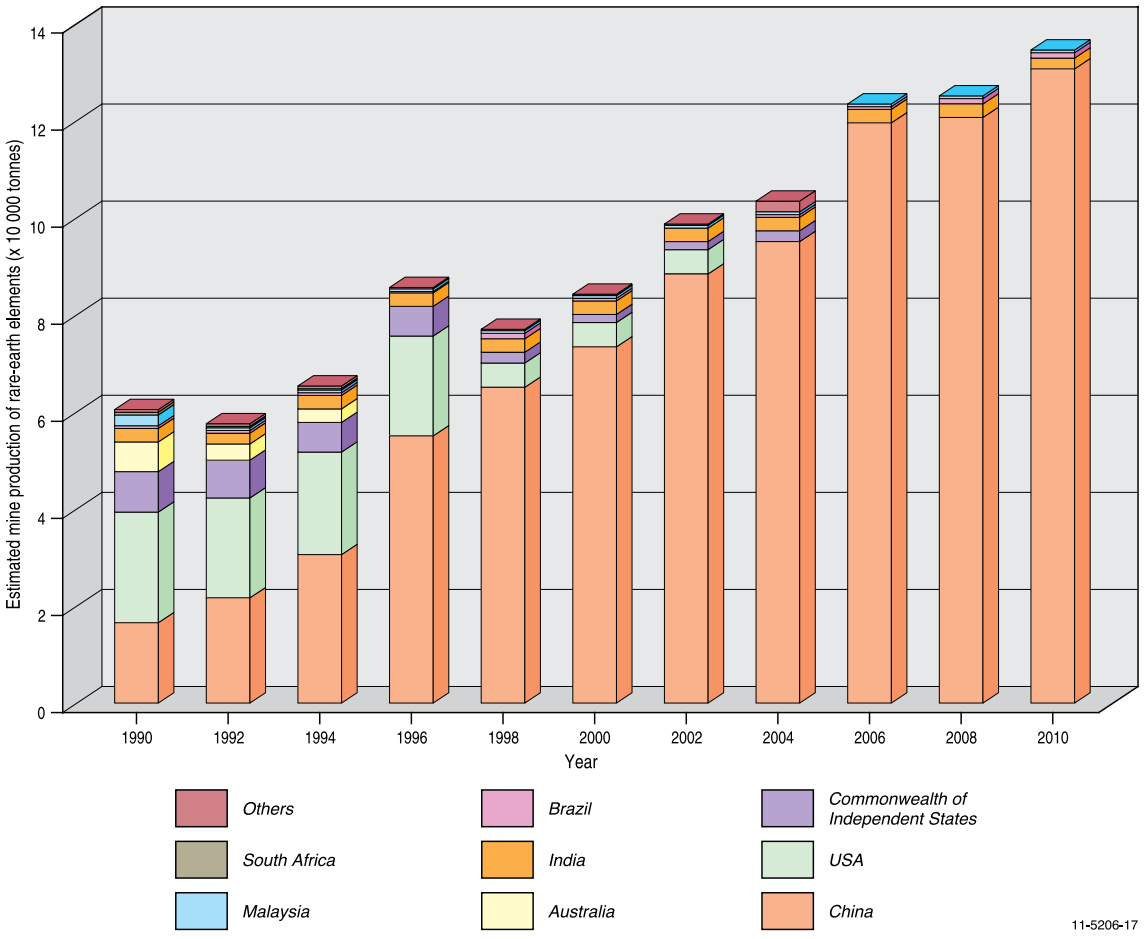

Figure 1.9. Estimated mine production of rare-earth elements for the major producing countries. Data from the United States Geological Survey Mineral Commodity Summaries, 1990 to 2011: Rare Earths (http://minerals.usgs.gov/minerals/pubs/commodity/rare_earths/). Others = other countries, including Madagascar, Sri Lanka, Thailand, Congo (Kinshasa), and Zaire.

either as a by-product of iron production at Bayan Obo, Inner Mongolia, or from lateritic REE-rich clays in southern China. The Bayan Obo iron-niobium-REE deposit (Drew et al., 1990; Fan et al., 2004) is the largest REE deposit in the world, as well as being a major producer of niobium and iron. It has geological similarities with both carbonatite REE deposits and to hydrothermal Cu-Au-U-REE iron-oxide deposits, such as Olympic Dam in South Australia and Kiruna in Sweden. Bayan Obo contains hydrothermal REE-enriched iron ores that have bastnäsite [(Ce, La, Y) CO_3F] and monazite as the main REE-bearing minerals. Resources at Bayan Obo total at least 48 million tonnes REO + Inferred + Subeconomic Resources) at grades of 3 to 6% REO. Another source of REE in China is ion-adsorption ores associated with lateritic clays developed on granitic and syenitic rocks in tropical southern China. Haxel et al. (2005) noted that these ores have the advantages of being enriched in the more valuable HREE and the metals are relatively easy to mine and extract. These deposits are currently the major supplier of these metals, as well as the focus of environmental controversy in China. By 2000, China accounted for 88% of world production, and some nine years later this has grown to 95.5%. Chinese leader Deng Xiaoping, recognised the strategic importance of these resources when he declared, "There is oil in the Middle East; there is rare earth in China" (Steinitz, 2010).

Global production trends of REE from 1950 to 2010 are summarised in Figure 1.8. Haxel et al. (2005) recognised four major global production periods, namely: a monazite-placer period starting in the late 1800s through to the mid-1960s; the Mountain Pass (USA) period commencing in 1965 and ending around 1984; a transitional period of mixed contributions from China, USA, and other countries from 1984 to 1991; and the Bayan Obo (China) period starting in 1991 and which continues to increase production to the present day. This figure clearly highlights the recent global dominance of China's impact at the expense of REE production from other countries including, most notably, the USA.

As mentioned above, China dominates the global REE scene, accounting for about 95% (129 000 tonnes TREO: Table 1.5; Figure 1.9) of total production in 2009, while both India and the Commonwealth of Independent States (former members of the Soviet Union) contributed about 2%. In 2010, China holds 55 million tonnes (48.3%) of the world's economic reserves of TREO, followed by the Commonwealth of Independent States with 19 million tonnes (16.7%) and the USA with 13 million tonnes (11.4%). Australia's global REE impact in 2009 was negligible, with no recorded production and total Economic Demonstrated Resources (EDR) in 2010 amounting to 1.65 million tonnes of REO (1.45%).

Table 1.5. World production (2009) and resources (2010) of rare-earth oxides (modified from Cordier, 2011).

	Production (2009)		Resources (2010)	
	TREO (tonnes)	Share (%) Excluding other countries	TREO (tonnes)	Share (%)
Australia[1]	0	0	1 650 000	1.45
Brazil	550	0.41	48 000	0.04
China	129 000	95.48	55 000 000	48.32
Commonwealth of Independent States[2]	2500	1.85	19 000 000	16.69
India	2700	2.00	3 100 000	2.72
Malaysia	350	0.26	30 000	0.03
United States of America	0	0	13 000 000	11.42
Other countries[3]	NA	NA	22 000 000	19.33
Total	135 100	100	113 828 000	100

[1] Economic Demonstrated Resources for Australia as estimated by Geoscience Australia.
[2] Production for Commonwealth of Independent States (former members of the Soviet Union) from Long et al. (2010).
[3] Other countries include South Africa, Sri Lanka, and Thailand.
NA = Not Available.

Figure 1.10 shows the relationships between the global supply (histograms) and demand (green graph) of REE for the period 1992 to 2010. Predicted trends are also shown up to 2014. In general, there has been a fairly consistent increase for both supply and demand for the REO until they experienced a significant decline during the global financial crisis, falling by a third in 2009. However, demand has since rebounded and the number of applications continues to soar. Current demand for REE is forecast to maintain a strong growth from the current level of around 124 000 tonnes per annum (tpa) REO, which has an estimated value of US$1.5 billion, to about 175 000 tpa in 2014 (Kingsnorth, 2010a). This forecasted rapid increase in demand is shown by the dashed green line in Figure 1.10. The most significant increases in demand are predicted for hybrid cars, followed by petroleum catalyst, glass manufacturing and polishing, and multi-level electronic components. Expansion in new potential technologies include tidal power generation turbines, hydro power generation, magnetic refrigeration, and eBikes (Steinitz, 2010). The main global consumers of REE are China, USA, Japan, Korea, and Thailand with China reportedly accounting for about 60% of the world's consumption.

The central Chinese government has recently imposed production and export restrictions, adding upward pressure on prices for REE and contributing to incentives for development of REE resources outside China. Galaxy Resources Limited reported (http://www.galaxyresources.com.au/documents/DocGXY-151GalaxyCompletesReviewofPontonRareEarthsProject110111_000.pdf) in late 2010, that the Chinese Ministry of Commerce announced a 35% reduction in the export quota for the first half of 2011, compared to the corresponding period in 2010. This coincided with the launch of a nationwide crackdown on illegal mining of REE in China. The Chinese Government has also encouraged large companies to consolidate the country's REE inventory to prevent the resource from being undervalued. With China's moves to reduce export quotas, and stricter controls on illegal mining, several of the REE (e.g., neodymium) significantly increased in price. Consequently, over 200 REE mining projects throughout the world are being closely assessed, and in many cases re-examined, for potential mining operations, including the Mountain Pass REE deposit in the United States.

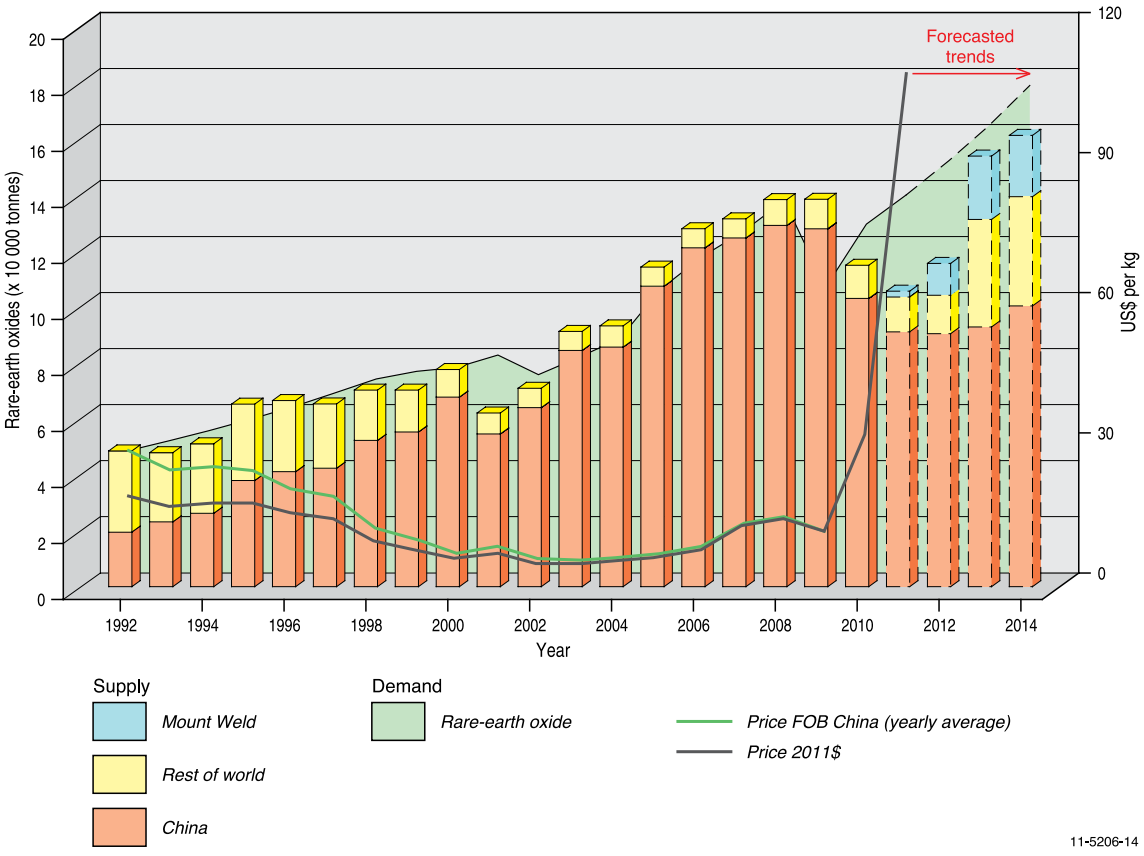

Figure 1.10. Historical and forecasted global supply, demand, and pricing trends of rare-earth oxides, 1992 to 2014. Modified from Lynas Corporation Limited (2011).

1.5. AUSTRALIA'S RESOURCES

Geoscience Australia estimated in 2010 that Australia's REO resources amounted to 1.65 million tonnes of Economic Demonstrated Resources (EDR: Appendix 5), 0.37 million tonnes Paramarginal Resources, and 34.48 million tonnes in the Submarginal Resources categories (Miezitis, 2010: Appendix 5). There is a further 24.56 million tonnes in the Inferred Resources category[3]. About 53 million tonnes of the Submarginal and Inferred Resources are in the Olympic Dam iron oxide-copper-gold deposit in South Australia (predominantly 0.2% La and 0.3% Ce) and are not currently economic. Small quantities of scandium (4620 t Subeconomic and 1690 t Inferred Sc) were also reported in 2010. In addition, about 4160 tonnes of Paramarginal Resources and 51 980 tonnes of Inferred Resources of scandium were reported as REE.

Very significant resources of REE are contained in the monazite component of heavy-mineral sand deposits, which are mined for their ilmenite, rutile, leucoxene, and zircon content. Monazite is a REE-thorium-bearing phosphate mineral found within heavy-mineral sand deposits in Australia. Geoscience Australia estimates Australia's monazite resources to be in the order of 6.1 million tonnes (Miezitis, 2010). Assuming the REO content of monazite to be about 60%, the heavy mineral deposits could hold a REO resource of around 3.65 million tonnes. Currently, extraction of REE from monazite is not viable because of the cost involved with the disposal of thorium (Th) and uranium (U) present in the monazite.

In a global context, Australia is well placed in the near future to have a significant impact on the potential supply of REO. Figure 1.11 shows that the Mount Weld (WA), Nolans Bore (NT), and Dubbo Zirconia (NSW) projects are well advanced with their development phases (at least to basic engineering status), and in the case of Mount Weld, of high *in situ* commodity value, compared to other operations in the USA, Africa, and Canada. In addition, the Dubbo Zirconia project despite its smaller relative production volume and value, contains the highest percentage (~60%) of the more valuable HREO relative to the other projects shown in Figure 1.12. The other eight projects shown in Figure 1.12 have HREO components less than 17%, with Mount Weld and Nolans Bore having HREO components of 3% and 4%, respectively.

Figures 1.13 and 1.14 show some of the concentration and kiln components at the Mount Weld operations in Western Australia and Malaysia. This planned engineering infrastructure timeframe for Mount Weld is highlighted in Figure 1.11.

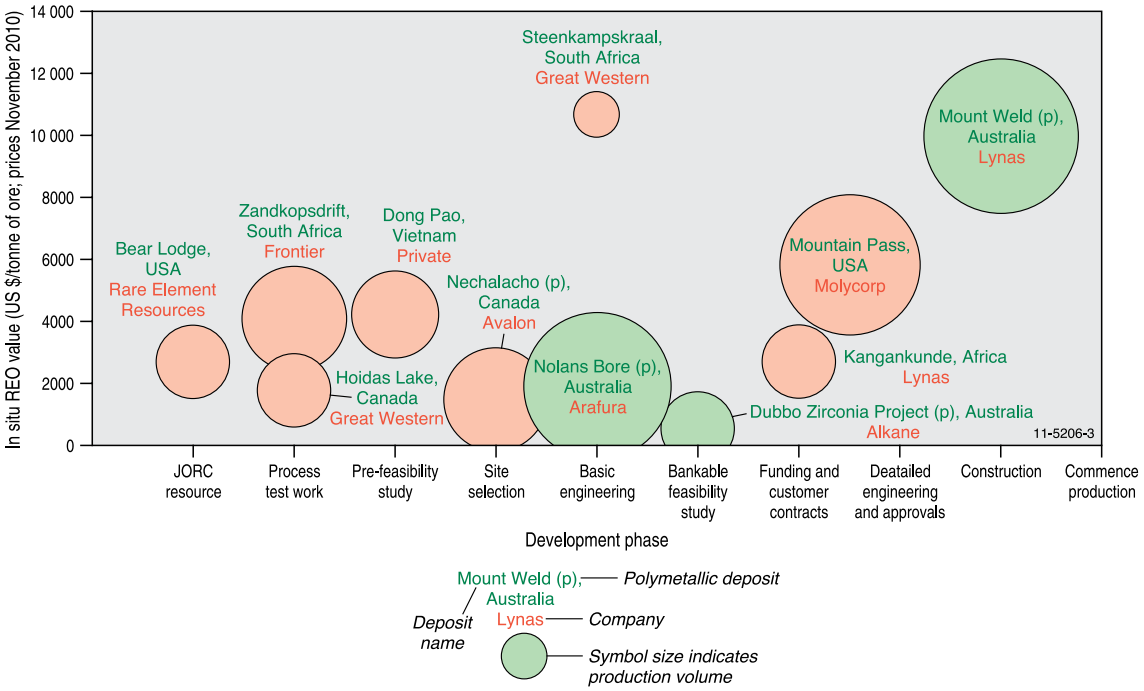

Figure 1.11. Relative value and development phase of major rare-earth-element projects. Australian projects are indicated by green spheres, and other projects by orange spheres. Modified from Lynas Corporation Limited (2011).

[3] Definitions of these resource terms are explained in Appendix 5

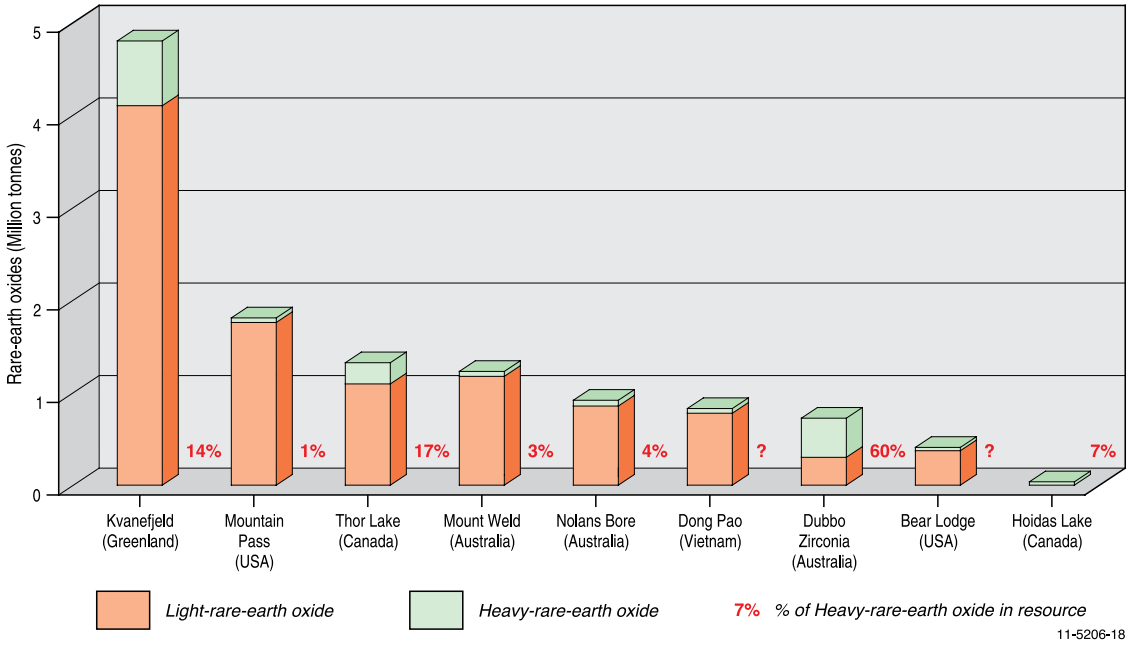

Figure 1.12. Relative percentage (shown in red numbers) of the heavy-rare-earth oxide component in deposits from Australia and elsewhere. Data from the Industrial Minerals Company of Australia Proprietary Limited (IMCOA).

1.6. EXPLORATION HISTORY OF RARE-EARTH ELEMENTS IN AUSTRALIA

Small-scale production of REE has taken place in Australia although information records on this activity are incomplete. REE-bearing minerals (monazite and xenotime) were produced as heavy mineral by-products from beach sand mining and as a very minor contribution from tin mining mainly in Tasmania. Australia was formerly the world's largest producer of monazite, almost entirely from beach sand deposits in Western Australia, New South Wales, and Queensland (Harben and Kužvart, 1996). During the 1970s and 1980s, Australia produced about 12 000 tonnes of monazite annually and, intermittently, about 50 tonnes per year of xenotime, largely from Western Australia as a by-product of beach sand mining (Cassidy et al., 1997). Production peaked in 1985, with 18 735 tonnes of monazite being mined. Australia's production of monazite (265 000 tonnes from 1952 to 1995) accounted for more than 50% of the world's total production (Towner et al., 1987).

Up to the mid-1990s, Australia was producing and exporting significant quantities of monazite, principally to Europe (Appendix 6). For example, in 1987, Australia supplied about 70% of the concentrates processed by western world producers. Some 98% of all monazite sold from Australia was exported to France. Cassidy et al. (1997) note that environmental issues

Figure 1.13. Filer press and thickener area at concentration plant, Mount Weld Project, Western Australia. Photographs provided by Georgia Bunn (Lynas Corporation Limited: http://www.lynascorp.com/)

Figure 1.14. Installation of rotary kilns, Mount Weld Project, Malaysia. Photographs provided by Georgia Bunn (Lynas Corporation Limited: http://www.lynascorp.com/)

in Europe were going to have an abrupt impact on the Australian REE industry. In March 1994, because of the increased sensitivity in France to toxic and radioactive waste disposal, a major French chemical and pharmaceutical company (Rhône-Poulenc) closed its monazite processing plant since it was unable to obtain a permit for a disposal site. In addition, the high disposal cost of thorium was considered prohibitive for the extraction of REE from the monazite. Consequently, imports of monazite were stopped, which in turn terminated Australian monazite mining activities in 1995. Monazite fractions from beach sand mining were subsequently returned to the mine site.

Appendix 6 provides annual statistics for the production of monazite in Australia for the period 1980 to 1995. Further historical production statistics can be found in Barrie (1965), Cassidy et al. (1997), and Towner et al. (1996).

During the latter half of the last century, a number of minor occurrences of REE were found in a variety of hard-rock environments throughout Australia. Such occurrences include the uranium deposits of Mary Kathleen in Queensland and Radium Hill in South Australia, and scandium was reported in some Australian tin (cassiterite) and tungsten (wolframite) deposits (Barrie, 1965). One of the earliest documented examples of hard-rock mining of REE in Australia is from a pegmatite in the Cooglegong region near Marble Bar, Western Australia. Minor amounts of yttrium-bearing ores were obtained from the pegmatite in 1913, but as typical of these small vein- and dyke-like deposits, production was restricted to only a few years due to low grades and/or tonnage. Barrie (1965) reports that ~1 ton of gadolinite was produced in 1913, and another similar amount of the same mineral is said to have been produced in 1920. With the exception of the beach sand mining described above, and the minor REE contributions from Cooglegong and monazite concentrates from Tasmania, there has been no historical commercial production of REE in Australia. However, in recent years, considerable exploration interest has been generated by much larger deposits associated with carbonatite (Mount Weld, WA) and trachyte (Toongi, NSW) intrusions, and apatite-bearing veins (Nolans Bore, NT). For example, the Mount Weld deposit has exceptionally high grades up to 13.8% REE and is the world's richest lanthanide deposit. Australia's impact on the global scene of REE from hard-rock sources has historically been insignificant, however, this will change when new deposits, such as Mount Weld and Nolans Bore, commence production.

Appendix 7 summarises the exploration activities and major events, both historical and current, for the REE industry in Australia.

How much are rare-earth elements worth?

The prices of REO prices show significant variance in the relative market value for selected elements. There have been dramatic increases in metal prices for the REO, with cerium oxide (4340%), lanthanum oxide (3940%), and samarium oxide (3235%) recording some of the largest increases since 2007. The prices are dependent on the purity level, which is largely set by the specifications for each application. The table below shows the average annual price for a 'standard' 99% purity of individual elements. Prices are quoted in US$/kg.

Prices US$/kg					
Rare-earth oxide	**2007**	**2008**	**2009**	**2010**	**02/05/2011**
Lanthanum oxide	3.44	8.71	4.88	52.49	139.00
Cerium oxide	3.04	4.56	3.88	52.62	135.00
Neodymium oxide	30.24	31.90	19.12	81.38	225.00
Praseodymium oxide	29.05	29.48	18.03	78.62	208.00
Samarium oxide	3.60	5.20	3.40	36.58	120.00
Dysprosium oxide	89.10	118.49	115.67	287.85	705.00
Europium oxide	323.90	481.92	492.92	611.54	1200.00
Terbium oxide	590.40	720.77	361.67	620.38	1200.00

Metal prices from Lynas Corporation Limited at: http://www.lynascorp.com/page.asp?category_id=1&page_id=25

CHAPTER TWO

GEOCHEMISTRY OF RARE-EARTH ELEMENTS—BEHAVIOUR IN THE GEOCHEMICAL CYCLE

2.1. GENERAL CHEMISTRY

The REE are a group of 17 metals that include the 15 lanthanide elements (lanthanum to lutetium) and two other elements scandium and yttrium which have chemical similarities to the lanthanides. There is some confusion in the scientific literature about the status of scandium in this group. Wedepohl (1970) and some other researches (e.g., Henderson, 1984; Rollinson, 1993) do not include scandium, but in more recent reviews (e.g., Walters et al., 2010: British Geological Survey; IUPAC: http://old.iupac.org/dhtml_home.html) scandium is often included in the REE group. In this report scandium is regarded as one of the REE.

Although the group is called REE, the abundances of many of these elements are not rare compared to other elements. For instance, cerium, lanthanum, yttrium, and neodymium are more abundant in igneous rocks in the upper earth's crust compared to lead, cobalt, tin, molybdenum, silver, and tungsten (Henderson, 1984; Wedepohl, 1970). Cerium is the most abundant of the naturally occurring REE (Table 1.1).

The similar chemical behaviours of the REE are largely determined by the fact that they all (except scandium) form stable trivalent ions of similar size (Table 2.1). Only a small number of the REE exist with an oxidation (valence) state other than +3, with those ions of geological significance being Ce^{+4} and Eu^{+2} (Rollinson, 1993). Small differences in the chemical behaviours of the REE (especially of the lanthanides) are a consequence of the small and steady decrease in the ionic size with increasing atomic number in both six- and eight-fold co-ordination (Fig. 2.1; Table 2.1). Typically the elements with low atomic numbers and masses (lanthanum to samarium) are termed LREE, and those with higher atomic numbers and masses (gadolinium to lutetium) are classified the HREE. Less commonly the middle members of the group (from about promethium to holmium) are known as the middle-rare earths (MREE; Henderson, 1984). Rollinson (1993) groups elements from samarium to holmium as middle rare earth elements.

The ratio defined by ionic charge/ionic radius of the element is used to distinguish geochemically compatible and incompatible elements (Fig. 2.2). This ratio is described as field strength or ionic potential. Small highly charged cations are known as high-field-strength

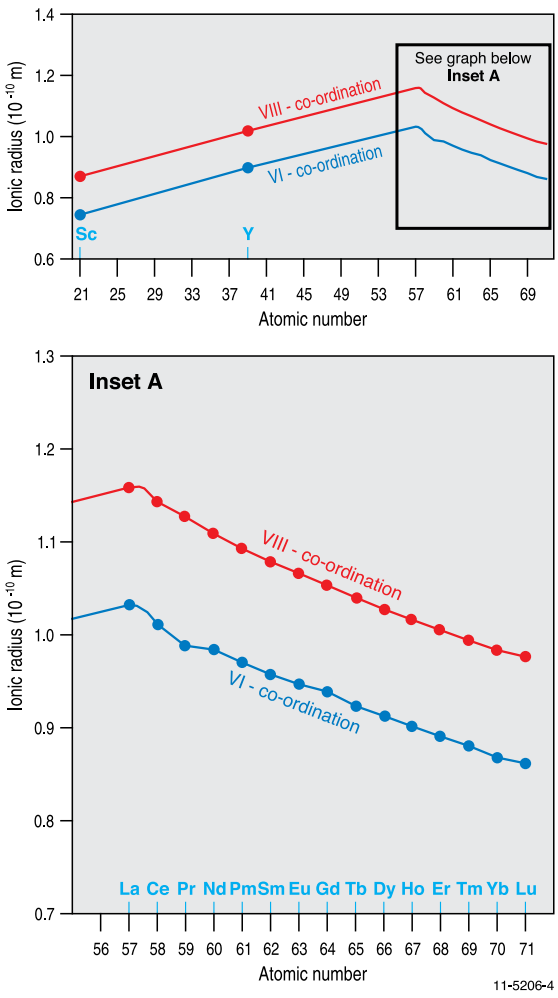

Figure 2.1. Ionic radii versus atomic number plot of rare-earth elements. Ionic radii data from Shannon (1976).

(HFS) cations (with ionic potential >2). And large cations with a small charge are known as low-field-strength (LFS) cations (ionic potential <2). They are also known as large-ion-lithophile elements (LIL). Elements with ionic potential <2 (low charge and large size) tend to be compatible, whereas those with ionic potential >2 (high charge and small size) are more incompatible. Scandium, yttrium, and the lathanides belong to the group of HFS ions, and hence tend to be incompatible (Fig. 2.2). The REE display lithophile behaviour since they concentrate predominantly in silicate minerals rather than in metal- or sulphide-bearing minerals (Henderson, 1984).

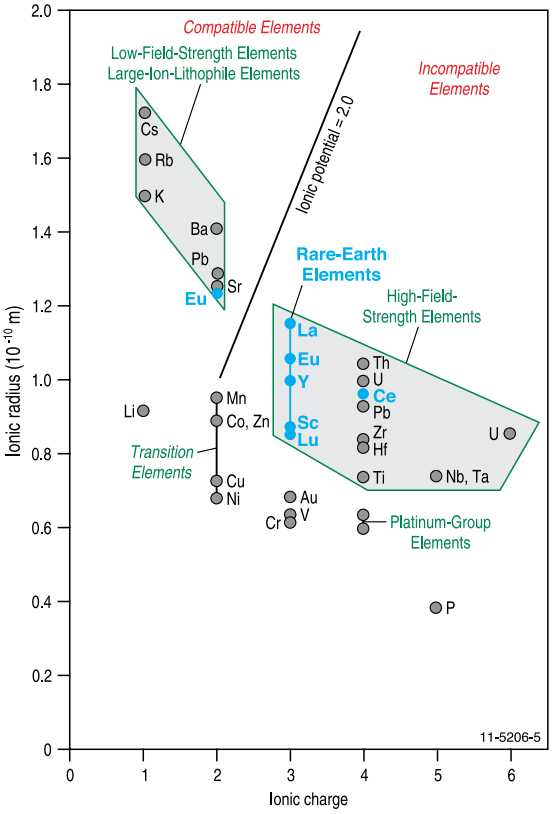

Figure 2.2 (shown right). Ionic radii versus ionic charge plot of trace elements showing that the rare-earth elements (except Eu^{+2} and Ce^{+4}) are incompatible elements. Modified from Rollinson (1993).

Table 2.1. Ionic radii (in 10^{-10} metres or angstrom units) of the rare-earth elements (Shannon, 1976).

Atomic number	Element	Symbol	Valency	VI co-ordination	VIII co-ordination
21	Scandium	Sc	+3	0.745	0.870
39	Yttrium	Y	+3	0.900	1.019
57	Lanthanum	La	+3	1.032	1.160
58	Cerium	Ce	+3	1.010	1.143
58	Cerium	Ce	+4	0.870	0.970
59	Praseodymium	Pr	+3	0.990	1.126
60	Neodymium	Nd	+3	0.983	1.109
61	Promethium	Pm	+3	0.970	1.093
62	Samarium	Sm	+3	0.958	1.079
63	Europium	Eu	+3	0.947	1.066
63	Europium	Eu	+2	1.170	1.250
64	Gadolinium	Gd	+3	0.938	1.053
65	Terbium	Tb	+3	0.923	1.040
66	Dysprosium	Dy	+3	0.912	1.027
67	Holmium	Ho	+3	0.901	1.015
68	Erbium	Er	+3	0.890	1.004
69	Thulium	Tm	+3	0.880	0.994
70	Ytterbium	Yb	+3	0.868	0.985
71	Lutetium	Lu	+3	0.861	0.977

2.2. ABUNDANCES OF RARE-EARTH ELEMENTS ON EARTH

Natural abundances of REE are often shown in geochemical plots in which the concentration in parts per million (ppm) of the element is plotted against the atomic number of the element (Fig. 1.2). However, REE with even atomic numbers are more stable and hence more abundant than REE with odd atomic number (for instance, concentration of lanthanum is lower than the concentration of cerium). As a result, abundance plots for the REE show zig-zag patterns (Fig. 1.2). Therefore the concentrations of REE are often normalised (concentration of an element in a mineral or a rock is divided by the abundance of the same element in a standard) relative to a standard such as a meteoritic chondrite. This normalisation fulfils two functions: firstly it eliminates the variation between odd and even atomic numbers, and secondly it allows to identify any fractionation amongst the various REE in the sample. This is because REE in chondrites do not show fractionation between LREE and the HREE. One complication associated with chondrite-normalised plots is that chondritic meteorites are quite variable in composition and no standardised values have been adopted to date. Some researchers use 'average chondrite', whilst others select C1 chondrites as standards.

2.2.1. The mantle

The principal division of the Earth into core, mantle, and crust is the result of principally two processes: the formation of a metal core very early in the history of the Earth (~30 million years after the beginning of the solar system; and the formation of the crust by partial melting of the silicate mantle (Palme et al., 2007). The mantle is thought to be the Earth's largest chemical reservoir constituting ~82% of its total volume and ~65% of its mass. It comprises most of the silicate Earth, extending from the base of the crust (average thickness of ~40 km) to the top of the metallic core at ~2900 km depth (Bennett et al., 2003).

Table 2.2. Rare-earth-element abundances (in ppm) of chondrite, primitive mantle, and continental crust.

Element	C1	Primitive mantle	Primitive mantle	Lower crust	Archean upper crust	Middle crust	Upper crust	Total crust
Sc	5.9	17.3	16.5	31	14.0	19	14	21.9
Y	1.6	4.55	4.37	16	18.0	20	21	19
La	0.237	0.7080	0.6860	8	20.00	24	31	20
Ce	0.613	1.8330	1.7860	20	42.00	53	63	43
Pr	0.0928	0.2780	0.2700	2.4	4.90	5.8	7.1	4.9
Nd	0.457	1.3660	1.3270	11	20.00	25	27	20
Sm	0.148	0.4440	0.4310	2.8	4.00	4.6	4.7	3.9
Eu	0.0563	0.1680	0.1620	1.1	1.20	1.4	1	1.1
Gd	0.199	0.5950	0.5710	3.1	3.40	4	4	3.7
Tb	0.0361	0.1080	0.1050	0.48	0.57	0.7	0.7	0.6
Dy	0.246	0.7370	0.7110	3.1	3.40	3.8	3.9	3.6
Ho	0.0546	0.1630	0.1590	0.68	0.74	0.82	0.83	0.77
Er	0.16	0.4790	0.4650	1.9	2.10	2.3	2.3	2.1
Tm	0.0247	0.0740	0.0717	0.24	0.30	0.32	0.3	0.28
Yb	0.161	0.4800	0.4620	1.5	2.00	2.2	2	1.9
Lu	0.0246	0.0737	0.0710	0.25	0.31	0.4	0.31	0.3
Total Y to Lu	4.08	12.0567	11.6477	72.55	122.92	148.34	169.14	125.15
Total LREE	1.60	4.80	4.66	45.30	92.10	113.80	133.80	92.90
Total HREE	0.91	2.71	2.62	11.25	12.82	14.54	14.34	13.25
Total HREE and Y	2.48	7.26	6.99	27.25	30.82	34.54	35.34	32.25
Ratio of LREE/HREE	1.77	1.77	1.78	4.03	7.18	7.83	9.39	7.01
Source	1	2	3	4	5	4	4	4

Source: 1. McDonough and Sun (1995); 2. McDonough et al. (1992); 3. Palme et al. (2007); 4. Rudnick et al. (2003); 5. Taylor and McLennan (1995).
The LREE include La to Eu, and the HREE include Gd to Lu.

The composition of the primitive mantle (the mantle before the onset of crust formation) has been estimated based on indirect approaches, such as: (a) analogy with chondritic meteorites; (b) critical evaluation of data derived from ultramafic mantle samples; and (c) chemical and petrological models of peridotite-basalt melting relations (pyrolite model; see discussions in Frey, 1984; McDonough et al., 1992; McDonough and Sun, 1995). The REE compositions of C1 chondrite and primitive mantle are summarised in Table 2.2.

The lower mantle is made of magnesium- and calcium-bearing perovskite ($MgTiO_3$ and $CaTiO_3$) and magnesiowustite [(Mg,Fe)O], whereas the upper mantle is largely composed of silicates (olivine, pyroxene, and garnet; Righter et al., 2003). According to Righter et al. (2003), fractionation of these minerals to form an initial magma could have controlled the concentrations of REE in the upper mantle. Similarly, as magnesium-perovskite/melt partition coefficients of samarium and neodymium are slightly different, the formation of magnesium-perovskite could have led to their fractionation from one another, thus affecting the evolution of neodymium isotopes in the mantle. It has been shown that the Lu/Hf and Sm/Nd ratios in some terrestrial basalt can be explained by their derivation from garnet- or majorite-bearing mantle (Righter et al., 2003).

There is some disagreement about the composition of the upper and lower mantle, although it is generally believed that the bulk composition of the mantle above the 660 km discontinuity (upper mantle) is similar to that of the lower mantle (McDonough and Sun, 1995). The analysis of REE abundances in upper mantle rocks, however, establishes that the upper mantle is heterogeneous in REE content, especially in LREE, which range from 0.001 to 25 times the LREE content of ordinary chondrites. The variation in HREE content is much less, ranging from 0.1 to 5 times ordinary chondrite (Frey, 1984).

2.2.2. The crust

The oceanic crust is thin (~7 km on average), is composed of dense rock types such as basalt, and is young (≤200 Ma old). In contrast, the continental crust is thick (~40 km on average), composed of highly diverse rocks with an average intermediate or 'andesitic' bulk composition (Taylor and McLennan, 1985).

Although the continental crust comprises only about 0.35% of the mass of the Earth, it contains substantial amounts (exceeding 30% of the bulk Earth budget) of the most incompatible elements, including the REE (Taylor and McLennan, 1985). Seismically the continental crust is interpreted to comprise three (upper, middle, and lower) layers. The upper crust, which is more readily accessible to sampling is shown to have a granodioritic bulk composition, and to be rich in incompatible elements and generally depleted in compatible elements (Rudnick et al., 2003). The middle crust contains a large variety of rocks and the estimated bulk composition of the middle crust is characterised by many uncertainties. Studies of crustal cross-sections show that the middle crust to be dominated by felsic gneisses of tonalitic bulk composition (Rudnick et al., 2003). Like the middle crust, the lower crust also contains a wide variety of rocks. Despite large uncertainties, the lower crust has a bulk mafic composition (Rudnick et al., 2003). The bulk REE compositions of upper, middle, and lower continental crusts are summarised in Table 2.2. The method of estimation and assumptions are described in Rudnick et al. (2003). The table also shows the bulk REE composition of the Archean upper crust estimated by Taylor and McLennan (1985).

The REE display show systematic variations in their concentrations in Table 2.2. The total concentration of REE increases from between 11 to 12 ppm in the primitive mantle to ~170 ppm in the upper crust. The upper crust is more enriched in REE than the middle and lower crusts. The concentration of LREE and HREE (including Y) also increases in the sequence from primitive mantle to lower crust to middle crust to upper crust. The ratio of LREE and HREE also follows the same pattern. The evolutionary processes involved with the crust have therefore concentrated REE in the crust.

2.3. RARE-EARTH-ELEMENT CONCENTRATIONS IN MAJOR ROCK TYPES

2.3.1. Igneous rocks

REE concentrations of major igneous rock types are summarised in Table 2.3. Both felsic and alkaline rocks show significant enrichment in REE compared to mafic rocks. The carbonatite melts represent extreme enrichment in REE and some orthomagmatic and magmatic hydrothermal deposits of REE are genetically associated with carbonatite (see following section for details). All rocks are more enriched in LREE relative to HREE. The enrichment with respect to LREE is even greater in carbonatites. Scandium on the other hand is enriched in basalt; its concentration in basaltic rocks is 4 to 10 times higher than in felsic and alkaline rocks (Table 2.3).

Table 2.3. Rare-earth-element abundances (in ppm) of some important igneous rocks.

Element	C1	Basalt	Granite	Syenite	Carbonatite, Phalaborwa, South Africa	Carbonatite, Oka, Canada
Sc	5.900	35.00	8.00	3.00		
Y	1.570	30.00	40.00	20.00		
La	0.237	10.00	55.00	70.00	213.00	1640.00
Ce	0.613	30.00	90.00	161.00	397.00	1450.00
Pr	0.093	4.00	10.00	15.00	58.00	144.00
Nd	0.457	20.00	35.00	65.00	249.00	494.00
Sm	0.148	5.00	9.00	18.00	47.70	64.30
Eu	0.056	1.50	1.00	2.80	11.80	17.39
Gd	0.199	6.00	8.00	18.00	28.60	40.90
Tb	0.036	0.80	1.50	2.80	3.08	4.97
Dy	0.246	4.00	6.50	13.00	12.90	26.30
Ho	0.055	1.00	2.00	3.50	2.13	5.00
Er	0.160	3.00	4.50	7.00	4.31	11.87
Tm	0.025	0.50	0.60	0.60		
Yb	0.161	2.50	4.00	7.00	1.57	9.52
Lu	0.025	0.50	0.70	2.10	0.15	1.29
Total Y to Lu	4.080	118.80	267.80	405.80	1029.24	3909.54
Total LREE	1.604	70.50	200.00	331.80	976.50	3809.69
Total HREE	0.91	18.3	27.8	54.0	52.74	99.85
Total HREE and Y	2.476	48.30	67.80	74.00	52.74	99.85
Ratio of LREE/HREE	1.77	3.85	7.19	6.14	18.52	38.15
Source	1	2	2	3	4	4

Source: 1. McDonough and Sun (1995); 2. Krasukopf (1989); 3. Turekian and Wedepohl (1961); 4. Hornig-Kjarsgaard (1998).
The LREE include La to Eu, and the HREE include Gd to Lu.

The REE patterns of igneous rocks are controlled by the concentrations of REE in the source rocks from which they are derived and the crystal-melt equilibria during their evolution. The average mineral/melt partition coefficients of REE provide a guide to understanding the behaviour of REE in melts. These coefficients depend on the ionic radii and the charge of the REE (see Section 2.1), temperature, pressure, oxygen fugacity, and composition of the system (see Henderson, 1984; 1996) for more detailed discussions). For the REE, the melt composition is the most significant single factor controlling partition coefficients. Experiments show that partition coefficients of all lanthanide REE for the same mineral are by an order of magnitude higher in a rhyolitic melt than for andesitic and basaltic melts (Figs 2.3 and 2.4; Table 2.4) suggesting that all lanthanide REE are more compatible in rhyolitic melts. In general, LREE are less compatible than HREE. The only exception is plagioclase, for which the partition coefficients show opposite trends; the HREE are less compatible than the LREE (Figs 2.3 and 2.4; Table 2.4). Compatibility with minerals increase in the sequence orthopyroxene–clinopyroxene–hornblende–sphene–garnet. In rhyolitic melts, pyroxene and hornblende show a small, but noticeable negative europium anomaly. Plagioclase shows a distinct positive europium anomaly for rhyolitic, basaltic, and andesitic melts.

The behaviour of europium in a felsic melt is controlled chiefly by feldspar because Eu^{+2} is compatible in feldspar in contrast to trivalent REE. Hence crystallisation and

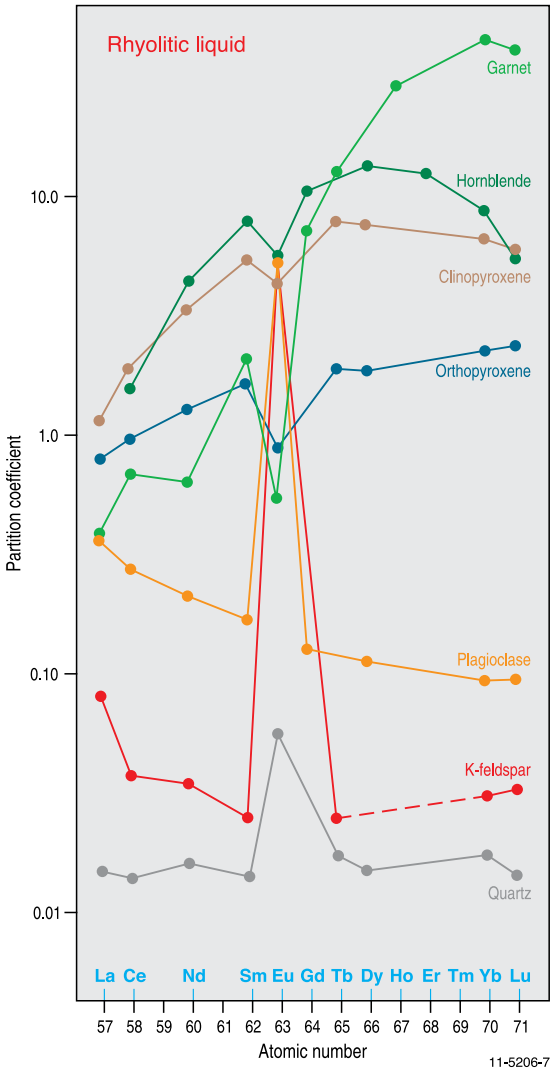

Figure 2.3. Mineral/melt partition coefficients of rare-earth elements for minerals in rhyolitic melt. Modified from Rollinson (1993).

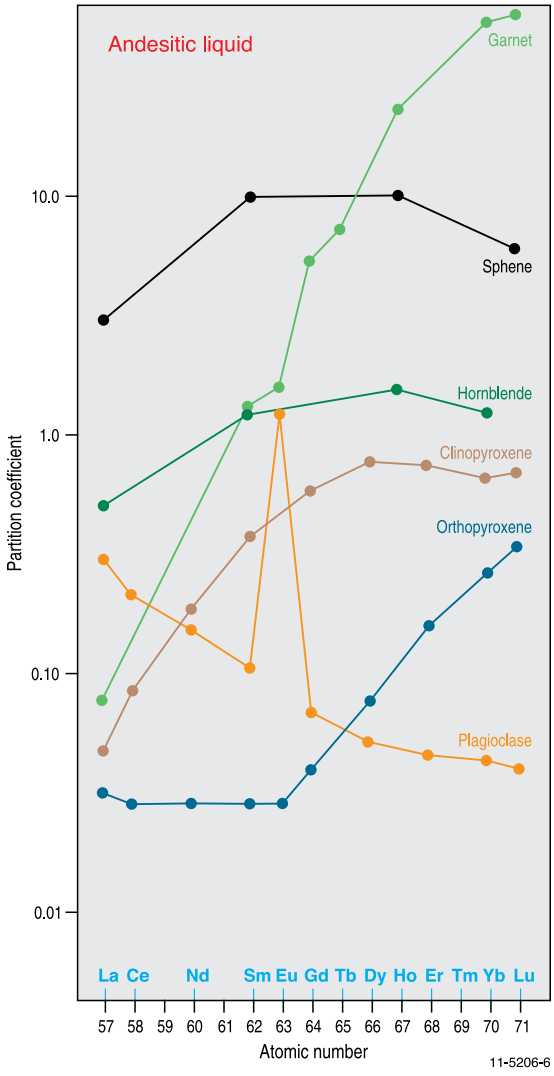

Figure 2.4. Mineral/melt partition coefficients of rare-earth elements for minerals in andesitic melt. Modified from Rollinson (1993).

removal of feldspar from a felsic melt creates a negative europium anomaly in the melt. A similar negative europium anomaly is generated during partial melting of a rock in which the feldspar is retained in the source rock. Other silicate minerals, such as hornblende, clinopyroxene, orthopyroxene, and garnet, can also create a negative europium anomaly in felsic melts. Hornblende is also the main control on the enrichment of the MREE (Sm to Ho) relative to the LREE and HREE (Rollinson, 1993). As the mineral/melt partition coefficients for hornblende are very large in felsic and intermediate melts, even a moderate amount of hornblende in the melt-rock systems can affect the concentration of MREE (Rollinson, 1993).

The fractionation of the LREE relative to HREE can be caused by the presence of olivine, orthopyroxene, and clinopyroxene because mineral/melt partition coefficients for these minerals increase by an order of magnitude from lanthanum to lutetium. The presence of garnet and hornblende (to a lesser extent) in the source rock will most likely cause extreme depletion of HREE relative to the LREE in the partial melt because of a large variation in the mineral/melt partitioning coefficient (Figs 2.3 and 2.4).

The presence of accessory minerals, such as sphene, zircon, allanite, apatite, and monazite can strongly influence the REE concentration of the melt because of the very high mineral/melt partitioning coefficients. Zircon can cause depletion in the HREE, sphene and apatite can partition MREE relative to the LREE and HREE, and monazite and allanite can cause depletion in the LREE (Rollinson, 1993).

Table 2.4. Average mineral-melt partitioning coefficients[1] of rare-earth elements of some important minerals (Henderson, 1984).

Element	Clinopyroxene (basaltic, andesitic rocks)	Clinopyroxene (dacitic and rhyolitic rocks)	Plagioclase (basaltic, andesitic rocks)	Plagioclase (dacitic and rhyolitic rocks)	Garnet (basaltic, andesitic rocks)	Garnet (dacitic and rhyolitic rocks)
La	0.08	0.6	0.14	0.32	0.05	0.39
Ce	0.34	0.9	0.14	0.24	0.05	0.62
Nd	0.6	2.1	0.08	0.19		0.63
Sm	0.9	2.7	0.08	0.13	0.6	2.2
Eu	0.9	1.9	0.32	2	0.9	0.7
Gd	0.9	3.1	0.1	0.16	3.7	7.7
Tb	1	3		0.15	5.6	12
Dy	1.1	3.3	0.09	0.13		29
Ho					19	28
Er	1		0.08	0.05		43
Tm	1.1			0.1		
Yb	1	2.1	0.07	0.08	30	43
Lu	0.8	2.3	0.08	0.06	35	38

[1] The Nernst partition coefficient is defined by K_d = (concentration in the mineral)/(concentration in the melt). A mineral-melt partition coefficient of 1.0 indicates that the element is equally distributed between the mineral and the melt. A value greater than 1.0 indicates that the element has a preference for the mineral phase (i.e., behaves compatibly) whereas a value less than 1.0 implies that the element prefers the melt (behaves incompatibly).

2.3.2. Sedimentary rocks

As REE are generally insoluble in sea and river water and present in very low concentrations (Tables 2.5 and 2.7), their concentrations in clastic sedimentary rocks are determined by their concentrations in the rocks from which they are sourced. Diagenesis has little affect on the redistribution of REE because only very high water/rock ratios during diagenesis can effect any significant change (Rollinson, 1993). Clastic sedimentary rocks show varied levels of enrichment in REE (Table 2.6) and they are normally enriched in the LREE.

Table 2.5. Abundances (in ppm) of rare-earth elements in water.

Element	Seawater	Sea water	River water
Sc	6.0×10^{-7}		
Y	1.0×10^{-6}	-	-
La	3.0×10^{-6}	8.84×10^{-5}	5.90×10^{-4}
Ce	1.0×10^{-6}	5.79×10^{-5}	8.42×10^{-4}
Pr	6.0×10^{-7}	-	-
Nd	3.0×10^{-6}	7.70×10^{-5}	5.26×10^{-4}
Sm	5.0×10^{-8}	3.47×10^{-6}	1.21×10^{-4}
Eu	1.0×10^{-8}	1.70×10^{-7}	3.14×10^{-5}
Gd	7.0×10^{-7}	4.34×10^{-6}	1.31×10^{-4}
Tb	1.0×10^{-7}	-	-
Dy	9.0×10^{-7}	5.49×10^{-6}	1.59×10^{-4}
Ho	2.0×10^{-7}	-	-
Er	8.0×10^{-7}	3.19×10^{-6}	1.08×10^{-4}
Tm	2.0×10^{-7}	-	-
Yb	8.0×10^{-7}	2.41×10^{-6}	8.94×10^{-5}
Lu	2.0×10^{-7}	-	-
Source	1	2	2

Source: 1. Krauskopf (1979); 2. Rollinson (1993).

Table 2.6. Abundances (in ppm) of rare-earth elements in C1 chondrite and some important sedimentary rocks.

Element	C1	Post-Archean Shale	Sandstone	Carbonate	Phosphorite	Coal
Sc	5.9	16.0	1.0	2.0		
Y	1.57	27.0	40.0	42.0		4.7
La	0.237	38.0	30.0	10.0	56	4.1
Ce	0.613	80.0	92.0	35.0	102	11.5
Pr	0.0928	8.9	8.8	3.3	14.5	2.2
Nd	0.457	32.0	37.0	14.0	57	4.7
Sm	0.148	5.6	10.0	3.8	11.2	1.6
Eu	0.0563	1.1	1.6	0.6	2.8	0.7
Gd	0.199	4.7	10.0	3.8	15	1.6
Tb	0.0361	0.8	1.6	0.6	2.1	0.3
Dy	0.246	4.4	7.2	2.7	12.3	
Ho	0.0546	1.0	2	0.8	3.3	0.3
Er	0.16	2.9	4.0	1.5	9	0.6
Tm	0.0247	0.4	0.3	0.1	1.06	0.1
Yb	0.161	2.8	4.0	1.5	6.7	0.5
Lu	0.0246	0.43	1.2	0.5	1.2	0.07
Total Y to Lu	4.080	210.00	249.70	120.20	294.16	32.97
Total LREE	1.604	165.60	179.40	66.70	243.50	24.80
Total HREE	0.91	17.4	30.3	11.5	50.66	3.47
Total HREE and Y	2.476	44.40	70.30	53.50	50.66	8.17
Ratio of LREE/HREE	1.77	9.52	5.92	5.8	4.81	3.04
Source	1	2	3	3	4	4

Source: 1. McDonough and Sun (1995); 2. Taylor and McLennan (1985); 3. Turekian and Wedpohl (1961); 4. Wedepohl (1970).
The LREE include La to Eu, and the HREE include Gd to Lu.

The concentration of REE in chemical sediments is most likely related to the concentration of sea water from which they are formed. The phosphate-rich rocks are more enriched in REE than carbonates (Table 2.6) and show more significant enrichment in the LREE. Both shallow- and deep-water manganese nodules are enriched in REE compared to sea water (Table 2.7). Manganese nodules from the Bauer Basin (south equatorial Pacific) are different from other nodules as they show enrichment with respect to HREE and also have Ce negative anomalies (Elderfield and Greaves, 1981) on a shale-normalised REE distribution geochemical plot. Their REE distribution is interpreted to be caused by an input of hydrothermal iron oxyhydroxides and by diagenetic reactions in the sedimentary rocks (Elderfield and Greaves, 1981).

Table 2.7. Average abundances (in ppm) of rare-earth elements in manganese nodules from the Pacific and Indian oceans. Data from Piper (1974).

Element	Seawater x 10^{-7}	Shallow water[1] nodules	Deep water[1] nodules
La	32	253	227
Ce	12	803	735
Pr	-	-	-
Nd	28	251	272
Sm	4.5	44	51
Eu	1.3	9.4	11
Gd	-	-	-
Tb	1.4	7.1	8.1
Dy	-	-	-
Ho	-	-	-
Er	-	-	-
Tm	-	-	-
Yb	8.2	25.5	19.2
Lu	1.5	4.4	3.2

[1] Shallow water nodules are collected from depths less than 3000–3500 m, and deep water nodules from depths greater than 3000–3500 m.

2.4. RARE-EARTH-ELEMENT ABUNDANCES IN MAJOR ROCK-FORMING AND MINOR MINERALS

The large ionic radii of the REE limits significant substitution of these elements into minerals, except where the ion which is substituted is also large. Substitution of trivalent REE are noted for mineral containing Ca^{+2}, Th^{+4}, U^{+4}, Mn^{+2}, and Zr^{+4}. The substitution of Zr^{+4} with a small ionic radius (0.72 Å[4] in VI-fold co-ordination) is not totally controlled by ionic radius (Henderson, 1984). Bivalent europium (Eu^{+2}; ionic radius of 2.17 Å in VI-fold co-ordination) can substitute for Pb^{+2} (2.19 Å), Ca^{+2} (1.00 Å), Sr^{+2} (2.18 Å) and Na^{+} (0.99 Å). Similarly, tetravalent (Ce^{+4}, ionic radius 0.87 Å in VI-fold co-ordination) can substitute for U^{+4} (0.89 Å), Th^{+4} (0.94 Å).

The substitution of a trivalent REE for a cation of different charge requires charge compensation either by coupled substitution or by production of a vacancy. In some cases the charge can be compensated by addition of an anion in an interstitial position in the crystal structure. Coupled substitution for a mineral like anorthite follows the scheme:
$(RRE^{+3}, Al^{+3}) = (Ca^{+2}, Si^{+4})$ and $(REE^{+3}, Na^{+}) = (2Ca^{+2})$.

The substitution of Ca^{+2} by REE in apatite occurs by production of a vacancy:
$2REE^{+3} + Ca_5(PO_4)_3OH = (REE_2\ Ca_2\ \square)(PO_4)_3OH + 3Ca^{+2}$; where $\square$ represents a vacant site.

[4] 1 angstrom (Å) unit = 1 x 10^{-10} metres.

Table 2.8. Abundances (in ppm) of rare-earth elements in some common rock-forming minerals (Taylor and McLennan, 1985).

Element	Olivine[1]	Clino-pyroxene[2]	Ortho-pyroxene[2]	Hornblende[3]	Plagioclase[3]	Alkali-feldspar[3]	Biotite[3]	Muscovite[4]	Garnet[5]
La								86	
Ce	0.569	5.94	0.442	22.5	1.36	0.264	2.2	127.3	20
Pr									
Nd	0.365	7.23	0.645	27.5	0.252	0.0769	1.03		15
Sm	0.09	3.3	0.347	8.67	0.02	0.0112	0.221	20.91	15.1
Eu	0.02	0.554	0.064	1.375	0.155	0.0821	0.0377	1.14	1.42
Gd	0.084			9.74			0.213		53.6
Tb								2.73	
Dy	0.079	6.75	1.35	8.29	0.00552	0.006	0.17		122
Ho									
Er	0.046	4.04	1.4	4.18	0.00308	0.0029	0.0913		77.9
Tm								14.48	
Yb			2.1	3.18	0.00301	0.0033	0.0792	2.12	70.13
Lu	0.0094		0.414						10.1
Total REE	1.26	27.81	6.76	85.44	1.80	0.45	4.04	254.68	385.25
LREE	1.04	17.02	1.50	60.05	1.79	0.43	3.49	235.35	51.52
HREE	0.22	10.79	5.26	25.39	0.01	0.01	0.55	19.33	333.73
LREE to HREE	4.78	1.58	0.28	2.36	153.92	35.59	6.30	12.18	0.15

Note: The LREE include La to Eu, and the HREE include Gd to Lu.
[1] Basalt.
[2] Andesite.
[3] Granodiorite.
[4] Granite.
[5] Dacite.

Table 2.9. Abundances (in ppm) of rare-earth elements of some common minor and accessory minerals (Taylor and McLennan, 1985).

Element	Zircon (granodiorite)	Apatite (granodiorite)	Monazite (granite)	Allanite (granodiorite)	Epidote (granodiorite)	Sphene (granodiorite)	Tourmaline (granite)
La			119 000				10.3
Ce	42.3	509	195 000	66560	152	3305	13.7
Pr			32 100				
Nd	14.9	302	98 000	16060	58.2	2680	
Sm	5.4	52.9	24 500	1260	9.45	655	1.86
Eu	1.27	15.2	635	133.3	3.38	165	0.11
Gd	17.4		14 700	460	8.15	564	0.213
Tb			1960				0.16
Dy	56.9	31.7	7710	118.4	5.67	470	
Ho			1400				
Er	116	17.1		28.5	2.69	237	
Tm							
Yb	253	13.9	540	17.4	2.1	207	0.59
Lu							0.1
Total REE	507.17	941.80	495 545	84 637.60	241.64	8283.00	27.03
LREE	63.87	879.10	469 235	84 013.30	223.03	6805.00	25.97
HREE	443.30	62.70	26 310	624.30	18.61	1478.00	1.06
LREE to HREE	0.14	14.02	17.83	134.57	11.98	4.60	24.43

Note: The LREE include La to Eu, and the HREE include Gd to Lu.

The steady change in the ionic radii with changing atomic numbers of REE causes fractionation of REE in various minerals. Larger LREE (La to Sm) readily go into minerals with large co-ordination polyhedra, such as allanite, while minerals with small co-ordination polyhedra, such as zircon, favour the smaller HREE (Gd to Lu). Minerals with intermediate-size polyhedra, such as apatite and sphene, don't show any preference for the LREE, HREE or the MREE.

The REE abundances of common rock forming and minor/accessory minerals are summarised in Tables 2.8 and 2.9. Olivine in basalt, plagioclase, alkali feldspar, and biotite from granodiorite have fairly low concentrations, except for europium which shows a positive europium anomaly (on chondrite-normalised plots). Muscovite, garnet, and hornblende show high abundances of all REE and distinct negative europium anomalies (on chondrite-normalised plots). All major minerals are enriched in LREE except clinopyroxene from andesite, but the relative enrichment is greatest for plagioclase and muscovite. Garnet on the other hand is enriched in HREE (Table 2.8).

All minor minerals listed in Table 2.9 are heavy minerals. They are characterised by high abundances of REE and some of them constitute main ore-forming minerals. Monazite and zircons are one of the principal ore-forming minerals of REE in heavy-mineral sand deposits. With the exception of zircon all other heavy minerals listed in Table 2.8 show similar pattern of REE distribution characterised by relative abundance of LREE. Zircon on the other hand is enriched in HREE (Table 2.9).

2.5. RARE-EARTH ELEMENTS IN HYDROTHERMAL FLUIDS

2.5.1. Fluid-melt partitioning

The existence of hydrothermal REE deposits shows that REE are mobile in hydrothermal fluids. The concentration of REE in high-temperature hydrothermal fluids generated from a melt depends on the fluid/melt partitioning coefficients of the REE. Experimental estimates of partitioning coefficients (e.g., Flynn and Burnham, 1978; Webster and Holloway, 1980; Bau, 1991; Bai and van Groos, 1999; Reed et al., 2000) show that some REE readily partition into fluids.

Flynn and Burnham (1978) studied partitioning of Ce, Eu, Gd, and Yb in a water-saturated silicate melt and vapour phase at 800°C and with pressures between 2.25 kilobars (kb) and 4.0 kb. They showed that the fluid/melt partitioning coefficients increased (from 0.02 to 0.3) with an increase in the salinity (from 0.646 mCl to 0.914 mCl) of the fluid. The partitioning coefficients for LREE were greater than those for HREE with the highest coefficients recorded for europium. The REE formed aqueous chloro complexes under these conditions. The partitioning coefficients at 2.25 kb were several times higher than at 4.0 kb. Studies by Bai and van Groos (1999) support results of the studies by Flynn and Burnham (1978) with the difference that no direct relation was observed between the partitioning coefficient of lanthanum and cerium and the concentration of chloride in the fluid. However, the partitioning coefficients increased sharply with an increase in the mHCl reaching ~30 for lanthanum and ≥3 for cerium. These studies found no correlation between partitioning coefficients and the concentration of dissolved carbonate and fluorine in the fluid suggesting that aqueous carbonate and/or fluoride complexes did not form at temperatures of ~800°C.

The partitioning of REE between a peraluminous monzogranitic melt and a chloride-bearing, sulphur- and carbon dioxide-free aqueous volatile phase at 800°C and 200 Megapascals (Mpa) pressure show that the partitioning of REE depends on the chloride concentration of the volatile phase (Reed et al., 2000; Fig. 2.5). In these experiments the LREE (e.g., La, Ce) partitioned into aqueous volatile phase to a greater extent than the HREE (e.g., Yb, Lu; Fig. 2.5). The difference in the behaviour of Eu is thought to be controlled by the two oxidation states (Eu^{+2} and Eu^{+3}) in which it occurs. All other REE (except Ce^{+4}) occur only in trivalent state. The Eu^{+2}/Eu^{+3} redox boundary is a function of the oxidation state of the system at a particular temperature. The calculations show that at temperatures of up to 600°C, the oxygen

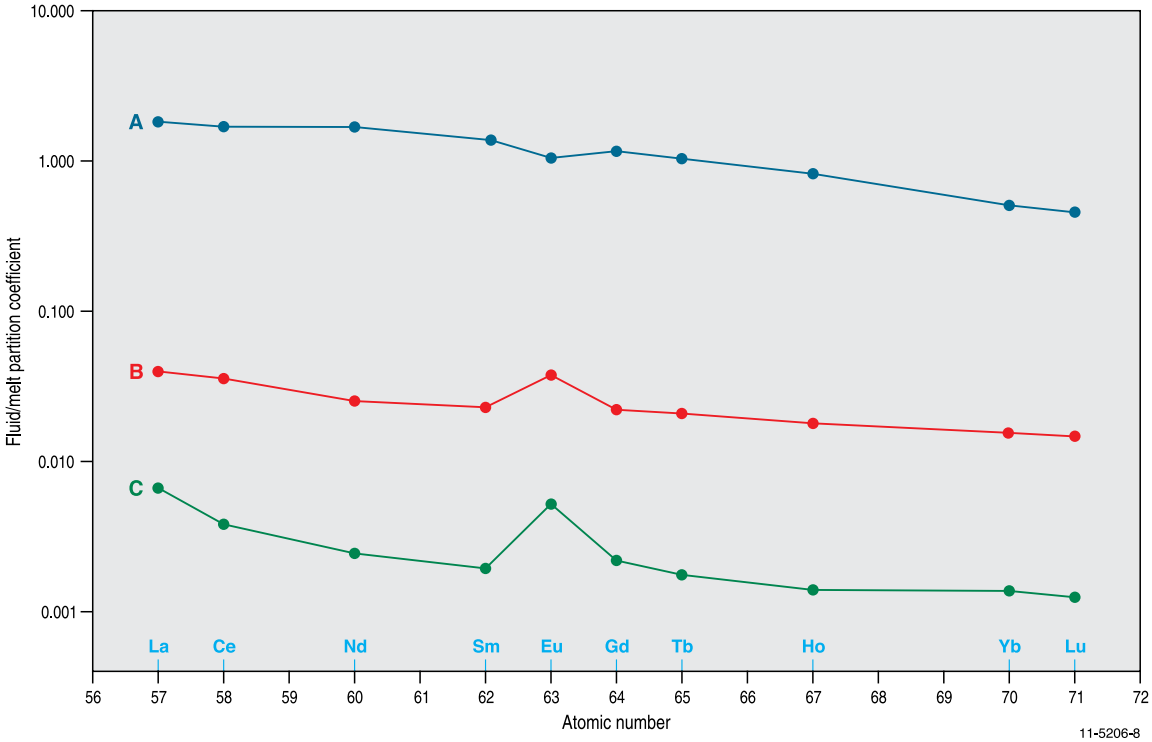

Figure 2.5. Fluid/melt partition coefficients of rare-earth elements for fluids with different salinities. Fluid A: salinity = 3.5 m Cl^-; Fluid B: salinity = 1.1 m Cl^-; and Fluid C: salinity = 0.4 m Cl^-. The partition coefficients increase with salinity. Modified from Reed et al. (2000).

fugacity at which Eu^{+3} is reduced to Eu^{+2} increases with increasing temperature suggesting that at high-temperatures, europium can be fractionated from the other REE (Bau, 1991). The numerical simulation of REE behaviour during isothermal decompression and degassing of water- and chloride-bearing granitic melts from 3 kb to 0.5–0.3 kb show that the first fluid formed during decompression is chloride-rich and shows high REE concentration higher than or similar to the REE content of the initial melt (Lukanin and Dernov-Pegarev, 2010). Fluids released at lower pressures have lower concentrations of REE. During all stages of decompression the fluid is enriched in the LREE relative to the HREE and the concentration of europium is controlled by the oxidation state of the melt-fluid system.

The above mentioned fluid-melt partitioning studies show that:

- partitioning of REE is a function of temperature, pressure, and salinity of the fluid. The fluid-melt partitioning coefficients increase with increase in the salinity (chloride concentration) of the fluid;
- REE most probably form aqueous chloro-complexes. The studies do not show a relationship between fluid-melt partitioning coefficients and the carbonate and fluorine concentrations of the fluid implying that REE do not form fluoro or carbonate complexes;
- the fluid-melt partitioning coefficients for the LREE are higher than those for the HREE suggesting that the fluids released from the melts are enriched in the LREE; and
- the behaviour of europium is controlled by the oxidation state of the system and that under reduced conditions it can fractionate from the other REE.

2.5.2. Rare-earth elements in fluids at temperatures below 350°C

The behaviour of REE in aqueous fluids has been reviewed in many publications (e.g., Brookins, 1989; Wood, 1990a,b; Lottermoser, 1992). The experimental studies on the stability of aqueous complexes of REE have been discussed amongst others by Gammons et al. (1996), Wood and William-Jones (1994), and Cetiner et al. (2005).

Gammons et al. (1996) estimate that at 300°C, a fluid with a composition similar to that observed in seafloor hydrothermal vents can dissolve a maximum of 1.9 ppb Nd. The REE in the analysed fluid were enriched by LREE, especially La, Ce, and Nd. The measured concentration of TREE in fluids of submarine hydrothermal vents (at temperatures of ~300°C) varies between 1 ppb and 4 ppb (Giere, 1996). Lower temperature (between 40°C to 100°C) fluids from continental hydrothermal waters can dissolve up to 2 ppb TREE. Much higher concentrations have been measured in fluid inclusions in quartz of some felsic rocks. An ICP–MS analysis of fluids extracted from fluid inclusions in hydrothermal quartz associated with the Capital Pluton in New Mexico yielded TREE concentrations of 200 ppm to 1300 ppm (Banks et al., 1994). Norman et al. (1989) report similar higher concentrations (8 ppm to 150 ppm TREE) in fluids extracted from fluid inclusions. Thus hydrothermal fluids can dissolve and transport REE in amounts significant to form hydrothermal deposits. These fluids can also remobilise and reconcentrate REE from REE-enriched rocks, such as pegmatites, alkaline rocks, and carbonatites.

As mentioned in Section 2.1, the dominant oxidation state of the REE is +3. Under more oxidising conditions Ce^{+4}, and more reducing conditions, Eu^{+2}, Sm^{+2}, and Yb^{+2} are formed (Wood, 1990a). Hence the aqueous geochemistry of most REE is dominated by their trivalent state. The trivalent REE are classified as hard acids and complex preferentially with hard bases-ligands, such as F^-, SO_4^{-2}, CO_3^{-2}, PO_4^{-3}, and OH^- (Table 2.10). REE are known to form complexes with intermediate bases such as Cl^-, but at 25°C they are weak and complexes with soft bases such as H_2S, HS^-, and CN^- are also weak or unknown (Wood, 1990a).

The above mentioned studies (Wood, 1990a,b) on the speciation of REE in aqueous fluids and their stability at temperatures below 350°C suggest that:

1. the stability of all REE complexes increases strongly with temperature, with the increase being greatest for fluoride and least for chloride complexes;
2. fluoride complexes of the REE may dominate over other complexes throughout a wide range of pH values and fluoride concentration expected in hydrothermal fluids; and
3. at low temperatures typical of surficial conditions and in natural waters (including shallow ground water), carbonate complexes of the REE tend to dominate in slightly acidic and alkaline conditions. In more acidic conditions sulphate, phosphate, and fluoride complexes become dominant.

As most common ore-forming minerals of REE contain REE in the trivalent state, the same oxidation state in which they are transported in hydrothermal fluids, oxidation-reduction reactions do not play a significant role in their formation. In general, the formation of REE-bearing minerals such as monazite and xenotime from hydrothermal fluids will be caused by factors such as

Table 2.10. Classification of metals and ligands in terms of Pearson's (1963) hard and soft acids and bases principle.

Hard	Borderline	Soft
Acids	**Acids**	**Acids**
H^{+}	$Fe^{+2} > Mn^{+2} > Co^{+2} > Ni^{+2} >$	$Au^{+} > Ag^{+} > Cu^{+} > Hg^{+2} > Cd^{+2}$
$Li^{+} > Na^{+} > K^{+} > Rb^{+} > Cs^{+}$	Cu^{+2}, $Zn^{+2} > Pb^{+2}$, Sn^{+2},	$Pt^{+2} > Pd^{+2}$ > other PGE^{+2}, $Tl^{+3} >$
$Be^{+2} > Mg^{+2} > Ca^{+2} > Sr^{+2} > Ba^{+2}$	As^{+3}, Sb^{+3}, Bi^{+3}	Tl^{+}
$Al^{+3} > Ga^{+3}$		
$Sc^{+3} > Y^{+3}$; REE^{+3} ($Lu^{+3} > La^{+3}$)		
$Ce^{+4} > Sn^{+4}$		
$Ti^{+4} > Ti^{+3} > Zr^{+4} \sim Hf^{+4}$		
$Cr^{+6} > Cr^{+3}$; $Mo^{+6} > Mo^{+5} > Mo^{+4}$;		
$W^{+6} > W^{+4}$; Nb^{+5}, Ta^{+5}, $Re^{+4} >$		
$Re^{+6} > Re^{+4}$; $V^{+6} > V^{+5} > V^{+4}$		
Mn^{+4}; Fe^{+3}; Co^{+3}; $As^{+5} \sim Sb^{+5}$		
Th^{+4}; U^{+6}; U^{+4}		
$PGE^{+5} > PGE^{+4}$		
Bases	**Bases**	**Bases**
$F^{-} > H_2O$, OH^{-}, O^{-2}; $NH_3 > NO_3^{-}$;	**Cl^{-}**	$I^{-} > Br^{-}$, CN^{-}; CO;
$CO_3^{-2} > HCO_3^{-2} > SO_4^{-2} > HSO_4^{-1}$;		$S^{-2} > HS^{-1} > H_2S$;
$PO_4^{-3} > HPO_4^{-2} > H_2PO^{4-}$;		Organic phosphines (R_3P),
Carboxylates (acetate, oxalate, etc)		organic thiols (RP); polysulphide,
$MoO_4^{-2} > WO_{4-2}$		thiosulphate, sulphite
		HSe^{-}, Se^{-2}, HTe^{-}, Te^{-2};
		AsS_2^{-}; SbS_2^{-}

Note: In the case of hard species, the symbol > denotes 'harder than', and in the case of soft species it denotes 'softer than'.
The symbol 'R' denotes an organic carbon chain.
Bold fonts indicate the REE as hard acids, and hard-base ligands with which REE readily form soluble complexes. The chloride ion (Cl^{-}) is not regarded very important because it is a borderline base.
PGE = Platinum-group elements (platinum, palladium, rhodium, iridium, ruthenium, and osmium).

cooling, changes in the concentration of the major ligands (carbonate, fluoride, sulphate, phosphate) in the fluids, changes in the fluid pH and boiling and associated loss of gases (e.g., CO_2), from the fluid. The oxidation state of the system and oxidation-reduction reactions can be important only for europium and cerium (which forms Ce^{+4} under highly oxidising conditions).

Precipitation of REE minerals can be represented schematically (reactions are not balanced) by the following general reactions:

$REE(CO_3)^{+}_{(aq)} + 2H^{+} = REE^{+3}$ (mineral) + $CO_{2(aq)} + H_2O$

$REE(F_2)_{(aq)} = REE^{+3}$ (mineral) + F^{-}

$REE(PO_4)_{(aq)}) = REE^{+3}$ (mineral) + $CO_{2(aq)} + H_2O$

These three reactions show that changes in pH and in the concentration of dissolved carbonate, phosphate, and fluoride ions in the fluids can cause precipitation of REE minerals.

2.5.3. Rare-earth-element mobility in surficial fluids

The concentrations of REE in sea and river waters are extremely low (Tables 2.5 and 2.7) reaching a maximum of ~1 ppb in river water. In spite of the low solubility of REE in surficial water, REE appear to be mobile in significant amounts to form economic-grade accumulations in sedimentary (phosphorite, lignite) and regolith (residual lateritic and bauxite) environments.

Brookins (1988) has complied Eh-pH diagrams at 25°C for yttrium and other light and HREE showing stability of REE carbonates, oxides, and hydroxides. The REE-bearing carbonates, oxides, and hydroxides

are stable in alkaline conditions (pH >6) and become more soluble in acidic conditions (pH <6). At a pH of 6, a fluid containing dissolved CO_2 can transport more than 1 ppm of REE. The increase in pH can cause precipitation of REE-bearing carbonates, oxides, and hydroxides. The pH at which LREE and HREE begin to precipitate varies between 6.2 and 7. Thus variations in pH alone are unlikely to explain the differentiation of HREE and LREE observed in some REE deposits formed in surficial conditions. When an acidic fluid reacts with a rock which increases the pH of the fluid, lanthanum carbonate will tend to precipitate at a pH of 6.2, lutetium at a pH of 6.4, and yttrium at a pH of 7. The solubility of all REE and the stability of REE-bearing minerals are independent of the oxidation state of the fluid. The only exceptions are europium and cerium. In acidic fluids, cerium is soluble as Ce^{+3}, and cerium oxide (CeO_2) can form by an increase in pH and/or in oxidation state.

The calculations by Brookins (1988) need to be taken with caution because the fluids do not include phosphate, fluoride, and sulphate species, the presence of which in surficial waters can affect the solubility and stability of REE-bearing minerals.

Mobilisation and redistribution of REE during lateritic weathering of a syenite was studied by Braun et al (1993). The study shows that during weathering, common REE-bearing accessory minerals, such as allanite, apatite, titanite ($CaTiSiO_5$), and epidote are destroyed in the first stages of weathering, resulting in most of the REE being released. During weathering, REE are fractionated and redistributed in the saprolite zone. The REE-phosphates formed in the process are strongly enriched in LREE. Cerium is deposited as cerianite (CeO_2) from changes in pH and oxidation state (Eh), whereas other LREE move to the base of the weathering profile. The majority of REE are leached from the iron-rich upper horizon of the weathering profile.

There is very little known about the behaviour of scandium in surficial waters. The Eh-pH diagrams at 25°C for a simple fluid (Brookins, 1988) show that the stability of scandium oxides and hydroxides is very similar to that of other REE-bearing minerals (stable at pH >6). Scandium is more abundant in mafic and ultramafic rocks (Table 2.3). Most favourable host minerals of scandium are pyroxene, hornblende, and biotite in basalt and gabbro. These minerals are destroyed during weathering and can release scandium. Scandium often follows Fe^{+3} in nature and the stability field of Sc_2O_3 occupies the same Eh-pH space as that of hematite, but scandium possess only one (+3) valence state (Brookins, 1988).

CHAPTER THREE

GEOLOGICAL SETTINGS OF RARE-EARTH-ELEMENT DEPOSITS IN AUSTRALIA

3.1. INTRODUCTION

In Australia, REE are associated with igneous, sedimentary, and metamorphic rocks from a wide range of geological settings. Elevated concentrations of REE have been documented in various heavy-mineral sand deposits, carbonatite intrusions, alkaline igneous complexes, iron-oxide breccia complexes, calc-silicate skarns, fluorapatite veins, pegmatites, phosphorites, lignites, cemented fluviatile sandstones, and unconformity-related uranium deposits. The age of the REE-bearing host rocks range from ~2890 million years (Archean) for pegmatites in Western Australia to late Cenozoic for residual lateritic deposits and heavy-mineral sand deposits widespread throughout eastern Australia. The geological settings of Australia's REE deposits and prospects are shown in Figure 3.1, and their operational status in Figure 3.2. Appendix 8 provides further details of individual deposits and prospects. The presence of REE in mineral occurrences and deposits have not been recorded in older sample analyses when there was a much lower demand for resources of REE, and such occurrences of REE are not shown on Figures 3.1 and 3.2 due to incomplete databases.

Australia's historic REE production has been dominated by monazite by-products from heavy-mineral sand mining largely in southwest and eastern Australia. Significant resources of REE are contained in the monazite component of the heavy-mineral sand deposits, which are mined for their ilmenite, rutile, leucoxene, and zircon contents. In current heavy-mineral mining operations, monazite is no longer recovered for extraction of REE. During the last decade there has been increasing industry interest in hard-rock REE deposits. A number of significant deposits (e.g., Mount Weld, WA; Nolans Bore, NT; Toongi, NSW) with different geological settings (i.e., age and style of mineralisation, rock types, tectonic environment, etc) have provided the catalyst for this exploration interest. These deposits have well advanced mining development programs and their impending production contributions (e.g., 2011 for Mount Weld) are likely to have an impact on the global supply of REE.

Primary hard-rock REE deposits are widely distributed throughout the continent, being particularly prominent in Proterozoic and Phanerozoic provinces (Fig. 3.1). The oldest REE deposits that have been dated in Australia are hosted by Archean pegmatites in the eastern Pilbara Craton (Pinga Creek, Cooglegong, WA). The pegmatites are interpreted to have been emplaced during two periods: an early phase at 2890 Ma to 2880 Ma and a later phase at between 2840 Ma to 2830 Ma (Sweetapple and Collins, 2002). Carbonatite complexes comprising stocks and dykes are prominent in Western Australia, with important examples in the Yilgarn Craton (Mount Weld, Ponton Creek), Capricorn Orogen (Yangibana), and Halls Creek Orogen (Cummins Range). Interestingly, no carbonatites of Archean age have been confirmed in Australia, with the oldest dated examples being the mineralised Mount Weld and nearby Ponton Creek, both emplaced at ~2025 million years in the eastern Yilgarn Craton. The mineralised regolith associated with the Mount Weld Carbonatite is much younger than the host rock and is interpreted to have developed during the Late Mesozoic to Early Cenozoic (Bunting et al., 1974; Duncan and Willett, 1990). Mineralised Proterozoic fluorapatite veins at Nolans Bore in the Arunta Region of the Northern Territory could have been derived from a carbonatite or alkaline magmatic source at depth that has so far not been recognised in geophysical surveys. Alkaline rock complexes with REE resources feature in the Halls Creek Orogen (Brockman) and in the Tasman Orogen (Toongi, Narraburra) of New South Wales. The type example of the iron-oxide breccia complex association is the world-class Mesoproterozoic Olympic Dam deposit in the Gawler Craton, where the REE are associated (but not extracted) with the copper-gold-uranium mineralisation. REE also occur in the similar iron-oxide-hosted Carrapateena deposit. In the Mount Painter–Olary regions of the Curnamona Province east

Australian Rare-Earth-Element (REE) Deposits and Prospects

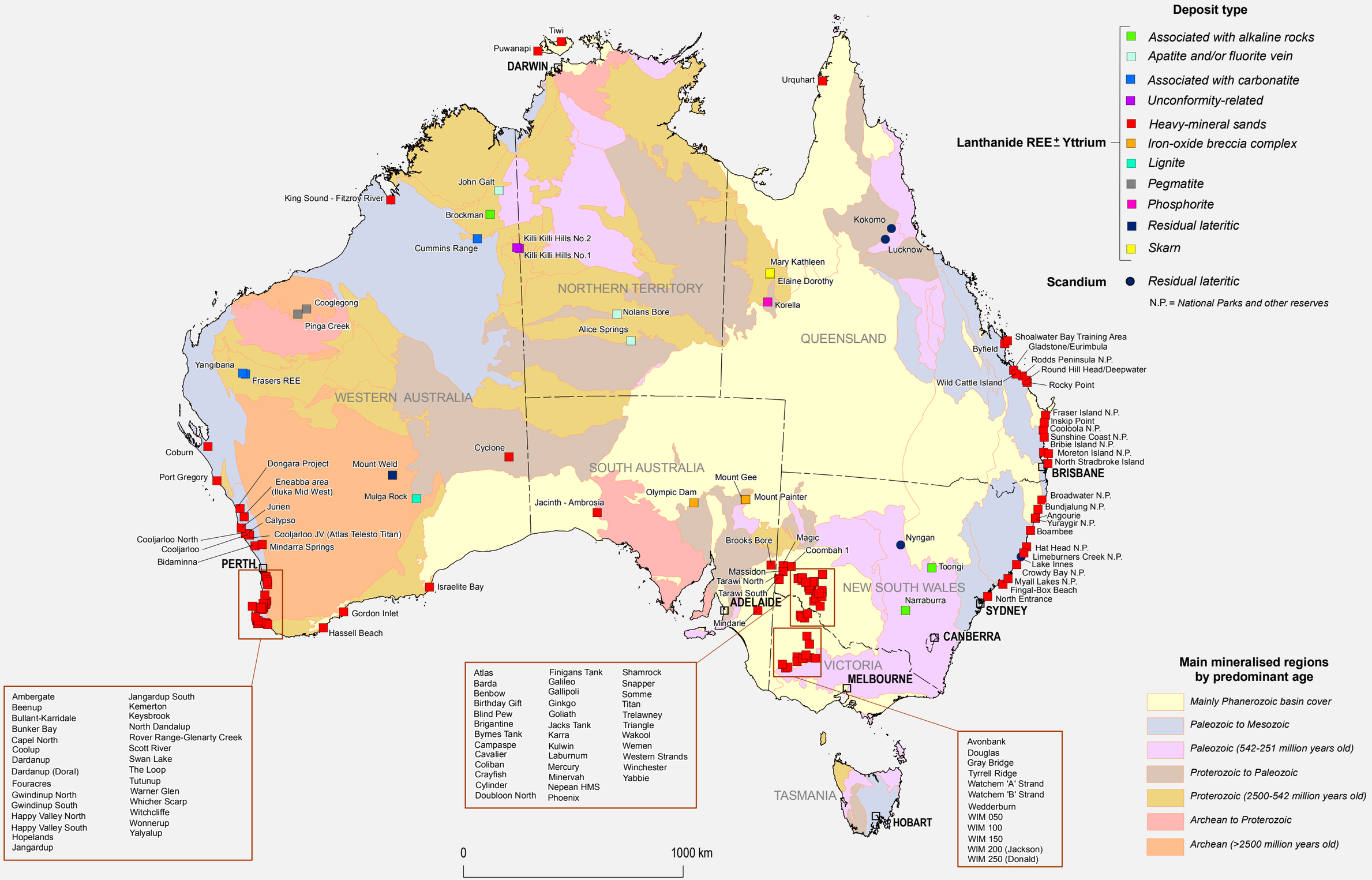

Figure 3.1. Distribution of Australian rare-earth-element deposits and prospects: Deposit type.

Australian Rare-Earth-Element (REE) Deposits and Prospects

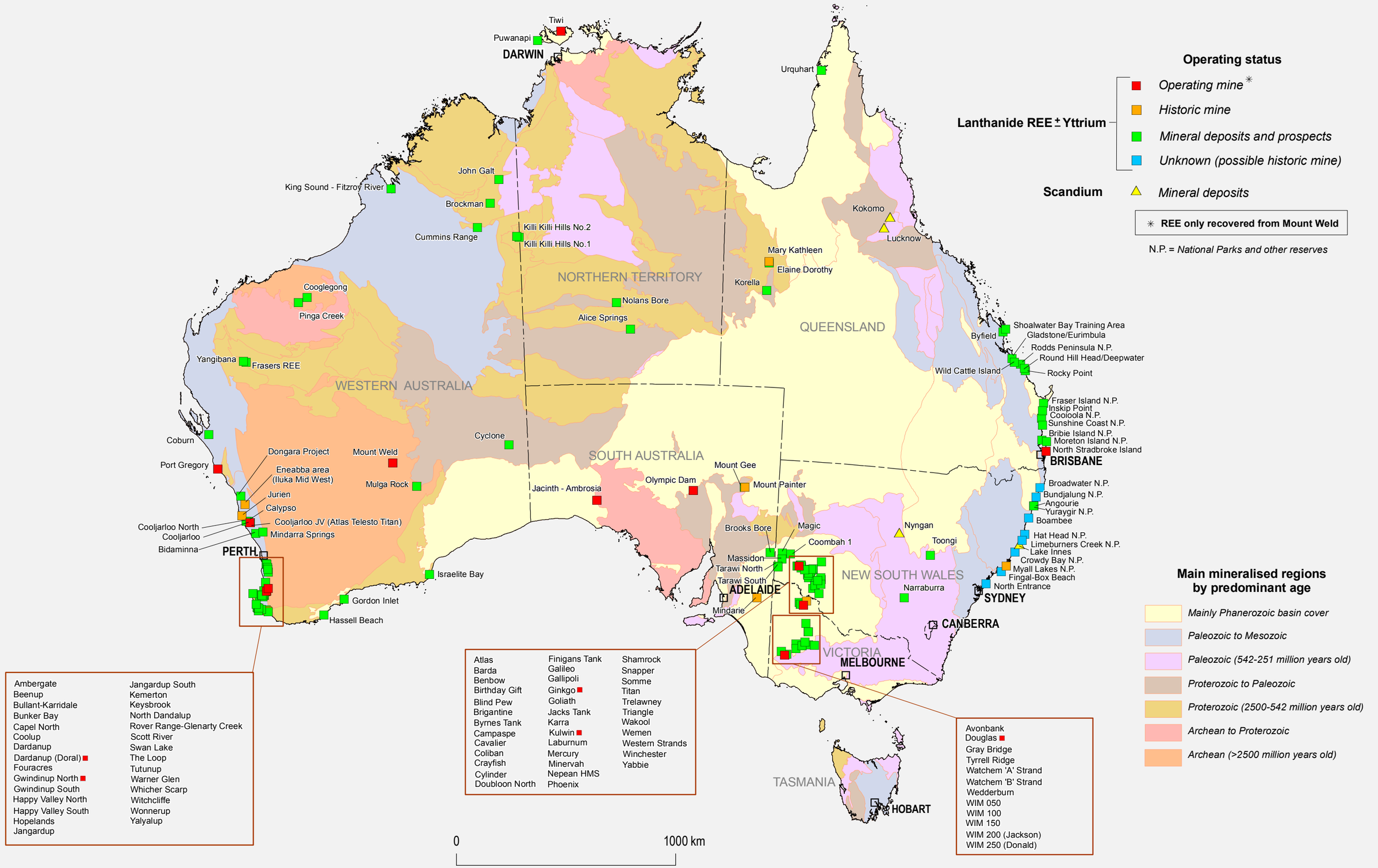

Figure 3.2. Distribution of Australian rare-earth-element deposits and prospects: Operating status.

of Olympic Dam are several Proterozoic REE-bearing iron-oxide uranium breccia deposits. One of the type examples of a metamorphic/metasomatic or skarn-bearing deposit containing REE is the Mary Kathleen uranium deposit in the Mount Isa Inlier, northwestern Queensland. Scandium-bearing nickel-cobalt laterites of Cenozoic age are associated with tectonically emplaced Phanerozoic ultramafic and mafic complexes in the Tasman Orogen of eastern Australia.

The heavy-mineral sand and placer deposits are concentrated along the coastlines of southern Western Australia, northern New South Wales, and southern Queensland. Major deposits occur along fossil shorelines inland in the Murray Basin centred near the junction of Victoria, New South Wales, and South Australia, and in the Eucla Basin in South Australia and Western Australia. Heavy-mineral deposits in beach, high dune, and offshore shallow marine environments are generally Cenozoic in age, whereas channel heavy-mineral deposits extend further back to the Mesozoic.

Currently, there are twelve REE-bearing deposits in Australia that are of operating status (Fig. 3.2; Appendix 8). Mount Weld (WA) is the only current REE mine in Australia from which REE are going to be produced once construction of a concentrator at the mine site and a processing plant in Malaysia are completed. REE are not recovered at the only other hard-rock REE-bearing deposit being mined at Olympic Dam (SA). The remaining ten active mines are heavy mineral sand deposits located at Cooljarloo, Dardanup (Doral), Gwindinup North and Port Gregory (all in WA); Douglas and Kulwin (Vic); Ginkgo (NSW); Jacinth-Ambrosia (SA); North Stradbroke Island (Qld); and Tiwi (NT). The REE in the heavy-mineral deposits are held in monazite, which occurs in minor amounts, usually 0.1 to 1.5%, in the heavy-mineral concentrate dominated by ilmenite, rutile, and zircon. As the monazite has a thorium content of around 5 to 7%, the REE are not recovered because of the cost of thorium disposal.

3.2. CLASSIFICATION OF RARE-EARTH-ELEMENT DEPOSITS

The distribution and concentration of REE into mineral deposits is influenced by various rock-forming processes including enrichment in magmatic or hydrothermal fluids, separation into mineral species and precipitation, and subsequent redistribution and concentration through weathering and other surface processes. Using this evolutionary framework, Walters et al. (2010) proposed that REE deposits can be broadly divided into: (1) primary deposits associated with igneous and hydrothermal processes; and (2) secondary deposits concentrated by sedimentary processes and weathering. Further sub-division of these general categories can be applied using such criteria as lithological association, mineralogy, and morphology of occurrence.

Traditional classification schemes of REE deposits are based on either descriptive-, or genetically (i.e., geological process)-derived criteria, or a combination of these. For example, the descriptive classification of REE deposits in China by Wu et al. (1996) is simply based on the type of host rocks, since they considered genetic-based classifications too controversial for many deposits (e.g., Bayan Obo). The major sub-groups in their 10-fold classification includes: carbonatitic rocks; quartz syenite; alkali granite; alkali complexes; alkali pegmatites; metamorphic rocks; phosphorites; bauxite; lateritic weathering crusts; and placers. Neary and Highley (1984) used a simple five-class structure for the major REE deposits of the world: alkaline rocks and carbonatites; vein; placer; apatite; and other deposits. The United States Geological Survey (Long et al., 2010) employed a rock-association scheme for their highest level categories, namely: peralkaline igneous rocks; carbonatite; iron-oxide copper-gold; pegmatite; porphyry molybdenum; metamorphic; stratiform phosphate residual; paleoplacer; and placer. The next hierarchical level, titled 'Type' with 34 sub-groups, has a much more 'process'-based emphasis, with such type examples as carbonate-rock replacement, metasomatic-fenite, and Climax-type. The classification scheme proposed by the British Geological Survey (Walters et al., 2010) is based on two criteria at the highest level, namely 'Primary deposit' or 'Secondary deposit', with carbonatite; alkaline igneous rocks; iron-REE; and hydrothermal (unrelated to alkaline igneous rocks) representing the sub-groups under the former criteria; and marine placer, alluvial placer, paleoplacer; lateritic; and ion-adsorption clays categorised under the latter criteria.

The classification of REE deposits in the world by Cassidy et al. (1997) is based on the relative 'abundance status' of the REE component in the deposit, i.e., where the REE are (1) a co-product or primary product, or (2) a by-product of the deposit.

1. A number of REE occurrences can be classified as a co-product or, in some cases, primary product deposits. The major deposit types in this class are those associated with carbonatites (sub-groups of primary, hydrothermal, supergene), alkaline igneous rocks and, to a lesser extent, hydrothermal iron-

oxide copper-gold-uranium (iron-rich, copper-uranium-gold-rich), and uranium-bearing skarns.

2. By-product deposits are dominated by heavy-mineral sands and placer deposits. However, discoveries of non-traditional REE resources in combination with new mining and processing techniques are now responsible for a significant proportion of TREE production. Such 'new' deposits include ionic adsorption clays (China), marine phosphorites (in several continents, including Australia), and anatase (Brazil) deposits.

Cassidy et al. (1997) have provided one of the few examples of classifying REE deposits in Australia. They divided the REE occurrences into six major groups, namely: shoreline placer; carbonatite; REE-enriched uranium; alkaline igneous rock; phosphorite; and unclassified (see their Fig. 2).

This report uses a mineral-systems approach to classify REE deposits in Australia and outside Australia (Table 3.1; Fig. 3.3). This approach focuses on mineral-forming process (see Chapter 4 for a definition of a mineral system) and has the advantage over more traditional descriptive classifications in that it attempts to identify those geological processes considered critical to the formation of a 'clan of deposit types' that share common parameters. This information can then be applied in a predictive sense to assist mineral exploration in the identification of potential new areas and types of REE mineralisation.

The mineral-systems classification is hierarchical in structure, with the most general grouping of deposits called 'Mineral-system association' (Table 3.1). This high-level category is divided into Regolith, Basinal, Metamorphic, and Magmatic associations, which are further subdivided into 'Deposit types'. An essential element of the magmatic association is the emplacement of REE-enriched melt. Various deposit types result either directly from the crystallisation of the melt and/or fluids predominantly derived from the melt. Deposit types of the basinal association can be formed from mechanical (e.g., placer) and chemical sedimentary (e.g., phosphorite) processes and from diagenetic fluids generated in sedimentary basins. Deposit types of the regolith association require a REE-bearing source rock to form economic-grade concentrations of REE. The REE deposits are formed either due to enrichment of REE in the residual material and/or from local remobilisation of REE. Deposit types of the metamorphic association are generated during regional and/or contact metamorphism and can involve metamorphic-derived fluids.

The mineral-system association concept used in this report can help relate mineral deposits to a general geochemical cycle (mantle-crustal-surface) of REE (Fig. 3.3). The data compiled for Figure 3.3 shows (see Chapter 2 for a detailed discussion) that REE are derived from the mantle and are enriched in the crust. Partial melting in the mantle generates (per)alkaline and carbonatitic melts enriched in REE. It has been generally recognised that highly alkaline melts can not readily be derived from 'normal' mantle melting of anhydrous chromium-diopside peridotite, which is poor in incompatible elements. This source material needs to be metasomatically enriched in incompatible elements to be a viable source of alkaline melts (e.g., Bailey, 1970; Roden and Murthy, 1985; Chesley et al., 2004). One possible source of fluids for the metasomatism of the mantle is the dehydration of the subducted slab, which can metasomatise asthenospheric mantle and subcontinental lithospheric mantle.

Partial melting of metasomatised mantle can generate (per)alkaline and carbonatitic melts, which can result in the enrichment of REE by about two orders of magnitude (Fig. 3.3). The partial melting of crustal material also produces felsic melts that are enriched in REE, but the enrichment factors are relatively smaller (by an order of magnitude). In general, sövitic carbonatitic melts show the highest levels of REE enrichment. They also show significant enrichment in LREE (LREE/HREE ratio of ~40, compared to ~7 for alkaline and felsic melts).

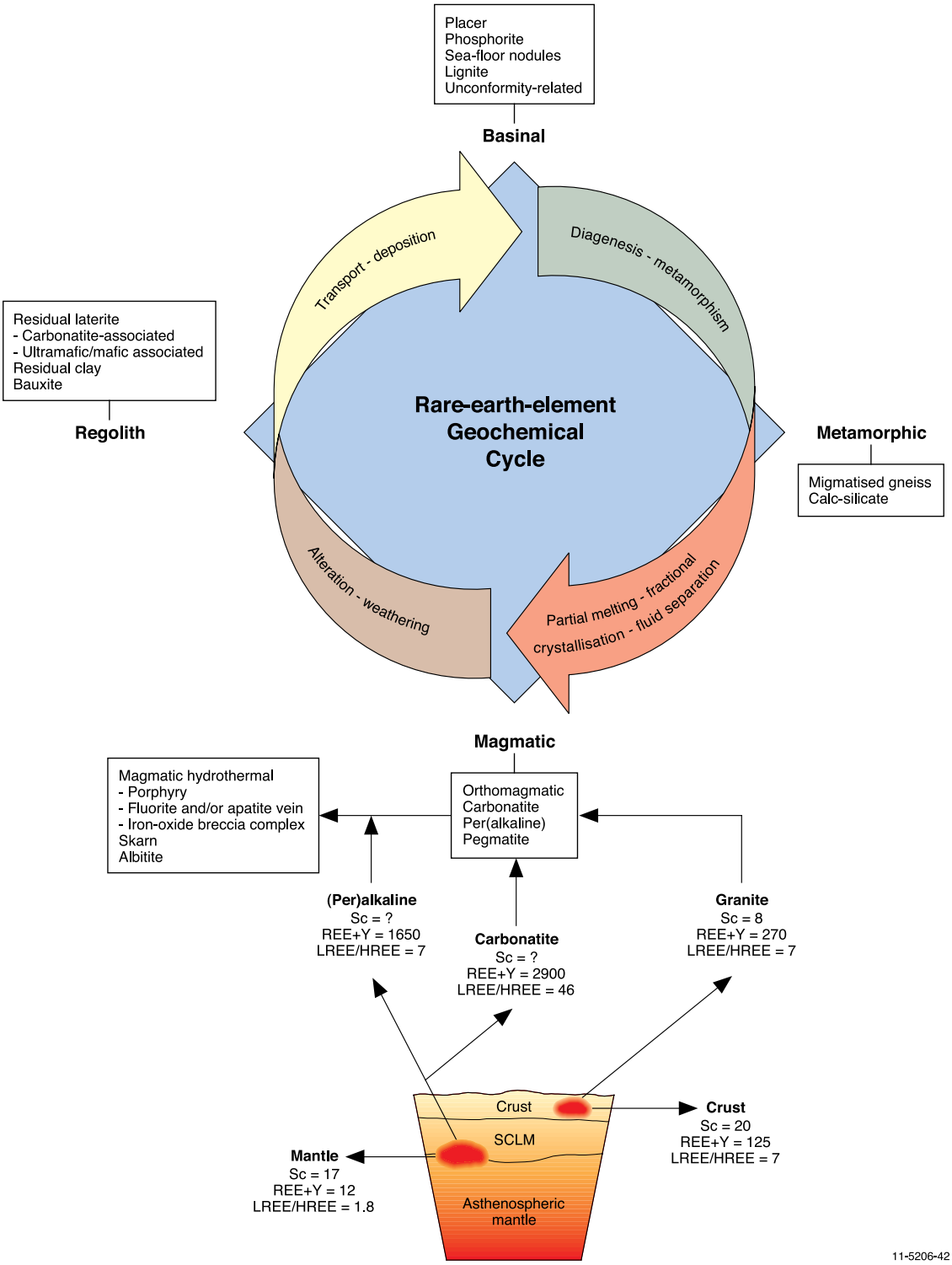

Figure 3.3. Mantle–crust–surface geochemical cycle for rare-earth elements (REE concentrations in parts per million). Alkaline and carbonatitic melts that are produced by the partial melting of metasomatised subcontinental lithospheric mantle (SCLM) transport the rare-earth elements from the mantle into the crust. Granites that are produced from the partial melting of crustal material are also enriched in rare-earth elements (less enriched than alkaline and carbonatitic melts). A more detailed classification of the rare-earth-element deposits is in Table 3.1. The rare-earth-element data for sövitic carbonatites are from Hornig-Kjarsgaard (1998), and the (per)alkaline rock data are from Gerasimovsky (1974). See Tables 2.2 and 2.3 for the other rare-earth-element data and LREE/HREE ratios shown in this figure.

Table 3.1. Mineral-system classification of rare-earth-element deposits. Australian deposit types and type examples are shown in **blue** font.

Mineral-system association	Deposit type	Example of Australian deposit/prospect
Regolith	Residual lateritic	
	• Carbonatite-associated	• Mount Weld, WA
	• Ultramafic/mafic rock-associated	• Lucknow, Qld
	Residual clay	
	Bauxite	
Basinal	Sedimentary	
	• Placer ◦ Quartz-pebble conglomerate ◦ Alluvial ◦ Heavy-mineral sands · Beach · High dune · Offshore shallow marine · Channel	 • Eneabba, WA • North Stradbroke Island, Qld • WIM 150, Vic • Calypso, WA
	• Phosphorite	• Korella, Qld
	• Sea-floor manganese nodule	
	• Lignite	• Mulga Rock, WA
	Diagenetic-hydrothermal	
	• Unconformity-related	• Killi Killi Hills, NT
Metamorphic	• Migmatised gneiss	
	• Calc-silicate	• Mary Kathleen, Qld[1]
Magmatic	Orthomagmatic	
	• Alkaline igneous rock	• Brockman, WA
	• Carbonatite	• Yangibana, WA
	• Pegmatite	• Cooglegong–Pinga Creek, WA
	Magmatic-hydrothermal	
	• Albitite	
	• Porphyry	
	• Skarn	• Mary Kathleen, Qld[1]
	• Apatite and/or fluorite vein	• Nolans Bore, NT
	• Iron-oxide breccia complex	• Olympic Dam, SA

[1] The Mary Kathleen example(s) shown was initially a skarn deposit that was subsequently modified to a calc-silicate-type deposit during regional metamorphism.

3.3. GEOLOGICAL SETTINGS OF RARE-EARTH-ELEMENT DEPOSITS IN AUSTRALIA

This section (3.3.1) describes the geological characteristics of the major REE deposits and occurrences in Australia. The first part (3.3.1) of the section summarises the geological features of fourteen deposits considered the type example of that deposit style in a pro forma containing the following attributes:

General description
Australian deposits/prospects
Deposits outside Australia
Type example in Australia
Location
Geological province
Resources
Current status
Economic significance
Geological setting
Host rocks
REE mineralisation
Source of REE
Age of mineralisation
Petrogenesis
Key references

The fourteen deposit types and their type example (see Table 3.1) are:

Deposit Type 3.1: Laterite associated with carbonatite complexes; Mount Weld, WA

Deposit Type 3.2: Scandium in laterite associated with ultramafic-mafic rocks; Lucknow, Qld

Deposit Type 3.3: Heavy-mineral sand—beach; Eneabba, WA

Deposit Type 3.4: Heavy-mineral sand—high dune; North Stradbroke Island, Qld

Deposit Type 3.5: Heavy-mineral sand—offshore shallow marine; WIM 150, Vic

Deposit Type 3.6: Heavy-mineral sand—channel; Calypso, WA

Deposit Type 3.7: Phosphorite; Korella, Qld

Deposit Type 3.8: Lignite; Mulga Rocks, WA

Deposit Type 3.9: Alkaline igneous rocks; Brockman, WA

Deposit Type 3.10: Carbonatite; Yangibana, WA

Deposit Type 3.11: Pegmatite; Cooglegong–Pinga Creek, WA

Deposit Type 3.12: Skarn; Mary Kathleen, Qld

Deposit Type 3.13: Apatite and/or fluorite veins; Nolans Bore, NT

Deposit Type 3.14: Iron-oxide breccia complex; Olympic Dam, SA

The second part (3.3.2) of the section describes the geological features of other REE occurrences (most without JORC-compliant resources: Appendix 7) not mentioned in the Deposit Types of Section 3.3.1.

3.3.1. Type examples of major rare-earth-element deposits in Australia

Deposit Type 3.1: Rare-earth-element-bearing laterite associated with carbonatite complexes

General description: Carbonatites are igneous rocks composed of more than 50% carbonate minerals, often spatially and temporally associated with alkaline felsic magmas, and have somewhat contentious origins. Primary carbonatites consist mainly of calcitic (sövite) and/or dolomitic (rauhaugite) rock types. Carbonate-rich melts can extract incompatible elements (e.g., REE, zirconium, niobium, phosphorus) from coexisting silicate melts or solids, concentrating them for subsequent deposition of rare-element cumulates from the carbonate magma (Mungall, 2007). Carbonatite complexes have generated considerable exploration interest in Australia because of their potential to host significant resources of REE, copper, niobium, tantalum, phosphorus, and uranium. Such intrusions occur near major structural features throughout the cratonic blocks and they range in age from Paleoproterozoic to Jurassic (Jaques, 2008). The largest deposits in Australia (Mount Weld, Cummins Range) formed from the supergene enrichment of REE in the laterite profile above large composite carbonatite bodies that are generally of Proterozoic age. Deeply weathered carbonatites also occur in Brazil, Canada, Finland, Guyana, Kenya, Tanzania, Uganda, and Zaire (see references in Lottermoser and England, 1988). In contrast to such world-class REE deposits as Mountain Pass in California, few Australian occurrences contain significant abundances of REE in the primary zones of carbonatite. Possible exceptions to this include two mineralised examples in Western Australia, namely Ponton Creek (see Appendix 7) and Yangibana (see Deposit Type 3.10 template).

Australian deposits/prospects: Mount Weld (Yilgarn Craton, WA); Cummins Range (near junction of Halls Creek and King Leopold orogens, Western Australia).

Deposits outside Australia: Araxá, Catalão, Goias, Minas Gerais, and Tapira (all Brazil); Mabounié (Gabon); Mrima (Kenya); Lueshe (Zaire); Dorowa and Shawa (Zimbabwe): Christie et al. (1998) and Lottermoser (1994).

Table 3.2. Resources for the Central lanthanide and Duncan deposits at Mount Weld (using cut-off grade of 2.5% REO).

	000 tonnes	REO%[1]	Total LnREO%[2]	Y_2O_3 ppm
Central lanthanide deposit				
Measured[3]	3550	14.4	14.3	820
Indicated	1440	8.2	8.1	960
Inferred	4884	8.6	8.5	1120
Total	9880	10.7	10.6	990
Duncan deposit				
Measured	3640	5.5	5.2	2700
Indicated	3560	4.1	3.9	2460
Inferred	410	4.3	4.1	2360
Total	7620	4.8	4.5	2570
Total REO resource				
Measured	7200	9.8	9.7	1770
Indicated	5000	5.3	5.1	2020
Inferred	5290	8.3	8.2	1210
Total	17 490	8.1	7.9	1680

Source: Lynas Corporation Limited www site: http://www.lynascorp.com/page.asp?category_id=2&page_id=4

[1] REO includes the oxides of the lanthanide group of REE and yttrium.

[2] Total LnREO includes the oxides of the lanthanide group of REE, but excluding yttrium.

[3] Category of resources.

Type example in Australia: Mount Weld, Western Australia (Figs 3.4 and 3.5).

Location: Longitude: 122.5475; Latitude: -28.8626
~35 km south-southeast of Laverton, Western Australia
1:250 000 map sheet: Laverton (SH 51–02)
1:100 000 map sheet: Burtville (3440)

The Mount Weld Carbonatite complex also hosts significant resources of niobium, tantalum, and phosphate. The Crown deposit in the northern part of the complex has an indicated and inferred resource of 37.7 Mt @ 1.07% Nb_2O_5, 1.16% total lanthanide oxides, 0.09% Y_2O_3, 0.3% ZrO, 0.024% Ta_2O_5, and 7.99% P_2O_5 (as of January, 2010), while phosphorous mineralisation in the Swan deposit in the northern half of the complex has an indicated and inferred resource of 77 Mt @ 13.5% phosphorous oxide (MiningNewsPremium.net, 16th March 2011). The Anchor deposit in the southwest of the Mount Weld complex contains niobium-tantalum mineralisation.

Geological province: Eastern Goldfields Province, Yilgarn Craton, Western Australia.

Resources: TREO resources (Table 3.2) at Mount Weld (as of 16th March 2011) to JORC Code standards are 17.49 Mt @ 8.1% REO for 1.416 million tonnes of contained metal (http://www.lynascorp.com/page.asp?category_id=2&page_id=4 and http://www.lynascorp.com/content/upload/files/Presentations/Investor_Presentation_March_2011_950850.pdf).

Current status: Advanced economic deposit with stockpiling of different grade ores and production planned to commence in 2011. Expected mine life is estimated to be at least twenty years.

Economic significance: 'World-class' economic deposit containing some of the highest REE grades (8.1% REO).

Geological setting: The ~2025 Ma Mount Weld Carbonatite complex (Figs 3.4 and 3.5) intrudes Archean sedimentary-volcanic sequences in the Eastern Goldfields Province of the Yilgarn Craton, Western Australia. The carbonatite intrudes the central part of the fault-bounded Laverton tectonic zone (linear graben-like zone) and it has been overprinted by greenschist facies metamorphism (Duncan and Willett, 1990). The Mount Weld Carbonatite belongs to a regional alkaline province represented by coeval low- to high-MgO alkaline ultramafic-mafic igneous rocks, kimberlites, and carbonatites that were emplaced into

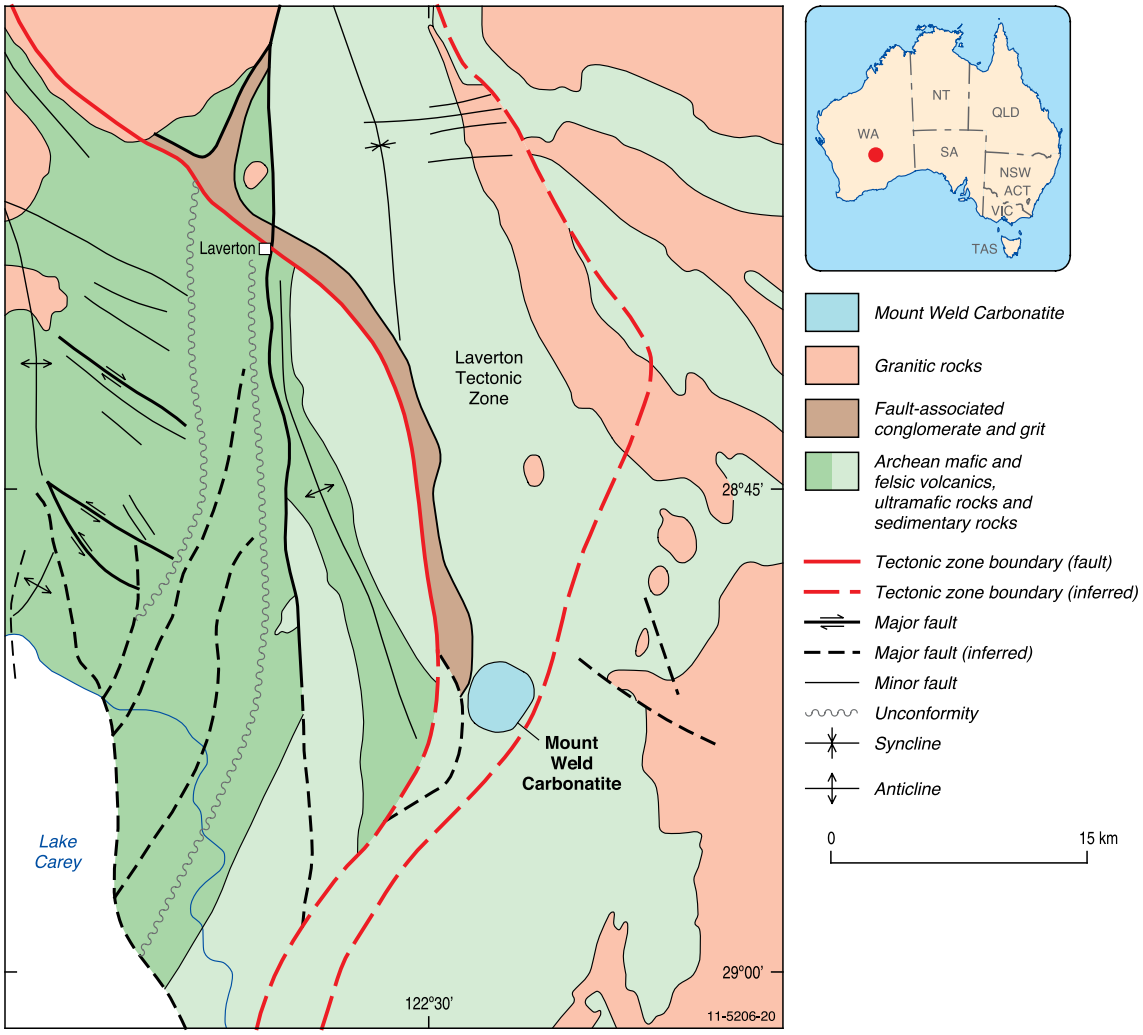

Figure 3.4. Regional geological setting of the Mount Weld Carbonatite, Yilgarn Craton, Western Australia. Modified from Duncan and Willett (1990).

the crust during the middle Paleoproterozoic (Graham et al., 2003; 2004). Incompatible element geochemistry, stable isotope, and Sm-Nd isotope data indicate that all these rocks are strongly enriched in incompatible elements and are comagmatic. The genetic and spatial relationships between the alkaline ultramafic and carbonatitic melts appear to be controlled by the depth and composition of the continental lithospheric mantle (Graham, et al., 2004).

The Mount Weld Carbonatite complex is a steeply plunging cylindrical body, 3 to 4 km in diameter, surrounded by a 500 m-wide fenitic (glimmerite) alteration zone (Fig. 3.5). Carbonatite dykes persist for up to 5 km from the main body. A thick (10 to 70 m) laterite overlying the unweathered carbonatite contains high-grade REO deposits and concentrations of niobium, tantalum, zirconium, and other 'rare' metals. The laterite regolith is covered by lacustrine and alluvial sedimentary rocks. The primary carbonatite consists mainly of calcitic (sövite) and dolomitic (rauhaugite) igneous rock types that contain more than 50% carbonate (Duncan and Willett, 1990). Relict cumulus textures involving carbonate minerals are locally preserved, with minor apatite, biotite, carbonate, and magnetite forming the intercumulus phases. The altered annulus surrounding the complex shows a gradational alteration transition from dominantly potassium-rich micaceous rock (glimmerite) to mafic volcanic country rocks. The altered zone contains phlogopite-rich rocks, brecciated wall-rocks, and is characterised by alkali

Figure 3.5 (see opposite). Geological map (Cenozoic units above carbonatite have been removed) and cross-section of the Mount Weld Carbonatite rare-earth-element deposit, Yilgarn Craton, Western Australia. Geological map and cross-section are modified from Fetherston and Searston (2004), and outlines of Central lanthanide and Duncan deposits are from Lynas Corporation Limited (2011). The minerals in the laterite profile (Inset A) are from Lottermoser and England (1988).

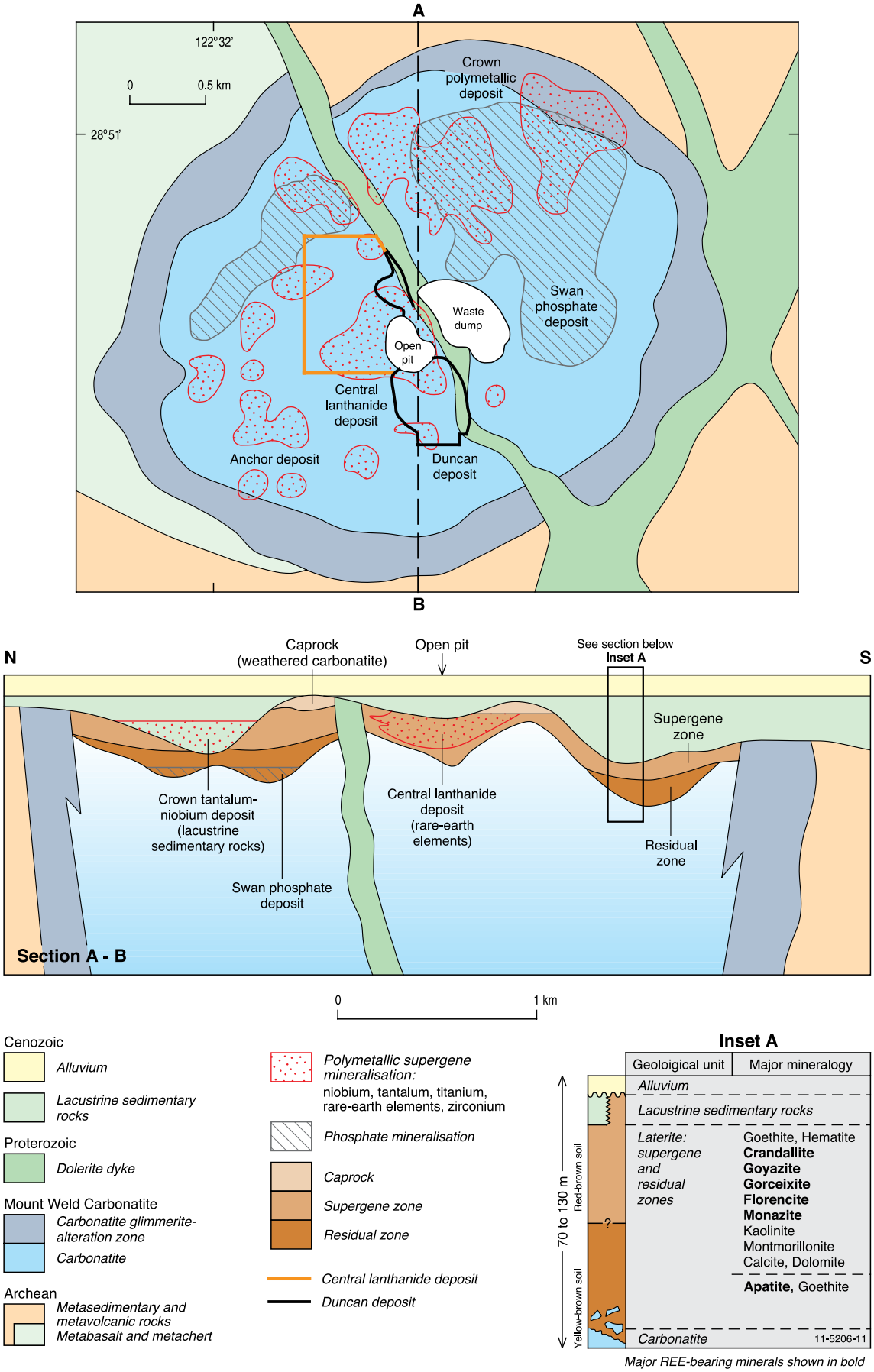
A
122°32'
0
0.5 km
28°51'
Crown polymetallic deposit
Swan phosphate deposit
Waste dump
Open pit
Central lanthanide deposit
Anchor deposit
Duncan deposit
B
N
Caprock (weathered carbonatite)
Open pit
See section below
Inset A
S
Supergene zone
Crown tantalum-niobium deposit (lacustrine sedimentary rocks)
Central lanthanide deposit (rare-earth elements)
Residual zone
Swan phosphate deposit
Section A - B
0
1 km
Cenozoic
Alluvium
Lacustrine sedimentary rocks
Proterozoic
Dolerite dyke
Mount Weld Carbonatite
Carbonatite glimmerite-alteration zone
Carbonatite
Archean
Metasedimentary and metavolcanic rocks
Metabasalt and metachert
Polymetallic supergene mineralisation:
niobium, tantalum, titanium, rare-earth elements, zirconium
Phosphate mineralisation
Caprock
Supergene zone
Residual zone
Central lanthanide deposit
Duncan deposit
Inset A
Geoloigical unit
Major mineralogy
Alluvium
Lacustrine sedimentary rocks
Laterite: supergene and residual zones
Goethite, Hematite
Crandallite
Goyazite
Gorceixite
Florencite
Monazite
Kaolinite
Montmorillonite
Calcite, Dolomite
Apatite, Goethite
Carbonatite
70 to 130 m
Red-brown soil
Yellow-brown soil
?
11-5206-11
Major REE-bearing minerals shown in bold

metasomatism under strongly oxidising conditions (i.e., fenitisation). As indicated by minor, but widely disseminated sulphides, periods of carbonate invasion that introduced calcite, dolomite, and ankerite, occurred under mildly reducing conditions.

Duncan (1990) estimated that during its evolutionary history about four vertical kilometres of the carbonatite intrusion and surrounding greenstone country rocks were removed by erosion. An important aspect of the economic status of the Mount Weld deposit is the geological preservation of the regolith profile. In contrast, the mineralised Ponton Creek carbonatite ~190 km south-southeast of Mount Weld, has no preserved paleo-regolith due to the scouring of the complex by Permian glaciation.

Host rocks: The lateritic regolith above the intrusive carbonatite contains all the currently known economic resources of REE in the Mount Weld deposit (Figs 3.5 and 3.6A). The following summary of the mineralogy and supergene enrichment processes that operated in the host lateritic rocks is from Duncan and Willett (1990) and Lottermoser (1990). Leaching and removal of carbonate by groundwater activity led to the progressive accumulation of primary igneous apatite and minor oxides, sulphides, and silicates. This was accompanied by the replacement, decomposition, and oxidation of primary igneous minerals, crystallisation of secondary minerals, and the formation of ferruginous cap rocks. These complex weathering-hydrological processes resulted in the formation of a mineralogically and chemically zoned laterite profile. The base of this profile is defined by a relatively sharp, karst-like interface with the underlying carbonatite. A residual zone containing relict igneous minerals (apatite, magnetite, ilmenite, pyrochlore, monazite, silicates) concentrated by the removal of carbonate directly overlies the unweathered carbonatite. The residual zone is overlain by a supergene-enriched zone containing abundant insoluble phosphates, aluminophosphates, clays, crandallite-group minerals, iron and manganese-bearing oxides that contain elevated concentrations of REE, Y, U, Th, Nb, Ta, Zr, Ti, V, Cr, Ba, and Sr. Of major exploration interest are the REE, niobium-tantalum, and phosphatic minerals concentrated in the laterite. The highest grades of niobium-tantalum occur in 6 to 15 m-thick horizontal units composed of unconsolidated, highly phosphatic lacustrine sedimentary rocks that grade upwards into smectite clays. Extreme conditions of lateritic weathering that prevailed in the supergene zone over a protracted period of time ensured the degradation of the residual magmatic REE-bearing minerals.

REE mineralisation: The Central lanthanide (9.88 Mt @ 10.7% REO) and the Duncan (7.62 Mt @ 4.8% REO) deposits contain the largest resources of REE in the carbonatite complex. The Crown and Coors polymetallic deposits in the northern part of the carbonatite body contain Nb, P, REO, Ta, Zr, Y, and Ti resources, and in addition, extensive phosphate-rich resources of the Swan phosphate deposit occur in the lower regolith. The Central lanthanide deposit (CLD) contains an indicative mix of predominantly LREE from CeO_2 (46.7%), La_2O_3 (25.5%), Nd_2O_3 (18.5%), Pr_6O_{11} (5.32%), Sm_2O_3 (2.27%), to Eu_2O_3 (0.443%), together with minor components of HREE: Dy_2O_3 (0.124%) and Tb_4O_7 (0.068%: Lawrence, 2006). The lower-grade Duncan REE deposit located southeast of the CLD contains about 25% of the TREO resource, but it has a higher component of the more valuable HREE relative to the CLD.

Very high-grade lanthanide concentrations (up to 45% combined lanthanide oxides) in the regolith are attributed to secondary monazite in polycrystalline aggregates that often pseudomorph apatite. This monazite is particularly rich in LREE and low in thorium. The weathered monazite (Fig. 3.6C) is 50 times less radioactive than monazite from beach sands, having only 0.07% thorium and 0.003% uranium (Lottermoser, 1990). Other REE-bearing minerals include crandallite, rhabdophane, cerianite, and churchite (Fig. 3.6B). Churchite contains considerable amounts of high-grade yttrium (up to 2.5% Y_2O_3) and is an important host to the HREE. Niobium and tantalum-bearing pyrochlore, ilmenite, and niobian rutile in the primary carbonatite are concentrated in the apatite and magnetite-rich residual zone. Grades are typically variable and locally high (up to 1.5% Nb_2O_5 and 0.05% Ta_2O_5: Duncan and Willett, 1990). Higher grades of niobium (up to 6% Nb_2O_5) characterise the supergene zone where crandallite and goethite have been partly derived from the lacustrine-fluviatile sedimentary rocks. Richardson and Birkett (1995a) note that the LREE-bearing minerals monazite and rhabdophane occur in the upper part of the residuum, whereas the HREE and Y are preferentially concentrated at depth as xenotime and churchite. The mineralogy and spatial distribution of the REE-bearing minerals in the laterite profile are discussed in detail by Lottermoser and England (1988) and Lottermoser (1990). A schematic section of the mineralised laterite is shown in the inset diagram of Figure 3.5.

Source of REE: The lanthanide group of REE and yttrium are widely dispersed throughout the laterite regolith. These metals are derived from the major REE-bearing minerals (apatite, monazite, synchysite)

of the primary igneous carbonatite, and to a lesser degree, from other silicate and carbonate minerals (feldspar, calcite, dolomite) that contain trace amounts of REE. Primary apatite has an average lanthanide oxide content of ~0.5%. REE-bearing phosphatic lacustrine sedimentary rocks appear to be derived from the weathering of fine-grained detrital apatite and pyrochlore deposited in the deeper parts of broad paleodrainage channels (Fetherston, 2004).

Age of mineralisation: The age of the mineralised laterite (Fig. 3.6A) above the Mount Weld Carbonatite is not known, however, an overlying sequence of bioturbated lacustrine clay and sand, up to 70-m thick, is by analogy with other similar sequences in the Eastern Goldfields Province, considered to be Late Cretaceous to Early Cenozoic in age (Bunting et al., 1974; Duncan and Willett, 1990). A further relative age constraint on the development of the carbonatite weathering profile is provided by a Permian glaciation event, which would have removed any previous weathering products. Thus the surface exposure of the carbonatite intrusion and subsequent weathering are interpreted to have taken place during the Late Mesozoic to Early Cenozoic.

A maximum age for the supergene REE mineralisation is constrained by the age of the carbonatite intrusive host, which has been dated by several isotopic methods with various levels of precision. K.D. Collerson (1982: unpublished data) obtained a Rb-Sr isotopic age from fresh rock of 2021 ± 13 Ma with an initial $^{87}Sr/^{86}Sr$ ratio of 0.70200 ± 0.00006. This ratio is similar to that of the upper mantle approximately 2025 million years ago, indicating the carbonatite was directly derived from the mantle without significant crustal contamination. A biotite-rich calcite and apatite-bearing fragment has a K-Ar age of 2064 ± 40 Ma (A.W. Webb, 1973, unpublished data), and two Pb analyses yield a Pb-Pb age of 2090 ± 10 Ma, within error of the K-Ar age (Nelson et al., 1988). Mineral and whole-rock Re-Os isotopic data indicate that the Mount Weld Carbonatite is part of a larger coeval suite of low- to high-MgO alkaline ultramafic rocks (Turkey, Melrose, Granny Smith) and carbonatites (Ponton Creek) that were emplaced into the crust in the middle Paleoproterozoic. Isotopic data for oxide minerals, and carbonatite, kimberlite, and melonite rock types yield a precise Re-Os isochron of 2025 ± 10 Ma (Graham et al., 2003; 2004).

The age constraints discussed above indicate that the Mount Weld Carbonatite intrusive was part of a regional alkaline magmatic event that occurred about 2025 million years ago in the eastern Yilgarn Craton.

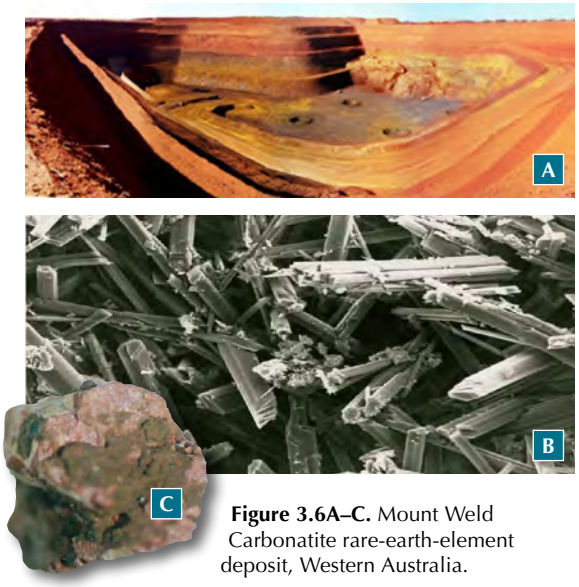

Figure 3.6A–C. Mount Weld Carbonatite rare-earth-element deposit, Western Australia.

A. Main open pit in the Mount Weld deposit. The REE-enriched laterite zone (yellow and orange colours) near the base of the pit is overlain by alluvium (red).

B–C. Two of the major REE-bearing minerals from Mount Weld are: B. churchite ($YPO_4 \cdot 2H_2O$: scanning-electron microscope image), and C. monazite $(Ce,La,Nd,Th)PO_4$.

Georgia Bunn (Lynas Corporation Limited: http://www.lynascorp.com/) provided the photographs.

Genetic model: The Mount Weld REE deposit formed from supergene enrichment processes that operated in the deep weathering profile of a large carbonatite body. Long-term leaching and redeposition by groundwater movement is the preferred model for REE enrichment (Cassidy et al., 1997). Lottermoser (1990) showed that the REE underwent pronounced lateral and vertical mobility during weathering, which was favoured by high-fluid/rock ratios, long fluid residence times, abundant REE complexing agents, and the decomposed condition of the primary igneous carbonatite minerals. Lottermoser (1990) also determined that the wide range of pH and alkaline conditions, and the carbonate anion concentrations in the groundwater variably influenced the different stabilities of LREE and HREE complexes which caused fractionation, separation, and deposition of LREE and HREE. The formation of a highly REE-enriched central laterite zone was facilitated by the lateral movement of groundwater flow towards a central topographic low of the laterite, and also the associated decreasing pH of the solutions favoured the mobilisation of large amounts of REE.

Key references: Duncan and Willett (1990): exploration history, regional and local geological setting, geochronology, mineral resources;
Lottermoser (1990), Lottermoser and England (1988): mineralogy, geochemistry; and
Graham et al. (2004): geochronology, petrogenesis.

Deposit Type 3.2: Scandium-bearing laterite associated with ultramafic-mafic rocks

General description: In contrast to the lanthanide group of REE (lanthanum to lutetium) and yttrium, which show a close genetical and spatial association with alkaline felsic igneous rocks, scandium has a closer affinity with high-magnesian ultramafic-mafic igneous rocks. In particular, the recent economic significance of scandium has been highlighted by its association with nickel and cobalt in deeply weathered laterite profiles superimposed above Phanerozoic mafic-ultramafic intrusions in New South Wales and ?older correlatives in Queensland. These intrusions have been variously described in the literature to having 'alpine'-, 'ophiolite'-, and 'Alaskan'-type affinities. Most of the Paleozoic intrusions are fault-bounded linear bodies that occur in anastomosing north-trending serpentinite belts associated with crustal-scale fault systems in the Lachlan Orogen of eastern Australia. The enrichment of scandium in the laterites appears to be a feature of the younger Phanerozoic bodies of eastern Australia, whereas the Ni-Co ± PGE laterites superimposed over Archean ultramafic (e.g., komatiitic) rocks in the Yilgarn and Pilbara cratons of Western Australia appear to have much lower concentrations of scandium. The most advanced projects with JORC-determined resources of nickel, cobalt, and scandium are the Lucknow and Greenvale deposits in Queensland and the Nyngan and Syerston deposits in New South Wales.

Australian deposits/prospects: Lucknow, Greenvale, and Kokomo (all Greenvale Province, Qld); Gilgai–Nyngan (Lachlan Orogen, NSW); Owendale-Tout–Fifield (Lachlan Orogen, NSW); Thuddungra (Lachlan Orogen, NSW), and Lake Innes near Port Macquarie (?New England Orogen, NSW).

Deposits outside Australia: Significant deposits of scandium associated with nickel-cobalt laterites appear to be rare, with few occurrences documented outside Australia. The Sipilou South nickel-cobalt-scandium laterite deposit is located in western Côte d'Ivoire, Africa (http://www.marketwire.com/press-release/Sama-Resources-Intersects-137-Metres-Up-25-Nickel-Its-Nickel-Cobalt-Scandium-Laterite-TSX-VENTURE-SME-1419535.htm). Drill intersections include 13.7 m @ 2.5% Ni, and scandium and cobalt concentrations in the limonitic section of the deposit attain 110 ppm and 0.34%, respectively. Similar scandium-bearing laterite deposits (Lola Project) also occur in the Republic of Guinea, West Africa.

Type example in Australia: Lucknow (part of NORNICO Project, Greenvale region), Queensland (Figs 3.7 and 3.8).

Location: Longitude: 144.9555; Latitude: -19.0284
~10 km southwest of Greenvale township, Queensland
1:250 000 map sheet: Clarke River (SE 55–13)
1:100 000 map sheet: Burges (7859)

Geological province: Greenvale Province (near boundary with Broken River Province), Lachlan Orogen, Queensland.

Resources: The Measured, Indicated and Inferred scandium resource (as of 19th January 2011; Table 3.3) for the Lucknow deposit that conforms to JORC guidelines is 6.24 Mt @ 169 g/t Sc (using 70 g/t Sc cut-off grade) including a higher-grade zone of 4.15 Mt @ 205 g/t Sc (using 120 g/t Sc cut-off grade).

Current status: Advanced projects with JORC-compliant resources.

Economic significance: The economic impacts of the scandium-bearing laterites in the Greenvale (Queensland) and Nyngan–Fifield (New South Wales) regions are generally not well understood at their early stages of development.

Geological setting: The southeastern part of the Georgetown Inlier in northern Queensland contains a number of mafic-ultramafic igneous complexes that have been the focus of exploration since nickeliferous laterites were first discovered in the Greenvale area in 1957 (see Appendix 7). The Boiler Gully, Sandalwood, Gray Creek and a number of smaller complexes occur in a structurally deformed region (Greenvale Province) located between the Precambrian rocks of the Georgetown Inlier and the Paleozoic rocks of the Broken River Province (Fergusson et al., 2007; Henderson et al., 2011). The complexes are spatially associated with the regional northeast–trending Gray Creek Fault Zone and Burdekin Fault Zone (Henderson et al., 2011). They show a common geological history of layered peridotite and gabbro intruded by gabbro and mafic dykes regionally metamorphosed and deformed (Arnold and Rubenach, 1976). Laterite cappings are developed on all types of basement rocks in the Greenvale region. For those associated with ultramafic rocks, the laterite profile is deep and mature, and nickel-cobalt concentrations attain ore grades in some deposits. The most significant scandium-enriched Ni-Co laterites are associated with the Gray Creek Complex (Lucknow deposit) and Boiler Gully Complex (Greenvale deposit).

The Gray Creek Complex is a ~25 km-long, northeast-trending lenticular body near Greenvale. This fault-bounded complex is surrounded by Paleozoic sedimentary and volcanic rocks of the Broken River

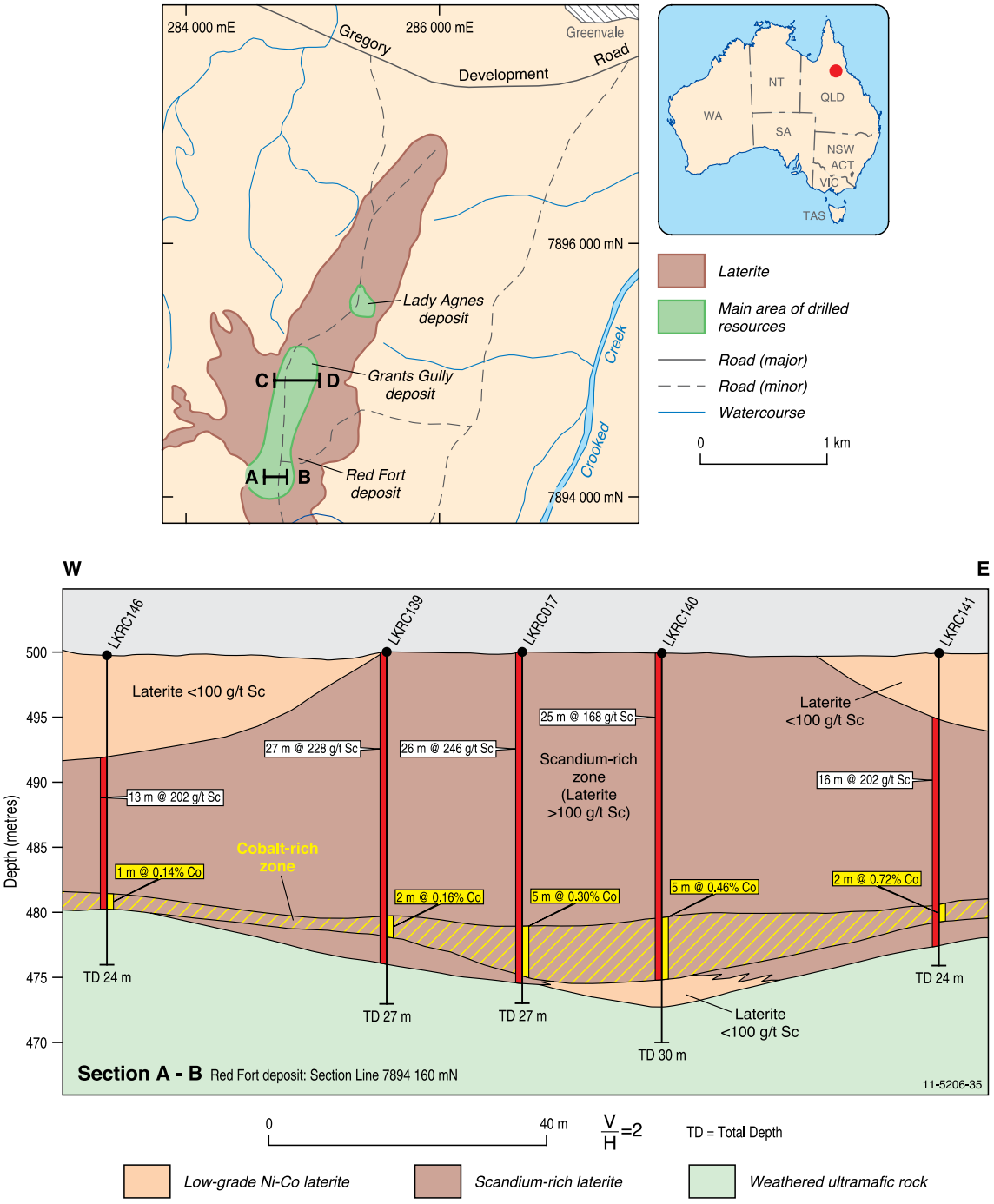

Figure 3.7. Distribution of scandium-bearing laterite (Lucknow Ni-Co-Sc Project) in the Greenvale region of northern Queensland. The Red Fort, Grants Gully, and Lady Agnes deposits have been the focus of drilling. The cross-section A–B for the Red Fort deposit highlights the wide thickness of scandium mineralisation (>100 g/t Sc) and the enrichment of cobalt in the lower part of the laterite profile. Modified from Metallica Minerals Limited (2010).

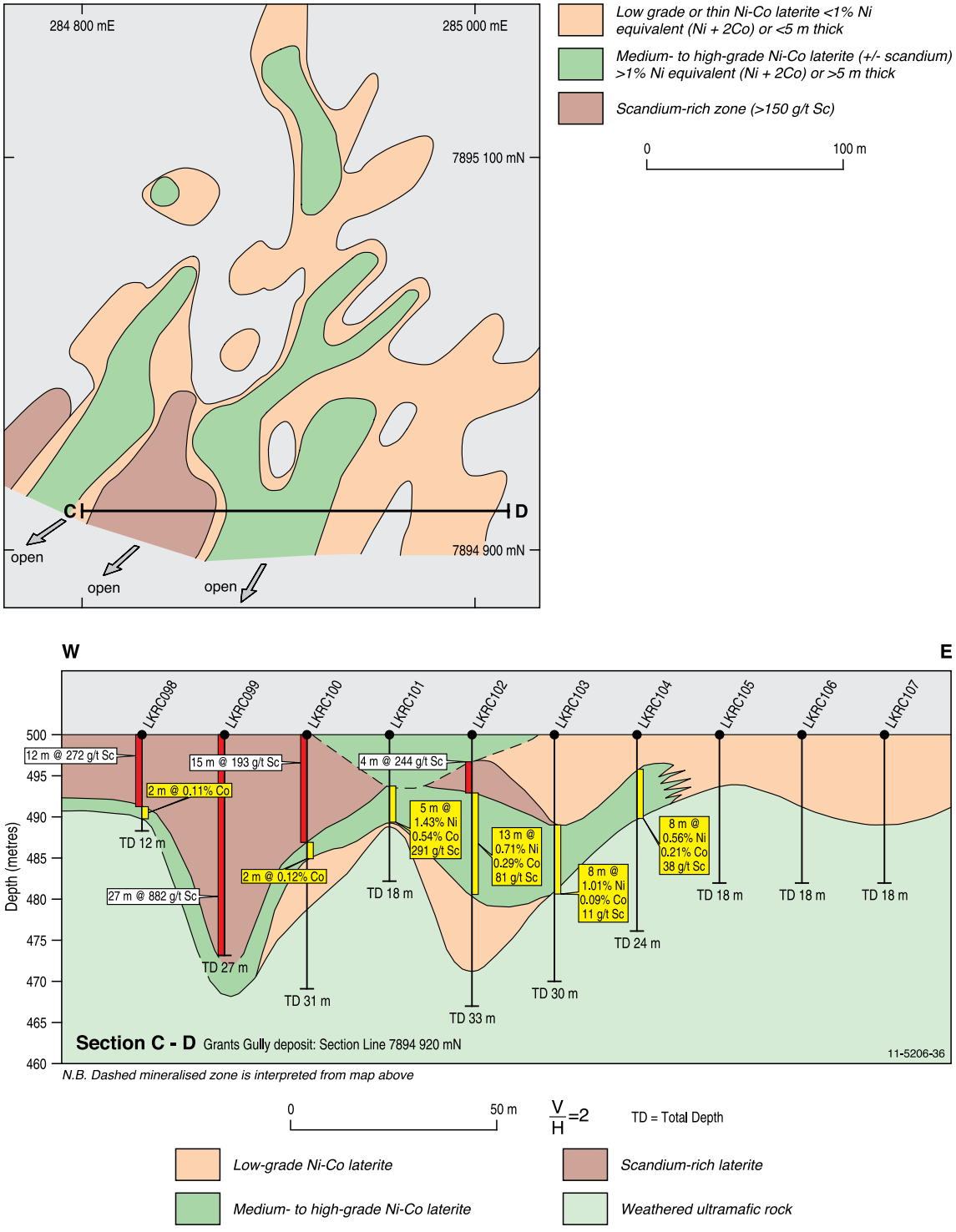

Figure 3.8. Metal distribution plan and cross-section C–D for the Grants Gully Sc-Ni-Co laterite deposit. The spatial distribution of metals has been generalised in the cross-section. The dashed mineralised zone in the cross-section is centred about drill hole LKRC101. The locations of the Grants Gully deposit and cross-section are shown in Figure 3.7. Modified from Metallica Minerals Limited (2010).

Province and is situated within the Gray Creek Fault Zone bounded by the Halls Reward Fault in the west and the Grey Creek Fault in the east (Henderson et al., 2011). Ultramafic and amphibolite rocks similar to those in the nearby Boiler Gully and Sandalwood complexes compose most of the northern and central parts of the complex. Dominant rocks include lateritised serpentinite, clinopyroxenite with interlayered wehrlite and gabbro, and amphibolite. The lateritised serpentinite is probably derived from dunite and peridotite. It contains relict olivine and enstatite, serpentine, chrysotile, chlorite, spinel, chromite, and magnetite. Cumulus textures are locally preserved in the pyroxenites. The northern end of the complex is characterised by a 500 m-wide core-zone of serpentinite flanked by clinopyroxenite that is interlayered with wehrlite and metagabbro. The southern part of the complex is represented by a younger phase of mafic magmatism that has produced a variety of rock types including extensive dykes, gabbro, tonalite, and trondhjemite. The complex has been intensely faulted both along the margins and internally, and it has been metamorphosed to amphibolite facies (Arnold and Rubenach, 1976). Fault zones have provided permeable zones for the advancement of alteration, and as major conduits for flushing away the soluble products of lateritisation. Rubenach (1982) notes that the mafic rocks of the Gray Creek and Boiler Gully complexes have geochemical characteristics of island-arc and ocean-floor tholeiites. Interpreted tectonic settings for the complexes range from Precambrian layered mafic-ultramafic intrusions, sills, and dykes emplaced along the southeastern margin of the Georgetown Inlier (Green, 1958; Arnold and Rubenach, 1976), to tectonically emplaced Precambrian ophiolites along the faulted margin of a Proterozoic craton (Rubenach, 1982), to fault-bounded Cambro-Ordovician bodies representing oceanic crustal components in an island-arc environment (Henderson et al., 2011).

Host rocks: Metallica Minerals Limited has defined high-grade nickel-cobalt and nickel-cobalt-scandium zones, as well as broad and thick scandium zones in the Lucknow deposit (Figs 3.7 and 3.8). The high-grade scandium mineralisation is contained within highly oxidised and weathered red-brown lateritic material and in many areas the mineralisation starts at surface and persists to a maximum depth of 40 m. Where the scandium is associated with high-grade nickel-cobalt grades, it usually occurs above these metals in the laterite profile. However, the scandium mineralisation is predominantly associated with low-grade nickel and cobalt abundances which possibly reflects the ultramafic rock protolith on which the laterite formed (Metallica Minerals Limited, 2010). The distribution of scandium in the laterite profile at Lucknow is summarised in Figures 3.7 and 3.8.

Table 3.3. Resource data for the Lucknow and Greenvale Sc-Ni-Co lateritic deposits.

Lucknow Sc-Ni-Co resource using a 70 g/t Sc cut-off grade (subject to Straits Resources Exploration Limited Joint Venture)						
Classification	Mt	Sc g/t	Ni%	Co%	NiEq%	Fe%
Measured	0.72	197	0.26	0.05	0.34	30.8
Indicated	2.67	171	0.19	0.04	0.27	35.4
Inferred	2.85	159	0.20	0.04	0.27	35.1
Total	6.24	169	0.20	0.04	0.28	34.7
Greenvale Ni-Co-Sc resource using a 0.70% nickel equivalent cut-off grade						
Classification	Mt	Sc g/t	Ni%	Co%	NiEq%	Fe%
Measured	2.63	33	1.08	0.09	1.26	22
Indicated	4.47	33	1.03	0.08	1.19	21
Inferred	0.90	30	0.99	0.07	1.12	19
Total	8.00	33	1.04	0.08	1.20	21

Source: Metallica Minerals Limited (2011).

The laterites at Greenvale are enriched in nickel (up to 2.5%), chromium (up to 3%), and to a lesser degree cobalt (up to 0.5%). Details of the behaviour and distribution of scandium in the Greenvale laterite are not available. The ore blanket extends over about 3.3 km^2 and averages about 8-m thickness with only minor lateral and vertical grade variation (Fletcher and Couper, 1975; Burger, 1982). Nickel in the ore horizon is fixed in goethite and népouite ($Ni_3Si_2O_5(OH)_4$), whereas cobalt is absorbed on smectite and manganese oxides (Burger, 1982). Fletcher and Couper (1975) divided the laterite profile at Greenvale into four zones; from the base they are:

1. weathered serpentinite laterite zone (average thickness ~10 m)—transition from fresh to weathered serpentinite corresponds to a specific gravity decrease from 2.7 to 1.4 and the development of saprolitic clays with parent-rock textures still preserved. Magnesite and goethite veinlets are developed along fractures, and chalcedonic and chrysoprase veins are abundant. Nickel is concentrated about 10 times the parent rock value and reaches a maximum near the upper boundary of this zone, whereas cobalt shows only minor enrichment. Almost 50% of the resources for the deposit are from this zone. The upper part of the zone is characterised by MnO_2 coatings and films on joints;
2. limonitic laterite zone (~5 m)—characterised by the lack of parent rock textures, with the mineralogy dominated by goethite and massive bands and irregular pods of secondary silica. Nickel concentrations are lower than the underlying zone, but cobalt attains maximum concentrations of 0.5% (25 times concentration) sympathetic with increased abundances of Cr_2O_3 and MnO_2;
3. pisolitic laterite zone (~7 m)—composed of ferruginous concretions, either partly cemented or unconsolidated, as pisolites, oolites, or irregular plates, which increase in abundance and diameter (to 5 cm) up the zone. A marked increase in density accompanies the mineralogical changes in this zone. Nickel and cobalt are depleted to background concentrations towards the top of the zone, with a marked increase in Al_2O_3; and
4. surface soils (~3 m)—red-brown unconsolidated residual soil with clayey layers, up to 10-m thick, but averaging 3 m, overlie pisolitic laterite or limonite.

REE mineralisation: Scandium is the only 'REE' documented in the laterite profile of the Lucknow deposit (Metallica Minerals Limited: http://www.metallicaminerals.com.au/). Serpentinised ultramafic rocks at the northern end of the Gray Creek Complex are mantled by a 500 to 1000 m-wide laterite layer containing several areas of Ni-Co-Sc mineralisation (Grants Gully, Red Fort, Lady Agnes). The Lucknow scandium-rich laterite deposit has significant bulk mineable drill intercepts of >200 g/t Sc that occur close to the Ni-Co ore zones. Extremely rich intersections of scandium (e.g., 27 m @ 882 g/t Sc) have been reported within these zones.

Source of REE: As with nickel, chromium, and cobalt, scandium is derived from the weathering of high MgO-bearing igneous rocks such as serpentinised dunite, peridotite, pyroxenite, and from more primitive basalts. Fresh serpentinite at Greenvale has a composition of about 37.1% SiO_2, 39.2% MgO, 0.63% Al_2O_3, 6.7% Fe_2O_3, 0.47% FeO, 0.28% Ni, and 0.01% Co. There are no known published references describing the scandium-bearing minerals concentrated in the Lucknow laterite deposit. In general, scandium is found in common rock-forming minerals, such as pyroxene, hornblende, and biotite, and in trace amounts (5 to 100 ppm) in basalt and gabbro. These three rock-forming minerals and mafic rock types are integral components of the igneous rock stratigraphy at Lucknow, and potentially could be a source(s) for the scandium. Scandium can also reside in the rare minerals thortveitite [$(Sc,Y)_2Si_2O_7$], which contains 44–48% scandium oxide Sc_2O_3, bazzite ($Be_3(Sc,Al)_2Si_6O_{18}$), wiikite (ill-defined mixture of REE), euxenite, and gadolinite.

Age of mineralisation: The precise age of the Ni-Co ± Sc laterites in the Greenvale region is not known. Fletcher and Couper (1975) proposed that erosion of cover rocks at Greenvale resulted in 5.5 km^2 of fractured hydrated serpentinite containing an evenly distributed 0.2% nickel being exposed to a Cenozoic land surface and climate. Burger (1982) suggested a possible mid-Cenozoic age for the main period of weathering and Ni-Co-Sc mineralisation, but there has been subsequent reworking and erosion of parts of the original laterite profile.

Similarly, the age(s) of the associated mafic-ultramafic protolith rocks are not well constrained with ages in the literature ranging from Late Proterozoic to early Paleozoic. Arnold and Rubenach (1976) showed that the Gray Creek Complex is structurally identical and chemically similar to the nearby Boiler Gully Complex suggesting a coeval/comagmatic association. Black et al. (1979) determined Mesoproterozoic Ar–Ar isotopic ages for S_1 hornblende from the Gray Creek Complex of 1111 ± 30 Ma and 1316 ± 40 Ma; the latter

providing a minimum age for the complex. However, Rubenach (1982) considers these ages equivocal due to possible complications of excess argon during isotopic analysis. Henderson et al. (2011) proposed that if a temporal relationship to other mafic-ultramafic belts in eastern Australia is used, then a Cambrian age is possible for the Greenvale complexes (Spaggiari et al., 2003). Recently, Huston (GA: pers. comm., 2011) determined a preliminary whole-rock Sm-Nd age of 466 ± 37 Ma for the Gray Creek Complex.

Similar laterites associated with 'Alaskan'-type mafic-ultramafic intrusions in the Fifield district of New South Wales are enriched in scandium (see Appendix 7). During the late Paleozoic, deep erosion exposed these intrusive complexes whilst continued weathering during the Mesozoic saw the development of up to 50-m thick laterite profiles and the scouring of paleo-alluvial channels in the underlying intrusions (http://www.platinaresources.com.au/files/projects/PC00736_Platina_Factsheet_Owendale_v1.pdf).

Genetic model: The following summary describing the genesis of the Ni-Co ± Sc laterite profiles in the Greenvale region is in part from Solomon and Groves (1994), and the references cited within. The prolonged weathering of serpentinised ultramafic rocks in a well drained, well aerated, and hence highly oxidised environment resulted in the removal of elements such as magnesium, and retention of nickel, chromium, cobalt, and scandium. Fracturing of the source serpentinite rock may have preceded weathering and facilitated the formation of a permeable profile. The water table probably was near the top of the saprolite zone. At a predicted rate of formation of 10 to 20 metres per million years, the Greenvale profile would have required at least one million years to become established during the Cenozoic. Fletcher and Couper (1975) suggested the rainfall was cyclic (monsoonal?), with periods of downward leaching by acid waters alternating with periods of oxidation; acidity derives from CO_2 in the atmosphere and NO_3^{2-} from the decay of vegetation. Steep groundwater gradients and lateral water movement allowed removal of soluble elements. The enrichment in nickel (factor of 10 times), chromium, cobalt, and scandium results in part from retention of primary metals in secondary silicates (e.g., népouite), and also from a concentration at the base of the profile of metal dissolved from higher levels. Dissolved nickel species migrate further down the profile due to higher solubilities compared to aqueous species of scandium, chromium, and cobalt. The development of lateritic profiles superimposed on ultramafic rocks in the Greenvale region is a function of the rate of downward movement of oxidation and surface erosion (Fletcher and Couper, 1975).

Key references: Fletcher and Couper (1975): petrology of ultramafic rocks, mineralisation and genesis of mineralised laterite;

Arnold and Rubenach (1976): regional geological setting, geology, and structure of mafic-ultramafic complexes;

Solomon and Groves (1994): genesis of mineralised laterites;

Fergusson et al. (2007): lithostratigraphy, structural, and deformational history of Greenvale region;

Henderson et al. (2011): regional geological setting, petrology, and geochemistry of country rocks, tectonic synthesis;

Metallica Minerals Limited: ASX Release 19th January 2011 (http://www.metallicaminerals.com.au/sites/default/files/MLM_Greenvale_Resource_Update.pdf); and

Metallica Minerals Limited: Quarterly Report to 31 December 2010, ASX Release 31st January 2011 (http://www.metallicaminerals.com.au/sites/default/files/MLM%20Qtly%20Dec10.pdf): mineralisation and resources of Lucknow and Greenvale laterite deposits.

Deposit Type 3.3: Beach sand heavy-mineral deposits with rare-earth-element-bearing monazite

General description: Heavy-mineral beach sand deposits have maintained Australia's position as a major world producer of rutile, ilmenite, and zircon for over four decades. Mining of beach sands first started on a major scale on the Australian east coast in the late fifties, then shifted to the fossil beach sand deposits of the Capel, Yoganup, and Happy Valley strandlines in the southwest of Western Australia, south of Perth, and on the fossil beach sand deposits at Eneabba (Fig. 3.9) and Cooljarloo north of Perth. The fossil beach sand deposits of the Murray Basin emerged in the mid nineties and now support mining operations at Ginkgo and Snapper in central New South Wales and the Douglas and Kulwin operations in Victoria. The latest emerging heavy-mineral province is the Eucla Basin where zircon is the dominant commercial mineral rather than the titanium-rich minerals of rutile, ilmenite, and leucoxene. The accessible beach sand heavy-mineral resources of the east coast of Australia have been mined out and all beach sand operations have closed down. The heavy-mineral beach sand deposits as defined here include a suite of beach placers comprising 'lag' deposits, 'transgressive' deposits, 'regressive' deposits, and 'aeolian' deposits in associated coastal

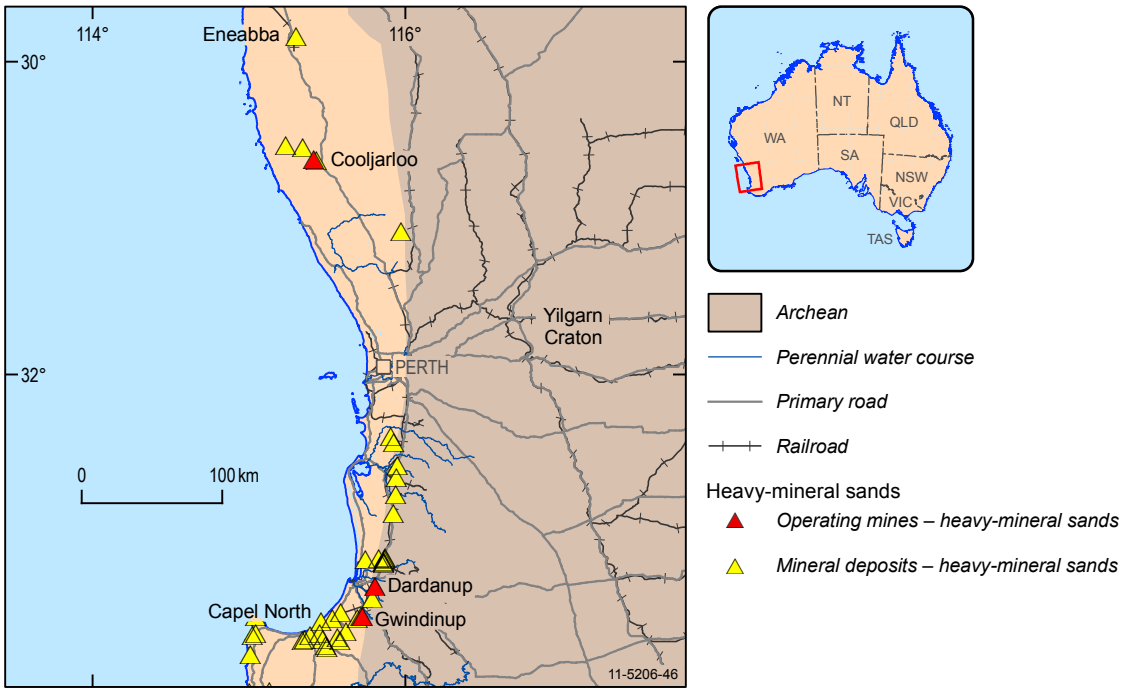

Figure 3.9. Beach sand heavy-mineral deposits along fossil beach strandlines in the Perth Basin, Western Australia.

dunes (Roy, 1999; Hou, 2005). The high dunes as described by McKellar (1975) are described separately under Deposit Type 3.4.

Australian deposits: Virtually all of the heavy-mineral resources in beach sand deposits in Australia are hosted in numerous deposits in inland fossil beach strandlines. The heavy-mineral sand deposits in fossil beach strandlines are located in the Murray Basin, of New South Wales, Victoria, and South Australia; in the southern Perth Basin along the Yoganup and Happy Valley strandlines and along the Eneabba and Cooljarloo fossil strandlines in the northern part of the Perth Basin in Western Australia. Some of the more important heavy-mineral sand developments in the Eucla Basin of South Australia include the recently commissioned heavy-mineral sand mine of Jacinth-Ambrosia, and the undeveloped deposit of Cyclone (Fig. 3.10).

Deposits outside Australia: Lake Malawi, Malawi; Srikurman, Andhra Pradesh, India; Chavara, Kerala, India; Alcobaca, Bahia, Brazil (Orris and Grauch, 2002).

Type example in Australia: Eneabba (Perth Basin, WA: Fig. 3.9); Jacinth-Ambrosia and Cyclone (both in Eucla Basin, SA: Fig. 3.10); Douglas and Ginkgo (both in Murray Basin: Vic and NSW, respectively).

Location: Eneabba: Longitude: 115.3003; Latitude: -29.8368
~240 km northwest of Perth, Western Australia
1:250 000 map sheet: Dongara (SH 50–05)
1:100 000 map sheet: Arrowsmith (1938)

Geological province: The Eneabba fossil beach strandlines are located on the Northern Swan Coastal Plain and overlie the Perth Basin, and there are also fossil beach strandlines on the Southern Swan Coastal Plain over the southern Perth Basin in southwest of Western Australia. The other provinces with fossil beach strandline heavy-mineral sand deposits are the Murray Basin in New South Wales, Victoria, and South Australia, and the Eucla Basin in South Australia and Western Australia (Fig. 3.10).

Resources: Beach sand placer deposits represent a major source of rutile, ilmenite, zircon, and in the past–of monazite. According to Lissiman and Oxenford (1975), the original resource at Eneabba was of the order of 25 to 30 million tonnes of recoverable heavy minerals with a monazite content of about 0.5%. Production of monazite at Eneabba, for extraction of REE and thorium, peaked between 1975 and 1985 (Shepherd, 1990).

Current status: Eneabba is a major heavy-mineral sand mine currently under care and maintenance, but REE have not been recovered from monazite since 1995.

Economic significance: Prior to 1995, Eneabba was a significant exporter of monazite for extraction of REE and thorium. Currently the REE are not extracted from the monazite which is returned back to the mine site.

Geological setting: Heavy-mineral deposits in coastal regions require a stable tectonic environment with efficient sorting and winnowing mechanism by wave action and wind which sort sediments derived from deeply weathered igneous–metamorphic terranes or from older sedimentary rocks derived from the original igneous–metamorphic terranes. Faulting during sedimentation has influenced the distribution of heavy-mineral deposits in the Murray Basin (Roy et al., 2000).

Host rocks: Pleistocene–Holocene dune sand, Middle Eocene to Miocene in Eucla Basin.

REE mineralisation: The REE are held within the monazite and xenotime contents of the heavy-mineral concentrate. The range of REO contents in monazite and xenotime in both minerals from concentrates from Western Australia is shown in Table 3.4. Table 3.5 shows REO and thorium oxide contents in monazite and xenotime concentrates from Eneabba, Capel, and Yoganup mines in Western Australia as produced prior to 1996. Figures from similar concentrates from the USA, India, and Malaysia are also included for comparison. Table 3.6 provides a comparison of the distribution of REO in monazite from three mines in Western Australia with mines in the USA, Taiwan, China, and India.

Table 3.4. Variation of the chemical composition (%) of individual monazite and xenotime grains from concentrates, Western Australia (Elsner, 2010).

	Monazite			Xenotime		
	Range	Mean	Standard deviation	Range	Mean	Standard deviation
La_2O_3	8.9–21.0	14.53	2.13	-	-	-
Ce_2O_3	21.7–35.0	28.52	2.17	-	-	-
Pr_2O_3	1.8–3.2	2.53	0.26	-	-	-
Nd_2O_3	4.8–12.7	8.85	0.26	-	-	-
Sm_2O_3	0.36–2.89	1.53	0.45	<0.16–1.82	0.47	0.22
Gd_2O_3	<0.16–2.71	0.88	0.51	<0.16–4.56	1.91	0.59
Dy_2O_3	<0.16–1.28	0.26	0.30	2.4–7.5	5.11	0.72
Ho_2O_3	-	-	-	<0.16–1.59	1.17	0.16
Er_2O_3	<0.16–0.45	0.02	0.08	2.5–6.6	4.63	0.49
Tm_2O_3	-	-	-	<0.16–0.70	0.70	0.14
Yb_2O_3	-	-	-	1.4–11.4	4.56	1.22
Lu_2O_3	-	-	-	<0.16–1.95	0.54	0.24
Y_2O_3	<0.06–6.25	1.19	0.66	40.2–53.2	46.82	1.91
ThO_2	1.2–21.9	8.79	0.08	<0.17–8.44	0.46	0.68
UO_2	<0.17[1]–0.75	0.08	0.23	<0.17[1]–5.82	0.57	0.86
CaO	0.12–2.50	0.98	1.10	<0.02[1]–0.54	0.06	0.06
SiO_2	0.12–4.01	1.09	0.66	<0.02[1]–1.98	0.38	0.26
P_2O_5	25.1–32.6	30.33	1.24	29.7–36.4	34.55	0.73
Total	92.5–103.1	99.58	2.10	96.0–105.2	101.93	1.17

[1] Below detection limit.

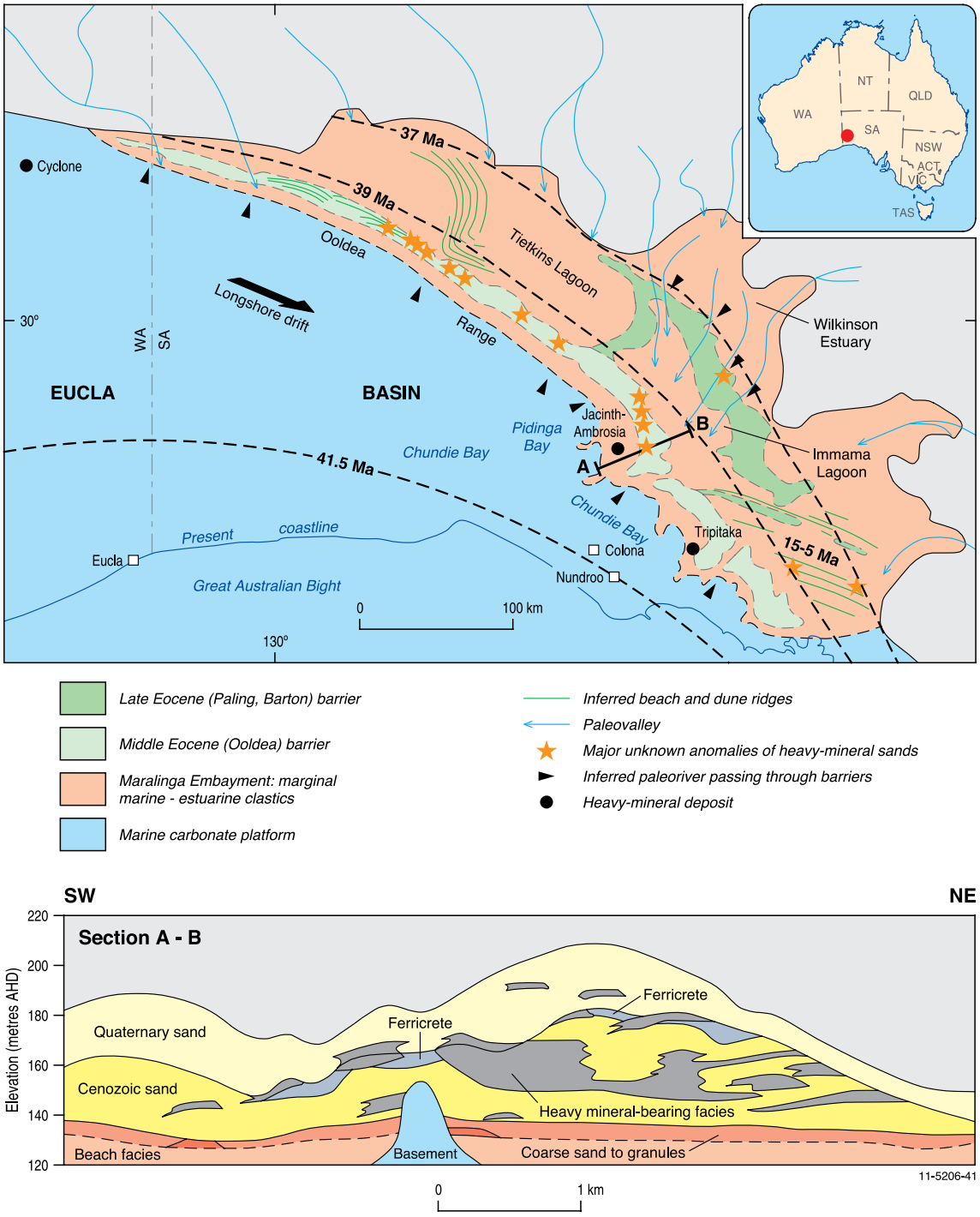

Figure 3.10. Fossil beach strandlines and heavy-mineral deposits in the Eucla Basin and cross-section, South Australia. Four generations of shorelines are shown by dashed lines at 41.5 Ma, 39 Ma, 37 Ma, and 15–5 Ma. Modified from Hou (2005).

Table 3.5. Chemical composition (%) of monazite and xenotime concentrates (Elsner, 2010).

Area of deposit or producer	REO	ThO_2	H_2SO_4-insoluble	TiO_2	P_2O_5
WA–Eneabba	58	6.4			
WA–Capel	57	7			
WA–Yoganup (guaranteed)	>55	>6	<10		
WA–Yoganup (typical)	56–58	6.5–7.0	7.0–8.5	0.3–0.6	
USA–Green Cove Springs	57	7			
India–KMML	57.5	7.96	5.05		28.2
Malaysia–monazite average		6			27
Malaysia–xenotime average		0.7			29

Source of REE: At Eneabba the immediate source for the REE-bearing monazite in the dune and beach sands is considered to be the underlying Mesozoic sedimentary rocks, but the Archean crystalline basement provided the original source rocks (Shepherd, 1990).

Age of mineralisation: The age range varies from late Neogene to early Pleistocene for the Eneabba region on the Northern Swan Plain. Elsewhere the age varies from Holocene along present day beaches to as old as Eocene in the Eucla Basin.

Genetic model: Heavy-mineral concentrations in beach sands form by high energy wave action and are built up along coastal regions of stable crustal margins with tectonic stability important for preservation of deposits. Environmental conditions for fractionating mechanisms to operate include: low rates of clastic sediment supply and long periods of weathering and abrasion to create a mature heavy-mineral suite, an energetic swell wave climate driving large sand fluxes onshore and alongshore, and changing sea levels (especially marine transgressions) that have the effect of moving heavy minerals from the shelf onto the present coast (Roy, 1999). The sorting action is most effective under conditions of surf wave action during storms and long-shore drift along 'J' curved shorelines preceding a headland (McKellar, 1975; Baxter, 1977). The heavier minerals are obstructed by the headlands to form deposits while the lighter grains are carried around the headlands by wave action. At Eneabba, monazite contents can be up to 7% near the southern end of the strandlines, i.e., in the direction of the longshore drift approaching a headland (Shepherd, 1999; page 1593). The Eneabba heavy-mineral deposits are located in a series of fossilised shorelines between 29 and 115 m above sea level. The highest heavy-mineral concentrations occur over a length of 20 km and a width of 9 km (Shepherd, 1990).

Key references: Baxter (1977) and Roy (1999): origin and resources of heavy-mineral deposits; and Elsner (2010): chemical analyses of monazite and xenotime from heavy-mineral deposits.

Deposit Type 3.4: High dune sand heavy-mineral deposits with rare-earth-element-bearing monazite

General description: McKellar (1975) noted that remnants of a system of old dunes exceeding 180 m in height occur at intervals along the east coast from the Hawkesbury River in New South Wales to Fraser Island in Queensland. The very large low-grade heavy-mineral resources in these high dune sand deposits are described here as a separate class from the usual transverse aeolian and beach foredunes associated with the suite of beach sand heavy-mineral deposits. The most significant high dune sand heavy-mineral deposits are along the east coast of Queensland between the North and South Stradbroke Islands near Brisbane in south and Fraser Island in the north. The Byfield deposit, 380 km northwest of Fraser Island, is also hosted in high dune sands. Generally the heavy-mineral content in dune sands is less than 0.05 %, but in places it attains ore grades of 1 to 2% heavy minerals with sand tonnages ranging from a few hundred million tonnes to large mineralised zones in dune sands in excess of a billion tonnes. The Byfield deposit, for example, has 2.4 billion tonnes of sand at 1.14% heavy minerals, or 0.09% ilmenite, 0.06% rutile, and 0.16% zircon (Strategic Minerals Corporation, 2004). Unpublished data indicate that the heavy minerals contain about 0.2% monazite. The high dune sand heavy-mineral deposits are often fringed by heavy-mineral beach sand deposits.

Table 3.6. Chemical composition of monazite concentrates from selected deposits world wide (Elsner, 2010).

	Manavalakurichi MK-Grade Indian Rare Earths Ltd. Tamil Nadu, India	**Beihai Processing Plant** Guangxi Province China	**Folkston (I)** Humphreys Gold Corp. Georgia, USA	**Folkston (II)** Humphreys Gold Corp. Georgia, USA	**Green Cove Springs (I)** Iluka Resources Ltd. Florida, USA	**Green Cove Springs (II)** Iluka Resources Ltd. Florida, USA	**Capel** Western Titanium N.L. Western Australia	**Eneabba** RGC Mineral Sands Ltd. Western Australia	**Yoganup** Westralian Sands Ltd. Western Australia	**Indonesia**	**Black Monazite** Taiwan	**Brazil**
REO total		**61.86**	**av. 58.9**	**60.53**	**58.57**	**55.04**			**56.0-58.0**			**59.2**
La_2O_3	15.7			11.99	11.98	10.03	16.20	14.82	13.5	14.29	25.41	8.64
CeO_2	30.6		av. 25.4	26.45	26.49	27.12	26.70	27.60	26.0	30.25	23.18	26.94
Pr_6O_{11}	2.9			3.07	2.99	2.55	2.60	2.93	2.85	3.35	1.27	3.55
Nd_2O_3	10.5			10.6	9.99	8.72	11.00	9.44	9.82	10.77	7.95	14.50
Sm_2O_3				2.09	2.09	1.72	1.30	1.45	1.43	2.01		3.26
Eu_2O_3				0.16	0.14	0.12	0.02		0.03			
Gd_2O_3				1.38	1.40	1.41	0.30		0.84			
Tb_4O_7				0.16	0.15	0.14			<0.02			
Dy_2O_3				0.77	0.63	0.53	0.20		0.39			
Ho_2O_3				0.14	0.107	0.087	+		<0.03			
Er_2O_3				0.312	0.168	0.139			0.12			
Tm_2O_3				0.038	0.018	0.014			<0.01			
Yb_2O_3				0.178	0.066	0.058			0.07			
Lu_2O_3				0.0200	0.0090	0.0068			<0.02			
Y_2O_3	0.04	2.22		3.16	2.35	2.39	0.60	1.42	1.36	2.51	1.07	
H_2SO_4-insol.[1]			av. 8.2			8.25	8.50		7.0-8.5		22.94	
TiO_2	0.4		av. 0.42			0.09		0.81	0.3-0.6	0.09		1.75
SiO_2	2.4	1.23	av. 2.6					2.55		2.17	18.08	2.2
ZrO_2	1.3	0.13	av. 3.8					2.05		0.20		
Al2O_3	0.1	0.14	av. 1.7					0.81		0.37		
Fe_2O_3	0.9	0.62	av. 0.63					0.33		n.d.		0.51
P_2O_5	29.2	30.00					27.00	26.55		27.46	20.55	26.0
ThO_2	9.0	6.31	av. 4.2			4.24	6.80	6.40	6.5-7.0	4.67		6.5
U_3O_8								0.31		0.32		0.17
CaO		0.16	av. 1.1					0.95		0.18	+	
LOI	0.1							0.52		0.60		

[1] Proportion of REO insoluble (insol.) in H_2SO_4.

Australian deposits: Byfield, Fraser Island, Cooloola, Moreton Island, and North Stradbroke Island (all Qld).

Deposits outside Australia: Richards Bay South Africa, Trail Ridge USA (Orris and Grauch, 2002; Jackson and Christiansen, 1993).

Type example in Australia: North Stradbroke Island, Queensland (Fig. 3.11).

Location: Longitude: 153.4425; Latitude: -27.4784
~30 km east-southeast of Brisbane, Queensland
1:250 000 map sheet: Brisbane Special (SG 56–15)
1:100 000 map sheet: Brisbane (9543)

Geological province: The high dune sands occur at intervals over a distance of about 1400 km along the east coast of Australia from the Hawkesbury River in New South Wales to Byfield in Queensland (Fig. 3.11).

Resources: The latest published resources for North Stradbroke Island, as in December 2008, amounted to Measured, Indicated, and Inferred Resources of 1195 million tonnes of sand at 0.9% heavy minerals, or 10.36 million tonnes of heavy minerals at 47% ilmenite, 11% zircon, and 14% rutile (Iluka Resources Limited, 2008). Gardner (1955) reported the monazite content in the heavy-minerals concentrate as 0.3%. Cassidy et al. (1997) reported a total resource for the North Stradbroke Island deposit in the order of 3000 million tonnes at about 1% heavy minerals with the proportion of monazite recovered from the heavy-minerals concentrate of about 0.2% of the heavy-mineral concentrate.

Current status: A major operating heavy-mineral sand mine but REE are not recovered from monazite.

Economic significance: The North Stradbroke Island dune sand deposit is the only heavy-mineral-mining operation remaining on the east coast of Australia. Fraser Island, Cooloola, and Moreton Island deposits are within various types of conservation reserves and these resources are not available for mining. The North Stradbroke Island deposit is mined for its rutile, zircon, and ilmenite content. The REE are not extracted from the monazite which is returned back to the mine site.

Geological setting: Heavy-mineral concentrations in dune sands form by the winnowing action of wind. Dune sands built up along coastal regions of stable crustal margins with tectonic stability important for preservation of deposits. North Stradbroke Island is a complex coastal sedimentary system comprising beach sand, parallel dune sand and high transverse dune sand deposits. Most of the heavy-mineral sand resource occurs as low-grade heavy-mineral zones in the large transverse dune sand. North Stradbroke Island forms part of the Pleistocene–Holocene heavy-mineral-bearing sand mass of the east Australia coastal zone between the Hawkesbury River in the south in New South Wales to Byfield in Queensland in the north.

Host rocks: Pleistocene–Holocene dune sand, some possibly as old as Miocene.

REE mineralisation: The REE is held within the monazite content of the heavy-mineral concentrate with the REO content in monazite at around 55% to 60%. The distribution of the REO in monazite from North Stradbroke Island is shown in Table 3.7 and a world-wide distribution of REO in monazite from undifferentiated types of heavy-mineral sand deposits is shown in Table 3.8.

Table 3.7. Distribution of types of rare-earth elements in monazite from North Stradbroke Island, Queensland (Hedrick, 2000).

REO	REO in monazite from North Stradbroke Island, Queensland (weight%)
La_2O_3	21.50
CeO_2	45.80
Pr_6O_{11}	5.30
Nd_2O_3	18.60
Sm_2O_3	3.10
Eu_2O_3	0.80
Gd_2O_3	1.80
Tb_4O_7	0.30
Dy_2O_3	0.60
Ho_2O_3	0.10
Er_2O_3	0.20
Tm_2O_3	-
Yb_2O_3	0.10
Lu_2O_3	0.01
Y_2O_3	2.10
Total	100.71

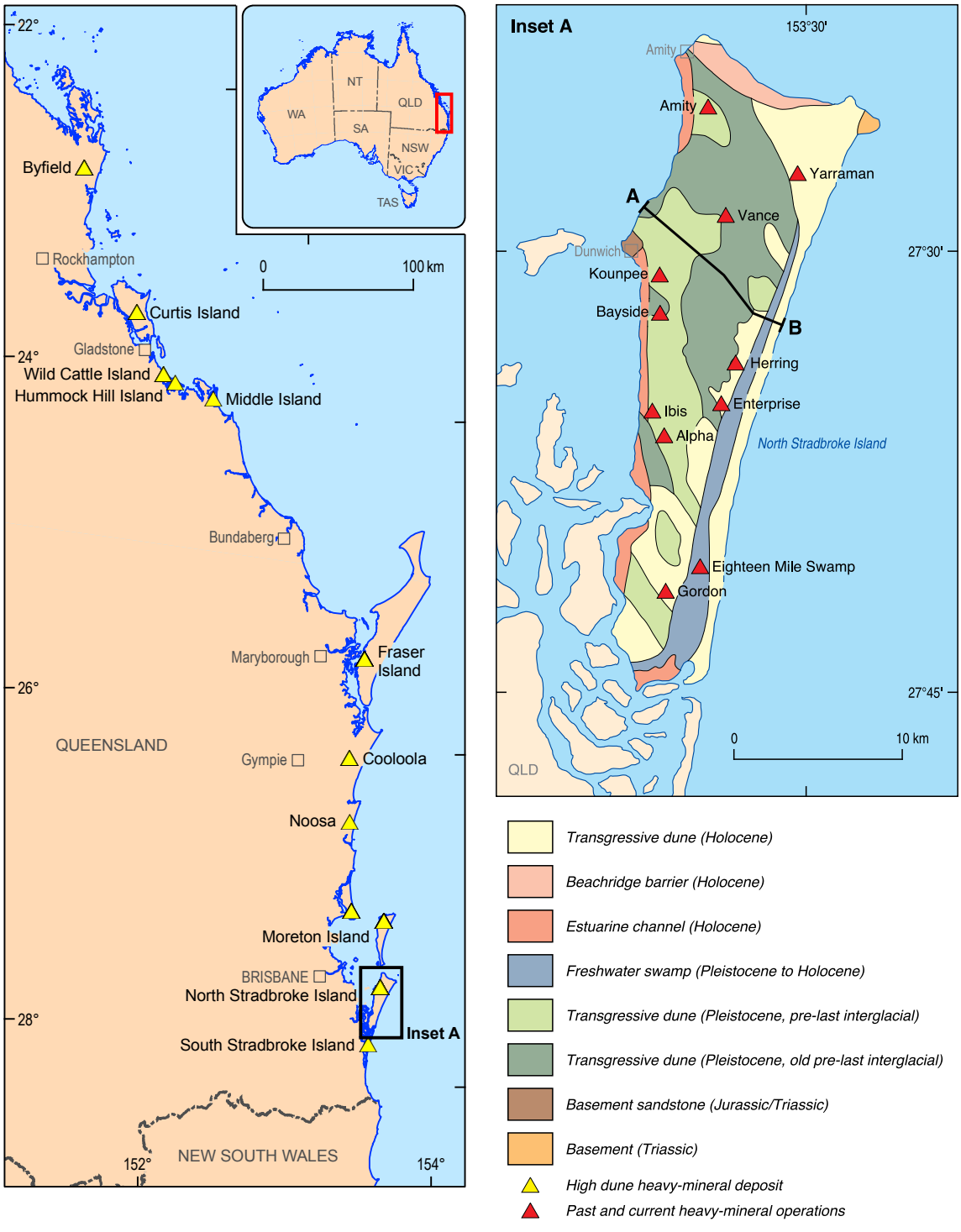
22°
24°
26°
28°
152°
154°
NEW SOUTH WALES
QUEENSLAND
Byfield
Rockhampton
Curtis Island
Gladstone
Wild Cattle Island
Hummock Hill Island
Middle Island
Bundaberg
Maryborough
Fraser Island
Gympie
Cooloola
Noosa
Moreton Island
BRISBANE
North Stradbroke Island
South Stradbroke Island
Inset A
0
100 km
NT
WA
SA
QLD
NSW
VIC
TAS
Inset A
153°30'
27°30'
27°45'
Amity
Yarraman
Vance
Dunwich
Kounpee
Bayside
Herring
Enterprise
Ibis
Alpha
North Stradbroke Island
Eighteen Mile Swamp
Gordon
A
B
0
10 km
QLD
Transgressive dune (Holocene)
Beachridge barrier (Holocene)
Estuarine channel (Holocene)
Freshwater swamp (Pleistocene to Holocene)
Transgressive dune (Pleistocene, pre-last interglacial)
Transgressive dune (Pleistocene, old pre-last interglacial)
Basement sandstone (Jurassic/Triassic)
Basement (Triassic)
High dune heavy-mineral deposit
Past and current heavy-mineral operations

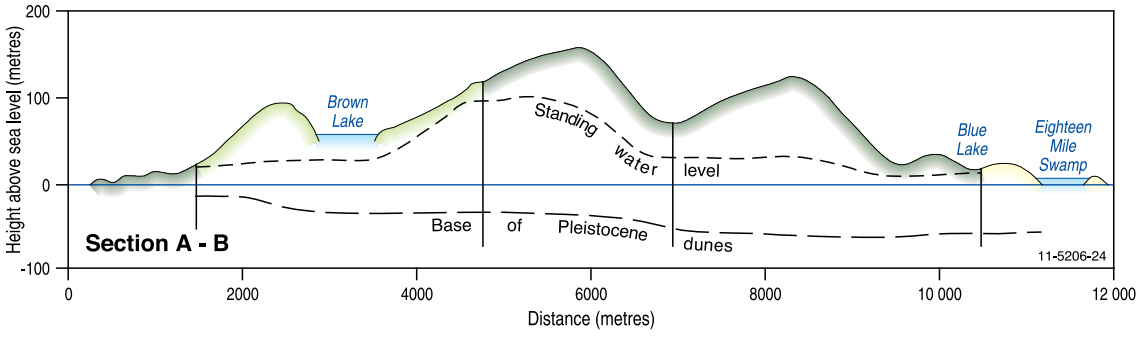
Height above sea level (metres)
200
100
0
-100
Brown Lake
Standing water level
Blue Lake
Eighteen Mile Swamp
Base of Pleistocene dunes
Section A - B
11-5206-24
0
2000
4000
6000
8000
10 000
12 000
Distance (metres)

Table 3.8. Distribution of types of rare-earth elements in monazite from different parts of the world (modified from Mukherjee, 2007).

Rare-earth oxide	Guangdong, China (wt %)	Taiwan (wt %)	Florida, USA (wt %)	India (wt %)	Australia (wt %)
La_2O_3	23	21	17.4	22	23.2
CeO_2	42.7	47.9	43.7	46	46.3
Pr_6O_{11}	4.1	5.4	4.9	5.5	4.9
Nd_2O_3	17	18.7	17.1	20	18.3
Sm_2O_3	3	3.3	4.9	2.5	2.5
Eu_2O_3	<0.1	0.54	0.16	0.016	0.04
Gd_2O_3	2	1.6	6.5	1.2	1.7
Tb_4O_7	0.7	0.19	0.26	0.06	0.22
Dy_2O_3	0.8	0.35	0.59	0.18	0.56
Ho_2O_3	0.12	0.03	0.11	0.02	0.08
Er_2O_3	<0.03	0.03	0.04	0.01	0.06
Tm_2O_3	Tr	-	0.03	Tr	-
Yb_2O_3	0.24	0.07	0.21	Tr	0.04
Lu_2O_3	<0.14	-	0.03	Tr	-
REO	55	48–62	-	58	58.5
Y_2O_3	2.4	0.19	3.18	0.45	1.57

Source of REE: The ultimate source for the REE-bearing monazite in the dune and beach sands is considered to be igneous–high-grade metamorphic rocks, but generally monazite was captured with zircon, rutile, and ilmenite in earlier depositional cycles and subsequently eroded.

Age of mineralisation: The age range of dune and beach sands is considered to be Miocene to Holocene, but generally Pleistocene to Holocene. Limited data summarised by Lees (2006) indicate that at least eight dune sand emplacements can be recognised in the sand masses of the Great Sandy region of southern Queensland that includes Fraser Island, Cooloola, the Peregian sandhills, Moreton, and the Stradbroke islands. Available optically stimulated luminescence (OSL) dating has identified episodes of dune emplacements at Cooloola at about 730 000 years ago (years before present (YBP)), at about 460 000 YBP, 395–280 000 YBP, 215–195 000 YBP, 170–130 000 YBP at between 9500–7500 YBP, 3100 YBP and 500 YBP. Lees (2006) noted that there were very few dates available for the other dune sand masses in the area.

New South Wales data summarised by Lees (2006) show a complex sequence of six dune forming events for Newcastle Bight–Myall Lakes area in New South Wales. Age estimates for these events range from 36–30 000 YBP (^{14}C), 18–17 000 YBP, 9–7000 YBP (7280 ± 220 ^{14}C YBP and 8850 ± ^{14}C YBP), one at about 3500 YBP, another at about 2500 YBP, and one between 800 and 400 YBP. Older dune-forming events (170–130 000 YBP) have been identified at other locations including Red Point and Port Stephens in New South Wales, but error ranges for these older events are considered to be too broad for meaningful analysis (Lees, 2006).

Genetic model: Heavy-mineral deposits in coastal regions require a stable tectonic environment with efficient sorting and winnowing mechanism by wave action and wind which sort sediments from a deeply weathered igneous–metamorphic terranes or from older sedimentary rocks derived from the original igneous–metamorphic terranes. The low-grade heavy-mineral concentrations in the dune sands are usually derived by wind action from higher-grade heavy-mineral concentrations on the beach previously formed by wave action. McKellar (1975) postulated that the

Figure 3.11 (see opposite). High dune sand heavy-mineral deposits along the southern Queensland coast, including geology of North Stradbroke Island (Inset A) and cross-section. Modified from Wallis and Oakes (1990).

high dune system on the east coast of Australia was formed during periods of maximum sea level depression under climatic extremes of the ice ages. According to Chappell and Shackleton (1986), sea level oscillations over the last 150 000 years are marked by a large marine recession 150 000 years ago when the sea level dropped to a maximum of 150 m below the present sea level followed by a similar drop of 150 m about 10 000 years ago. At times of maximum low sea levels, broad expanses of unconsolidated sand would have been exposed and swept inland by wind to form high dune systems which reach heights in excess 180 m and above the current sea level. According to Lees (2006), while the bulk of the dunes on the north and northeast Australian coast were emplaced during glacial maxima, this does not appear to be the case for the east coast where the high dunes on the North Stradbroke Island are located and more dates are required to determine the formation of the dunes in the eastern region.

Key references: McKellar (1975): distribution and origin of the high dune sands; and
Lees (2006): age estimates of dune formation.

Deposit Type 3.5: Offshore-shallow-marine heavy-mineral deposits with rare-earth-element-bearing monazite–(WIM 150 type)

General description: The resources of the five fine-grained (less than 80 micron) WIM deposits (WIM 50, 100, 150, 200 (now renamed as Jackson deposit) and 250 (Donald deposit)) have not been fully assessed and are currently under investigation for their zircon, rutile, and ilmenite content (Fig. 3.12). The presence of thorium and uranium in monazite discourages commercial interest in processing monazite for its rare earth content. Mining companies generally do not publish detailed resource assessments of monazite in heavy-mineral deposits, including those of the WIM deposits. Detailed assessments of the REO content in the monazite also are not generally available in the public domain. According to historic resource estimates, the five WIM heavy-mineral sand deposits could contain of the order of 3 million tonnes of REO in over 200 million tonnes of heavy-mineral (HM) concentrates and could represent a major proportion of the REO resources in monazite in Australian beach sands (Cassidy et al., 1997). Description of the model derived from descriptions by Williams (1990), Stitt (1999), Mason (1999), and Roy and Whitehouse (1999).

Australian deposits: WIM 150, Donald (WIM 250), Jackson (WIM 200), WIM 100, and WIM 50 (all in the Murray Basin, Vic). Beenup? (WA).

Deposits outside Australia: Not known.

Type example in Australia: WIM 150, Victoria (Fig. 3.13).

Location: Longitude 142.3400; Latitude -36.8062 ~18 km southeast of Horsham, Victoria

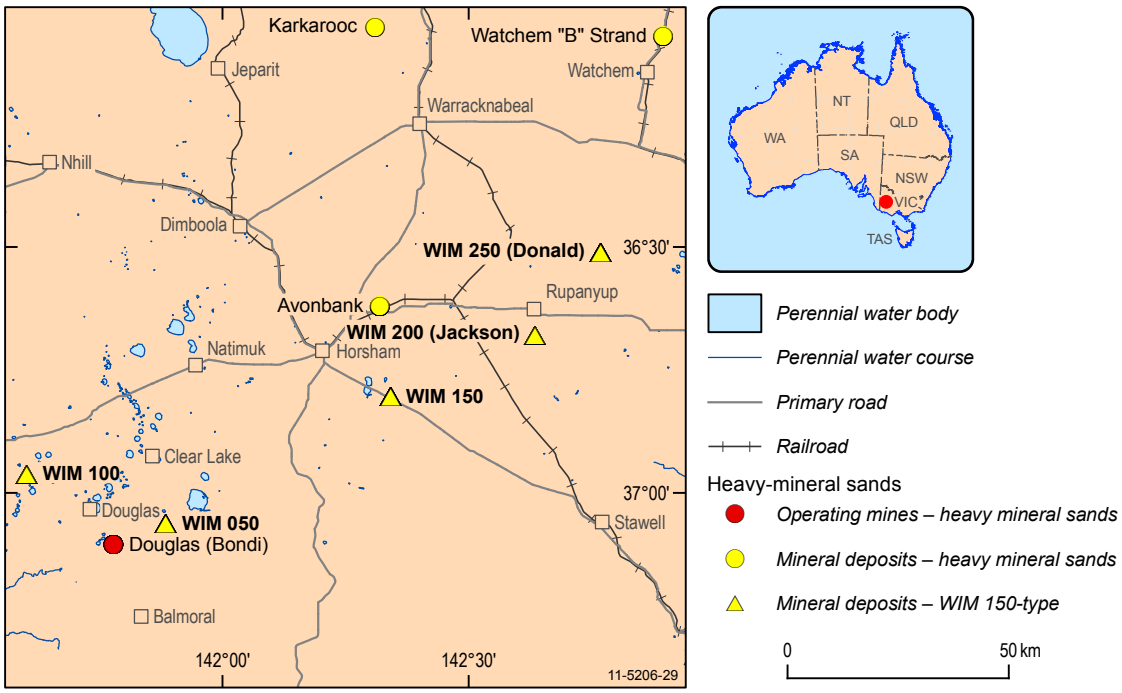

Figure 3.12. Regional map of WIM 150-type heavy-mineral deposits near Horsham, Victoria.

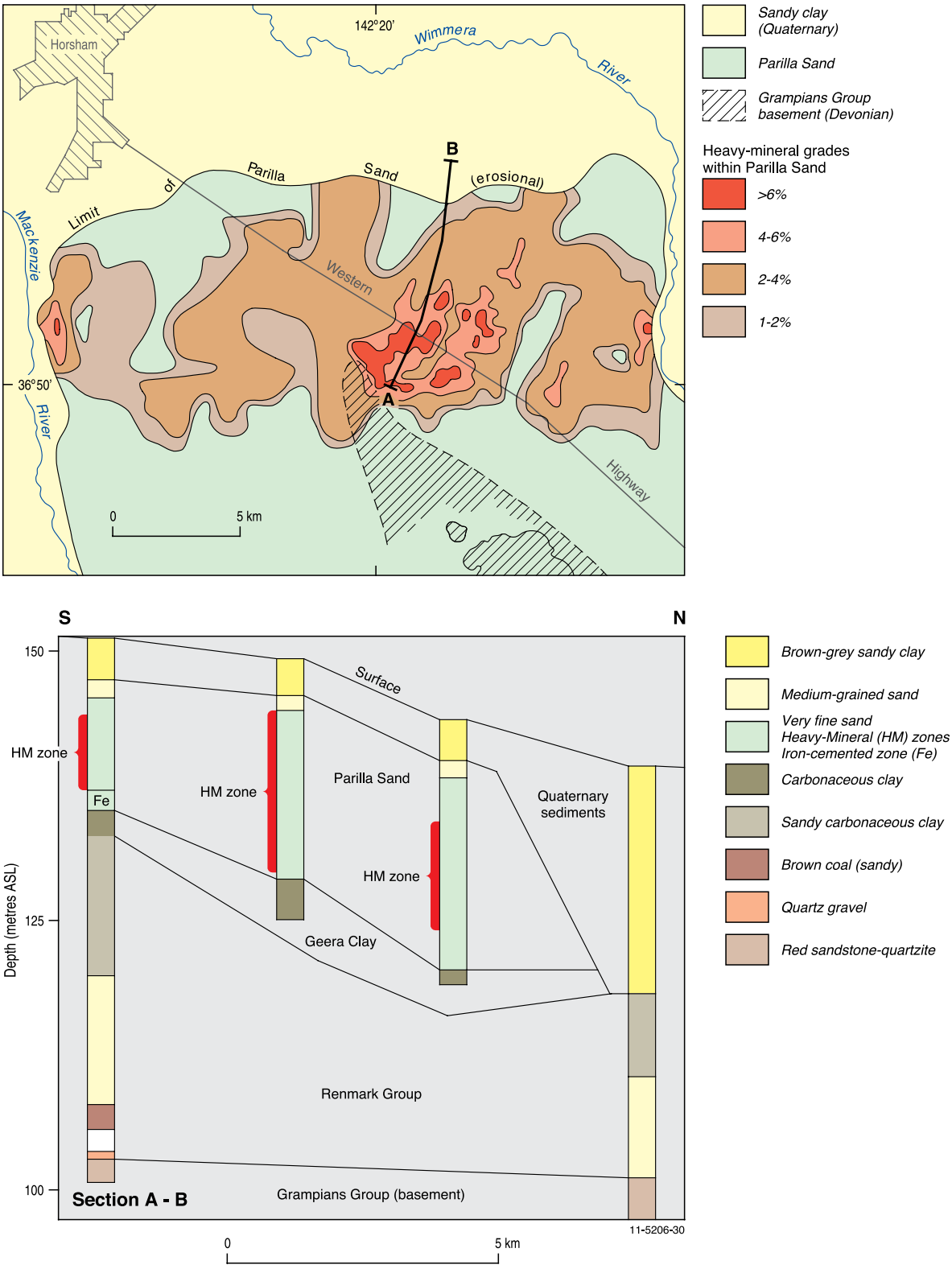

Figure 3.13. Geological map and cross-section of the WIM 150 heavy-mineral deposit (see Fig. 3.12), Victoria. Modified from Williams (1990).

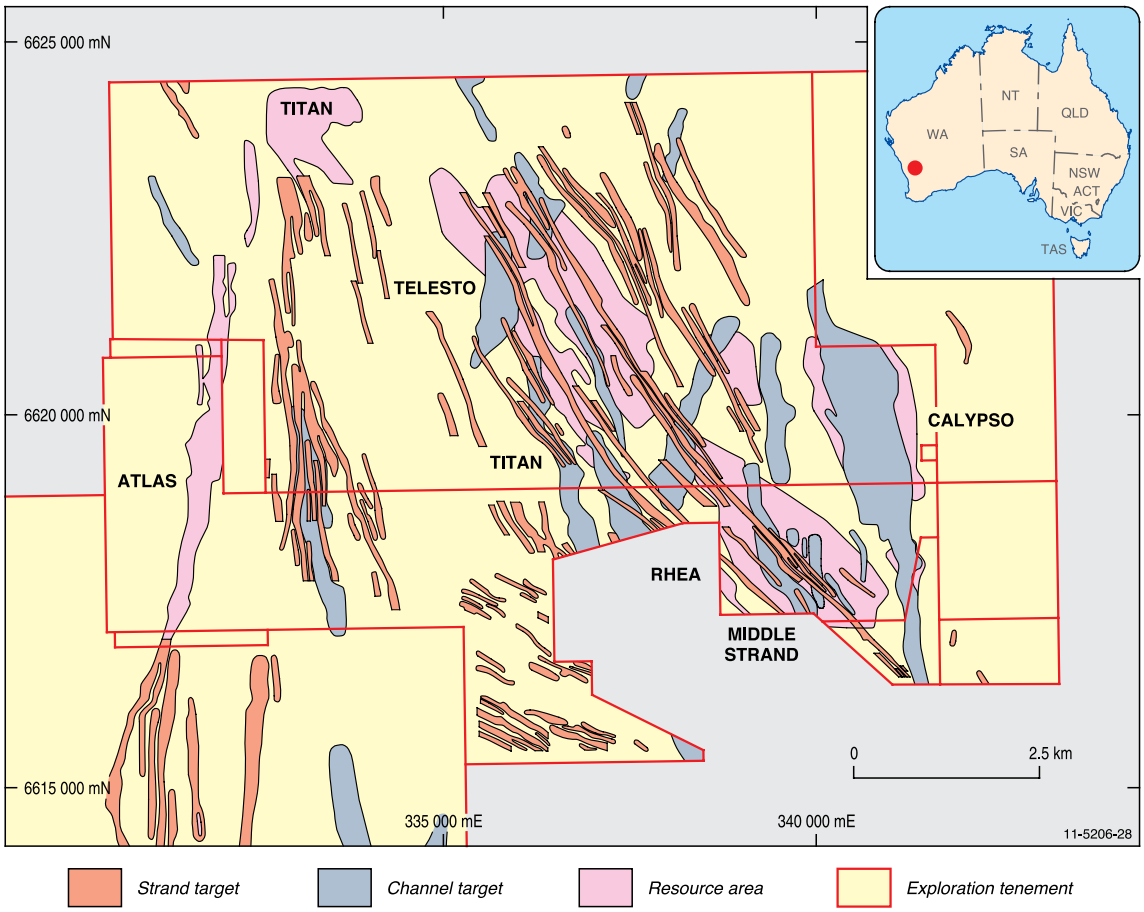

Figure 3.14. Strand and channel heavy-mineral deposits as interpreted from magnetic surveys near Calypso, Western Australia. Modified from Image Resources Limited (2010).

1:250 000 map sheet: Horsham (SJ 54–03)
1:100 000 map sheet: Horsham (7324)

Geological province: Murray Basin in Victoria, New South Wales, and South Australia.

Resources: Current published Indicated and Inferred Resources for WIM 150 stand at 727 million tonnes of sand at about 3.9% HM giving about 28.5 million tonnes of HM. The zircon, rutile, ilmenite, and monazite contents in the HM have not been published, but Williams (1990) reported the HM constituents for the WIM 150 deposit as 13.3% zircon, 8.7% rutile and anatase, 31.6% ilmenite, 11.6% leucoxene, 1.4% monazite, and 0.4% xenotime.

On 27 April 2010, Astron Limited announced a combined Indicated and Inferred Resource for the Donald (WIM 250) and Jackson (WIM 200) deposits of 4.5 billion tonnes of sand grading at 4% HM (Astron, 2010a). On 27 July 2010, Astron also announced areas of higher-grade HM within this resource, which contained 370 million tonnes of Indicated Resources of sand grading 6.1% HM (Astron, 2010b). The HM contained 32% ilmenite, 19.0% leucoxene, 4.5% rutile, and 19% zircon; and 1010 million tonnes of sand grading 5.7% HM containing 33% ilmenite, 16.0% leucoxene, 1% rutile, and 18% zircon.

Current status: Large undeveloped deposit.

Economic significance: In the past the fine grain size of the offshore shallow marine deposits have presented difficulties in processing the heavy-mineral concentrates. Such problems are currently being overcome and government approvals in regard to environmental and mining regulations are currently under way to mine the Donald deposit (previously WIM 250) in Victoria. As noted above, the presence of thorium and uranium in monazite discourages commercial interest in processing monazite for its rare-earth content.

Geological setting: Very fine-grained HM concentrations form as large, tabular deposits thought to be deposited on the lower shoreface/inner shelf under low-energy conditions. Sediment derived from

deeply weathered igneous and metamorphic terranes of sillimanite or higher grade. The origin of these deposits is not well understood.

Host rocks: Fine-grained silt in offshore deposits.

REE mineralisation: The REE is held mainly within the monazite and to a lesser extent within the xenotime content of the HM concentrate, with the REO content in monazite at around 55% to 60% and the thorium content of around 6% Th.

Source of REE: The ultimate source for the REE-bearing monazite in the dune and beach sands is considered to be igneous–high-grade metamorphic rocks but generally monazite was captured with zircon, rutile, and ilmenite in earlier depositional cycles and subsequently eroded.

Age of mineralisation: Age range of Miocene to Holocene, with the WIM-type deposits considered to be part of the Miocene to Pliocene Murray Basin sedimentary sequence.

Genetic model: Margin of craton or intracratonic basin. Crustal stability during deposition and preservation of deposits.

Williams (1990) noted that the major features of the WIM-type deposits (Fig. 3.13) are:

- broad lobate plan geometry;
- lateral continuity of individual heavy-mineral lenses;
- continuity of grades over large areas;
- uniformity of the heavy-mineral assemblage;
- fine-grain size of heavy minerals and host sand; and
- undulating to hummocky cross-stratified heavy-mineral concentrations.

Williams (1990) noted that these features are not shared by heavy-mineral sand deposits formed in coastal beach and dune sand environments and suggested that undulating and hummocky cross-stratification may indicate offshore deposition below the fair weather wave base during storms.

Key references: Williams (1990): regional and local descriptions of WIM 150 deposit.

Deposit Type 3.6: Channel placer heavy-mineral deposits with rare-earth-element-bearing monazite

General description: Heavy-mineral sand concentrations as placers in terrestrial drainage channels rather than in coastal environments.

Australian deposit: Calypso (WA).

Deposits outside Australia: Fluvial deposits of rutile in Sierra Leone and Cameroon; Sao Gancalo do Sapucal (Minas Gerais), Brazil (Jackson and Christiansen, 1993; Orris and Grauch, 2002).

Type example in Australia: Calypso, Western Australia (Fig. 3.14).

Location: Longitude: 115.3423; Latitude: -30.5509
~155 km northeast of Perth, Western Australia
1:250 000 map sheet: Hill River (SH50–09)
1:100 000 map sheet: Wedge Island (1936)

Geological province: Perth Basin, Western Australia.

Resources: The published resources for the Calypso deposit are 51.5 million tonnes of sand grading 1.7% HM at a cut off of 1% HM giving 850 000 tonnes of HM. The HM is reported to contain 598 000 tonnes of ilmenite, 44 000 tonnes of leucoxene/rutile, 90 000 tonnes zircon, 16 000 tonnes monazite, 70 000 tonnes garnet + staurolite and 31 000 tonnes of other heavy minerals (Image Resources NL, 2008).

Current status: Undeveloped deposit, currently under investigation.

Economic significance: Preliminary scoping studies indicate that the deposit could be economic. Under prevailing economic conditions the REE are not extracted from the monazite which would be returned back to the mine site.

Geological setting: According to Image Resources NL (2008), the Calypso mineralisation shown in Figures 3.14 and 3.15 is interpreted to be of fluvial origin. It is hosted in Mesozoic sediments, and appears to be facies controlled. The sediments hosting the mineralisation are typically a very clean fine- to medium-grained sand up to 70 m in depth. They are bounded by clay-rich sediment barren of heavy minerals. The sands are interpreted to be braided streams and the clays thought to represent quiet swamp environs. There are clay intercalations within the sands. The heavy-mineral channel type deposits occur in close association with, and are overlain, by younger fossil beach strandline heavy-mineral deposits (Figs 3.14 to 3.16).

Host rocks: Mesozoic fluvial sands.

REE mineralisation: The REE content in the monazite of this deposit is unknown, but is probably of the order of 45% to 60%.

Source of REE: The ultimate source for the REE-bearing monazite in the dune and beach sands is considered to be igneous–high-grade metamorphic

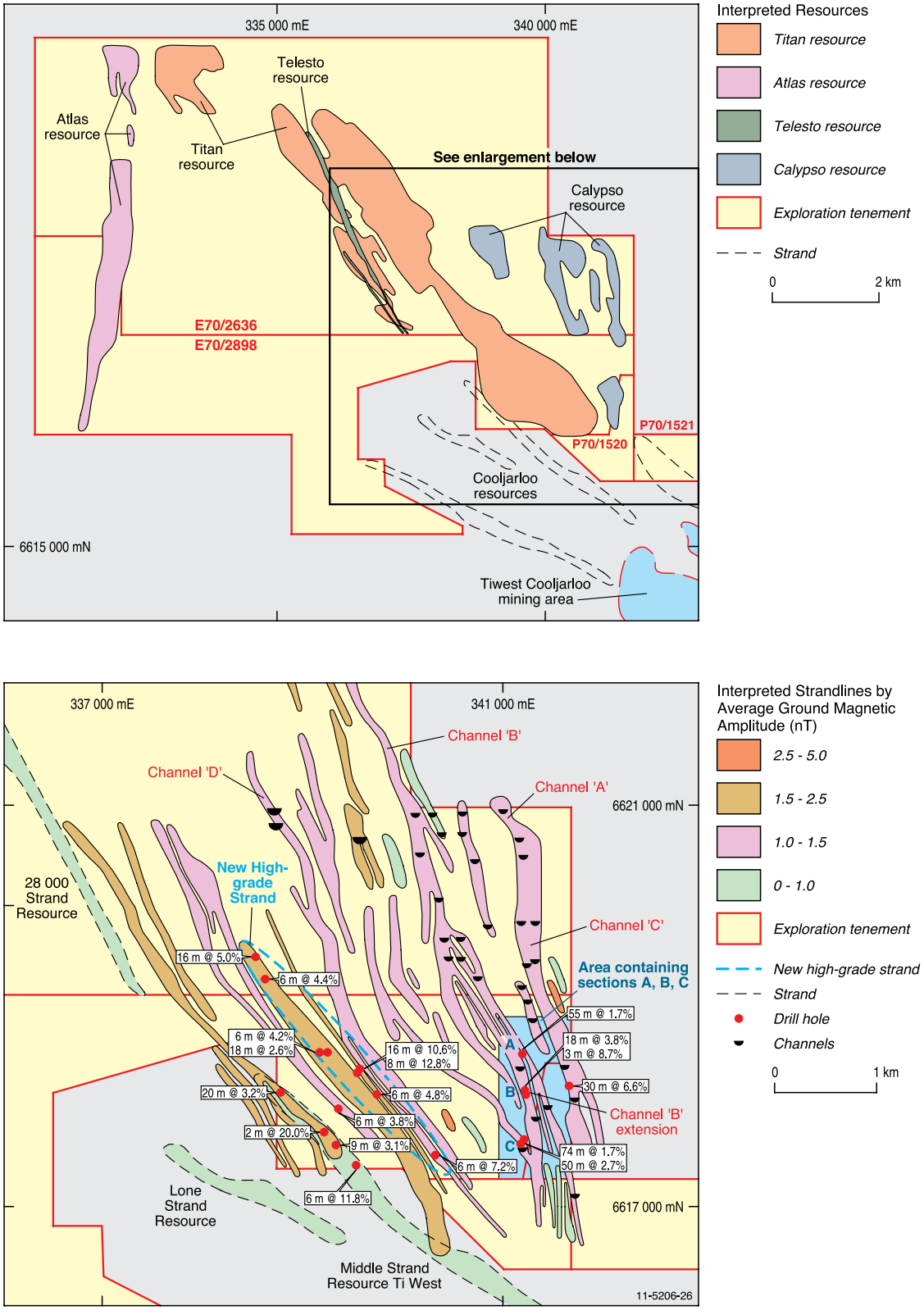

Figure 3.15. Regional and detailed maps of channel-type heavy-mineral deposits near Calypso, Western Australia. Modified from Image Resources Limited (2007a,b; 2008).

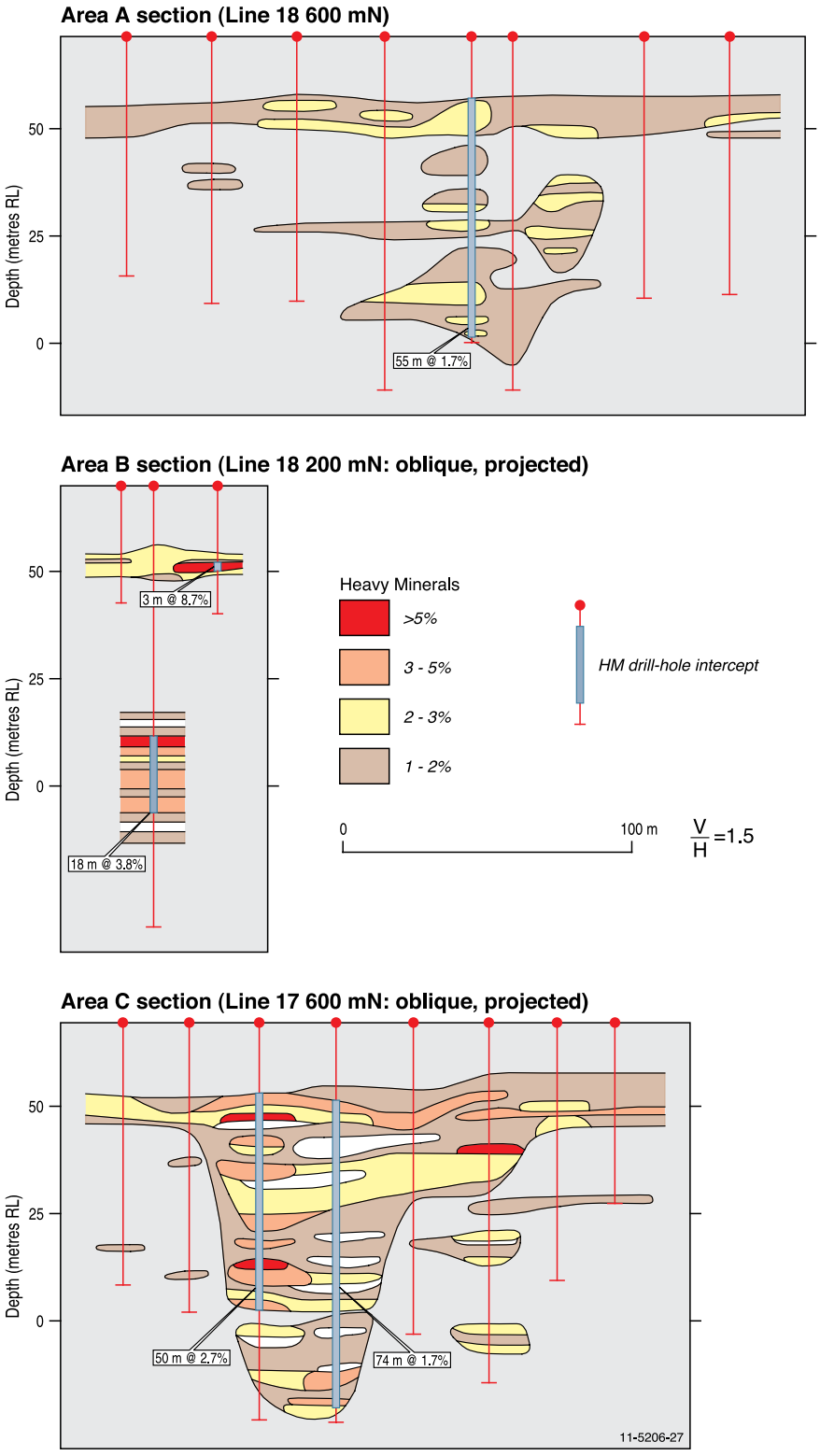

Figure 3.16. Cross-sections showing heavy-mineral concentrations in deposits near Calypso, Western Australia. Modified from Image Resources Limited (2007a,b). Locations of section lines A, B, and C are shown in Figure 3.15.

rocks, but generally monazite was captured with zircon, rutile, and ilmenite in earlier depositional cycles and subsequently eroded.

Age of mineralisation: Mesozoic (?).

Genetic model: Unknown.

Key references: Image Resources NL (2007a,b; 2008): descriptions of channel-type deposits and resources.

Deposit Type 3.7: Rare-earth elements associated with phosphorites

General description: Elevated levels of REE are reported to be associated with deposits of phosphorites in Australia and overseas.

Australian deposits: Korella, Sherrin Creek, D Tree, and Wonnarah (all Georgina Basin, Qld and NT: Fig. 3.17).

Deposits outside Australia: Schevchenko, Kazakhstan (Will et al., 1995); Abu Tartar, Egypt (Hussein and El Sharkawi, 1990); Zhijin, China (Li et al., 2007).

Type example in Australia: Korella, Queensland (Figs 3.17 and 3.18).

Location: Longitude: 139.9667; Latitude: -21.9500
~145 km southeast of Mount Isa, Queensland
1:250 000 map sheet: Duchess (SF 54–06)
1:100 000 map sheet: Dajarra (6854)

Geological province: Georgina Basin, Queensland and Northern Territory.

Resources: Inferred phosphate and REE resources have been published for the Korella phosphate-yttrium deposit as 4.2 Mt @ 746 g/t Y (0.96 kilogram/tonne Y_2O_3) and Nd and Dy are also reported to be present, but their resources have not been estimated (Krucible Metals Limited, 2011). The Korella deposit also has an Inferred Resource 8.3 Mt @ 27.36% P_2O_5 at a cut-off grade of 20% P_2O_5 (Krucible Metals Limited, 2010). The anomalous zone of yttrium enrichment at Korella appears to remain open towards the Duchess deposit to the north. There is little published data in regard to REE resources in phosphorite in Australia. Total phosphate resources in the Georgina Basin are considered to be of the order of 4 billion tonnes (Lottermoser, 1991), but TREE contents in the phosphorites are generally much less than 1000 ppm.

Current status: Korella is an undeveloped phosphate-yttrium deposit (Fig. 3.18).

Economic significance: Korella is a significant phosphate-yttrium deposit being considered for possible development. The economic significance of the elevated values of yttrium in the Sherrin Creek phosphate deposit is unknown. The recovery of europium as a by-product of phosphate mining has been reported for the Schevchenko deposit in Kazakhstan (Orris and Grauch, 2002) and research by Li et al. (2007) have investigated the feasibility of extracting REE as a by-product of phosphate mining from the Zhijin phosphorite deposit in China.

Geological setting: According to Howard (1986), the time and location of major phosphogenesis in Australia was in the Middle Cambrian of the Georgina Basin. About 20 known early Middle Cambrian phosphorite deposits in the Georgina Basin, comprising a major world resource of phosphate, are located along the paleo-periphery of the basin over a distance of 1000 km (Fig. 3.17). The paleogeography and the nature of the contained sediments indicate the Georgina Basin occupies a mild structural downwarp in the pre-Cambrian basement. Three different structural/depositional environments have been postulated for the Georgina Basin phosphorites (Howard, 1986):

- the Duchess phosphorites were deposited across the seaward flanks of the Smokey Anticline structural rise and in the depression of the Burke River Structural Belt;
- the Lady Annie, D Tree, and Sherrin Creek phosphorites were deposited in coastal subtidal, intertidal, and supratidal environments related to a shallow-marine epicontinental basin containing large hypersaline banks surrounded by subtidal channels fringed by embayments, lagoons, and estuaries; and
- the Wonarah and Alroy phosphorites were deposited on the Alexandria-Wonarah Basement High, which was actively rising during sedimentation and the structure was the site of phosphogenesis. The phosphorite beds drape over basement highs which were related to reactivated Paleoproterozoic faults.

Host rocks: Middle Cambrian Phosphorite. The Beetle Creek Formation and the Inca Formation are the main hosts and consist of a sequence of phosphatic siltstone (phosphorite) and chert that overlies limestone, sandstone, and conglomerate.

REE mineralisation: Analyses of phosphorite samples collected by Howard and Hough (1979) show a significant enrichment in yttrium.

- Fourteen samples from the Sherrin Creek deposit exceeding 200 ppm Y and seven of those exceeding 300 ppm reaching a maximum of 624 ppm Y.

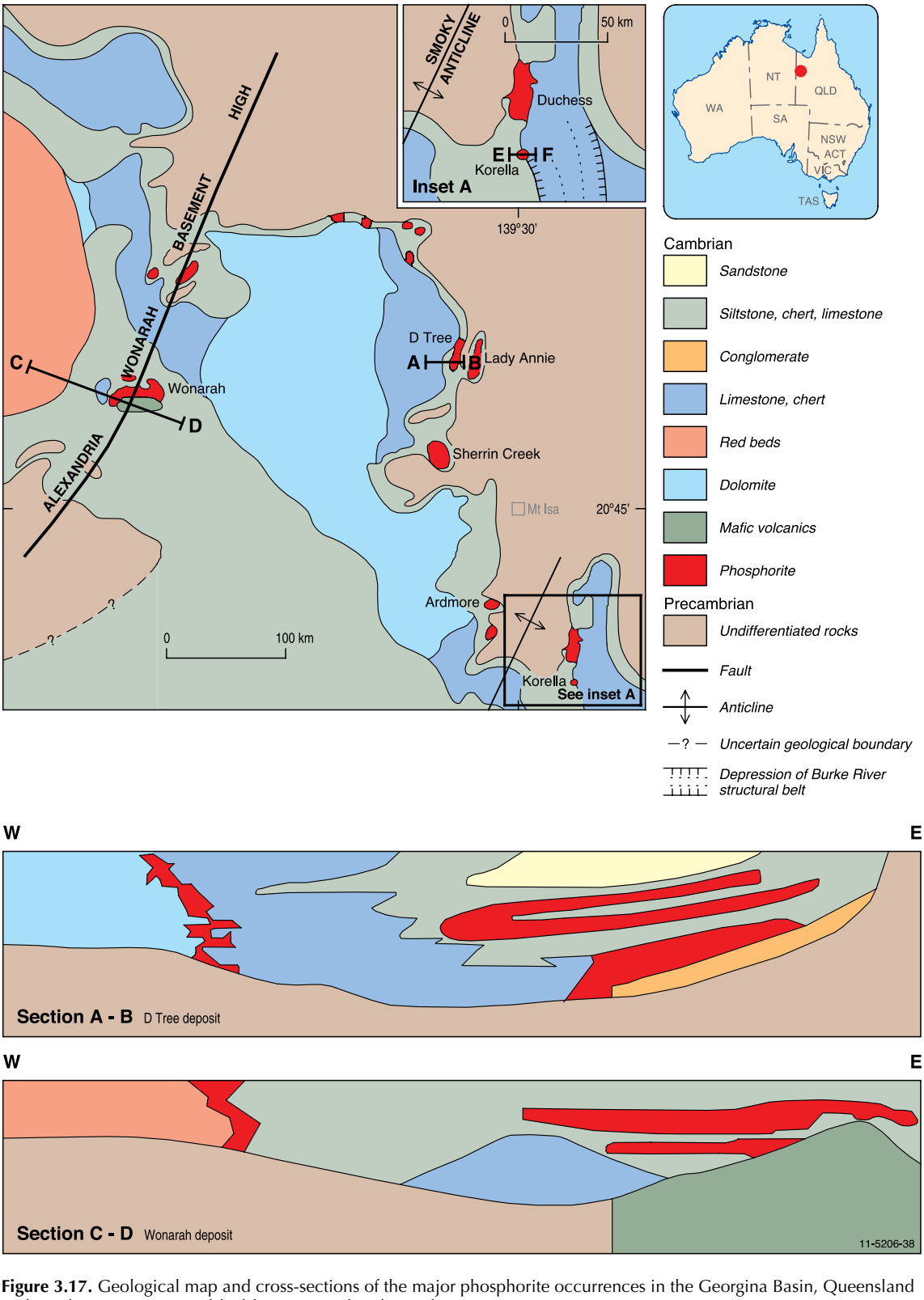

Figure 3.17. Geological map and cross-sections of the major phosphorite occurrences in the Georgina Basin, Queensland and Northern Territory. Modified from Howard and Hough (1979).

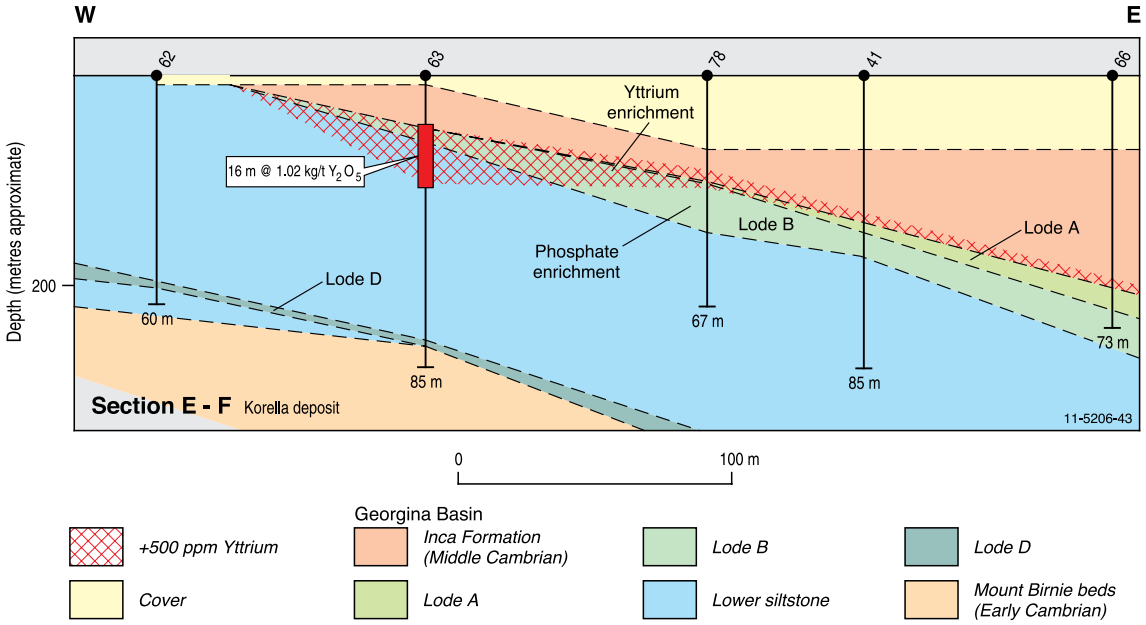

Figure 3.18. Geological cross-section of the Korella phosphorite deposit, Georgina Basin, Queensland. Modified from Krucible Metals Limited (2011).

- The sample with maximum Y value also had a maximum value of 148 ppm La and 214 ppm Ce.
- The plus 300 ppm Y values are usually associated with the higher-grade phosphate samples (>30% P_2O_5).
- Howard and Hough (1979) noted that in unleached Sherrin Creek (and D Tree) phosphorites, yttrium, lanthanum, and cerium correlate with apatite where they substitute for calcium.

- Seven phosphorite samples from the D Tree deposit also exceeded 200 ppm Y, reaching a maximum value of 482 ppm Y, which also had maximum values of 142 ppm La and 214 ppm Ce.
- The Wonarah deposit only had two samples yielding plus 200 ppm Y with a maximum of 336 ppm Y, which also had 41 ppm La and 5 ppm Ce.

Russell and Trueman (1971) noted that the phorphorite in the Dutchess deposit averaged 500 ppm La and 600 ppm Y. Analyses of 17 samples of pelletal phosphorite from the Georgina Basin as published by de Keyser and Cook (1972) indicate higher values of yttrium ranging from 800 to 1500 ppm Y.

Source of REE: Source of REE may be influenced by the nature of the seabed rock. The samples with the highest values of yttrium published in Howard and Hough (1979) are from unleached samples of phosphorite from Sherrin Creek and from unleached and partly leached samples from D Tree. The lowest yttrium values are from Wonarah where all of the samples were leached. However, both Sherrin Creek and D Tree are relatively close to the Mount Isa Inlier, as is the Korella phosphorite deposit, which has the only published resource of yttrium in the Georgina Basin. The close proximity of these deposits to the Mount Isa Inlier may suggest the Precambrian basement as a possible source for yttrium and other REE.

Age of mineralisation: Middle Cambrian age.

Genetic model: Howard and Hough (1979) reviewed the available data on the phosphorite types of the Georgina Basin epicontinental sea and concluded that:

1. phosphate formed in restricted and shallow to very shallow water environments ranging from subtidal to intertidal;
2. contained faunas in different areas of the Georgina Basin are very different in overall composition, and it appears that they developed independently of each other. In this study the geochemical data indicate that there were discernible differences in the chemistry of the waters of these depressions;
3. outside of the restricted areas, phosphogenesis declined rapidly and ceased basinward, even though shallow open-marine conditions persisted. There is a change from a restricted paleodepression containing phosphorites into open basin with a change to phosphatic siltstone and limestone; and
4. phosphogenesis was confined to a specific faunal time zone (Xystridura zone).

The favoured interpretation by Howard and Hough (1979) to account for the characteristic features of the Georgina Basin phosphorites listed above is that there was a set of circumstances which coincided to form a phosphate 'pump'. These were normal sea water saturated in carbonate fluorapatite but supplemented by phosphate from coastal streams in areas of lagoons, estuaries, or more restricted embayments, and a rapid concentrating mechanism which could maintain a high bottom-water concentration. The concentration agent was a prolific phytoplankton population which on death sank and released phosphate in the oxidising environment at the sediment-water interface Howard and Hough (1979).

Key references: Howard (1986), Howard and Hough (1979), and Cook (1972): geological setting and geochemistry;
Krucible Metals Limited (2011): describe first reported REE resource in Georgina Basin.

Deposit Type 3.8: Rare-earth elements associated with lignite in sandstone-hosted polymetallic uranium deposits

General description: Rare-earth elements are associated with lignite in the sandstone-hosted polymetallic uranium deposit at Mulga Rock, in Western Australia.

Australian deposits: Mulga Rock (?Eucla Basin, WA).

Deposits outside Australia: Enrichment of REE occur in germanium-bearing Cretaceous lignite at the Wulantuga deposit, Inner Mongolia, China (Qi et al., 2007), and at the Spetsugli germanium-bearing coal deposit in the Promor'e region, Russia (Seredin, 2005). Gallium-bearing coals at Jungar, Inner Mongolia, are enriched in REE (Dai et al., 2006). Rare earths in acidic waters are being investigated in regard to environmental issues, in pits from a former lignite mine at Lusatia, Germany (Bozau et al., 2008).

Type example in Australia: Mulga Rock, Western Australia (comprises three separate deposits Ambassador, Shogun, and Emperor: Fig. 3.19).

Location: Longitude: 123.5906; Latitude: -29.9057
~220 km northeast of Kalgoorlie, Western Australia
1:250 000 map sheet: Minigwal (SH 51–07)
1:100 000 map sheet: Narnoo (3638)

Geological province: ?Eucla Basin, Western Australia.

Resources: 55.44 million tonnes of Inferred Resources at 0.490 kg/t U_3O_8 (Energy and Minerals Australia Limited, 2010a).

Current status: An undeveloped polymetallic sandstone-hosted uranium deposit currently at a stage of advanced exploration.

Economic significance: A significant polymetallic uranium deposit currently being considered for possible development. Commercial significance of REE undetermined.

The germanium-bearing coal deposits of Wulantuga (referred to as the Wulantuga germanium deposit), Inner Mongolia, and at Spetsugli in Russia are very large. Similarly, the gallium-bearing coal deposit at Jungar (referred to as a superlarge gallium ore deposit), Inner Mongolia is also large. However, the commercial significance of the REE in these overseas deposits is not clear.

Geological setting: The Mulga Rock polymetallic uranium deposit occurs within a buried paleochannel sequence of Phanerozoic age, underlain by predominantly Archean and Proterozoic granites of the Yilgarn Craton and the Albany–Fraser Province. According to Douglas et al. (2011), Pb-Pb data together with a high Th/U ratio suggest that lamproites and carbonatites may be present in the Mulga Rock region of the Yilgarn Craton. The deposit is hosted in lignite and underlying sandstones in the paleochannel which is 5–15 km wide and at least 100 km long. The paleochannel may have received input from drainage systems that extended for over 400 km northwest across the Yilgarn Craton. At Mulga Rock the paleochannel sequence comprises:

- fluviatile sands and interbedded lacustrine sediments (30 m-thick);
- lacustrine to paludal sediments, kaolinitic clays overlying lignite (peat), clay-rich lignite and carbonaceous sands and clays (30 m); and
- basal fluviatile sands and gravels (40 m).

The upper units have been weathered, ferruginised, and silicified. Oxidation, extends to 20–30 m depth with a sharp redox boundary between kaolinitic clay and lignite, usually close to the water table. The oxidation is possibly related to weathering under humid conditions during Oligocene to mid-Miocene followed by later weathering under more arid environment.

Host rocks: At the Ambassador deposit, uranium is hosted in lignite and in the underlying sandstone, but the REE appear to be confined to the mineralised lignite. The abundances of REE in the Emperor and Shogun deposits have not been reported.

REE mineralisation: The uranium mineralisation in the Ambassador deposit is distributed as follows:

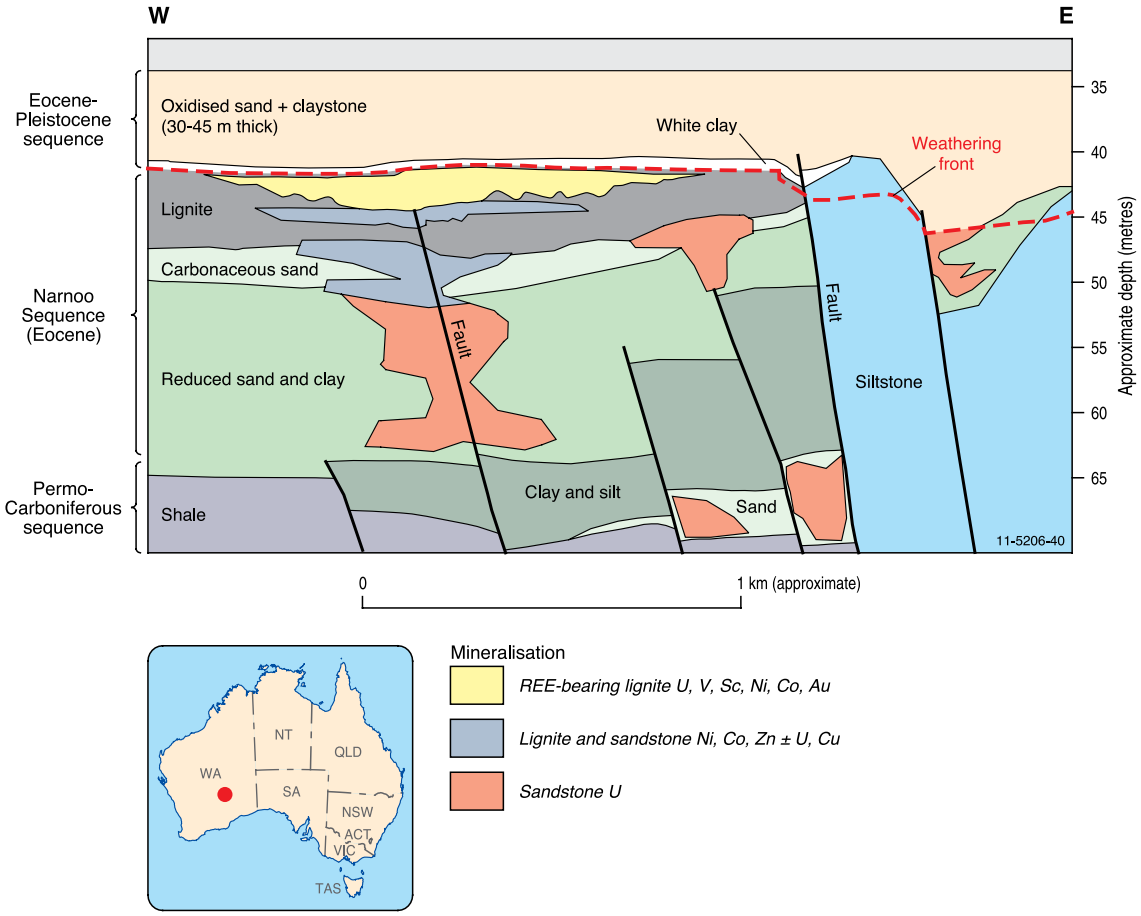

Figure 3.19. Geological cross-section of the Mulga Rock lignite sandstone-hosted uranium deposit, Yilgarn Craton, Western Australia. Modified from Davis (2010).

- Upper lignite—16.7 Mt @ 600 ppm with 10 000 t of contained U_3O_8; main elements are–U, Ni, Co, Cu, Zn, Sc, REE, V, Au, Ag;
- The proportion of REE in upper lignite was reported as 10.8% La, 39.8% Ce, 6.1% Pr, 24.1% Nd, 6.0% Sm, 1.2% Eu, 4.2% Gd, 0.6% Tb, 3.4% Dy, 0.6% Ho, 1.5% Er, 0.2% Tm, 1.2% Yb, and 0.2% Lu: Energy and Minerals Australia Limited (2010c).
- Lower lignite—3.7 Mt @ 320 ppm with 1 200 t of contained U_3O_8; main elements are–U, Ni, Co, Cu, Zn; and
- Sandstone—7.2 Mt @ 240 ppm with 12 900 t of contained U_3O_8; main elements are: U, Ni, Co, Cu, Zn, Au (Energy and Minerals Australia Limited, 2010a).

Some of the best drill-hole intersections in the Ambassador deposit (Energy and Minerals Australia Limited, 2010b) include:

- 5.50 m @ 1900 ppm U_3O_8, 0.24% Ni, 0.09% Co, 153 ppm Sc_2O_3, 390 ppm V_2O_5, and 0.18% Zn;
- 10.0 m @ 2200 ppm U_3O_8. Within this intersection, there is an intersection of 7 m @ 2.2% Zn, 0.14% Ni, 0.06 Co%, and 529 ppm V_2O_5; and
- 5.0 m @ 2200 ppm U_3O_8, 0.27% Ni, 0.11% Co, 192 ppm Sc_2O_3, and 0.30% Zn.

The distribution of the mineralisation at the Emperor and the Shogun deposits has not been published.

Source of REE: Douglas et al. (2011) consider that the Pb-Pb isotopic data suggest a very distinctive lithology, Archean or Proterozoic in age, with a high Th/U ratio is the likely source for the Ambassador mineralisation. In particular, the isotopic composition corresponds to that of Western Australian lamproites and carbonatites. The Mount Weld Carbonatite is adjacent to a paleochannel system, 180 km to the northwest, and other carbonatites are known, or are inferred, to occur in the Mulga Rock area (e.g., Ponton Creek–Cundeelee; Lewis, 1990). Both Sr and Nd isotopic results also support the hypothesis that lamproites or carbonatites could be the source of the mineralisation, however, the Sr and Nd isotopic data are also compatible with a number of granitic lithologies in the Yilgarn

Craton. Douglas et al. (2011) state that lamproites and carbonatites are also geochemically compatible source rocks because they are commonly enriched in a wide range of trace elements, in particular U, Th, and the REE. These rocks could represent a source of mineralisation located either within the basement proximal to the paleochannel, or directly linked via one of the branches of the Minigwal paleochannel system.

In regard to sources of REE in overseas deposits, published information on the REE-enriched germanium-bearing lignite at Wulantuga, the germanium-bearing coal at Spetsugli, and the gallium-bearing coal at Jungar are summarised below:

- Qi et al. (2007) note that the TREE contents of 42 samples from the Wulantuga germanium deposit (WGD) range from 9 ppm to 533 ppm, with a maximum TREE + Y content of 648 ppm.
  - The average REE contents of the WGD samples are slightly higher than those of USA coals and world-wide coals.
  - REE contents of most lignite samples are highly positive correlated with ash yields indicating a mainly detrital source and an association with syngenetic mineral matter.
  - There are no distinct correlations between germanium and any individual REE, or TREE + Y content.
  - The germanium contents of the lignite samples range from 23.3 to 1424 ppm, with an average of 300 ppm.
- According to Seredin (2005) the TREE + Y concentrations of germanium-bearing coals from the Spetsugli deposit range from 86 to 316 ppm.
  - The germanium-bearing coals are strongly enriched in yttrium and HREE as compared with coals located beyond the zone of germanium mineralisation.
  - The REE distribution in the coal seams show no correlation between the REE and germanium contents.
  - Anomalously high REE contents in germanium-bearing coals are of epigenetic origin and accumulated after the formation of germanium mineralisation.
  - The deposits formed from metalliferous REE-enriched and germanium-free or germanium-poor solutions of volcanic origin that circulated during the Pliocene–Early Quaternary period.
- According to Dai et al. (2006):
  - the TREE + Y contents of coal average 255 ppm with a maximum value of 715 ppm;
  - the TREE + Y contents of laboratory ash averages 830 ppm with a maximum value of 2586 ppm;
  - Dai et al. (2006) also state that the average REE + Y concentrations for coal from other regions are as follows:
    - Late Paleozoic coal from North China–111 ppm;
    - most Chinese coal–137.9 ppm;
    - USA coal–62.1 ppm; and
    - most world coal–46.3 ppm.
  - The gallium content of the main minable coal averages 51.9 ppm and 89.2 ppm in laboratory high-temperature ash.
  - The main carrier of the gallium is in the boehmite content of the coal.
    - Boehmite is derived from bauxite in the weathered crust of the underlying Benxi Formation in the north of the basin during peat accumulation.
  - The source of the REE + Y is unknown.

Age of mineralisation: Initially uranium and other metals precipitated syngenetically with organic phases in late Eocene followed by remobilisation during periods of weathering and associated diagenesis with the latest episode in the last 300 000 years (Douglas et al., 2011).

Genetic model: Douglas et al. (2011) favour a chemically syngenetic model where uranium and other trace elements were transported in solution from one or more sources and precipitated in the organic matter as it accumulated, and subsequently mobilised and concentrated during diagenesis/weathering. Solution and mobilisation are postulated to have occurred during a humid weathering event during the late Eocene, based on the palynological dating of the lignite, transported in solution and/or adsorbed to organic colloids in paleorivers. Post-depositional remobilisation and concentration may have occurred at any period since late Eocene, related to changes in water-table during post-Eocene uplift, burial by presumed Miocene sediments and/or related to episodes of more intense weathering.

Key references: Douglas et al. (2011): geology and genesis of Ambassador polymetallic uranium deposit; and
Fulwood and Barwick (1990): exploration history, regional geology, mineralisation, ore genesis.

Deposit Type 3.9: Rare-earth elements associated with alkaline igneous rocks

General description: Significant resources of zirconium-hafnium-niobium-yttrium, and REE occur in highly fractionated sequences comprising A-type alkaline lavas, tuffs, mafic volcanics, and subvolcanic intrusives. Such rare-metal deposits associated with volatile-rich alkaline magmas are typical of intraplate tectonic settings. Mineralisation is the product of early pyroclastic eruption of alkaline trachytic magma enriched in volatiles (in particular, fluorine and water) and incompatible elements (e.g., Zr, Hf, Nb, Ta, Be, Y, REE), that are concentrated in the upper parts of the magma chamber. Late-stage hydrothermal fluids involving fluorine and chlorine associated with the intrusions are important for the enhancement of rare-metal grades in these deposits. The two most important examples of this deposit type in Australia are Brockman (Western Australia) and Toongi (New South Wales). Both these deposits contain significant resources of REE and other rare metals that are currently being assessed.

Australian deposits/prospects: Brockman (Halls Creek Orogen, WA); Toongi–Dubbo Zirconia Project (Lachlan Orogen, NSW).

Deposits outside Australia: Khibini and Lovozero complexes (Kola Peninsula, Russia); Mount Pajarito (New Mexico); Thor Lake (Northwest Territories, Canada: Lake Zone has 64 Mt @ 1.99% REO); Strange Lake/Lac Brisson (Labrador-Quebec, Canada: open-pit mineable reserve of 52 Mt @ 0.54% REE, 0.31% Y_2O_3).

Type example in Australia: Brockman, Western Australia (Fig. 3.20).

Location: Longitude: 127.7820; Latitude: -18.3192
~18 km southeast of Halls Creek, Western Australia
1:250 000 map sheet: Gordon Downs (SE 52–10)
1:100 000 map sheet: Halls Creek (4461)

Geological province: Halls Creek Orogen, Western Australia.

Resources: The Brockman deposit has an estimated JORC-compliant resource (as of September 2010) totalling 22.084 million tonnes grading 0.79% ZrO_2, 0.10% Y_2O_3, 0.31% Nb_2O_5 and 0.023% Ta_2O_5 (http://www.hastingsraremetals.com/?page=88). This resource comprises an Indicated Resource of 8.83 million tonnes grading 0.76% ZrO_2, 0.09% Y_2O_3, 0.31% Nb_2O_5 and 0.022% Ta_2O_5 from surface to 100 m depth, and an Inferred Resource of 13.25 million tonnes grading 0.81% ZrO_2, 0.10% Y_2O_3, 0.32% Nb_2O_5, and 0.024% Ta_2O_5 from 100 m to 250 m depth. The resources are based on a cut-off of 1500 ppm Nb_2O_5.

Current status: Advanced prospect with JORC-compliant resource.

Economic significance: The economic importance of this deposit has traditionally been hindered by the fine-grained (<20 um), hydrous nature of the ore minerals, which requires a specialised chemical leaching process to achieve high degrees of recovery of rare metals (Ramsden et al., 1993; Taylor et al., 1995b). With the advent of more recent, sophisticated metallurgical techniques, these potential complications may be alleviated.

Geological setting: The polymetallic Brockman deposit occurs in the Halls Creek Orogen (HCO), a well-exposed north-northeasterly-trending orogenic belt about 400 km long and at least 120 km wide along the southeastern margin of the Kimberley Basin in northern Western Australia. The HCO is a complex province comprising low- to high-grade metasedimentary and metavolcanic rocks, and voluminous granitic, mafic, and mafic–ultramafic intrusions that collectively range in age from about 1920 Ma to 1800 Ma. Alkaline volcanics and intrusives are a minor component of the igneous stratigraphy. Younger Mesoproterozoic and Neoproterozoic lamprophyric-kimberlitic diatreme intrusions in the Kimberley have significant economic significance (e.g., world-class Argyle diamond deposit: Jaques et al., 1985). Major phases of tectonism occurred along in the HCO during the Paleoproterozoic, Mesoproterozoic, and Neoproterozoic (see references in Chapter 3 of Hoatson and Blake, 2000).

The Brockman deposit occurs in a Paleoproterozoic sequence (>1000-m thick) of alkaline lavas, volcaniclastic sedimentary rocks, felsic volcanics, that is intruded by subvolcanic sheets and interlayered with greywacke, siltstone, and mudstone (Fig. 3.20). Major lithologies include: trachyandesite, trachyte, quartz trachyte, and rhyolitic lavas; pillowed mafic lavas; subvolcanic syenite sheets; volcanic breccias, pyroclastics, and volcaniclastic rocks (including the mineralised 'Niobium Tuff'). Some of the thicker flow may be remnants of lava domes. The lavas are generally amygdaloidal, and they include pillowed and columnar-jointed types. Scoriaceous flow-tops and carbonate-cemented volcanic breccias are preserved locally. Some pillow lavas can be traced into feeder

Figure 3.20 (see opposite). Geological map of the Brockman rare-earth-element deposit area, Halls Creek Orogen, Western Australia. Modified from Sanders (1999).

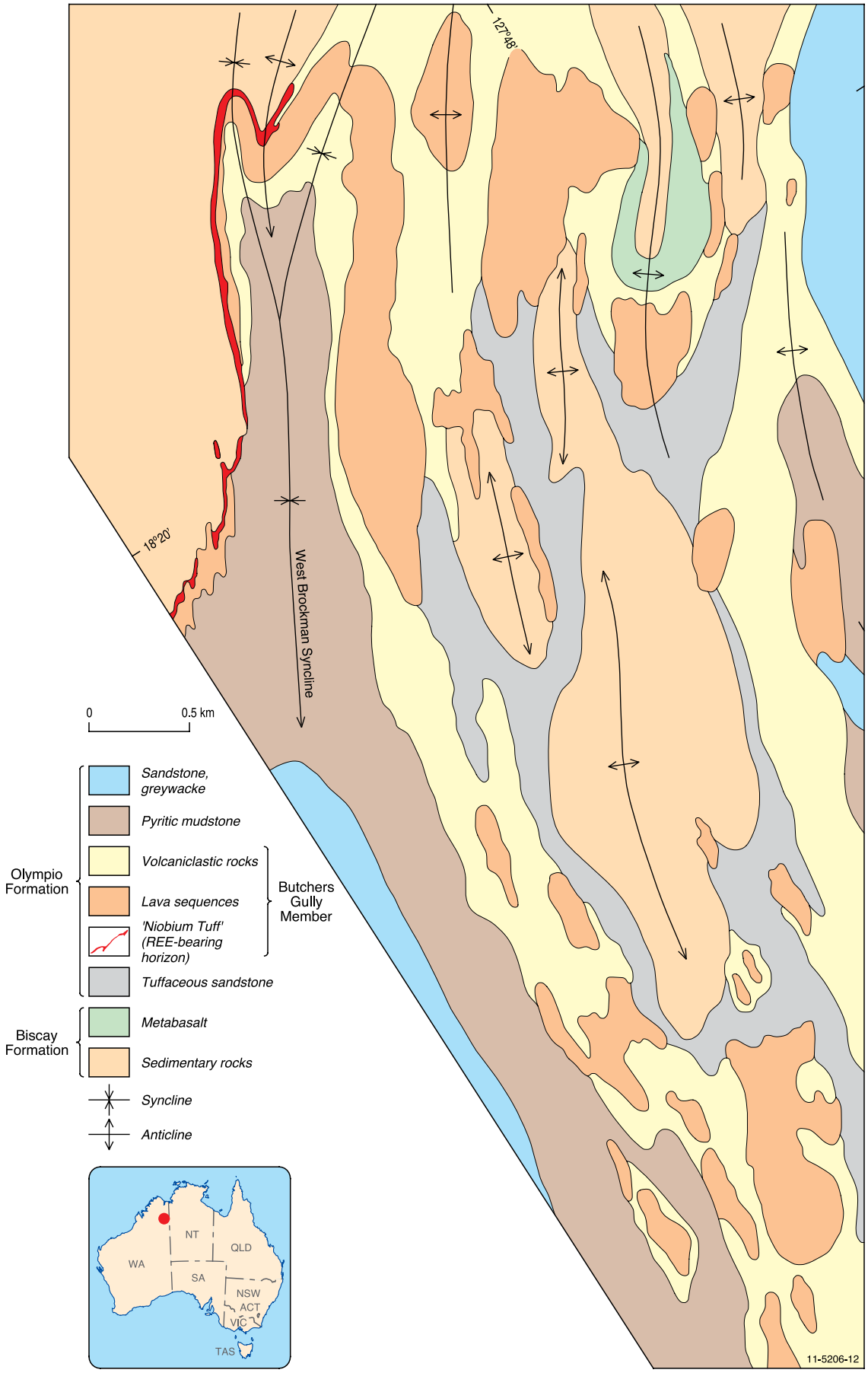
127°48'
18°20'
West Brockman Syncline
0
0.5 km
Sandstone, greywacke
Pyritic mudstone
Volcaniclastic rocks
Lava sequences
'Niobium Tuff' (REE-bearing horizon)
Tuffaceous sandstone
Olympio Formation
Butchers Gully Member
Metabasalt
Sedimentary rocks
Biscay Formation
Syncline
Anticline
NT
QLD
WA
SA
NSW
ACT
VIC
TAS
11-5206-12

dykes and sills (Taylor et al., 1995b). Extensive flows of altered mafic trachyte and sills of altered mafic syenite host gold mineralisation elsewhere (Butchers Creek and Golden Mile mines). The rock types commonly have a penetrative cleavage and are metamorphosed to greenschist facies. Weathering is limited, with oxidation observed down to depths of 30 m below the current surface. The presence of turbidites underlying and overlying the mineralised sequence, and of pillow lavas and pillow breccias within the sequence, indicate that the Butchers Gully alkaline volcanism was dominantly subaqueous.

Chemical analyses show that the alkaline volcanics were derived from quartz normative and metaluminous A-type magmas enriched in Nb, REE, Zr, Y, Ga, and Zn (Taylor et al., 1995a). The common presence of accessory fluorite indicates a significant fluorine content, and gamma-ray spectrometric data show that some of the volcanics have anomalously high thorium contents. The overall chemistry is indicative of intraplate magmatism (Taylor et al., 1995a,b; Blake et al., 1999). The interpreted tectonic setting of the Brockman deposit of intraplate alkaline magmatism in a shallow rift-related marine basin overprinted by orogenic events differs from most Cenozoic to Holocene trachyte volcanic complexes which are largely subaerial, are built on relatively thick continental crust, and show no post-eruptive orogenic activity (Taylor et al., 1995b).

Host rocks: The polymetallic mineralisation is hosted by a fluorite-bearing volcaniclastic unit informally known as the 'Niobium Tuff', which occurs at the base of the Butchers Gully Member of the Olympio Formation (Chalmers, 1990; Ramsden et al., 1993; Taylor et al., 1995a,b). The trachytic ash-flow tuff appears to be composed of two closely spaced units that formed from different eruptive episodes; namely a crystal-rich lower unit with a similar thickness to an overlying pumice-rich unit that collectively cooled as a single unit (Fig. 3.20). Taylor et al. (1995b) describes the 'Niobium Tuff' as a tuffaceous volcaniclastic unit grading into a volcaniclastic sandstone in the distal facies. It varies in thickness from 5 to 35 m and crops out for at least 3.5 km along the western flank and northern closure of a major southwest-plunging syncline, where it has a vertical to steep dips towards the east (Chalmers, 1990). Sub-surface data indicate that the 'Niobium Tuff' unit gradually thickens down-dip to the east where the source volcanic vent is interpreted to be located some 1000 m below the present land surface (Ramsden et al., 1993). The tuff contains strongly foliated microcrystalline quartz and potassium mica, with scattered albite microphenocrysts, lithic fragments, pumice, and possible glass shards set within a devitrified microcrystalline groundmass. Accessory minerals include limonite, carbonate, biotite, chlorite, epidote, and the REE-bearing minerals aeschynite, bastnäsite, parisite, and rhabdophane have been recorded in veins and amygdales. Purple fluorite is common throughout the deposit intimately associated with the ore minerals. It also occurs with coarse-grained biotite, quartz, and muscovite, infilling pumice, and in late-stage discordant carbonate veins at the footwall contact with coarse quartz, carbonate, chlorite, and sphalerite (Ramsden et al., 1993; Taylor et al., 1995b; Blake et al., 1999). The 'Niobium Tuff' contains extreme enrichment in high-field-strength incompatible elements (average 1660 ppm Y, 9700 ppm Zr, 3200 ppm Nb, 175 ppm Yb: Taylor et al., 1995a). Trachytic lavas overlying the 'Niobium Tuff' contain many of the ore minerals, but in trace amounts.

REE mineralisation: The Brockman deposit contains significant quantities of zirconium, yttrium, niobium, tantalum, hafnium, gallium, and HREE, such as terbium and dysprosium. Chalmers (1990) provides the following summary of the mineralogy of the REE. Electron microprobe studies by CSIRO have shown that the ore minerals are extremely fine grained with few species greater than 20 µm and most less than 10 µm in diameter. They are dispersed throughout the quartz, potassium mica, and albite host, usually occurring in layers and on grain boundaries. Major ore minerals include zircon and gel-zircon (unusual hydrous Y-Th-Nb-bearing variety of zircon: Ramsden et al., 1993), columbite, and Y-bearing rare-earth niobates. The hydrous gel-zircon contains about 5000 ppm Dy, 5000 ppm Er, 6000 ppm Yb, 1400 ppm Gd, 600 ppm Sm, in addition to anomalous Y, Th, and Nb. The REE minerals bastnäsite, calcian-bastnäsite, parisite, and synchysite, have been documented with chalcopyrite, galena, pyrite, sphalerite, thorite, gel-thorite, and ilmenite. Gel-zircon is the principal host of the HREE, and disseminated bastnäsite (± parisite and synchysite) carries the LREE. Bertrandite ($Be_4Si_2O_7(OH)_2$), in late-stage calcite veins, is the main host for Be, and Ga is enriched in potassium mica (300 ppm Ga) in the groundmass (Ramsden et al., 1993). The textures of the ore minerals are in part controlled by the fabric of the host tuff unit, and there is much evidence for remobilisation and redistribution associated with fluoritisation. However, there is not a typical texture and the ore minerals are generally disseminated throughout the 'Niobium Tuff'.

Source of REE: Taylor et al. (1995a) state that the large degrees of crystallisation required to derive the more differentiated rocks of the Brockman deposit are

best explained by a process of 'liquid fractionation' resulting in internal compositional stratification of the magma chamber with extreme differentiates such as the 'Niobium Tuff' forming a volatile-enriched 'cap' in the magma chamber-roof zone. The REE and other rare metals were derived from fertile (i.e., REE-bearing) quartz-oversaturated, metaluminous alkaline magmas which underwent a widespread and protracted fractionation process, and progressive contamination with upper crustal granitic-metasedimentary rocks. This very efficient mineralising system was overprinted by late-stage fluorine-rich fluids. The fine-grained rare-metals mineralisation is the result of alteration and remobilisation of magmatic columbite and zircon. Chondrite-normalised REE distributions for the 'Niobium Tuff' show strong enrichment in HREE, which is in marked contrast to the LREE-enriched overlying trachytic lavas (Ramsden et al., 1993).

Age of mineralisation: A trachytic pillow lava belonging to the Butcher's Gully Member has a SHRIMP U-Pb zircon age of 1848 ± 3 Ma (Blake et al., 1999). The pillow lava, from a sequence of trachytic to rhyolitic volcanics overlying the 'Niobium Tuff', provides the most reliable age for the timing of the alkaline magmatic event. Older zircons dated at 1870 ± 4 Ma (Taylor et al., 1995b) and 1868 ± 3 Ma (Blake et al., 1999) from the mineralised 'Niobium Tuff' at the base of the Butcher's Gully Member are interpreted to be volcanic detritus in the host rock.

Genetic model: Brockman-style rare-metal deposits are characterised by preservation of subaqueous volcanics beneath a thick sedimentary sequence, eruption of early incompatible-element-enriched products followed by less differentiated magmas, widespread activity of volatile-rich fluids (particularly fluorine and water), and fine-grained mineralogy influenced by alteration processes (Taylor et al., 1995a,b). Taylor et al. (1995b) interpreted the geological setting of the mineralised 'Niobium Tuff' in the Brockman deposit as either a pyroclastic-flow deposit, or as a subaqueously-deposited mass-flow that incorporated pyroclastic debris. An initial pyroclastics ash-flow eruption of crystal-rich magma enriched in incompatible elements and F formed the lower part of the 'Niobium Tuff' unit, followed by pyroclastic eruption of pumice-rich material also enriched in incompatible elements formed the upper part. The REE mineralisation is believed to have formed from extreme enrichment of the tuff unit during deuteric alteration of an unusual suite of highly fractionated, A-type felsic lavas, tuffs, and subvolcanic intrusives. The mineralisation is believed to be essentially syngenetic, with fluorine-rich fluids moving through the cooling and consolidating tuff units soon after deposition (Chalmers, 1990). These volatile-rich fluids reacted with precursor magmatic minerals, such as zircon and columbite, and transported the REE, Be, and Ga as stable fluoride complexes. The fluorine-rich fluids played an important role in enhancing rare-metal abundances by increasing the efficiency of crystal-liquid separation and decreasing mineral-melt K_d's (Taylor et al., 1995a). Ramsden et al. (1993) and Taylor et al. (1995a) provide comprehensive interpretations for the petrogenesis of the Brockman polymetallic deposit.

Key references: Chalmers (1990): regional and local geological setting, mineralisation;
Ramsden et al. (1993): mineralogy and geochemistry, mineralisation; and
Taylor et al. (1995a,b): geochemistry, geochronology, petrogenesis.

Deposit Type 3.10: Rare-earth-element-bearing carbonatite

General description: Carbonatites (rocks with more than 50% modal carbonate) occur both as intrusive and volcanic rocks and are invariably associated with a wide range of alkalic rocks (see Chapter 4 for a description of important mineral system features of mineralised carbonatite). They are generally surrounded by a zone of sodic and/or potassic metasomatic rocks called fenites. The REE mineralisation can be both magmatic and metasomatic (formed from fluids released from a carbonatitic melt). Mineralisation can be found in lava flows and tuff, plugs, cone sheets, dykes, and rarely sills. Generally, large homogenous plutons of carbonatites are rarely mineralised. REE-mineralisation shows strong enrichment in light REE. In many carbonatites, economic mineralisation is associated with supergene processes (see Deposit Type 3.1).

Australian deposits/prospects: Yangibana (Capricorn Orogen, WA); Ponton Creek (Yilgarn Craton, WA); Yungul dykes (Halls Creek Orogen, WA); Cummins Range (Cummins Range (junction of Halls Creek and King Leopold orogens, WA). Mud Tank (Arunta Region, NT). Carbonatites and/or related veins are also reported at Mordor Igneous Complex (Arunta Region, NT) and Walloway (Gawler Craton, SA).

Deposits outside Australia: Mountain Pass (USA); Phalaborwa (South Africa); Kangakunde Hill (Malawi); Gallinas Mountain (USA); Saima (China); Bayan Obo (China), Mato Preto (Brazil); Qaqarssuk (Greenland), Sarfartoq (Greenland), Aley (Canada); Argor (Canada); Oka (Canada).

Type example in Australia: Yangibana, Western Australia (Fig. 3.21).

Location: Yangibana: 116.197215,
Latitude -23.890331
~300 km northeast of Carnarvon, Western Australia
1:250 000 map sheet: Edmund (SF 50–14)
1:100 000 map sheet: Edmund (2150)

Geological province: Gascoyne Complex, Capricorn Orogen, Western Australia.

Resources: The Yangibana 'ironstones' prospect has a recorded resource of 3.5 Mt @ 1.7% REO. The REE are in coarse-grained monazite and carbonatite containing up to 20% Nd_2O_5 and 1600 ppm Eu_2O_3. Flint and Abeysinghe (2000; cited in Sheppard et al., 2010) estimated a similar total resource of about 2.77 Mt @ 1.52% REO.

Current status: Prospect.

Economic significance: Unknown.

Geological setting: The REE-bearing ~1.25 Ga Yangibana 'ironstones' are part of the ~1.68 Ga Gifford Creek alkaline complex in the Capricorn Orogen (Pearson, 1995; Pearson and Taylor, 1996; Pearson et al., 1996). The alkaline complex intrudes Paleoproterozoic migmatite and granite and is spatially bound by two major west-northwest-trending lineaments (Fig. 3.21). The Yangibana and nearby Fraser prospects are also spatially close to a regional northeast-trending lineament delineated by O'Driscoll (1990). The REE-bearing ferrocarbonate-magnetite-hematite dykes occur as lenses and pods.

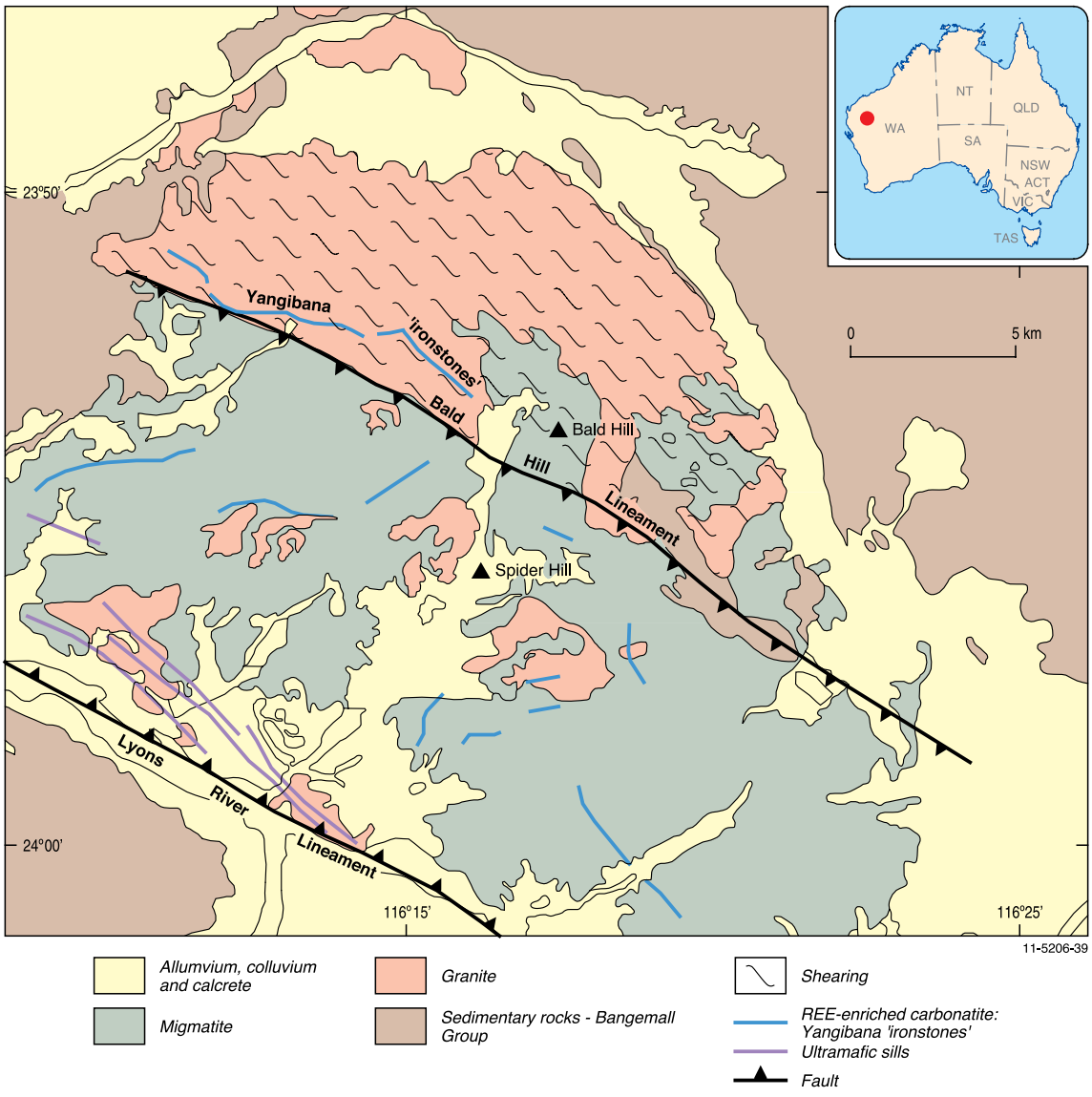

Figure 3.21. Simplified geological map of the Gifford Creek Complex and Yangibana 'ironstones'. Modified from Pearson and Taylor (1996).

Other components of Gifford Creek alkaline complex include carbonate-rich ~1.68 Ga ultramafic sills (Lyons River sills), pyrochlore-bearing sills (Spider Hill sill), limonitic weathered intrusions (Bald Hill intrusion), and fluidisation breccias (Pearson, 1995; Cassidy et al., 1997; Jaques, 2008).

Host rocks: Pearson et al. (1996) subdivided the alkaline rocks into five groups: alkali-amphibole and/or sodic pyroxene-rich ultramafic sills; magnetite- and hematite-rich pods (the Yangibana 'ironstones') and ferrocarbonatite dykes; aegirine-phlogopite-magnetite-apatite-pyrochlore-bearing sills and dykes; limonitic and weathered intrusions with basal layers of the Bangemall Group sedimentary rocks; and fluidisation breccias. The Yangibana dykes are generally 2 to 25 m in width and extend for up to 25 km along strike over an area of 500 square kilometres. The dykes have narrow zones of K-feldspar-magnetite alteration and are subconformable to metamorphic and shear foliations. Drilling has intersected carbonate-rich (ferrocarbonatite) rocks underneath the dykes.

REE mineralisation: The REE- and uranium-thorium mineralisation is hosted by ferrocarbonatite dykes and is enriched in LREE. The main minerals in the mineralised zones comprise dolomite, siderite, fluorite, magnetite, phlogopite, ilmenite, allanite, apatite, pyrite, sodic amphibole, and aegerine. The zones contain traces of sphalerite, galena, and molybdenite. Weathering has leached carbonates to form strongly cemented ironstones (Lottermoser, 1991). The ironstones contain up to 40% REO, with bastnäsite and monazite the major REE-bearing minerals. Significant zirconium (3.2%), niobium (1.8%), hafnium (0.3%), and scandium (110 ppm) are probably related to pyrochlore (Nb), zircon, and baddeleyite (Zr, Hf: Lottermoser, 1991).

Source of REE: Mineralised ferrocarbonatites represent the final stage of fractionation of a carbonatitic melt intimately associated with the emplacement of the Gifford Creek ultramafic-alkaline complex (Pearson et al., 1996). Hence the REE could have been sourced from the ultramafic-alkaline melt. The REE-enrichment observed in the ironstones could have been caused by supergene processes affecting ferrocarbonatites and associated fenites. Scandium was most probably sourced from ultramafic sills (Table 2 of Pearson et al., 1996).

Age of mineralisation: A SHRIMP U-Pb zircon age of 1679 ± 6 Ma obtained from a xenolith of metasomatised granite within an ultramafic sill (Lyons River sills) gives the age of the intrusion of the sills and of metasomatism. This age is similar to the SHRIMP U-Pb zircon age of 1674 ± 6 Ma from the alkaline feldspar granite with trachytic texture (Dingo Granite), which provides the age of emplacement for the Gifford Creek Alkaline Complex (Pearson et al., 1996). Pearson and Taylor (1996) suggest that the emplacement of the Gifford Creek Complex occurred as two episodes: first episode comprising ~1.68 Ma ultramafic sills, which also generated extensive fenitic alteration; and a second episode involved the emplacement of carbonatitic rocks at ~1.25 Ma. The first episode occurred prior to the sedimentation of the Bangemall Group rocks, whereas the second episode occurred after the initial phase of sedimentation (Pearson et al., 1996). The primary REE mineralisation was partially remobilised during weathering.

Genetic model: According to Pearson et al. (1996) the early phase of the Gifford Creek Complex may be related to the initial stage of rifting and opening of the Bangemall Basin at ~1.68 Ma. This was followed by the emplacement of carbonatitic magma after sedimentation in the basin had begun and was related to the continuing extension in the basin. Remobilisation of the ultramafic sill in the second phase was caused possibly due to reactivation of faults. REE mineralisation hosted by ferrocarbonatites was formed in the second phase and could have been magmatic and/or hydrothermal. It is possible that this involved remobilisation of magmatic and/or metasomatic REE-mineralisation formed during the first stage. Primary REE-mineralisation was also remobilised during weathering of ultramafic, fenitic, and ferrocarbonatitic rocks.

Key references: Pearson et al. (1996): geology, petrography, geochemistry; and
Pearson and Taylor (1996): mineral chemistry, whole-rock chemistry, stable isotopes, genesis.

Deposit Type 3.11: Rare-earth-element-bearing pegmatite

General description: REE-bearing pegmatites are formed from peraluminous, metaluminous, and peralkaline felsic melts (Fig. 3.22; Table 3.9; Long et al., 2010). Most pegmatites show an overprinting by magmatic-hydrothermal fluids. According to Cerny (1991a), REE-bearing pegmatites belong to NYF (Niobium-Yttrium-Flourine) and mixed families of rare-element pegmatites (Table 3.10). Pegmatites often form structurally controlled lenticular and tabular bodies within or in proximity to felsic intrusions and are characterised by homogenous, zoned and layered internal structures (Cerny, 1991a). In the NYF pegmatites, the late (hydrothermal) units show

a dramatic increase in the concentration of REE. The main REE minerals in pegmatites are gadolinite, fergusonite, euxenite, and monazite (Cerny, 1991a). The pegmatites are generally formed at temperatures between ~750°C and 150°C, with temperatures decreasing from the margins to the internal zones and secondary (hydrothermal) units.

Australian deposits/prospects: Cooglegong and Pinga Creek Tin fields (Abydos), (Pilbara Craton, WA); Waddouring Rock Pegmatite Group (Yilgarn Craton, WA); Wodgina Pegmatite districts (Pilbara Craton, WA).

Deposits outside Australia: Khibina Massif, Aldan (Russia); Motzfeldt, Greenland; Shatford Lake Field, Bancroft-Renfrew Field, Five Mile (Canada); Spruce Pine, South Plate, Topsham, Mount Antero, Wasau Complex (USA); Ytterby (Sweden).

Type example in Australia: Cooglegong–Pinga Creek, Western Australia (Fig. 3.23)

Location: Cooglegong: 119.4167, Latitude -21.5834; Pinga Creek (Abydos): Longitude 119.00, Latitude -21.75
~150 km southeast of Port Hedland, Western Australia
1:250 000 map sheet: EDMOND (SF5014)
1:100 000 map sheet: EDMOND (2150)

Geological province: Pilbara Craton, Western Australia.

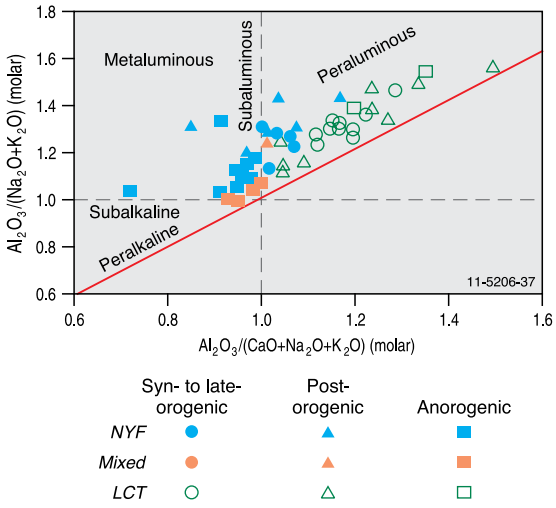

Figure 3.22. Fertile granites and associated pegmatite types coded by tectonic affiliation. Three major groups of pegmatites are shown, namely: NYF: Niobium–Yttrium–Fluorine; LCT: Lithium–Cesium–Tantalum; and Mixed. REE-bearing NYF-type pegmatites are associated predominantly with metaluminous and peraluminous granites (see Table 3.1 for definitions of granite types). Modified from Cerny (1991b).

Resources: The pegmatites and associated alluvial placers were mined for tin. It is not clear if REE were extracted with the tin.

Current status: Old mine. Prospect.

Economic significance: Unknown. The pegmatites in the region need more work to assess the potential of REE mineralisation.

Geological setting: The Cooglegong and Pinga Creek pegmatite fields (Figs 3.23 and 3.24) are associated with the 2890 Ma to 2830 Ma granite suites emplaced in the Eastern Pilbara tectonic zones (Sweetapple and Collins, 2002). The NYF family and mixed Lithium–Cesium–Tantalum pegmatite (LCT)–NYF-family pegmatites are predominantly located in domains 3 and 2 of the Eastern Pilbara Craton as defined by Krapez and Eisenlohr (1998). Some pegmatites constitute part of a 120-km-long north-northeast-trending linear array (Wodgina-Strelley belt). More than 55% of the pegmatites in the Pilbara Craton are interpreted to be spatially related to major faults. Pegmatites were emplaced into brittle and ductile deformation regime and their shapes appear to be determined by the nature of the host rocks. The pegmatite veins and swarms often use narrow tension gashes, dilational jog-type, and horse-trail brittle structures in granite-gneiss (Sweetapple and Collins, 2002).

Host rocks: The mineralisation is hosted by NYF and mixed LCT–NYF-family pegmatites which are emplaced in Archean gneissic granites, migmatites, and monzogranites (Table 3.11). The Cooglegong pegmatites are associated with the Cooglegong and Spear Hill monzogranties of the Shaw Granitoid complex whereas the Pinga Creek pegmatites are associated with the Numbana Monzogranite of the Yule Granitoid complex (Figs 3.23 and 3.24). The internal structure of the pegmatites is layered and simple. Some pegmatites in the Pinga Creek field are aplitic (Table 3.11).

REE mineralisation: The primary REE mineralisation in the pegmatites is poorly described. The presence of REE mineralisation is interpreted from REE-bearing minerals in the alluvial concentrates derived from them. The main REE-bearing minerals include tanteuxenite, gadolinite, yttrotantalite, fergusonite, monazite, and samarskite (Sweetapple, 2000). The alluvial concentrates also contain cassiterite and tantalite-columbite.

Source of REE: The peraluminous nature of granites and a high initial $^{87}Sr/^{86}Sr$ ratio of the Cooglegong Granite suggest that the NYF-type pegmatites were

most likely derived from partial melting, or reworking of older felsic material that also generated the granites (Sweetapple, 2000). Like most other pegmatites of this type the REE were most probably derived from a fluid-rich pegmatitic melt.

Age of mineralisation: SHRIMP $^{206}Pb/^{207}Pb$ analyses of cassiterite from the Cooglegong pegmatites yielded an age of 2839 ± 16 Ma. This is slightly younger than the age obtained from cassiterite by secondary ion mass spectrometry (2901 ± 16 Ma). Geochronological data from rare-metal pegmatites in the region indicates that emplacement of associated granites (post-dating peak metamorphism at 2950 Ma and 2900 Ma) occurred between 2800 Ma and 2900 Ma. The pegmatites are interpreted to have been emplaced during two periods: an early phase at 2890 to 2880 Ma and a later phase between 2840 Ma and 2830 Ma (Sweetapple and Collins, 2002).

Genetic model: The REE mineralisation was most probably formed during crystallisation of a fluid-rich pegmatitic melt. In the pegmatites of the Wodgina Pegmatite Group, tantalum mineralisation is interpreted to have formed in the early stages of crystallisation from the melt. Some tantalum was remobilised later and dispersed within secondary (hydrothermal) albite and lepidolite. It is possible that similar process occurred for the NYF-type pegmatites in the Cooglegong and Pinga Creek fields, however, more detailed information on the mineralogy and paragenesis is required to indicate an evolutionary model for the REE-bearing pegmatites.

Key references: Cerny (1991a,b): regional to global environments, petrogenesis, evolution;
Sweetapple and Collins (2002): classification, petrogenesis, metallogeny; and
Sweetapple (2000): age, classification, exploration methods.

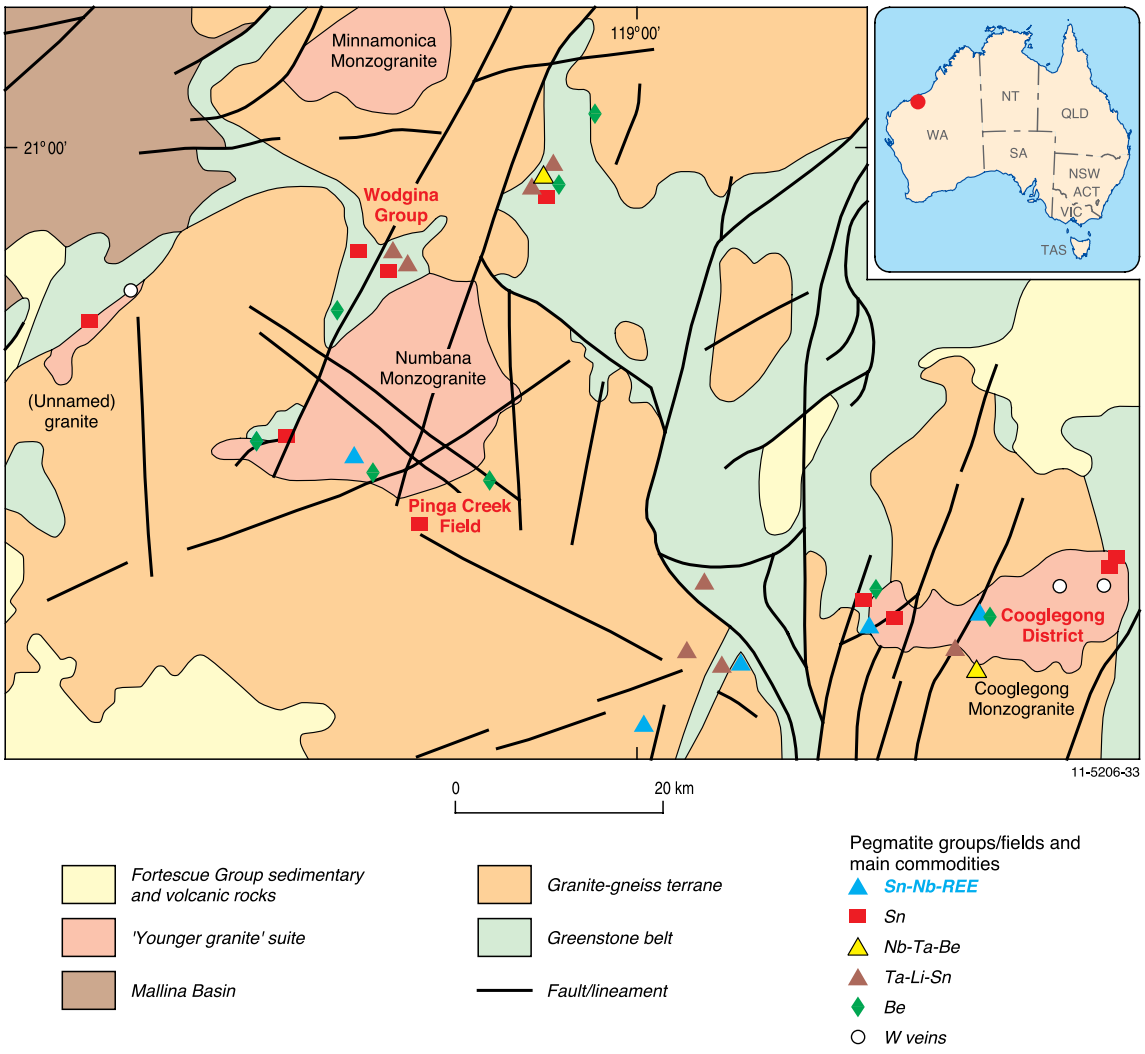

Figure 3.23. Regional geological map of the major mineralised pegmatite fields in the east Pilbara Craton, Western Australia. Modified from Sweetapple and Collins (2002).

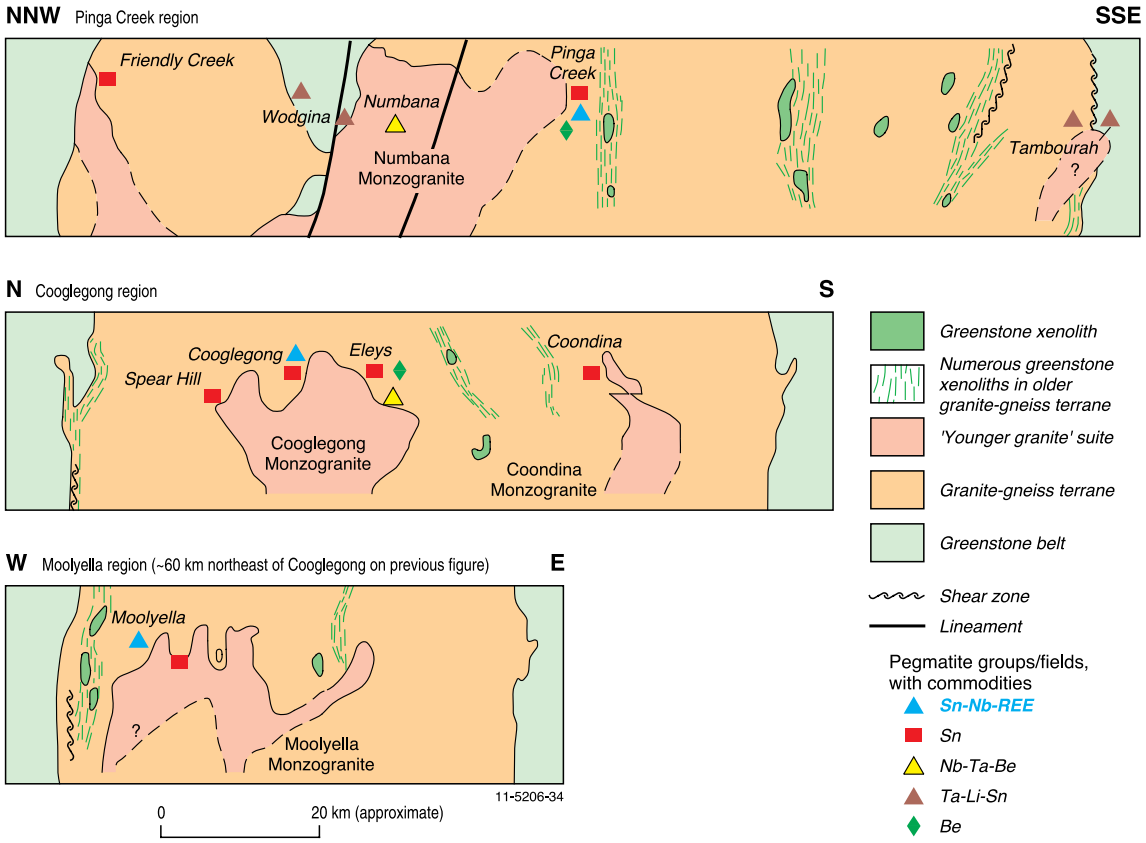

Figure 3.24. Schematic cross-sections through the Yule, Shaw, and Mount Edgar granitic complexes showing general location of rare metal and rare-earth-element-bearing pegmatites. Modified from Sweetapple and Collins (2002).

Table 3.9. Three petrogenetic families of rare-earth-element-bearing pegmatites (Cerny, 1991a).

Family	Pegmatite types	Geochemical signature	Pegmatite bulk composition	Associated granites	Source lithologies	Examples
LCT	Beryl, complex albite-spodumene, albite	**Li**, Rb, **Cs**, Be, Sn, Ga, **Ta** > Nb (B, P ,F)	Peraluminous	Syn- to late-orogenic; Peraluminous S, I or mixed types	Undepleted upper- to middle- crust supracrustals and basement gneisses	Biktia field, Zimbabwe; Uto-Mysingen field, Sweden,; White Picacho field, New Mexico; Wodgina, Pilbara (WA)
NYF	Rare earth	**Nb** > Ta, Li, **Y**, Sc, REE, Zr, U, Th, **F**	Subaluminous, metaluminous (subalkaline)	Mostly anorogenic; peraluminous to metaluminous (rarely peralkaline) A and I types	Depleted middle to lower crustal granulites, or undepleted juvenile granites	Shatford Lake group, Canada; Stockholm area, Sweden; Cooglegong and Abydos, Pilbara (WA)
Mixed	'Cross-bred' LCT and NYF	Mixed	Metaluminous to moderately peraluminous	Post-orogenic to anorogneic; subaluminous to slightly peraluminous; mixed geochemical signature	Mixed protolith; or assimilation of supracrustals by NYF granites	Tordal district, Norway; Kimito, Finland; Moolyella, Pilbara (WA)

LCT = Lithium–Cesium–Tantalum pegmatite; NYF: Niobium–Yttrium–Fluorine pegmatite. Peraluminous = (A/CNK) >1; subaluminous = (A/CNK) ~1; metaluminous = (A/CNK) <1 at (A/NK) >1; subalkaline = (A/NK) ~1; peralkaline = (A/NK) <1. A = molecular Al_2O_3; CNK = CaO + Na_2O + K_2O; and NK = Na_2O + K_2O.

Table 3.10. Four classes of granitic pegmatites (modified from Cerny, 1991a).

Class	Family	Typical minor elements	Metamorphic environment	Relation to granites	Structural features
Abyssal		U, Th, Zr, Nb, Ti, **Y**, **REE**, Mo; poor to moderate mineralisation	Upper amphibolite to low- to high-P granulite facies	None (anatectic segregations)	Conformable to mobilised cross-cutting veins
Muscovite		Li , Be, **Y**, **REE**, Ti, U, Th, Nb > Ta; poor to moderate mineralisation; ceramic minerals	High P, Barrovian amphibolite facies (kyanite– sillimanite)	None (anatectic segregations) to marginal and exterior	Quasi-conformable to cross-cutting
Rare-element	LCT	Li, Rb, Cs, Be, Ga, Sn, Hf, Nb > or < Ta, B, P, F; poor to abundant mineralisation; gemstock, industrial minerals	Low P, Abukama amphibolite to upper greenschist facies (andalusite–sillimanite)	(Interior to marginal to) exterior	Quasi-conformable to cross-cutting
	NYF	**Y**, **REE**, Ti, U, Th, Zr, Nb > Ta, F; poor to abundant mineralisation; ceramic minerals	Variable	Interior to marginal	Interior pods, conformable to cross-cutting
Miarolitic	NYF	Be, **Y**, **REE**, Ti, U, Th, Zr, Nb > Ta, F; gemstock; poor mineralisation	Shallow to sub-volcanic	Interior to marginal	Interior pods, conformable to cross-cutting dykes

LCT = Lithium–Cesium–Tantalum pegmatite; NYF: Niobium–Yttrium–Fluorine pegmatite.

Table 3.11. Rare-earth-element-bearing pegmatites in the Pilbara Craton, Weatern Australia (modified from Sweetapple and Collins, 2002).

Pegmatite field/district/ group	Associated granite complexes	Host rock	Morphology	Internal structure	REE minerals	Pegmatite class/ and type/subtype
Pinga Creek	Numbana Monzogranite; Yule Granitoid complex	Gneissic granite, migmatite, greenstone xenoliths	Unknown	Layered aplite-pegmatites	Gadolinite	Rare element/rare earth/gadolinite
Cooglegong	Cooglegong Monzogranite; Spear Hill Monzogranite; Shaw Granitoid Complex	Granite gneiss, migmatite, monzogranite	Swarms of shallow-dipping sheets	Layered and simple pegmatites	Tanteuxenite, yttrotantalite	Rare element
White Springs	Unknown	Granite gneiss, migmatite	Dyke	Simple unzoned pegmatites	Gadolinite, monazite, tanteuxenite	Rare element/rare earth/gadolinite
Abydos	Unknown	Granite gneiss, migmatite	Sheets and dykes	Simple to complex zoned pegmatites	Gadolinite, monazite	Rare element/rare earth/gadolinite
Wodgina	Numbana Monzogranite	Mafic-ultramafic metavolcanics	Veins	Layered and massive pegmatites		Rare element
Moolyella	Moolyella Monzogranite	Gneissic granite	Veins	Layered aplite-pegmatites and simple pegmatites	Monazite	Rare element

Deposit Type 3.12: Rare-earth-element-bearing skarn

General description: Skarn is a rock dominated by calcium and magnesium silicates typically formed from the alteration of carbonate rocks as a result of metasomatic replacement by fluids derived from felsic melts. Some skarns can be formed from thermal and regional metamorphism. In skarns, often the initial thermal-metamorphic hornfels are overprinted by anhydrous and hydrous silicates of calcium, iron and magnesium. Economic-grade concentrations of ore minerals are generally formed in the later stages of cooling of the fluids (Eckstrand et al., 1995; Meinert, 1993). REE mineralisation in skarn is hosted by calc-silicate rocks formed from fluids derived from predominantly felsic magmatic melts, which also form granites intruding calcareous rocks. Some REE-bearing skarns are also derived from fluids sourced from carbonatites (e.g., Saima in China; Long et al., 2010). In some REE-bearing skarns, the mineralisation involves two stages—in the first stage skarns with REE-bearing minerals are formed, which are remobilised by metamorphic fluids generated from regional metamorphism at the second stage.

Australian deposits/prospects: Mary Kathleen (Mount Isa Orogen, Qld).

Deposits outside Australia: Saima (China); Skye (Scotland).

Type example in Australia: Mary Kathleen, Queensland (Fig. 3.25).

Location: Longitude 140.013, Latitude -20.746
~50 km east of Mount Isa, Queensland
1:250 000 map sheet: Cloncurry (SF 54–02)
1:100 000 map sheet: Marraba (6956)

Geological province: Mount Isa Orogen, Queensland

Resources: Significant REE mineralisation has been intersected at the Mount Dorothy and Elaine Dorothy prospects. An inferred Resource of 83 000 tonnes at 280 ppm U_30_8 and 3 200 ppm TREO was reported in March 2010.

Current status: Mined out. The deposit was mined for uranium, but the REE were left in the tailings dumps.

Economic significance: Unknown, but high for other prospects in the area.

Geological setting: The Mary Kathleen deposit is located within the Mary Kathleen Belt (10 to 30 km wide and >200 km long) of metasedimentary rocks metamorphosed to amphibolite facies (Bierlein et al., 2008). An ENE–WSW-directed extension created a rift basin (Leichhardt Superbasin), which was filled (between ~1800 Ma to ~1750 Ma) with a thick pile of mafic rocks and fluvial to lacustrine siliciclastic and lesser carbonate-bearing sedimentary rocks (Jackson et al., 2000; Gibson et al., 2008). The metasediments of the Corella Formation hosting the Mary Kathleen deposits were deposited during this event. Felsic magmatism related to the Wonga Extension Event occurred in the belt between 1760 Ma and 1720 Ma during which the Wonga and the Burstall Suites were emplaced (Neumann, 2007). This Phase 1 was overprinted by a Phase 2 comprising regional metamorphism and deformation between 1550 Ma and 1500 Ma (Oliver et al., 1999).

Host rocks: The REE and uranium mineralisation is hosted by hornfelsed calc-silicate rocks, skarns, quartzite, and marble. The precursor rocks of the skarns comprised calcareous pebble conglomerate, an ophitic-textured 'monzonitic' intrusion and minor banded calcareous sediments (Fig. 3.25). Stratigraphically these rocks belong to the upper parts of the Corella Formation (Derrick, 1977; Oliver et al., 1999). The mineralisation is structurally controlled by Phase 1 and Phase 2 skarns occupying the axial zone and the western limb of the Mary Kathleen Syncline (Fig. 3.25). Paragenetic studies show two episodes of skarn-formation (Oliver et al., 1999).

REE mineralisation: The high-grade uranium, thorium, and REE mineralisation forms infilling- and replacement-style veins. A later phase of REE mineralisation is represented by anastomosing array of veins and 'metasomatic' breccia (Oliver et al., 1999). The main REE-ore minerals are allanite and stillwellite [$(Ce,La,Ca)BSiO_5$] associated with uraninite, garnet, pyroxene, and apatite. Apatite, garnet, and titanite also contain REE. The REE mineralisation overprints skarns. In the marginal zone fractured skarn is cut by a network of allanite veins. In the main ore zone, coarse bladed allanite is accompanied by second-generation garnet, apatite, and uraninite sheathed with silica. A late generation of allanite forms alteration patches and infills post-ore fractures. The post-ore assemblage also contains calcite, prehnite, albite, and variable amounts of epidote, garnet, chalcopyrite, and hematite (Oliver et al., 1999). The mineralisation is cross-cut by late calcite veins with accessory chalcopyrite, garnet, and rare clinopyroxene. The late veins are interpreted to be related to a ~1500 Ma deformation event (Oliver et al., 1999). The REE content of the deposit is around 4% (Scott and Scott, 1985), with the REE

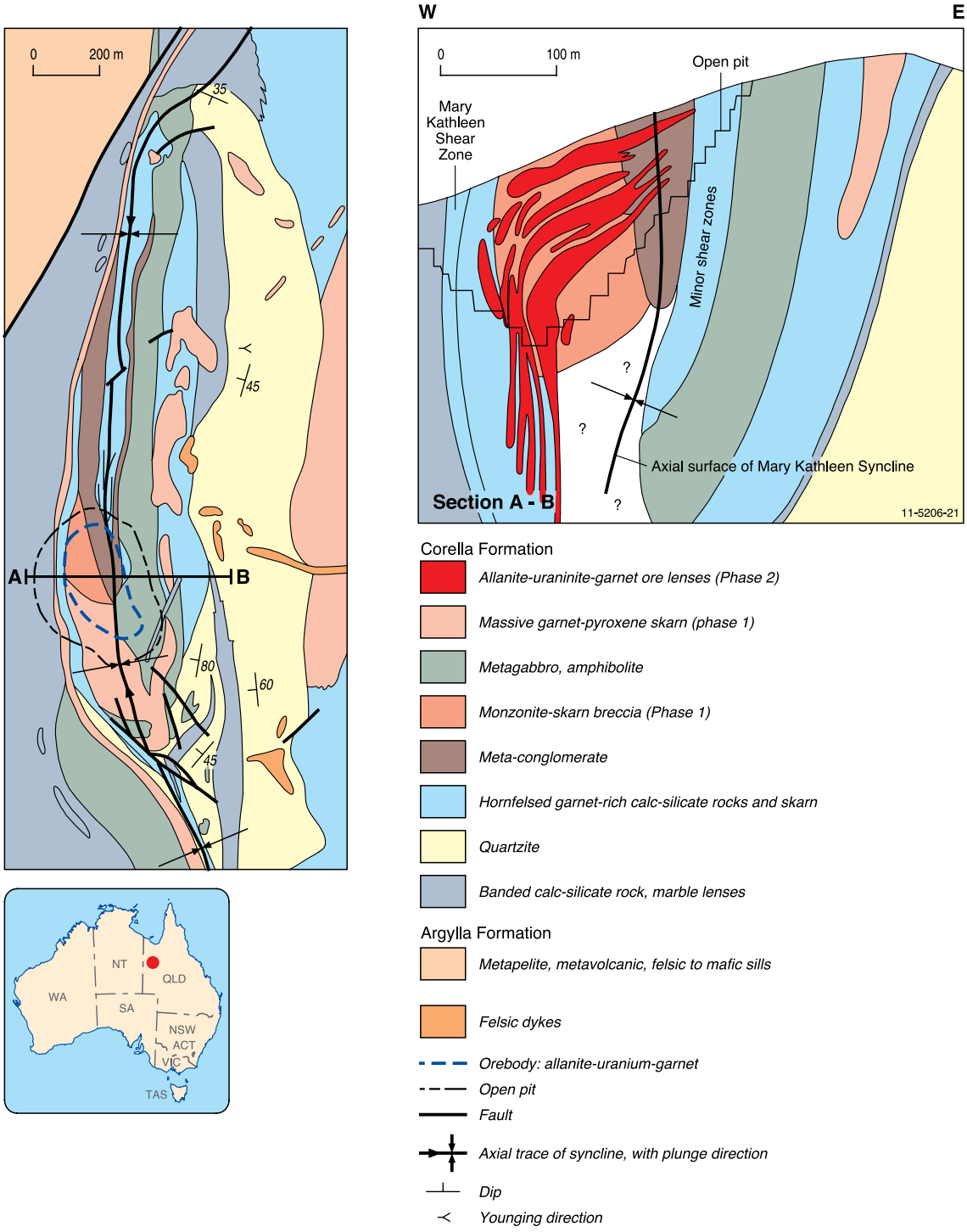

Figure 3.25. Geological map and cross-section of the Mary Kathleen uranium-rare-earth-element deposit, Queensland. Modified from Oliver et al. (1999).

content of individual ore samples ranging from 14 to 16 wt% (Table 3.12). The ore samples show extreme enrichment in LREE (Tables 3.12 and 3.13). Amongst the skarns, paragenetically early banded skarns are more enriched in REE than massive skarns. Recent drilling at the Mount Dorothy project located near Mary Kathleen shows intervals containing up to ~5000 ppm TREE, with HREE + yttrium accounting for more than 50% of the TREE (ASX/media announcement by China Yunnan Copper Australia Limited, 6th January 2011). This hole intersected a strongly weathered/oxidised zone rich in iron-oxides and clay.

Source of REE: Available data do not permit clear identification of the source of REE. The REE distributions and initial $^{143}Nd/^{144}Nd$ ratios in the ores suggest that magmatic fluids associated with the Burstall Granite could have leached REE from the Corella Formation to form a REE-rich skarn protore (Maas et al., 1987). Oliver et al. (1999) proposed a more complex model in which REE are derived from two (or more) sources which include extremely light REE-enriched old (>2300 Ma) rocks and rocks within the Mary Kathleen Syncline (skarns and the Burstall Granite).

Age of mineralisation: The age of mineralisation is contentious. U-Pb dating of uraninite from an apatite-allanite assemblage gave an age of 1550 ± 15 Ma (Page, 1983). This age is close to the age of D_3 deformation and peak metamorphism in the belt (Oliver et al., 1999). The Burstall Suite granites, which are interpreted to be related to the formation of skarns, yield a U-Pb TIMS age of ~1740 Ma (Page, 1983). More recent SHRIMP U-Pb ages confirm a magmatic age of 1740–1735 Ma (Neumann, 2007). Mineral separates from the garnet ± pyroxene skarn assemblage yield a Sm–Nd isochron age of 1766 ± 80 Ma (Maas et al., 1987) which overlaps the age of the Burstall Suite granites.

Genetic model: The mineralisation is interpreted to have formed in two stages (Maas et al., 1987; Oliver et al., 1999). The first stage resulted in the formation of skarns from predominantly magmatic fluids associated with the Burstall Suite granites. In the second-stage metamorphic fluids generated during peak metamorphism recrystallised and upgraded REE and uranium mineralisation. The second-stage fluid-flow was structurally controlled.

Key references: Page (1983): U-Pb geochronology, lead isotopes;
Maas et al. (1987): Sm-Nd isotopes, REE abundances, geochronology; and
Oliver et al. (1999): mineral chemistry, petrography, structure, geochronology, ore genesis.

Table 3.12. Concentration (in ppm) of rare-earth elements in ore and granite, Mary Kathleen deposit (Maas et al., 1987).

Element	Ore (MK 68)	Ore (MK 69)	Ore (MK 70)	Fresh Burstall Granite (237 G)	Fresh Burstall Granite (241 A)	Altered Burstall Granite (240 A)	Altered Burstall Granite (240 E)
La	54 675	60 845	46 922	51	79.3	4.1	3.3
Ce	77 113	87 015	80 692	93.6	160.1	13.9	31.7
Pr	7648	7503	5325				
Nd	16 252	15 680	10 584	45.5	59.4	6.5	3
Sm	1002	638	487	8.4	9.6	2.2	0.83
Eu	35	34	33	0.25	0.81	0.37	0.13
Gd				13.6	6.9	4.4	3.8
Tb				1.56	1.27	1.59	1.58
Dy	28	46	33				
Ho				2.02	1.75	1.08	0.88
Yb		2	1	4.16	4.56	3.31	2.61
Lu				0.59	0.7	0.41	0.36
LREE	156 725	171 715	144 043	199	309	27	39
HREE	28	48	34	22	15	11	9
LREE/ HREE	5597	3615	4224	9	20	3	4
Total REE	156 753	171 763	144 077	221	324	38	48

Note: The number in brackets indicates the sample number.

Table 3.13. Concentration (in ppm) of rare-earth elements in skarns, Mary Kathleen deposit (Maas et al., 1987).

Element	Banded Skarn (1262D1)	Banded Skarn (1262D5)	Banded Skarn (5013A1)	Banded Skarn (5013A3)	Massive Skarn (0832A2)	Massive Skarn (0822C1)	Massive Skarn (0822C2)
La	17.3	23.3	183	40.2	3.6	10.7	13
Ce	39.7	37.8	205	58.9	12.9	34.3	38.6
Pr							
Nd	19.3	21	62.6	34	21.9	23.8	23.7
Sm	3.5	4	6.8	7.7	7.4	4.9	4.4
Eu	0.45	0.58	0.89	1.25	2.3	1.9	1.68
Gd	2.36	3.98	6.6	6.6	5.2	4.6	4.3
Tb	0.39	0.66	0.39	1.08	0.65	0.76	0.66
Dy							
Ho	0.54	1.02	0.41	1.44	0.77	1.26	1.04
Yb	1.37	2.92	1.65	3.65	2.02	3.79	3.11
Lu	0.19	0.44	0.15	0.55	0.31	0.58	0.49
LREE	80	87	458	142	48	76	81
HREE	5	9	9	13	9	11	10
LREE/HREE	17	10	50	11	5	7	8
Total REE	85.1	95.7	467.49	155.37	57.05	86.59	90.98

Note: The number in brackets indicates the sample number.

Deposit Type 3.13: Apatite and/or fluorite veins

General description: The vein deposits include REE-enriched veins of apatite and/or fluorite. In some deposits mineralisation is hosted in quartz veins. The veins are formed from hydrothermal fluids predominantly derived from alkaline and/or carbonatite melts. In many regions the veins may be distal to alkaline and carbonatite complexes. In some deposits the veins may have formed from non-magmatic fluids or fluids related to later magmatic melts.

Australian deposits/prospects: Nolans Bore (Arunta Region, NT); ?John Galt (Halls Creek Orogen, WA).

Deposits outside Australia: Lehmi Pass, Idaho (USA); Gallinas Mountains, New Mexico (USA); Kangakunde Hill (Malawi).

Type example in Australia: Nolans Bore, Northern Territory (Figs 3.26 and 3.27).

Location: Longitude 133.238557, Latitude -22.59385
~135 km north-northwest of Alice Springs
1:250 000 map sheet: Napperby (SF 53–09)
1:100 000 map sheet: Aileron (5552)

Geological province: Arunta Region, Northern Territory.

Resources: Measured, Indicated and Inferred Resources totalling 30.3 million tonnes to a depth of 130 m which grades at 2.8% REO, 12.9% P_2O_5, 0.44 pounds per tonne U_3O_8, and 0.27% Th. According to Arafura, the distribution of the LREE currently being considered for extraction, (La, Ce, Pr, and Nd) amount to 95%, whereas the HREE (Sm, Eu, Gd, Tb, Dy) amount to 4.23% (Miezitis, 2010).

Current status: Deposit–advanced project (Fig. 3.28).

Economic significance: High.

Geological setting: The Nolans Bore deposit is spatially close to several tin and tantalum pegmatites, and REE-bearing carbonatite/alkaline complexes (Mud Tank and Mordor Igneous Complex). This mineral field of carbonatites, pegmatites, and other REE occurrences is in a region transacted by three major lineaments delineated by O'Driscoll (1985), which include the north–northwest-trending G2-gravity lineament that is considered to be spatially related to the Olympic Dam deposit and northwest-trending G3-gravity

and R16 lineaments (Fig. 3.26). At a more local scale both the Mud Tank Carbonatite and Mordor Igneous Complex are located near the Woolanga Lineament, a deep-seated NW-trending crustal structure which may have controlled the emplacement of alkaline rocks in the Aileron Province (Jaques, 2008; Hoatson et al., 2005). The mineral field traverses the northern Willowra Gravity Ridge high (Fig. 3.26) that forms the boundary between the Aileron Province in the south and the Tanami Orogen in the north and which is interpreted to be a suture zone where the thickness of the crust (in the Aileron Province) increases to ~60 km (Goleby et al., 2009). Thus like many other alkaline and carbonatite provinces, the Nolans Bore deposit and other pegmatites and carbonatites in the area can be spatially related to a zone of thickened crust (lithospheric?) crosscut by deep crustal structures.

Host rocks: The mineralised fluorapatite veins at the Nolans Bore deposit are hosted predominantly by granite (metamorphosed to gneiss) which intruded the Lander Rock beds consisting of schist, phyllite, hornfels, granofels and tourmaline-bearing quartzite (Fig. 3.27; Huston et al., in press). The granites are correlated with the Boothby Gneiss (dated at 1806 ± 4 Ma) and the Napperby Gneiss (1778 ± 8 Ma; cited in Huston et al., in press).

REE mineralisation: The mineralisation at the Nolans Bore deposit (Fig. 3.29) is hosted in a series of east-northeast-trending, and steeply dipping to the northwest, fluorapatite veins and breccia zones (Fig. 3.27). The granite-gneiss host has been strongly kaolinised due to weathering. The weathering zone shows secondary enrichment with REE. Huston et al. (in press) describe four styles of mineralisation: (1) massive fluorapatite veins that typically contain 4–6% REE oxides and constitute most of the defined resource; (2) very high-grade (7%–10% REE oxide) zones found in cheralite-bearing, apatite-poor kaolinitic zones outside of the veins; (3) apatite-allanite-epidote zones hosted by calc-silicates; and (4) low-grade stockwork zones in gneiss and kaolinitised rock adjacent to the veins and mylonite zones. The main ore minerals are cheralite, thorite, allanite, bastnäsite, monazite, and

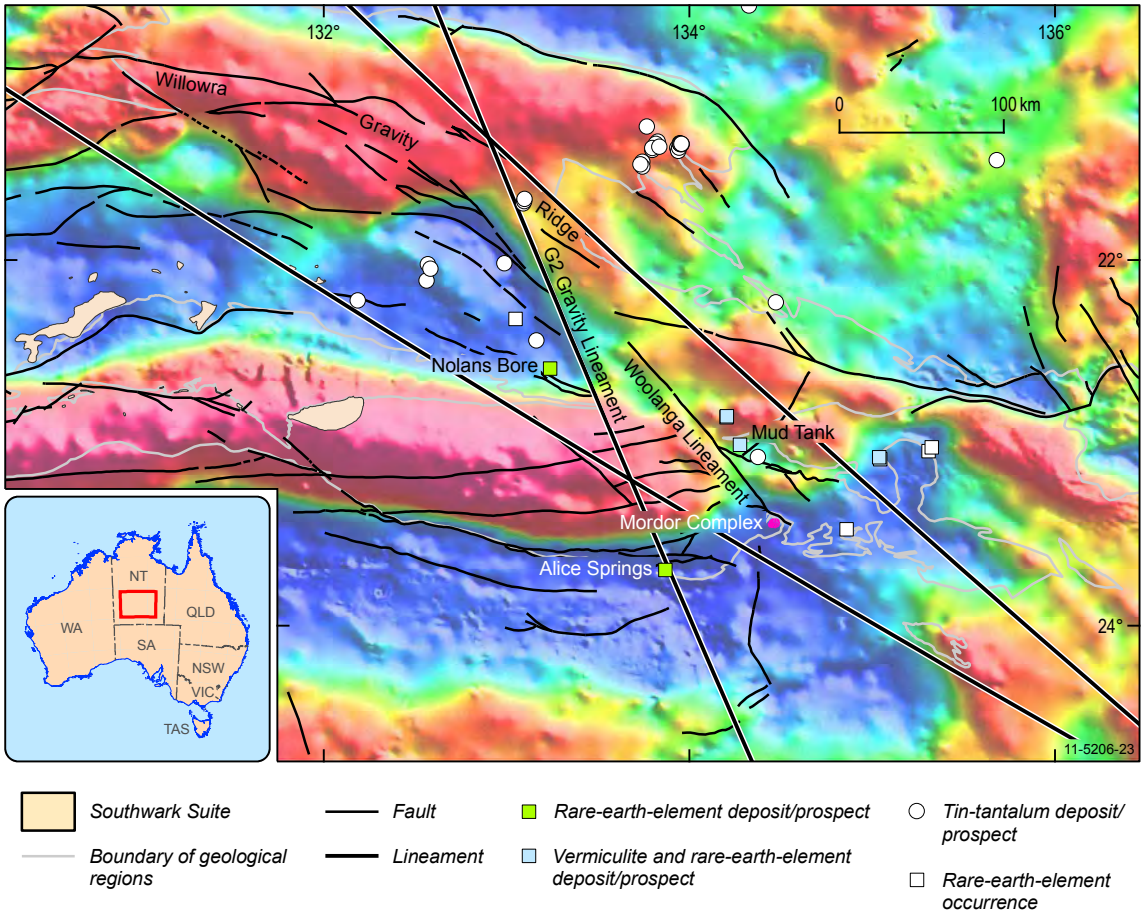

Figure 3.26. Locations of Nolans Bore and other rare-earth-element-bearing prospects and deposits in central Australia. The major structural and gravity lineaments are shown on a background gravity image. Locations of deposits and prospects are from Geoscience Australia's OZMIN database.

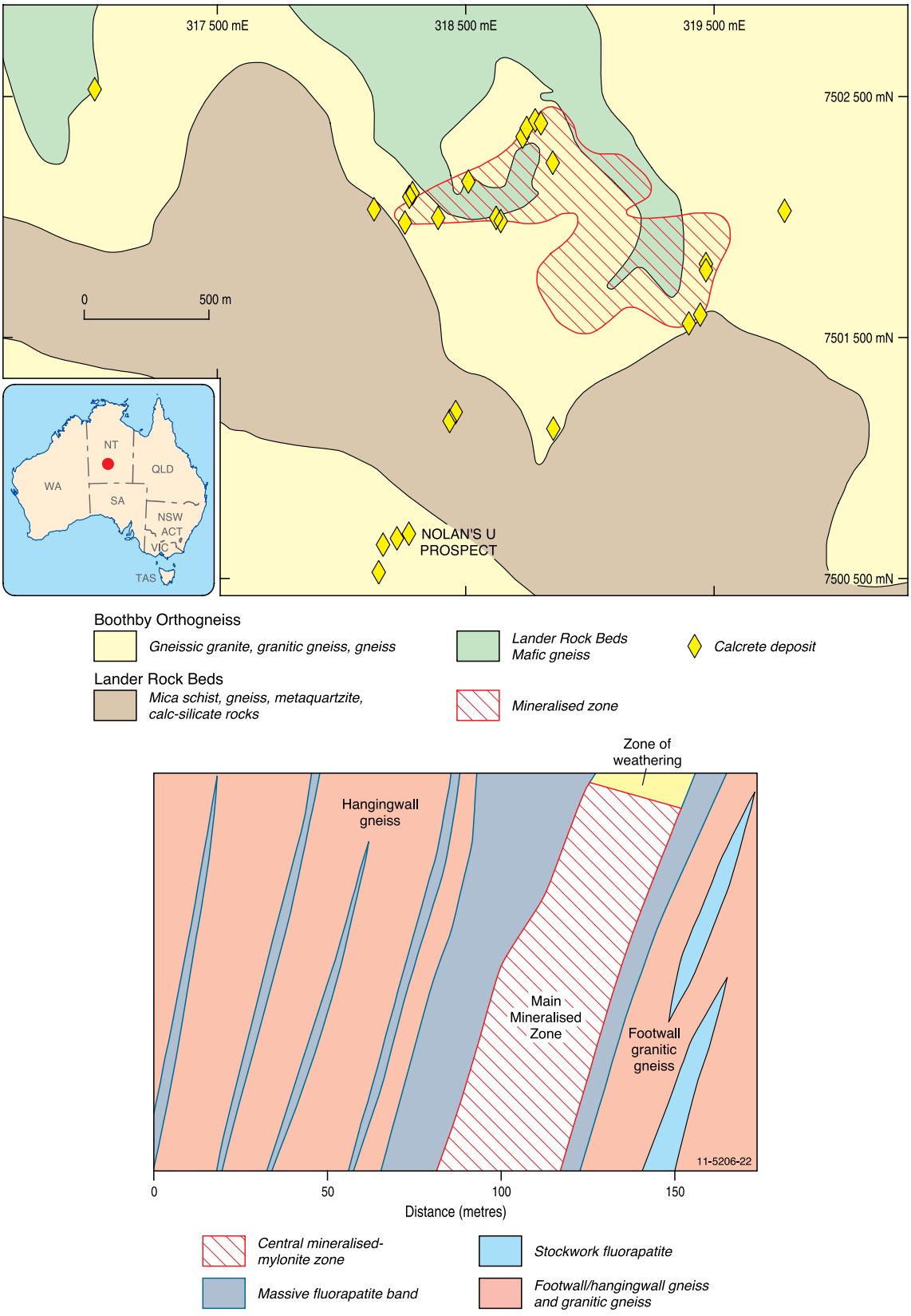

Figure 3.27. Geological map and cross-section of the Nolans Bore rare-earth-element deposit. The section is from the northwestern part of the deposit. Modified from Lockyer and Brescianini (2007).

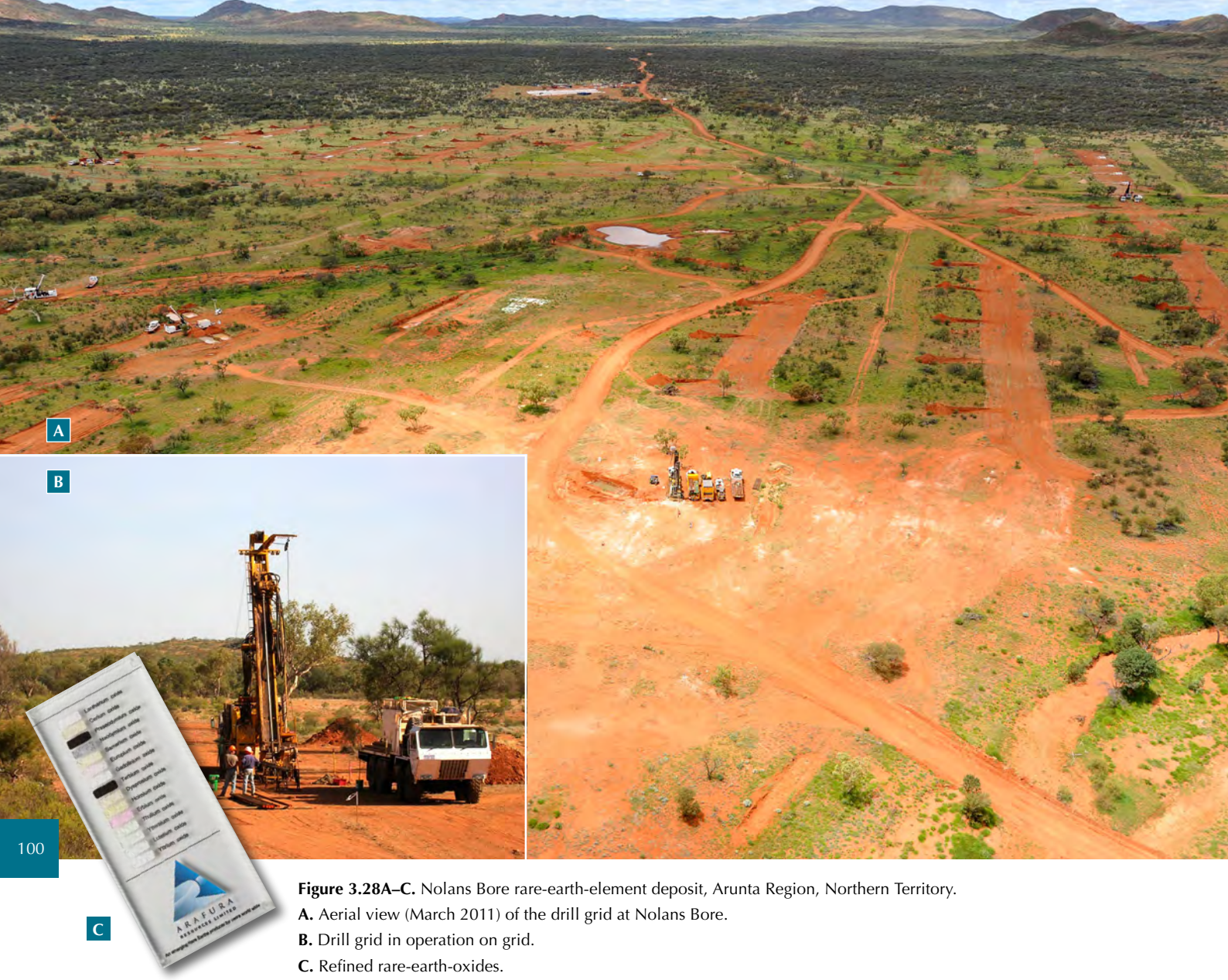

Figure 3.28A–C. Nolans Bore rare-earth-element deposit, Arunta Region, Northern Territory.
A. Aerial view (March 2011) of the drill grid at Nolans Bore.
B. Drill grid in operation on grid.
C. Refined rare-earth-oxides.
Richard Brescianini (Arafura Resources Limited: http://www.arafuraresources.com.au/) provided the photographs.

several REE-bearing fluorocarbonates (Lockyer and Brescianini, 2007; Huston et al., in press). Often brecciated apatite is infilled and replaced with Ce- and La-bearing cheralite monazite and bastnäsite (Lockyer and Brescianini, 2007).

Source of REE: The Nolans Bore deposit is located in a zone that also contains the Mud Tank Carbonatite, Mordor Igneous Complex, and several tin- and tantalum-bearing pegmatites. It is possible that REE in the deposit were derived from alkaline and/or carbonatite melts or from felsic melts which formed tin-tantalum pegmatites. On the basis of high thorium content of the Nolans Bore fluorapatite, Hussey (2003) suggests that it was unlikely to be related to a carbonatite or carbonatite-derived fluid, but is more likely to be sourced from a NYF-type (Niobium-Yttrium-Fluorine type, Cerny, 1991a) pegmatite melt. The REE patterns for fluorapatite, however, are similar to that of apatite from both peralkaline and carbonatitic melts (Hussey, 2003). Juvenile initial $^{87}Sr/^{86}Sr$ (0.705-0.707) and evolved Nd isotopes (Nd 1250 = -12 to -4) suggest an enriched mantle source of REE (Korsch et al., 2009).

Age of mineralisation: The mineralised veins and breccias are hosted by granite gneisses interpreted to be emplaced at ~1880 Ma to 1780 Ma (see above). This provides a maximum age for mineralisation. Preliminary U-Pb dating of apatite from the veins yields an age of 1244 ± 10 Ma (Korsch et al., 2009). If this age is correct the mineralisation is neither related to the Mordor Igneous Complex (with a SHRIMP U-Pb crystallisation age of 1133 ± 5 Ma, Hoatson et al., 2005), nor with the Mud Tank Carbonatite, which has a much is younger emplacement age of 732 ± 5 Ma (Black and Gulson, 1978). Although the ~1244 Ma age is thought to broadly coincide with the age of the Mudginberri phonolite dykes (Rb-Sr isochron age of 1316 ± 40 Ma, Page et al., 1980) in the Pine Creek

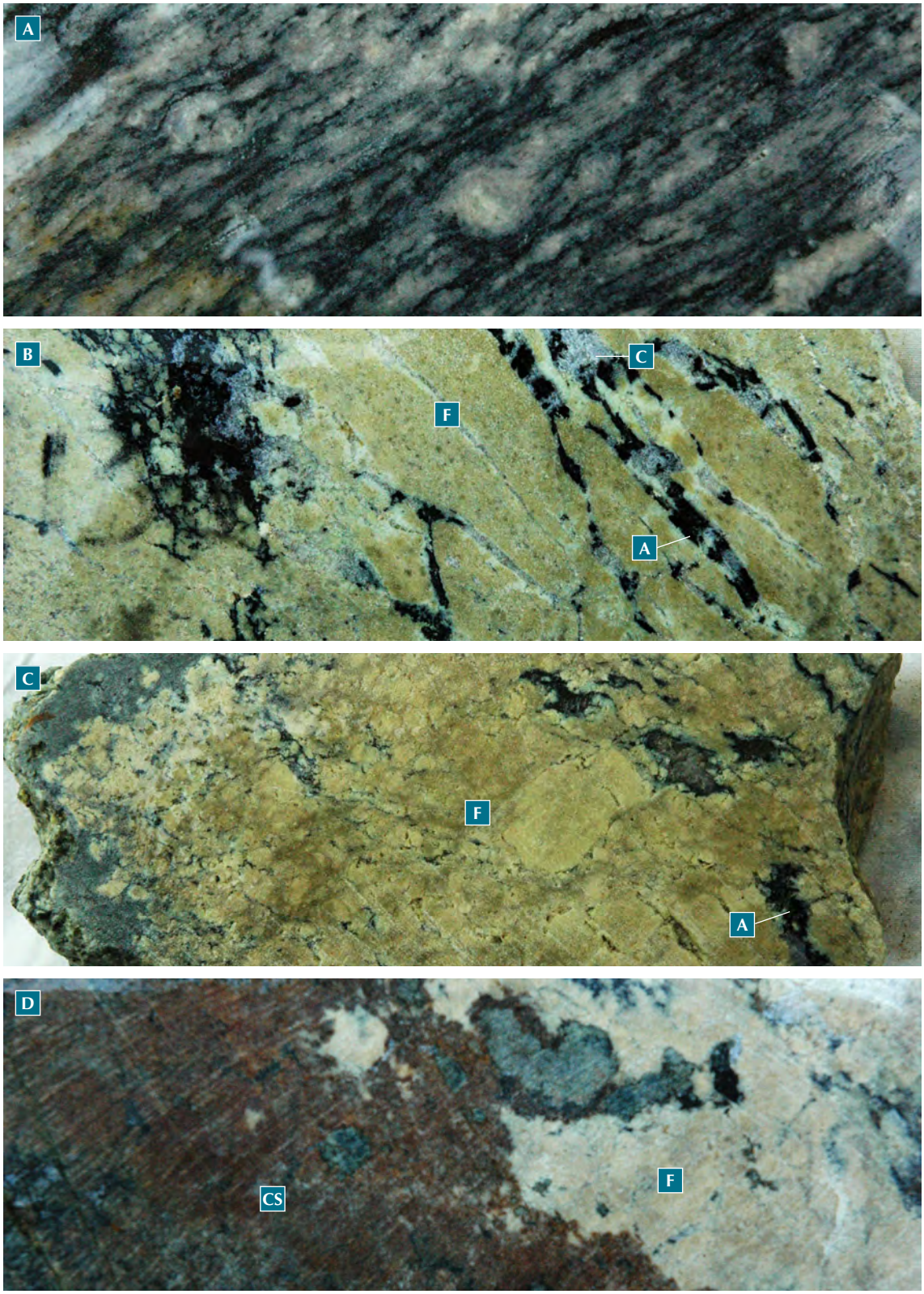

Figure 3.29A–D. Major rock types from the Nolans Bore rare-earth-element deposit, Northern Territory.

A. Gneissic granite country rock (Boothby Orthogneiss).

B. REE-bearing fluorapatite (F) cut by calcite (C) and REE-bearing allanite (A) veins.

C. Moderately to slightly weathered, brecciated fluorapatite (F) with irregular allanite (A) veins.

D. Irregular contact between massive fluorapatite and calc-silicate assemblage (CS). Field of view (short dimension) of drill core is ~5 cm. Reproduced with permission from Arafura Resources Limited (http://www.arafuraresources.com.au/).

David Huston (GA) and Kelvin Hussey (Arafura Resources Limited) provided the photographs.

Orogen and a global carbonatitic and alkalic magmatic event between 1300 and 1130 Ma (Pidgeon, 1989) it could also be related to the tin and tantalum pegmatites in the area, the age of which is unknown. Korsch et al (2009) suggest that the mineralisation was emplaced during a widespread Mesoproterozoic thermal event which included syn- to post-tectonic felsic magmatism (ranging between 1235 Ma and 1195 Ma) in the Musgrave Province.

Genetic model: The close spatial association between the mineralisation at the Nolans Bore deposit and other carbonatite, alkaline, and tin- and tantalum-bearing pegmatites suggests that it could have formed from magmatic fluids released from any of the above mentioned melts. The ~1244 Ma age of mineralisation however indicates that it could represent a distal hydrothermal event (Hussey et al., 2008) related from an intensive Mesoproterozoic thermal event (between 1235 Ma and 1195 Ma) during which REE were remobilised. The REE mineralisation also shows a thermal overprint during the Alice Springs Orogeny (Hussey, 2003). REE in the zone of secondary enrichment indicate that primary REE mineralisation was remobilised during weathering and/or calcrete formation in the area.

Key references: Hussey (2003): regional geology, deposit types, mineralisation;
Korsch et al. (2009): U-Pb, K-Ar, Rb-Sr geochronology, regional geology, stratigraphy; and
Huston et al. (in press): geology, mineralisation, genesis.

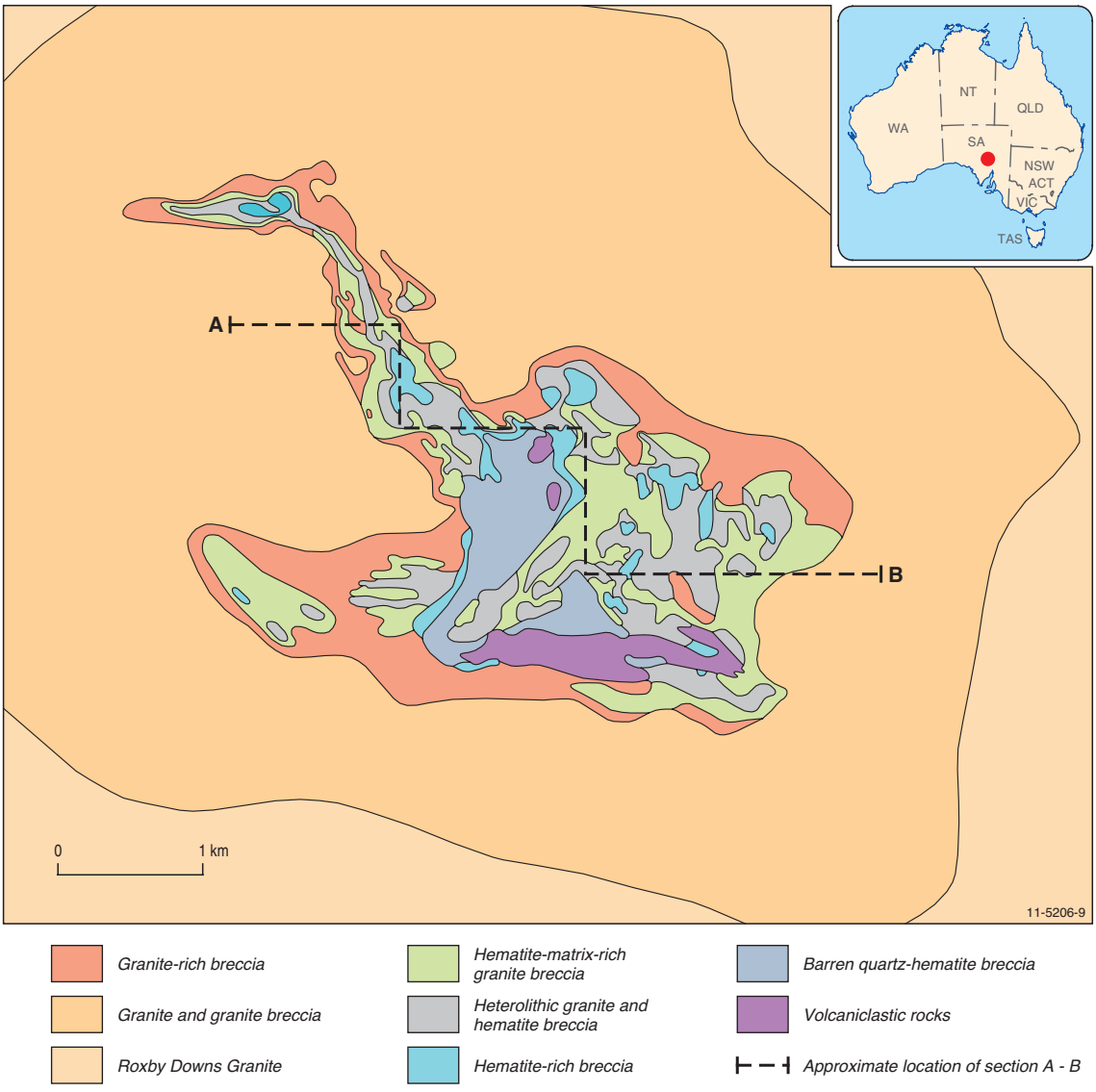

Figure 3.30. Schematic geological map of the Olympic Dam Cu-Au-U deposit, South Australia. Modified from Reynolds (2001).

Deposit Type 3.14: Iron-oxide breccia complex (or iron-oxide copper, gold, uranium deposits) with rare-earth elements

General description: Iron-oxide copper-gold-uranium (IOCG) deposits generally form in extensional environments and range in age from the present at least back into the Late Archean. Many deposits of this type are enriched in a distinctive, geochemically diverse suite of minor elements, including F, P, Co, Ni, As, Mo, Ag, Ba, LREE, Th, and U. These deposits contain mineable resources of more than one commodity, such as copper, gold, uranium, and iron. Although some of these deposits are enriched in REE, these elements are not currently extracted.

Australian deposits/prospects: Olympic Dam, Prominent Hill, Carrapateena (all Gawler Craton, SA); Mount Gee (Mount Painter Inlier, SA); Ernest Henry (Mount Isa Orogen, Qld).

Deposits outside Australia: Salobo, Cristallino, Sossego, Alemão (Carajás, Brazil), and Candeleria-Punta del Cobre and Manto Verde (Chile). (Williams et al., 2005).

Type example in Australia: Olympic Dam, South Australia (Figs 3.30 and 3.31).

Location: Longitude: 122.547515;
Latitude: -28.862596
~560 km north-northwest of Adelaide
1:250 000 map sheet: Andamooka (SH 53–12)
1:100 000 map sheet: Mattaweara (6237)

Geological province: Gawler Craton, South Australia.

Resources: Submarginal and Inferred Resources of REO of ~53 million tonnes (predominantly 0.2% La and 0.3% Ce). Currently not economic (Miezitis, 2010).

Current status: Operating mine, but REE are currently not extracted.

Economic significance: Unknown (REE).

Geological setting: According to Williams et al. (2005) these deposits occur in crustal settings with very extensive and pervasive alkali metasomatism. Skirrow et al. (2007) highlight the importance of pre-deposit continental margin setting for the Olympic Dam deposit and the Olympic Dam IOCG province in the Gawler Craton that produced during orogenesis over-thickened crust and mantle lithosphere. This setting was conducive in generating large volumes of high-temperature crustal melts emplaced during compression. The deposit lies at the intersection of major north–northwest-trending and west–northwest-trending gravity lineaments (O'Driscoll, 1985). Regional geophysical datasets indicate that the deposit is located at one of numerous coincident, but slightly displaced magnetic and gravity anomalies caused by hematite alteration of the host rocks.

Host rocks: The Olympic Dam deposit is hosted within a large body of hydrothermal breccia (Figs 3.30 and 3.31) occurring entirely within the Roxby Downs Granite (Reynolds, 2001). The funnel-shaped breccia complex primarily comprises a barren, hematite-quartz breccia core surrounded by variably mineralised and zoned hematite-granite breccia bodies. The breccia complex is interpreted to have formed from polycyclic events of alteration and brecciation. Heterolithic breccias contain a wide variety of altered clasts of granite, porphyritic volcanics, ultramafic to felsic intrusives, vein fragments of copper sulphides, fluorite, barite, siderite, and fine-grained laminated arkosic sedimentary rocks. The breccia complex is intruded by a variety of ultramafic, mafic, and felsic dykes. The breccias are interpreted to have formed in a phreato-magmatic diatreme structure located in the central part of the breccia complex (Reeve et al., 1990).

REE mineralisation: Hematite is the main iron-oxide which replaces magnetite, preserved now only at depth and within less evolved breccia at the peripheries of the breccia complex. Hematite is more abundant and intense towards the centre of the deposit (locally >95% of the rock) and replaces minerals and also forms veins and fills vugs. Ore zones form only a small fraction of breccia complex but weak mineralisation at background level is widespread within it. There is a general spatial correlation between higher grade copper-uranium mineralisation and more hematite-altered rocks, although the central hematite-quartz breccia zone is essentially barren of copper-uranium mineralisation. Low-grade economic gold mineralisation occurs in the copper-uranium ore zones, but higher grade gold mineralisation also occurs in small zones locally separate from or adjacent to copper-uranium zone (Reeve et al., 1990).

Most lithologies of the breccia complex are strongly enriched in REE, especially the LREE. REE mineralisation averaging 3000–5000 ppm combined lanthanum and cerium occurs throughout the breccia zones, including the central hematite-quartz core, where concentrations are generally higher (Reynolds, 2001). Typically there is about 0.59% TREO in the orebody (Roberts and Hudson, 1983). As granite breccia with hematite matrix and hematitised granite contain

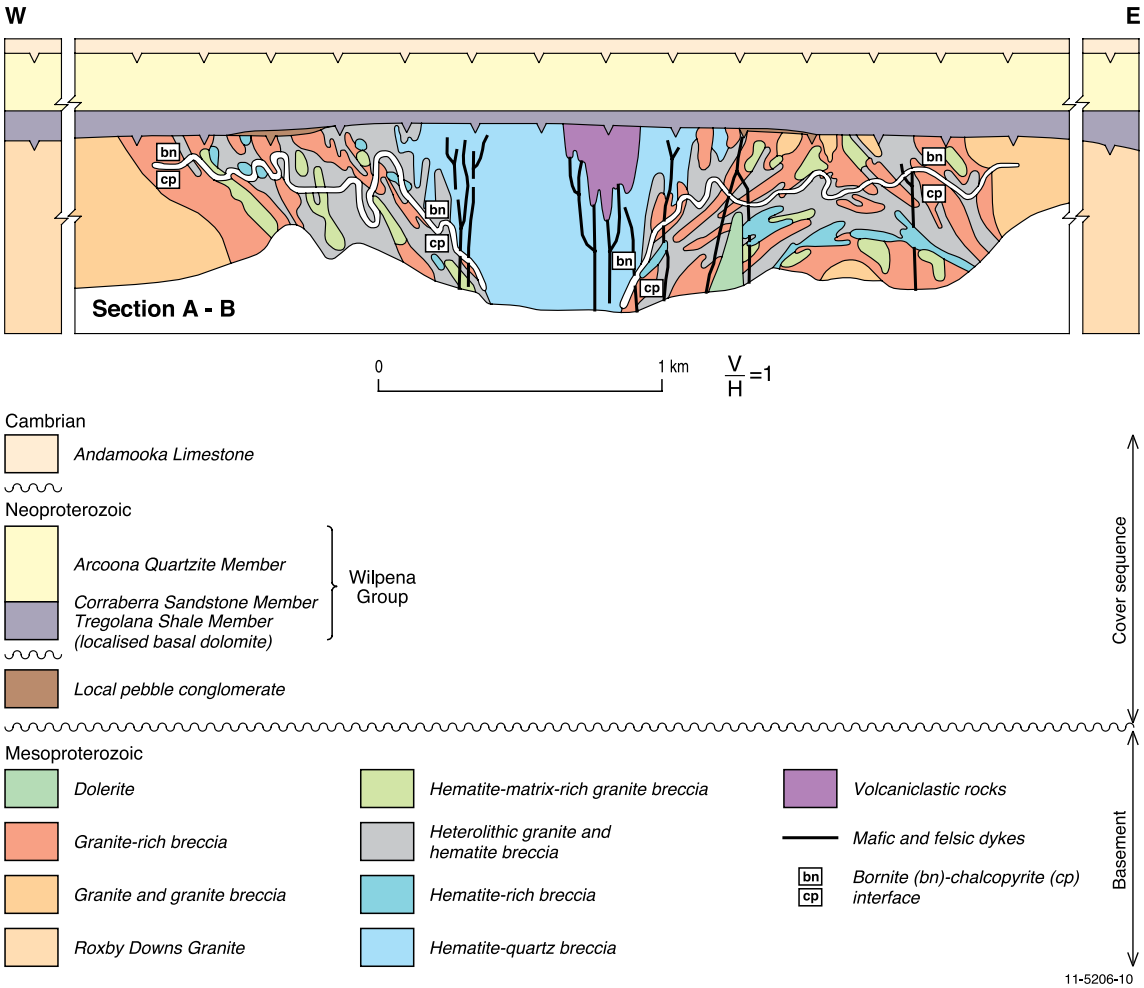

Figure 3.31. Schematic cross-section of the Olympic Dam Cu-Au-U deposit, South Australia. The approximate location of the stepped cross-section A–B is indicated on Figure 3.30. Modified from Reynolds (2001).

similar relative and absolute abundances of REE, the distribution of REE is not controlled by the mode (replacement or infilling) of hematite introduction (Oreskes and Einaudi, 1992). The absolute abundance of REE increases with increasing hematite content of the breccia. REE are also enriched in quartz-sericite veins and laminated barite fragments. According to Oreskes and Einaudi (1992), the REE were introduced into the altered rocks during breccia formation. LREE were mobile during all stages of alteration whereas the mobility of HREE was restricted to the most extreme stages of iron metasomatism.

Four major minerals of REE have been identified in the breccias: bastnäsite [(Ce, La)CO_3(F.OH)], florencite [(Ce,Al_3(PO_4)$_2$(OH)$_6$], monazite, and xenotime. In addition a U-Y-Si-P phase (probably a britholite series mineral) is also present. Oreskes and Einaudi (1992) did not report the presence of REE in zircons. However, LA–ICPMS analysis of zircons from an altered dyke show enrichment in HREE (Jagodzinski, 2005).

Mineral paragenetic studies indicate that REE minerals were deposited during much of the hydrothermal history of the deposit.

Source of REE: The high concentration of REE in the Olympic Dam deposit is in agreement with a general REE-enrichment of magmatic rocks of the Hiltaba Suite. According to Agangi et al. (2010), rhyolites of the Gawler Range Volcanics are enriched in REE, Y, and fluorine. The whole-rock geochemistry of these rocks suggests that because of high-fluorine concentration in the melt the REE behaved incompatibly during magmatic crystallisation and were enriched in a volatile-rich late-stage magmatic fluid, which deposited REE-rich minerals in vesicles, micromiaroles, and interstices between major mineral phases of rhyolites. On the basis of the differences in Nd isotopic values of the hematitic ores and of less mineralised granite host rock Johnson and McCulloch, (1995) suggested that the REE were derived in part from a source more primitive (possibly mantle) than that of the granitic host. They also noted

a correlation between Nd isotope value (εNd) and copper concentration in highly altered breccia and argued that copper and REE had a common source. These conclusions were supported by a later province-scale study (Skirrow et al., 2007) that also established the difference in Nd values of the hematitic ores in the Olympic Dam deposit (higher εNd values and hence a primitive source of REE) and of all other prospects in the Olympic Dam province, such as Titan and Emmie Bluff (lower εNd values hence crustal or evolved source of REE). Thus REE in the supergiant Olympic Dam deposits and other smaller prospects were probably derived form different sources.

Age of mineralisation: The SHRIMP U-Pb zircon age of 1588 ± 4 Ma age (Creaser and Cooper, 1993) of the Roxby Downs Granite constrains the maximum age of brecciation at the deposit. SHRIMP U-Pb analysis from three felsic dykes within the breccia complex yield an age of ~1590 Ma. These ages are confirmed by more recent data (Jagodzinskii, 2005). On the basis of textural relationships between sulphides and iron-rich breccias and the crosscutting relationship between the igneous units and the mineralised breccia it has been argued that brecciation, mineralisation, and magmatic activity were broadly contemporaneous and occurred at ~1590 Ma (Johnson and Cross, 1995). Based on Ar/Ar age of alteration muscovite, and SHRIMP U-Pb ages of titanite and zircon in the Olympic Dam district, Skirrow et al (2007) postulated another younger hydrothermal magnetite alteration event followed by hematitic alteration in the district at ~1575 Ma.

Genetic model: The current consensus among researchers is that mineralisation at the deposit was formed form an evolving hydrothermal system in which most of the metals and hydrothermal fluids were derived from a magmatic source. The hydrothermal system was driven by high-level felsic Hiltaba Suite plutons coeval with Gawler Range Volcanics. The fluid inclusion and silicate geothermometry data suggest the involvement of at least two fluids (Oreskes and Einuadi, 1992) one of which was hot (~ 400°C) and saline (up to ~ 42 wt% eq. NaCl), and the other relatively cooler (160°C to 250°C) and of moderate salinity. It is argued that early magnetite was formed from the first fluid, whilst hematite was deposited from the second fluid (Oreskes and Einuadi, 1992). The fluid inclusions associated with the magnetite-stage alteration and mineralisation in the Olympic Dam province are enriched in copper (from 300 to 600 ppm to 2 to 4 wt%, Bastrakov et al., 2007). These fluids were thus capable of transporting large quantities of copper and iron (Reeve et al., 1990). The low- to moderately-high-temperature fluids were relatively enriched in fluorine and relatively more oxidised and hence capable of transporting uranium, REE, and possibly copper (Reeve et al., 1990). Haynes et al. (1995) proposed a fluid-mixing model in which the two above-mentioned fluids mixed in a shallow phreato-magmatic setting. Bastrakov et al. (2007) suggest a similar two-stage model in which the early magnetite-bearing stage of alteration and mineralisation was overprinted by a hematitic stage during which copper, gold, and uranium were remobilised.

Key references: Reynolds (2001): regional geology, geology of deposit, mineralisation, structure, U-Pb zircon geochronology, genesis; and
Reeve et al. (1990): regional geology, alteration, igneous intrusions, mineralisation, ore genesis.

3.3.2. Additional geological information on rare-earth-element-bearing deposits not included in Section 3.3.1.

Heavy-mineral sands: The most common REE-deposit type in Australia is associated with heavy-mineral sands which are formed by enrichment of heavy minerals in marine and aeolian sands (generally of low grade). These placer deposits are concentrated along Cenozoic and older shorelines on both the southwest and east coasts of Australia. Beach, high dune, and offshore shallow marine deposits of Eocene to Holocene age occur mainly along coastal strips in southwestern Western Australia and they also extend for about 1300 km from near Gosford in New South Wales to just north of Rockhampton in Queensland. Shallow-marine-tidal deposits of similar age occur inland in the Murray Basin near the junction of South Australia, Victoria, and New South Wales. Older channel heavy-mineral deposits extend back into the Mesozoic with the Calypso deposit north of Perth being the type example. The heavy-mineral placers contain varying concentrations of monazite, xenotime, zircon, and titanium-bearing oxides, such as ilmenite, rutile, and leucoxene.

The importance of heavy-mineral deposits as a source of REE depends upon the content of monazite, and to a lesser degree xenotime, in the heavy-mineral concentrate. Up to 1995, Australia exported significant quantities of monazite, as a by-product from heavy-mineral-sand mining, for the extraction of REE and thorium overseas. Monazite was separated from heavy-mineral concentrates containing as little as 0.1% to 0.3% monazite. The bulk of Australia's monazite production was derived from the Eneabba and Cooljarloo regions in the Phanerozoic Perth Basin, north of Perth. Heavy-mineral concentrates for deposits

in these two regions contain 0.5 to 1.0% monazite, and from the Capel area, again in the Perth Basin, south of Perth, the heavy-mineral concentrates contain around 0.4% monazite (Cassidy et al., 1997). The heavy-mineral sand mines on the east coast of New South Wales and Queensland generally accounted for less than 10% of the monazite production, where the monazite contents in the heavy-mineral concentrates were generally 0.1 to 0.3%. The fine-grained fossil shallow marine deposits of the WIM 150-type in the Murray Basin, western Victoria, have reported monazite and xenotime contents of ~1.4% and ~0.4%, respectively (Williams, 1990).

Detailed descriptions of individual heavy-mineral deposits can be found in Shepherd (1990), Wallis and Oakes (1990), Williams (1990), Towner et al. (1996), Cassidy et al. (1997), Roy (1999), and Roy and Whitehouse (1999). The heavy-mineral sand deposits are described in detail in Section 3.3.1.

Carbonatite: Most carbonatite complexes in the world are localised within stable continental tectonic units. Within these large regional structures, the carbonatites are generally confined to alkaline magmatic provinces controlled by intracontinental rift and fault systems (Berger et al., 2009). Carbonatite and alkaline igneous magmatism produces several types of significant REE deposits. Some deposits are closely related to the cooling and crystallisation of magma, whereas others are formed from hydrothermal fluids released by magmatic melts, or from supergene-enrichment processes operating in the weathered zone of the carbonatite body.

Jaques (2008) divided Australia's major carbonatite occurrences into two major groups: (1) those associated with kimberlites and/or ultramafic lamprophyres; and (2) those occurring in alkaline complexes or discrete bodies. Examples of the first group include Mount Weld, Ponton Creek (Cundeelee), veins at Granny Smith and Wallaby gold mines (all Yilgarn Craton, WA), Yungul (Halls Creek Orogen, WA), and Walloway (Gawler Craton, SA). Occurrences with alkaline affinities in the second group include Cummins Range and Copperhead (Halls Creek Orogen), Yangibana 'ironstones' of the Gifford Creek alkaline complex (Capricorn Orogen, WA: see Section 3.3.1), and the Mud Tank and Mordor igneous complexes (Arunta Region, NT). The geological features and mineral resources of these carbonatite-associated deposits are summarised in Table 3.14. REE mineralisation is associated with both groups of carbonatites, with the most significant deposits hosted by large carbonatite bodies at Mount Weld and Cummins Range (Duncan and Willett, 1990; Andrew, 1990). Although rare-earth minerals can be formed during crystallisation of carbonatite melt and also from later hydrothermal fluids, most of the known resources are concentrated in the regolith cover over the main intrusive carbonatite complex. The base of the regolith is commonly defined by a karst-like interface with the underlying carbonatite. Leaching of soluble minerals such as carbonates and silicate produces a residual zone enriched in rare restite minerals, such as primary and secondary monazite, apatite, zircon, pyrochlore, cerianite, churchite, and crandallite. Enrichment of REE in the residual zones can attain up to 10 times their original concentration. The Ponton Creek and Yangibana (see Deposit Type 3.10) are rare examples in Australia where the REE are hosted in the unweathered primary zone of the carbonatite body.

The ~2025 Ma (Re-Os isochron) Ponton Creek carbonatite (previously called Cundeelee) is located at the southeastern margin of the Archean Yilgarn Craton near the intersection of a shear system associated with the Fraser Complex to the southeast and the southern extensions of the Laverton Tectonic Zone. The emplacement of the Ponton Creek complex may have been facilitated by the intersection of these two regional structural corridors. The main basement lithologies comprise granitic gneiss, migmatite, and intrusives overprinted by the northeast-trending tectonic fabrics of the Proterozoic Albany–Fraser Orogen. The complex is overlain by 350 to 500 m of Permian tillite. The 10 km-wide central core of alkaline ultramafic cumulates is cut by veins of primary apatite-rich rauhaugite (hypabyssal dolomitic carbonatite), secondary calcite-magnetite-bearing rocks, and pods and veins of pegmatitic aegirine syenite. The best drill intersections in the primary zone are 16 m @ 14.48% TREO + Y, and 28 m @ 10.50% REO. There is no paleo-regolith profile due to the action of Permian glaciation (Lewis, 1990).

The Cummins Range Carbonatite (Fig. 3.32) in the Halls Creek Orogen of Western Australia consists of a central carbonatite plug with a weathered capping of silicified, limonitic collapse breccia that is enclosed by an envelope of carbonated, mica-rich pyroxenite that is largely altered to amphibolite (see Appendix 7). Calcite (sövite)- and dolomite (rauhaugite)-dominant carbonatites contain apatite, phlogopite, magnetite, and clinopyroxene (Lewis, 1990). Steeply dipping carbonatite veins, up to 60-m wide, traverse the weathered zone (Andrew, 1990). Isotopic dating (1012 ± 12 Ma U-Pb zircon and 905 ± 2 Ma Rb-Sr) indicates that the carbonatite pre-dates the ~800 Ma kimberlites

of the Kimberley region, but it may be coeval with Bow Hill lamprophyres further to the north (Jaques et al., 1985; Jaques, 2008). Weathering and leaching of the oxidised zone above the carbonatite has enriched (by up to 10 times) LREE, Y, U, Nb, V, and P mineralisation with associated high levels of Ta, Zr, Nb, Sc, Sr, Ti, and Th, in such minerals as monazite, apatite, zircon, pyrochlore, and magnetite. As of September 2009, the Cummins Range deposit has an Inferred Resource of 4.17 Mt @ 1.72% TREO, 11.0% P_2O_5, and 187 ppm U_3O_8.

The Yungul carbonatite dykes and the associated Speewah fluorite deposit occur on a north-trending splay from the northeast-trending Greenvale Fault which defines the western margin of the Halls Creek Orogen, Western Australia (Rogers, 1998; Alvin et al., 2004). The carbonatite is spatially associated with Neoproterozoic (~800 Ma) kimberlites and lamprophyres (e.g., Bow Hill lamprophyre dyke), but its intrusion age is unknown (Jaques, 2008). The dykes in the Speewah Dome are up to 15-m wide and are concentrated in a 150 m-wide zone along a fault splay of the regional northeast-trending Greenvale Fault. The dykes are massive calcite carbonatites that host very coarse, pegmatitic veins and pods of calcite (Gwalani et al., 2010). They have carbonatised and fenitised the ~1790 Ma Hart Dolerite country rocks.

The Mordor Complex (Langworthy and Black, 1978; Barnes et al., 2008) in the eastern Arunta Region is a composite plug-like alkaline-ultramafic body that has been explored for REE, PGEs, Ni, Cu, Cr, diamonds, vermiculite-phlogopite, and U. The complex crops out over 6 by 6 km and can be broadly subdivided into a western zone of homogeneous syenite and an eastern zone comprising a highly fractionated comagmatic suite of alkaline felsic and mafic rocks (syenite, monzonite, melamonzonite, shonkinite) spatially associated with phlogopite-bearing ultramafic cumulate rocks (wehrlite, olivine clinopyroxenite, lherzolite, dunite, pyroxenite). The ultramafic rocks make up less than 5% of the intrusion. Pegmatites and carbonate-rich dykes and veins cut the intrusion. Previous investigators have interpreted these dykes and veins to be carbonatites with associated fenitic alteration. Geochemical data show that the Mordor Complex forms a differentiated ultrapotassic suite of uniform silica content (43–53%) enriched in K, Al, Rb, Ba, Sr, and La (Appendix 7). Plagioclase pyroxenite from the northeastern corner of the intrusion has a U-Pb zircon crystallisation age of 1133 ± 5 Ma (Claoué-Long and Hoatson, 2005), which is consistent with the mineral Rb–Sr isochron ages of 1128 ± 20 Ma and 1118 ± 17 Ma (Langworthy and Black, 1978). The alkaline felsic rocks and discordant carbonate-bearing dykes have been a focus for REE exploration, however, drilling programs have generally returned disappointing results. Stratabound PGE mineralisation (8 m @ 0.67 ppm Pt+Pd+Au) hosted by cyclic sequences of ultramafic rocks (Barnes et al., 2008), and base-precious mineralisation (1 m @ 1.4% Cu, 0.3% Ni, 0.4 ppm Pt+Pd, and 0.1 ppm Au) at the Braveheart ironstone on the southeast margin of the intrusion highlight the polymetallic character of the complex.

The Mud Tank Carbonatite (Knutson and Currie, 1990; Currie et al., 1992), located 52 km north-northwest of the Mordor Complex, was the first

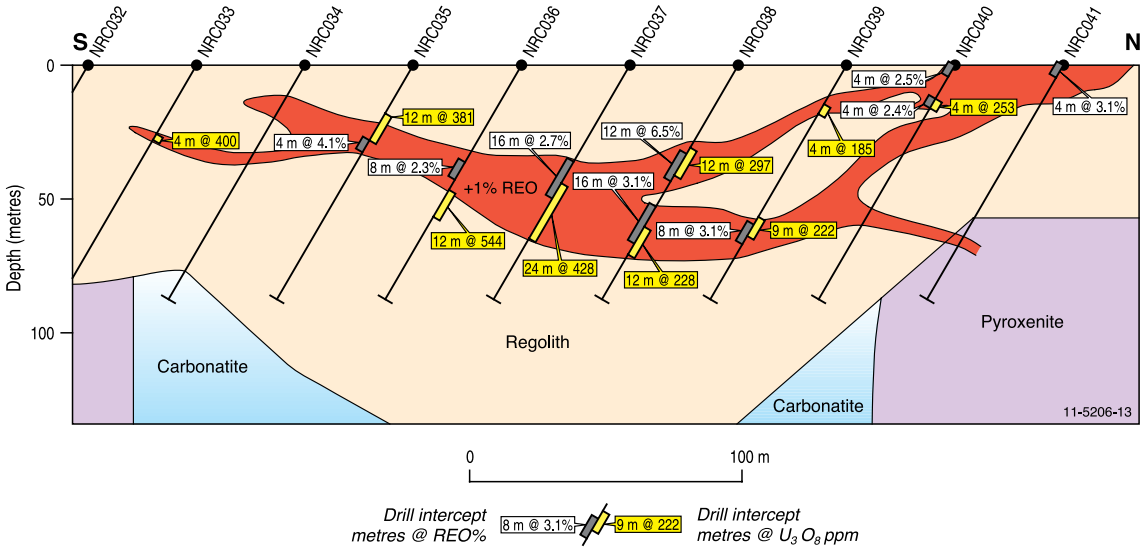

Figure 3.32. Geological cross-section of the Cummins Range Carbonatite rare-earth-element deposit, Halls Creek Orogen, Western Australia. Modified from Navigator Resources Limited (2010).

Table 3.14. Major carbonatite occurrences in Australia.

Carbonatite	Geological setting	Size	Resources	Reference(s)
Mount Weld, Yilgarn Craton, WA	Paleoproterozoic (~2025 Ma) carbonatite intrusive with thick mineralised laterite[2] profile	4 km[1]	17.49 Mt @ 8.1% TREO; significant resources of P_2O_5	Duncan and Willett (1990); Lottermoser (1990); Graham et al. (2003, 2004)
Ponton Creek, Yilgarn Craton, WA	Large Paleoproterozoic (~2025 Ma) carbonatite stock covered by 500 m of Permian tillite	10 km[1]	28 m @ 10.5% REO and 16 m @ 14.48% REO; no resource defined	Jaques (2008)
Copperhead, Halls Creek Orogen, WA	Small Paleoproterozoic (1821 Ma) carbonatite plug-like body	110 m by 80 m	Low anomalous REE concentrations: <76 ppm Y; <600 ppm Ce; <86 ppm La	Rugless and Pirajno (1996); Jaques (2008)
Yangibana 'ironstones', Capricorn Orogen, WA	Mesoproterozoic (~1250 Ma) ferrocarbonate-magnetite-hematite dykes	10-m wide, up to 25 km long	3.53 Mt @ 1.64% REO	Pearson and Taylor (1996); Jaques (2008)
Mordor, Arunta Region, NT	Mesoproterozoic (1133 Ma) alkaline ultramafic plug cut by carbonate-rich dykes and veins	6 by 6 km (plug)	Anomalous REE, PGEs, Ni, Cu, U, Au	Barnes et al. (2008); Hoatson et al. (2005;) Langworthy and Black (1978)
Cummins Range, Halls Creek Orogen, WA	Mesoproterozoic (~1012 Ma) carbonatite intrusive stock with mineralised laterite profile	1.8 km[1]	4.17 Mt @ 1.72% TREO, 11.0% P_2O_5 , 187 ppm U_3O_8	Andrew (1990); Jaques (2008)
Mud Tank, Arunta Region, NT	Neoproterozoic (732 Ma) carbonate-rich lenses in granite, schist, and mafic granulite	Four separate lenses crop out over 4 km by 700 m	Vermiculite; gem-quality zircon	Currie et al. (1992); Knutson and Currie (1990); Black and Gulson (1978)
Yungul, Halls Creek Orogen, WA	Phanerozoic (not dated: probably post-Early Cambrian) carbonatite dykes	Less than 15-m wide	Low REE abundances (174 to 493 ppm TREE); fluorite resources	Alvin et al. (2004); Gwalani et al. (2010)
Walloway, Gawler Craton, SA	Jurassic (~170 Ma) carbonate-rich lamprophyric plugs and dykes	Small	NA	Tucker and Collerson (1972); Ferguson and Sheraton (1979)
Granny Smith and Wallaby gold mines, Yilgarn Craton, WA	Carbonatite veins (not dated) associated with ~2.66 Ma monzodiorite-syenite stocks, dykes, and carbonate-rich rocks	Less than 2-m thick	NA	Jaques (2008); Mueller et al. (2008)

[1] Maximum diameter dimension of plug- and stock-like bodies.
[2] Age of mineralised laterite ranges from approximately Late Mesozoic to Early Cenozioc.
NA = Not Available.
Locations for the carbonatites listed in this table are shown in Figure 5.4.

carbonatite recognised in Australia (Gellatly, 1969). The carbonatite consists of four separate carbonate-rich lenses within a north–northeasterly-trending zone some 4 km long. It was emplaced into granitic and mafic granulite rocks at mid-crustal levels and was subsequently remobilised to higher-crustal levels (Currie et al., 1992). Most of the carbonatite is altered and ferruginised at the surface, and was originally found by the large detrital concentrations of coarse apatite, magnetite, and zircon. Three major types of carbonatite have been recognised (Black and Gulson, 1978): (1) an abundant foliated micaceous carbonatite containing phlogopite, carbonate, soda-amphibole, apatite, and magnetite that grade into; (2) a calcite- and dolomite-bearing carbonatite with apatite, magnetite, phlogopite, chlorite, soda-amphibole, zircon, and pyrite; and (3) feldspathic carbonates with andesine, carbonate, aegirine, soda-amphibole, hastingsite, biotite, apatite, and Fe-oxides. Currie et al. (1992) report maximum REE concentrations of 335 ppm La, 595 ppm Ce, 264 ppm Nd, 68 ppm Pr, 67 ppm Sc, and 70 ppm Y from the carbonatite lithologies. The Mud Tank Carbonatites have significantly higher Cu, Ni, and Cr contents, and lower Sr, Zr, Nb, Mo, La, and Ce contents than the average carbonatite (Currie et al., 1992). The Mud Tank Carbonatite and Mordor Complex occur near the northwest-trending Woolanga Lineament—a deep-seated crustal dislocation that may have facilitated the emplacement of these unusual plug-like bodies. The younger emplacement of the Mud Tank Carbonatite (U-Pb zircon age of 732 ± 5 Ma: Black and Gulson, 1978) relative to the Mordor Complex may indicate reactivation along this regional lineament or associated fault structures.

Unconformity-related: The Killi Killi Hills uranium-REE prospects, located about 150 km southeast of Halls Creek, in the Proterozoic Birrindudu Basin near the Western Australian–Northern Territory border represent an interesting style of mineralisation where the main ore mineral xenotime is thought to have formed from fluids released during diagenesis of the Mesoproterozoic Gardiner Sandstone (Vallini et al., 2007). The presence of xenotime and florencite highlights the potential for

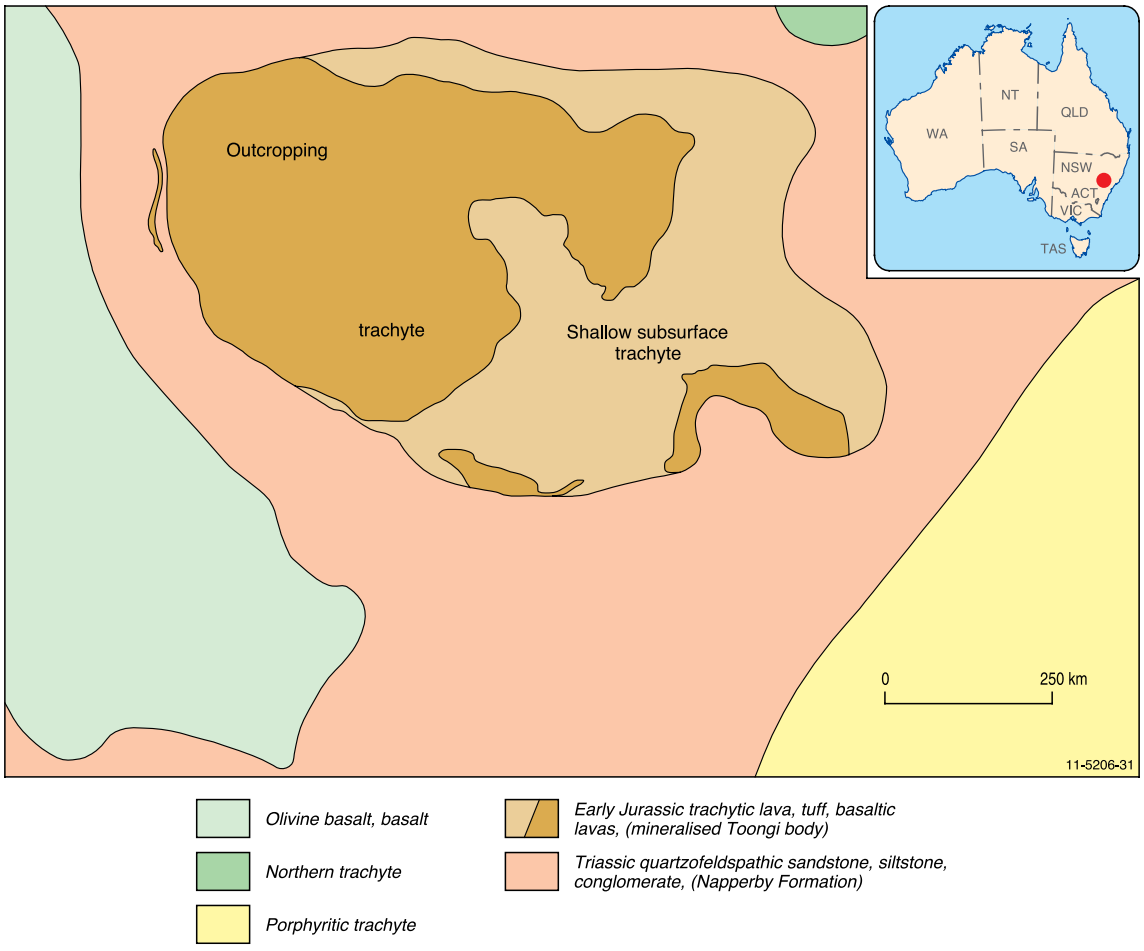

Figure 3.33. Geological map of the Toongi polymetallic deposit, Lachlan Orogen, New South Wales. Modified from Alkane Resources Limited (2011).

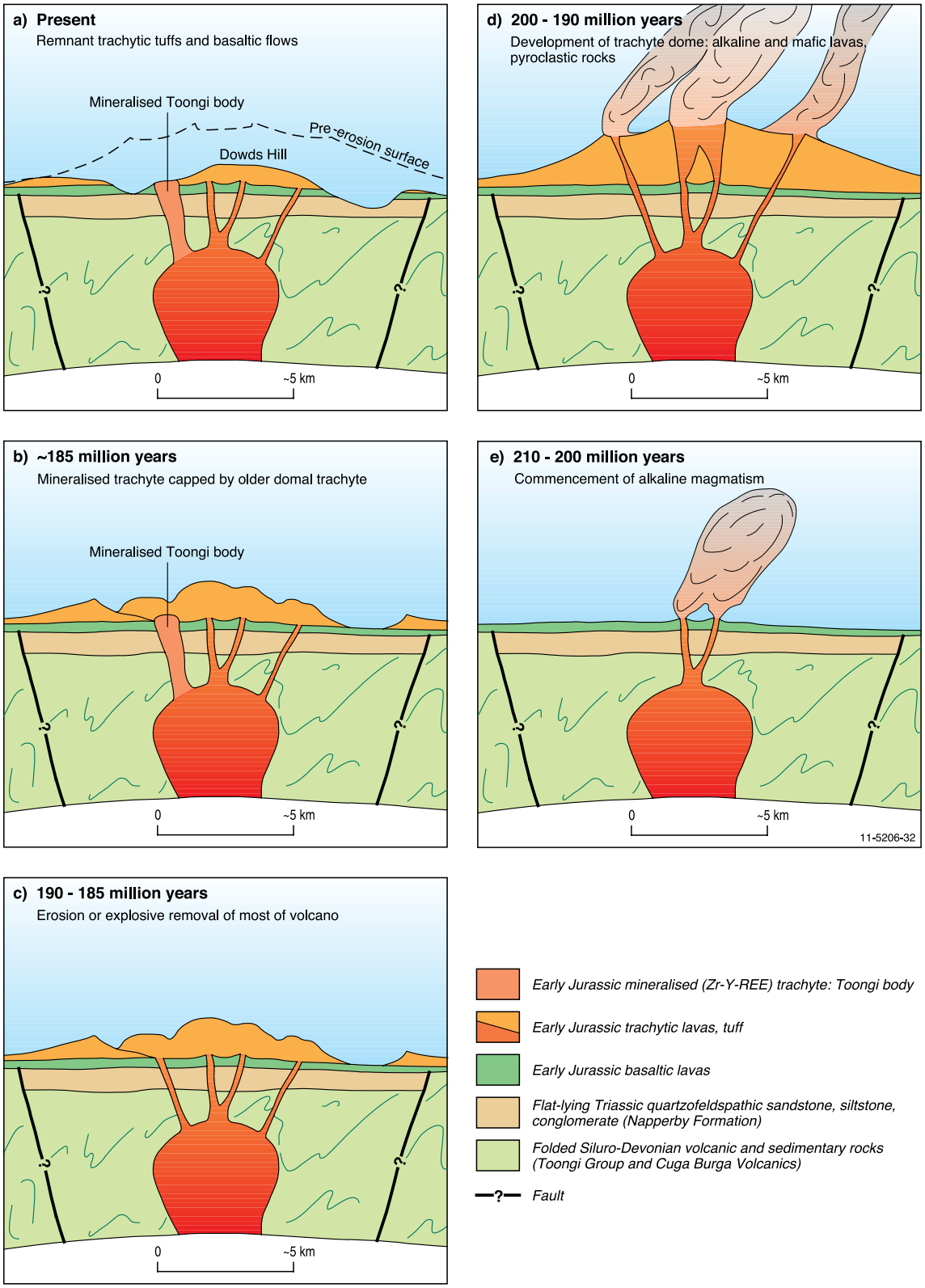

Figure 3.34. Time-event evolution of the Toongi deposit, New South Wales. Modified from Alkane Resources Limited (2007).

HREE and uranium. Xenotime from the Gardiner Sandstone has high concentrations of yttrium and phosphorous, with an average of 48% yttrium oxide and 16–20% phosphorous oxide. The mineralisation is confined to conglomerates at the base of the Gardiner Sandstone, which unconformably overlies steeply dipping, Paleoproterozoic shale and greywacke of the Killi Killi Formation (Blake et al., 1979). Similar diagenetic-fluid processes occur in other sedimentary basins, which unconformably overlie carbonaceous-rich rock and host world-class unconformity-related uranium deposits in the Pine Creek Orogen of the Northern Territory. Ores and altered host rocks in unconformity-related uranium deposits show elevated concentrations of REE (Jefferson et al., 2007; Fisher and Cleverley, 2010) indicating that some of these deposits may have economic resources of REE (see Caramel in Appendix 7).

Alkaline igneous rocks: The Dubbo–Mudgee region of New South Wales contains a number of Mesozoic alkaline complexes that range in age from about 225 million years to 165 million years (Warren et al., 1999). The complexes comprise stocks, sills, dykes, and flows that appear to be structurally controlled and aligned along regional lineaments. They range in composition from basalt, alkali diorite, trachyte, syenite, to quartz monzonite, with the trachytic variants having the greatest potential for REE. The Dubbo Zirconia Project (Toongi: Figs 3.33 and 3.34), located 25 km south of Dubbo, contains one of the world's largest in-ground resources of zirconium, hafnium, niobium, tantalum, yttrium, and REE. It was discovered in 1988, although serious investigations did not commence until 1999. The Toongi deposit has a Measured Resource of 35.7 million tonnes grading 1.96% ZrO_2, 0.04% HfO_2, 0.46% Nb_2O_5, 0.03% Ta_2O_5, 0.14% Y_2O_3, 0.75% TREO, 0.014% U_3O_8, and 0.0478% Th, and an Inferred Resource of 37.5 million tonnes of similar grades (http://www.dpi.nsw.gov.au/__data/assets/pdf_file/0003/316839/Rare_Earth_Elements.pdf). The mineralisation is hosted in a hydrothermally altered pipe-like body that outcrops over an area of about 400 m by 600 m, with shallow subsurface extensions of alkaline rocks indicating the overall dimensions of the body are approximately 900 m east-west by 600 m north-south (Fig. 3.33). Trachytic lavas, tuffs, and olivine basaltic lavas are interpreted to represent the volcanic phase of an alkaline magmatic event that occurred during the late Triassic to early Jurassic. The pipe-like body cuts folded Siluro-Devonian volcanic and sedimentary rocks (Toongi Group and Cuga Burga Volcanics) and a flat-lying Triassic sequence of quartzofeldspathic sandstone and minor siltstone and conglomerate (Napperby Formation). Narrow (up to 3 m) basaltic dykes intrude the body. Figure 3.34 shows a schematic time sequence of the major geological events Chalmers (1999) describes the Toongi body as a remarkably uniform, very fine-grained (<0.5 mm) massive alkali trachyte comprising K-feldspar (partly sericitised), albite, and aegerine pyroxene microphenocrysts, with minor carbonate, quartz, and 'ore' minerals. The intrusive contact is defined by a 2 to 10 m-wide zone of silicified trachyte with chalcedonic veining and a possible preserved vesicular cap to the body. Hydrothermal alteration involving significant carbonate, chloritic, potassic, and argillic alteration has modified the Toongi prospect (Christie et al., 1998). Weathering persists for up to 15 m below the surface, but its effect on the host trachyte and ore minerals is limited, causing only minor variations in the mineral species. The trachyte body exhibits uniformly elevated abundances of Zr, Hf, Nb, Ta, Y, and REE laterally and vertically. The orebody also contains low levels of uranium and thorium, but it is not classified as a radioactive ore. Scanning electron mineralogical studies indicate that the ore minerals are very fine-grained, being less than 100 µm in size (most less than 20 µm) and generally having unusual compositions. Un-named calcium- and REE-bearing zirconium silicates (similar to eudialyte and armstrongite: $ZrSiO_4$ ± Ca, Y, REE, H_2O, ?U) are the dominant ore minerals of zirconium and yttrium, while natroniobite ($NaNbO_3$) and calcian bastnäsite ($Ca(REE)CO_3F$) are the major sources of niobium and REE, respectively (Chalmers, 1999).

Elevated levels of zirconium, thorium, and REE are associated with deeply weathered and fresh peralkaline granite at the Narraburra deposit, 12 km northeast of Temora in central New South Wales (Wormald et al., 2004). A Late Devonian total-rock Rb-Sr isochron age of 365 ± 4 Ma for the emplacement of the granite has been implied by Wormald et at. (2004). This deposit contains an inferred resource of 55 Mt @ 60 ppm Y_2O_3, 300 ppm REO with up to 50 ppm thorium.

Pegmatite: Pegmatites in the Wodgina–Mount Francisco area (see Section 1.6 and Appendix 7) of the Pilbara Craton, Western Australia, are known to contain REE (Witt, 1990). The albite pegmatites and associated tourmaline lodes have been mined for tin, tantalum, and lithium (Ferguson and Ruddock, 2001).

Fluorite veins: The high-grade John Galt hard-rock resource and adjacent Corkwood Yard alluvial REE deposit are located near the western end of the Osmond Range, in the East Kimberley. REE mineralisation at John Galt consists of disseminations of xenotime in lithic quartz sandstone and conglomerate of

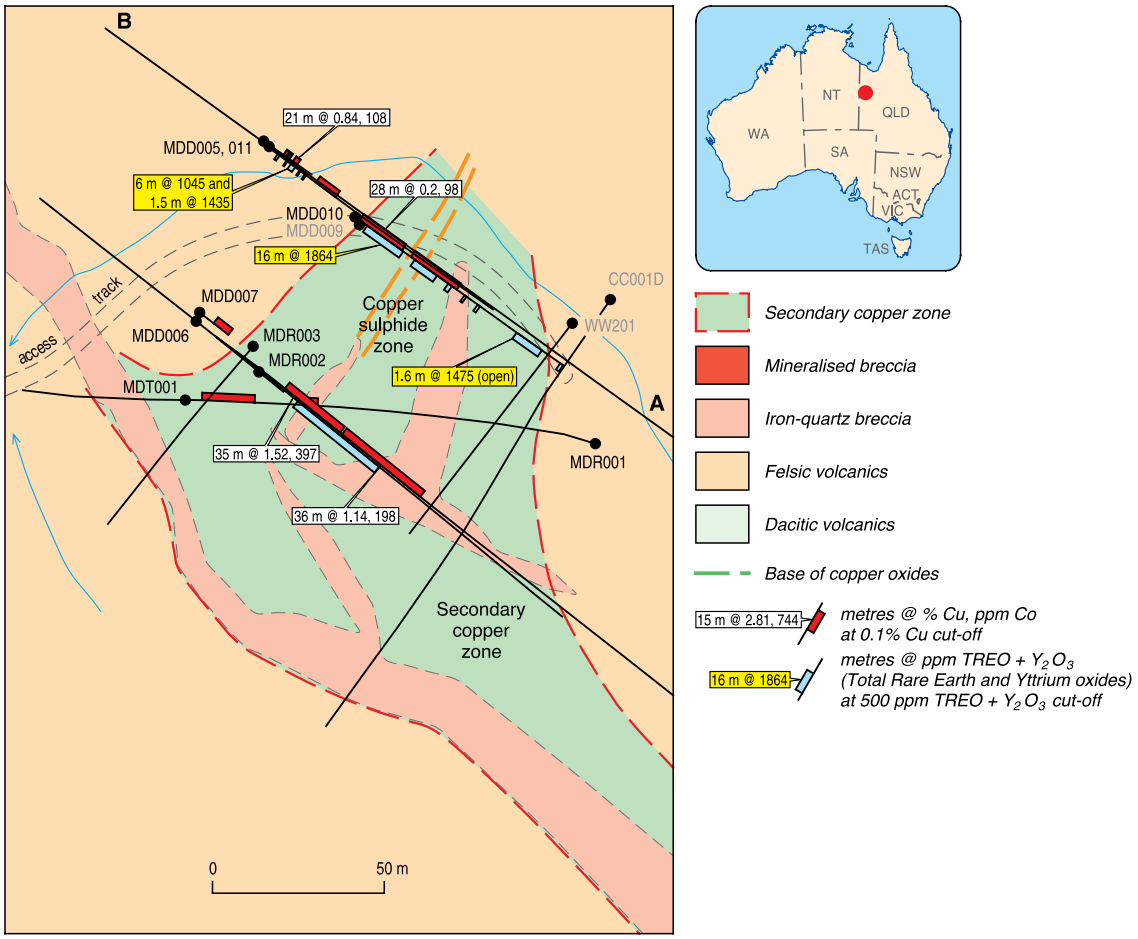
B
A
21 m @ 0.84, 108
MDD005, 011
6 m @ 1045 and
1.5 m @ 1435
28 m @ 0.2, 98
MDD010
MDD009
16 m @ 1864
CC001D
WW201
track
MDD007
MDD006
MDR003
MDR002
access
Copper
sulphide
zone
1.6 m @ 1475 (open)
MDT001
35 m @ 1.52, 397
MDR001
36 m @ 1.14, 198
Secondary
copper
zone
0
50 m
NT
QLD
WA
SA
NSW
ACT
VIC
TAS
Secondary copper zone
Mineralised breccia
Iron-quartz breccia
Felsic volcanics
Dacitic volcanics
Base of copper oxides
15 m @ 2.81, 744
metres @ % Cu, ppm Co
at 0.1% Cu cut-off
16 m @ 1864
metres @ ppm TREO + Y2O3
(Total Rare Earth and Yttrium oxides)
at 500 ppm TREO + Y2O3 cut-off

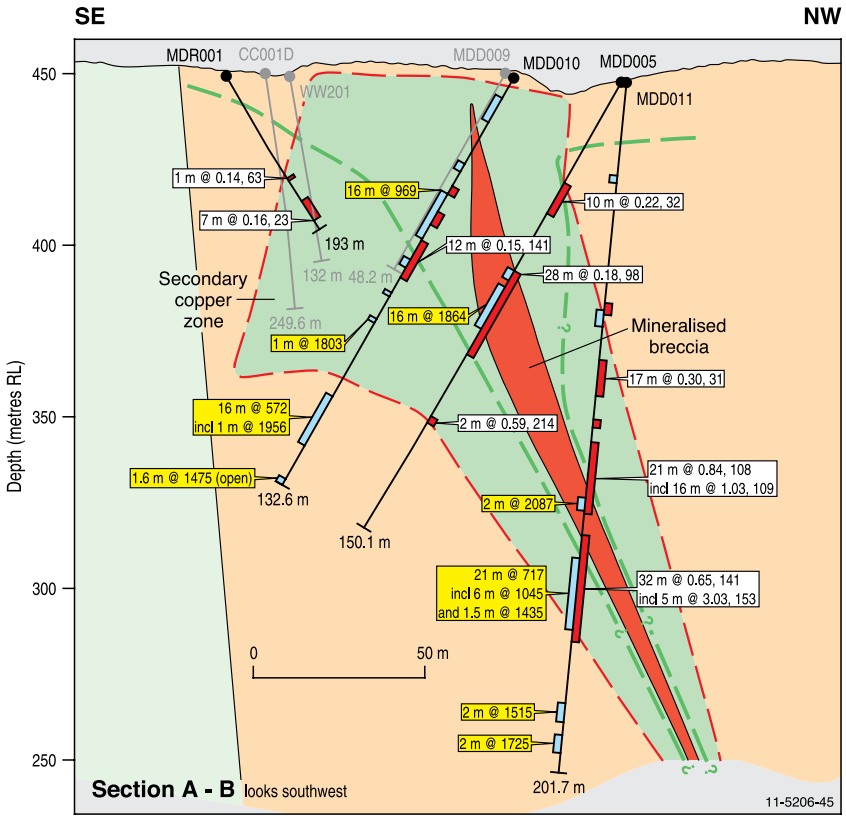
SE
NW
MDR001
CC001D
MDD009
MDD010
MDD005
WW201
MDD011
1 m @ 0.14, 63
7 m @ 0.16, 23
193 m
16 m @ 969
10 m @ 0.22, 32
12 m @ 0.15, 141
132 m
48.2 m
28 m @ 0.18, 98
Secondary
copper
zone
249.6 m
16 m @ 1864
1 m @ 1803
Mineralised
breccia
17 m @ 0.30, 31
16 m @ 572
incl 1 m @ 1956
2 m @ 0.59, 214
1.6 m @ 1475 (open)
132.6 m
21 m @ 0.84, 108
incl 16 m @ 1.03, 109
2 m @ 2087
150.1 m
21 m @ 717
incl 6 m @ 1045
and 1.5 m @ 1435
32 m @ 0.65, 141
incl 5 m @ 3.03, 153
0
50 m
2 m @ 1515
2 m @ 1725
201.7 m
Depth (metres RL)
450
400
350
300
250
Section A - B looks southwest
11-5206-45

the Proterozoic Red Rock Formation, as well as in joint- and fault-controlled veins up to 30 cm wide (Fetherston, 2008). The epithermal quartz veins are hosted by a brittle variant of the sedimentary rocks about 1 km east of the regional Halls Creek Fault. The veins form a cliff up to 30-m wide and 10 m high, and have been investigated over a distance of 4.5 km (Lottermoser, 1991). The mineralisation appears to be structurally controlled and possibly related to fluids from deeper level, alkaline source rocks (Sanders, 1999). Noble Resources (1992) determined inferred resources of 0.051 Mt @ 0.35% REO. Similarities in deformational style and vein morphology, and a possible association with late-tectonic alkaline source rocks, indicate comparisons with very late-stage epithermal mineralisation (Yungul carbonatite, fluorite) in the Speewah Dome.

Iron-oxide breccia complex: In addition to the world-class Olympic Dam copper, gold, uranium deposit, several large breccia complexes are also developed in the Mount Painter and Mount Babbage inliers of the Curnamona Province of South Australia. The Inliers consist of Proterozoic granites, metasedimentary rocks, and volcanic rocks that have been intruded by Paleozoic granites (Cassidy et al., 1997). Large bodies of breccia (e.g., Radium Hill breccia) occur in the Mount Painter Complex and the Paleozoic granites. The Radium Hill hematitic breccia contains base-metal sulphides, uraninite, monazite, chlorite, carbonate, fluorite, quartz, and magnetite (Drexel and Major, 1990). They are enriched in REE with reported concentrations of 1% TREO. The hematitic breccia and sinter at Mount Gee contain elevated concentrations of uranium, copper, and cerium (average concentrations of up to 6100 ppm; Drexel and Major, 1990). Many investigators have made comparisons between the hematitic breccias at Mount Painter with those at Olympic Dam (Cassidy et al., 1997).

The Radium Hill uranium deposit in the Olary district of South Australia is located within shears of Precambrian feldspathic gneiss, aplitic gneiss, and schist, which are intruded by mafic and felsic bodies (Cassidy et al., 1997). The main uraniferous-REE ore mineral mined was davidite. Approximately 136 kg of high-purity scandium was produced as a by-product of the uranium (Towner et al., 1987).

Skarn: The Mary Kathleen-Mount Isa region of northwestern Queensland may represent a new REE province with a number of significant discoveries in the last few years. Previous exploration in the region largely targeted uranium with little exposure devoted to REE. The Mount Dorothy (Fig. 3.35) and Elaine Dorothy REE ± Cu ± Co prospects have similar broad magmatic-metamorphic signatures to the previously mined Mary Kathleen uranium-REE breccia-skarn deposit (see Table 3.13). China Yunnan Copper Australia Limited announced the discovery of the Mount Dorothy HREE prospect in January 2011, with a broad zone of yttrium and HREE mineralisation in drill-hole MDD005, e.g., 16 m @ 1249 ppm (1.24 kg/tonne) total HREE-Y from 71 m. A northeast-trending, steeply plunging mineralised breccia occurs in a native copper-bearing zone hosted in felsic volcanics. High-grades of HREE and yttrium are spatially associated with secondary copper-cobalt mineralisation and the breccia (http://www.cycal.com.au/IRM/Company/ShowPage.aspx?CPID=1428&EID=49766522&PageName).

Figure 3.35 (see opposite). Geological map and cross-section of the Mount Dorothy rare-earth-element-copper-cobalt deposit, Queensland. Modified from Chinalco–China Yunnan Copper Australia Limited (2011).

CHAPTER FOUR

PRINCIPAL FEATURES OF RARE-EARTH-ELEMENT MINERAL SYSTEMS

4.1. WHAT IS A MINERAL SYSTEM?

In general, current schemes for the classification of ore deposits and most ore deposit models used in both exploration and resource assessment are largely empirical (Cox and Singer, 1986; Eckstrand et al., 1995). An alternative mineral-system approach to classify deposits conceptually is to focus on mineral deposits as a mineralising process and/or event. A mineral-system-based concept has some clear parallels with the petroleum systems approach which has proven to be a useful in oil and gas exploration. Such an approach provides a framework that is applicable at both basin and prospect scales and, unlike the empirical concept, can be used for frontier basins (Bradshaw et al., 1998).

A mineral system is generally defined by its constituent elements, which include:

1. sources of energy driving the system;
2. sources of fluids, metals, and ligands;
3. pathways along which melt or fluid move;
4. chemical and/or physical traps in proximity to pathways;
5. outflow zones for discharge of residual fluids (Wyborn et al., 1994; Knox-Robinson and Wyborn, 1997; Jaques et al., 2002); and
6. preservation.

The mineral-systems framework has been used to develop process based conceptual models of ore systems (e.g., Skirrow et al., 2009) and to create flexible probabilistic structures for conducting quantitative risk analysis in mineral exploration (Kreuzer et al., 2010). It has also been used to map essential ingredients of fertile mineral systems and conduct prospectivity analysis (e.g., Wyborn et al., 1994; Barnes et al., 1999). A similar approach was used to describe ore-forming processes in volcanic-associated massive sulphide deposits (Huston et al., 1997) and Archean lode-gold deposits (Phillips et al., 1996; Hagemann and Cassidy, 2000).

A classification of REE mineral deposits based on a general mineral-systems framework was discussed in Chapter 3. In that chapter, a type example of a particular Australian deposit was discussed in detail. In this chapter we summarise principal features of significant REE-forming mineral systems.

In tables presented in this chapter the original concept of the mineral system has been expanded to include information about geological setting, age, relative timing of mineralisation, and preservation. The focus in Chapter 3 was on type examples of Australian deposits, whereas in this chapter the description includes information from deposits outside Australia.

In compiling these tables, individual mineral systems have been grouped into larger categories represented by association types, such as those associated with the regolith (Table 4.1), heavy minerals (Table 4.2), alkaline rocks (Table 4.3), carbonatites (Table 4.4), pegmatites (Table 4.5), and skarns (Table 4.6). A separate table (Table 4.7) for REE-bearing iron-oxide breccia complexes is included because deposits of the type could be economically significant. A summary for phosphorites (Table 4.8) concludes the association types.

The genetic association of fluorapatite veins at the Nolans Bore deposit (NT) is at this point unknown. Such vein deposits can be formed from fluids generated by alkaline, carbonatite, and even pegmatitic melts, the mineral-system features of which are described in Tables 4.3, 4.5, and 4.6.

Table 4.1. Mineral-system features of rare-earth-element deposits associated with the regolith (deposit types: residual REE related to carbonatite; residual scandium related to ultramafic-mafic igneous rocks).

Geological setting
- Carbonatite and associated alkaline complexes and metasomatic rocks (for setting see Table 4.4)
- Mafic-ultramafic igneous rocks (for scandium). Phanerozoic 'alpine'- and 'Alaskan'-type mafic-ultramafic igneous rocks
- Blanket-like layers draped over weathered surface of carbonatite
- Humid tropical climate with moderate to high rainfall

Source (melt/fluid, metal, energy)

Fluids
- Surficial and/or/shallow ground water

Metals and ligands
- REE-enriched carbonatite and/or associated alkalic and metasomatic rocks
- Fluorine, CO_2 , PO_4 and Cl sourced from carbonatite and/or associated alkalic rocks
- Scandium sourced from mafic/ultramafic igneous rocks

Energy
- Hydrostatic head for shallow ground water

Fluid pathway
- Aquifers, faults, joints, fractures, karstic cavities

Depositional processes (Trap)

Structural/mechanical
- Faults, fractures, joints, cavities
- Topographic lows associated with karstic terranes are favourable for eluvial accumulations of REE-bearing minerals; such terranes are not conducive for significant concentrations of secondary REE minerals
- In areas without karst development internal drainage and basin-type topography create favourable traps for eluvial accumulations

Chemical
- Dissolution of carbonates leaves REE-enriched residual material with minerals, such as apatite, magnetite, pyrochlore, ilmenite, rutile, and zircon (eluvial)
- Decalcification of perovskite
- Changes in the concentration of dissolved fluoride, carbonate, and phosphate ions are important for the formation of secondary REE-bearing carbonates and phosphates, such as monazite, xenotime, parisite, and churchite
- LREE-bearing minerals concentrate in the upper part of the regolith, whereas HREE and Y are more prominent in the deeper parts of the regolith

Age
- Mesozoic to Cenozoic

Relative timing of mineralisation
- Mineralisation post carbonatite and alkalic rocks, but generally synchronous with karst formation and related supergene processes

Preservation
- Preservation is important. In the east Yilgarn Craton, regional glaciation during the Permian scoured pre-existing regolith and superficial deposits (e.g., Ponton Creek carbonatite). Post-mineralisation topography determines the preservation of supergene zones (zone of low hills are eroded)
- Preservation of eluvial accumulation is controlled by the chemistry of surficial water (concentration of CO_2 and sulphate) and nature of internal drainage

References

Richardson and Birkett (1995b); Duncan and Willett (1990)

Table 4.2. Mineral-system features of rare-earth-element-bearing placers (deposit types: heavy-mineral sands: beach; high dune; offshore shallow marine; channel).

Geological setting
- Coastal regions with stable crustal margins
- Lower shoreface/inner shelf area with low-energy conditions (for offshore shallow marine deposits)
- Transverse dune sands (for dune sand-type deposits)
- Braided river sand

Source (melt/fluid, metal, energy)

Heavy minerals
- REE-enriched minerals are derived from igneous and high-grade metamorphic rocks. For heavy minerals in dune sands the REE-bearing minerals are sourced from beach sands

Energy
- Wind, wave, fluvial

Fluid pathway

Not significant

Depositional processes (Trap)

Structural/mechanical
- Topography of coastal region. 'J' curved shoreline preceding headlands, which trap heavy minerals (for beach sands)
- Changes in wave and wind energy, sea-level changes
- Transverse dune sand (dune-type)
- Sorting of heavy minerals by wind action from previous heavy-mineral beach concentrations formed by wave action
- For channel placer-type deposits: zones of changes in water flow in fluvial system. Sands bounded by clay-rich sediments (formed in quiet swamp environment)

Age
- Miocene to Holocene, but generally Pleistocene to Holocene. Some as old as Eocene. Mesozoic for channel deposits

Relative timing of mineralisation
- Sorting and upgrading in many cycles. Monazite initially trapped with zircon, rutile, and ilmenite, but sorted in subsequent cycles
- In REE-bearing heavy minerals in dune sands, sorting of initial beach sands by wind

Preservation
- Tectonically stable regions are important for preservation

References

McKellar (1975); Wallis and Oakes (1990); Stitt (1999); Williams (1990); Roy (1999); Hou (2005)

Table 4.3. Mineral-system features of rare-earth-element deposits associated with (per)alkaline rocks (deposit types: orthomagmatic; volcanic; hydrothermal (vein); metasomatic (albitite)).

Geological setting
- Cratonic, anorogenic setting with magma generation and intrusion possibly associated with crustal extension; intraplate
- Igneous complexes are often bimodal (basaltic and rhyolitic). In some cases, (per)alkaline magmas are spatially related to peraluminous magmas
- Shallow-level environment: ring complexes of intrusive and volcanic rocks along ring fractures

Source (melt/fluid, metal, energy)

Melt/fluids
- Source of the melt: fractional crystallisation of alkali basaltic magma formed from small degree of partial melting of the mantle
- Source of fluids for hydrothermal and metasomatic (albitite) deposits: melt

Metals and ligands
- The first-stage source of REE is mantle; partial melting of which produces a REE-bearing melt
- For magmatic deposits: the source melt is of (per)alkaline composition
- For hydrothermal and metasomatic deposits: the source melt is (per)alkaline
- Fluorine and CO_2 sourced from melt

Energy
- High-geothermal gradient
- Intrusive and intrusive-volcanic complexes

Fluid pathway
- For igneous complexes: major deep crustal (lithospheric?) structures. At shallow levels, complexes are controlled by ring fractures
- For fluids: structures within and in proximity to igneous complexes

Depositional processes (Trap)

Structural
- Faults and ring fractures within igneous complexes

Chemical
- Cooling of melt and crystal fractionation
- Reaction of residual fluids with the pre-crystallised zones of the complex
- For metasomatic and hydrothermal deposits: cooling, and changes in pH could be significant
- In some deposits, such as Lovozero (Russia), bituminous substances could have played some role in forming hydrothermal mineralisation within pegmatites

Age
- Any age from Proterozoic to Cenozoic. A large number are Proterozoic

Relative timing of mineralisation
- Mineralisation is generally associated with the final phase of a multiple-stage batholith
- In deeper level settings mineralisation associated with small satellite phases of the main pluton
- Metasomatic and hydrothermal mineralisation either late, or postdates, magmatic phase

Preservation
- Post-emplacement tectonic history is important to preserve shallow intrusive-volcanic ring complexes

References

Mungall (2007); Jaques et al (1985); Jaques (2008); Richardson and Birkett (1995c)

Table 4.4. Mineral-system features of rare-earth-element deposits associated with carbonatites (deposit types: orthomagmatic; hydrothermal (vein and replacement); metasomatic (skarn, fenite); regolith-related).

Geological setting
- Continental (anorogenic) rift zones. Some carbonatites are near plate margins (collisional as well as divergent)
- Near margins of cratons
- Carbonatitic complexes invariably occur in association with alkalic rocks
- Spatially related to deep crustal (lithospheric?) structures controlling multiple intrusion events
- Mineralisation in lava, flows, and plugs, cone sheets, dykes, and rare sills, but never in large homogeneous plutons

Source (melt/fluid, metal, energy)

Melt/fluids
- Source of the melt: partial melting of carbonate-rich peridotite mantle; partial melting of carbonate-rich eclogite in subducted oceanic crust; liquation (i.e., separation of metals) and segregation from CO_2-rich alkaline melts in the crust; fractional crystallisation of alkali basaltic magma formed from small degree of partial melting of the mantle
- Source of fluids for hydrothermal and metasomatic (skarn, fenite) deposits: carbonatitic melt

Metals and ligands
- The first-stage source of REE is mantle; partial melting of which produces a REE-bearing melt
- For magmatic deposits: the source is carbonatitic melt. REE-bearing carbonatite deposits are strongly enriched in LREE
- For hydrothermal and metasomatic deposits: the source is carbonatitic melt
- For regolith-related deposits: the source is mineralised carbonatite
- Fluorine and CO_2 sourced from melt

Energy
- High-geothermal gradient
- Intrusive and intrusive-volcanic complexes

Fluid pathway
- For igneous complexes: major deep crustal (lithospheric?) structures. At shallow level complexes controlled by ring fractures
- For fluids: structures within and in proximity to igneous complex

Depositional processes (Trap)

Structural
- Faults and fractures within igneous complexes

Chemical
- Cooling of melt and fractionation. REE-bearing minerals formed in the cumulates during the early stages of crystallisation of carbonatitic melt, or from the late residual melt enriched in F, Ba, Sr, U, and Th
- Reaction of residual fluids with the pre-crystallised zones of the complex
- For metasomatic and hydrothermal deposits: cooling, changes in the concentration of CO_2, dissolved phosphorus and fluorine could be important

Age
- Any age from Archean to Cenozoic. More abundant in Proterozoic, Mesozoic, and Cenozoic

Relative timing of mineralisation
- Orthomagmatic REE mineralisation formed with cumulates in the early stages of crystallisation of carbonatitic melt and is tied up with minerals, such as perovskite, pyrochlore, apatite, and calcite. Main REE-mineralisation formed from the late residual melt enriched in REE, F, Ba, Sr, U, and Th. Mineralised ferrocarbonatites (dykes and veins) crosscut and replace early phases of carbonatite
- Metasomatic and hydrothermal mineralisation either late, or postdates, magmatic phase
- Carbonatite melts may be related to major extensional events (such as breakup of Rodinia)

Preservation
- Post-emplacement tectonic history is important for preservation of shallow intrusive-volcanic ring complexes

References

Mungall (2007); Jaques (2008); Richardson and Birkett (1995a)

Table 4.5. Mineral-system features of rare-earth-element-bearing pegmatites (some REE-bearing apatite/fluorite veins may be related to pegmatite system).

Geological setting
- Late tectonic stages of compressive dynamo-metamorphic event in orogenic zones. Collisional environments: continent–continent collision, continent–island arc, island arc–island arc, closures of ensialic rift
- Archean pegmatites in greenstone belts and mobilised sedimentary troughs
- Proterozoic pegmatites in belts marginal to the Archean basement
- Phanerozoic pegmatites within granite belts in orogens
- Anorogenic related to long-lived rift systems
- Structures formed during continuing compression and thickening after peak metamorphism

Source (melt/fluid, metal, energy)

Pegmatitic melt/fluids
- For NYC[1]-type: peraluminous to metaluminous (rarely (per)alkaline); A- and I-type felsic melts
- For mixed NYC- and LCT[1]-types: subaluminous to peraluminous
- Felsic melts are mildly fractionated. REE abundances show depletion in HREE
- Source of felsic melts: for NYF-type: depleted middle to lower crustal granulites. For mixed pegmatites: either mixed protoliths, or melts formed from assimilation of supracrustal rocks by NYF-type granites
- Fluids are sourced from the pegmatitic melt

Metals and ligands
- REE: pegmatitic melt and associated fluid. From breakdown of ferromagnesian minerals and accessory minerals, such as ilmenite, monazite, zircon, and titanite during melting of protolith
- Ligands: pegmatitic melt and associated fluid
- LCT-type: pegmatite with Li, Rb, Cs, Be, Sn, Ga, Ta > Nb (B, P, F); NYF-type: pegmatite with Nb > Ta, Ti, Y, Sc, REE, Zr, U, Th, F

Energy
- Compressive dynamo-metamorphism in orogenic zones;
- Steep thermal gradients established after peak (Abukama-type) metamorphism
- Felsic melts

Fluid pathway
- Regional faults formed during continuing compression and thickening after peak metamorphism. Faults along boundaries of metamorphic zones

Depositional processes (Trap)

Structural
- Faults, folds for pegmatites
- Fractures and cavities within pegmatites

Chemical
- Cooling and fractionation of pegmatitic melt
- Cooling of pegmatitic fluid

Age
- Any age

Relative timing of mineralisation
- NYF-type mostly post-orogenic to anorogenic
- Hydrothermal REE mineralisation late- and/or post-pegmatitic

Preservation
- As pegmatites are formed at pressures (4 to 1.5 kbar) generally similar to the pressures at which the host rocks of upper-greenschist to lower-amphibolite facies metamorphism are formed, the pegmatites are generally well preserved

References

Cerny (1991a); Cerny (1991b)

[1] These types of pegmatites are defined in Tables 3.9 and 3.10.

Table 4.6. Mineral-system features of rare-earth-element deposits associated with skarn.

Geological setting
- Orogens with metaluminous to peraluminous felsic rock intruding calcareous (meta)sedimentary rocks
- Skarn associated with alkaline and (per)alkaline rock (see Table 4.3 for general setting)
- Skarn associated with carbonatite complexes (see Table 4.4 for general setting)

Source (melt/fluid, metal, energy)

Fluids
- Alkaline, peralkaline, carbonatite melts
- For Mary Kathleen-style deposits multiple sources: metaluminous to peraluminous felsic melt and fluid generated during regional metamorphism

Metals and ligands
- Alkaline, peralkaline, carbonatite melts
- For Mary Kathleen-style deposits multiple sources which include felsic melts and (meta)sedimentary rocks

Energy
- High-geothermal gradient
- Intrusive and intrusive-volcanic complexes
- Regional metamorphism

Fluid pathway
- Fault within and in proximity to igneous complex. For metamorphic fluids regional faults and other penetrative structures could be significant

Depositional processes (Trap)

Structural
- Faults and fractures within igneous complexes and calcareous (meta)sedimentary rocks

Chemical
- Cooling and changes in pH and locally redox state
- Changes in the concentration of ligands, such as carbonate, phosphate, chloride, and fluoride, could be important. This change caused by reaction with paragenetically early skarns

Age
- Any age. The relative age is constrained by the age of the intrusive complexes

Relative timing of mineralisation
- In skarn deposit, REE-bearing minerals either synchronous or post-date skarn
- In regions where skarn formation is followed by deformation and metamorphism, REE mineralisation can be remobilised
- Weathering and regolith-formation can also remobilise REE

Preservation
- Post-emplacement tectonic history is important to preserve skarns formed with intrusive-volcanic complexes, such as carbonatite and (per)alkaline rocks

References

Oliver et al. (1999); Wu et al. (1996); Zhao et al. (2005)

Table 4.7. Mineral-system features of rare-earth-element-bearing iron-oxide breccia complex.

Geological setting
- Pre-deposit: continental margin, extensional basin along margin
- Syn-deposit: 'far-field' back-arc or intracontinental setting
- Coeval mafic and high-temperature I-or A-type intrusive-volcanic complexes. In some regions, no or limited coeval volcanics
- Brecciation at high-crustal level; diatreme/maar volcanic setting; brecciation not prominent in a relatively deeper crustal setting

Source (fluid, metal, energy)

Fluids
- Fluid 1: magmatic; high temperature (~400°C), high-salinity (up to 40 to 50 wt% eq. NaCl) fluid (fluorine-rich)
- Fluid 2: evolved meteoric water; moderate temperature (150°C to 250°C) of low to moderate salinity; fluorine-rich, more oxidised than Fluid 1

Metals and ligands
- Copper: magmatic; A-type granites, mafic rocks
- Iron: magmatic; (meta)sedimentary rocks
- Gold: magmatic; A-type granites, mafic rocks
- Uranium: A-type granites, gneiss in basement
- REE: magmatic (granites, and alkaline, mafic, and ultramafic rocks)
- Ligands: magmatic; locally evaporite-bearing sequences

Energy
- High-geothermal gradient
- Intrusive-volcanic complex
- Hydrostatic head for oxidised fluid 2

Fluid pathway
- Crust-penetrating shear/fault zones separating crustal blocks or orogens
- District-scale fault networks reactivated during mineralisation event

Depositional processes (Trap)

Structural
- Faults, folds
- Diatreme/maar, breccia zones

Chemical
- Redox: mixing of fluids and/or reaction between reduced rocks and oxidised fluid
- Iron-rich host rocks

Age
- Any age, but Proterozoic more important for world-class deposits

Relative timing of mineralisation
- Related to a switch from compressional to extensional deformation
- Mineralisation closely linked with emplacement of intrusive-volcanic complexes and brecciation

Preservation
- Important for shallow-level breccia complexes. Rapid cratonisation during or before mineralisation and/or basin formation is over

References

Reeve et al. (1990); Reynolds (2001); Johnson and McCulloch (1995); Skirrow et al. (2007)

Table 4.8. Mineral-system features of rare-earth-element-bearing phosphorite.

Geological setting
- Continental margin
- Continental shelves and shelf breaks. Atop submarine highs (seamounts and drowned carbonate build ups)
- Coastal subtidal, intertidal, and supratidal environments
- Basements highs over and around which phosphorites are deposited

Source (fluid, metal, energy)

Fluids
- Sea water

Metals and ligands
- Phosphorus: organic matter, bones and microbial mats. Locally run-off of rivers where phosphorus is adsorbed to iron hydroxides
- REE: the source unknown (possibly from REE-rich rocks, which also provide the sediments; bedrock of the basin?)

Energy
- Wave and currents provide upwelling of phosphorus-rich water

Fluid pathway
- Continental shelf

Depositional processes (Trap)

Structural
- Shelf-breaks. Shelf topography conducive for mixing of shallow water with upwelling currents

Chemical
- Mixing of cold relatively deeper upwelling currents with warmer shallower water and loss of CO_2

Age
- Favourable ages for phosphorite formation: Neoproterozoic, Cambrian, Permian, Late Cretaceous/Early Cenozoic, and Miocene

Relative timing of mineralisation
- Timing of REE-minerals in phosphorites is not clear. Some may precipitate with sedimentary apatite. The possibility of enrichment during diagenesis can not be excluded

Preservation
- Post-depositional tectonics and transgression and regression events important for preservation. Later transgression events may destroy REE-enriched phosphorite

References

Einsele (1992); Howard and Hough (1979)

CHAPTER FIVE

EXPLORATION FOR RARE-EARTH ELEMENTS

5.1. INTRODUCTION

The exploration for REE in Australia has had a much lower profile and a shorter evolution than most other widely sought commodities, such as gold, tin, iron, and the base metals (copper, lead, zinc, nickel). The Australian mining industry was initiated back in 1839 with the discovery of base metals near Adelaide (Solomon and Groves, 1994). In contrast, there has been no significant production of REE from a hard-rock source since REE were first mined in 1913 from pegmatites near Marble Bar in Western Australia (see Section 1.6). During the past century there were very few exploration programs dedicated solely to REE in Australia. However, in recent years, dramatically increasing metal prices have generated considerable exploration interest for the REE. The increased demand for REE in a number of emerging technologies and their narrow supply base (dominated by China) have provided the stimulus for the development of any potential new resources of the REE. This trend is reflected by the significant number of prospects now being explored for in Australia, and in particular Western Australia and the Northern Territory. Of the 74 prospects (2011 data) represented in the histograms of Figure 5.1, 40 are at the initial grassroots phase of exploration, and another 23 prospects are slightly more advanced with their exploration. A similar number of grassroots projects occur in Western Australia and the Northern Territory, with each jurisdiction accounting for about 40% of all grassroots prospects. A relative small number of new prospects (<12%) occur in Queensland, New South Wales, and South Australia. Less than 5% of all REE projects are at the feasibility development stage in Queensland, New South Wales, and South Australia.

The discovery of diamonds in the Kimberley region of Western Australia in the 1970s stimulated a major phase of exploration for diamonds across the country. During this period a wide range of alkaline igneous rocks including kimberlite, lamproite, lamprophyre, and carbonatite were identified (Jaques et al., 1985; Atkinson et al., 1990). Most of these rock types are strongly enriched in LREE but, with the exception of carbonatites, typically do not host economic REE deposits. The association of REE with uranium in unconformity-related settings in the Proterozoic regions (e.g., Pine Creek Orogen, Halls Creek Orogen) of northern Australia also provided exploration interest, but no major REE resources were found. Schofield (2010) has outlined the potential for magmatic-related uranium mineral systems in Australia. In recent years, a broader range of rock types (mafic, ultramafic, alkaline, regolith, clay, phosphorite, etc) and different geological settings are now being considered for REE exploration.

Potentially one of the most favoured geological settings for high-grade, large tonnage polymetallic

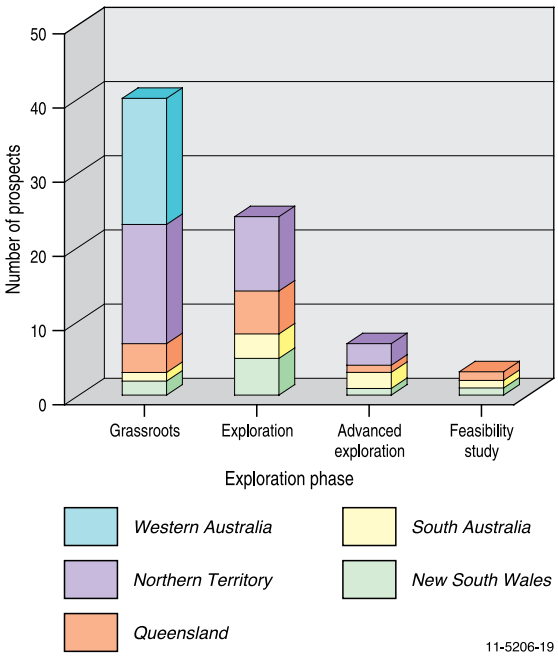

Figure 5.1. Exploration phase of rare-earth-element prospects in Australia. Total number of prospects shown is 74. Data from Intierra Resource Intelligence database, January 2011, (http://www.intierra.com/Homepage.aspx).

REE deposits are the supergene deposits localised in the weathering profile above carbonatites and alkaline igneous complexes (e.g., Mount Weld, Cummins Range; Cassidy et al., 1997). Exploration techniques that have been traditionally used for such prospective alkaline igneous source rocks, include high-resolution airborne and surface gamma-ray spectrometric (to detect Th and U contents), magnetic (presence of magnetite), and gravity (dense lithologies) surveys, and heavy-mineral studies (Lottermoser, 1991). However, such regional surveys can have limitations. For example, the Mount Weld and Cummins Range Carbonatites are steeply plunging cylindrical bodies that have relatively small cross-section dimensions that could be missed during regional gravity surveys. Both carbonatite bodies were found on the basis of significant aeromagnetic anomalies. In addition, the chemical susceptibility of the dominant minerals (calcite and dolomite) in carbonatites, means these alkaline complexes often have recessive landscape profiles and are totally covered by alluvium. Airborne radiometric data only records gamma-rays emanating from the near surface (less than ~30 cm), thus areas of thick surficial cover may mask a K-U-Th-bearing source.

Figure 5.2 summarises the temporal distribution of the major REE deposits in Australia. It is apparent that most hard-rock associations (carbonatites, alkaline rocks, fluorapatite veins, iron-oxide breccias) feature most prominently in the Early Proterozoic (Paleoproterozoic to Mesoproterozoic), with only the pegmatite deposit type (e.g., Pinga Creek) representing the Archean. Two notable hard-rock examples in the Phanerozoic include the REE-bearing Cambrian phosphorite deposits (Korella) and the Mesozoic trachyte-hosted deposits (Toongi). Mineralised laterites associated with carbonatite (Mount Weld) and ultramafic-mafic rocks (Lucknow) have similar time lines in the Late Mesozoic to Early Cenozoic, whereas the major lignite occurrence (Mulga Rock) occurs in the Eocene. Most heavy-mineral sand deposits formed in the Cenozoic, whereas channel types are older mineral systems that formed as far back as the Mesozoic. Thus, as an initial exploration criterion, it appears from the different tie lines in Figure 5.2, that the Proterozoic Eon is a favourable time period for different types of hard-rock REE deposits, whereas the Cenozoic Era offers more exploration opportunities for regolith-related, lignite, and heavy-mineral sand deposits. Further robust age data on other REE deposits are required to confirm this preliminary chronological record of Australia's REE deposits.

A synthesis of the major exploration methods that have been used for REE in Australia is provided in Section 5.2. Table 5.1 summarises the relative importance of these various geological and geophysical methods, and it also highlights the main method(s) responsible for the discovery of the deposit. Section 5.3 introduces several national digital datasets produced by GA since 2008 that have potential applications for REE exploration.

Major developments relating to the exploration and metallurgy of the REE by the Australian Government and other organisations are summarised in Appendix 9. A compilation of useful www links is provided in Appendix 10.

5.2. EXPLORATION METHODS AND STRATEGIES

5.2.1. Rare-earth-element deposits associated with carbonatites

- Mapping of deep crustal (lithospheric) structures using gravity, aeromagnetic, seismic, and magneto-telluric surveys.
- Radiometric survey can identify carbonatite complexes (outcropping and shallow under-cover) because they are commonly enriched in U and Th. The fenitic halo of altered rocks, which are also enriched in U and Th, can also be mapped by radiometric surveys.
- On aeromagnetic maps, carbonatites form positive magnetic anomalies (e.g., Mount Weld and Cummins Range, both WA: Dentith et al., 1994; Gunn and Dentith, 1997). The fenitic rocks generally do not contain magnetite hence circular to elliptical magnetic anomalies can be associated with magnetically negative halo of altered rocks. Because many carbonatite complexes are surrounded by mafic alkaline rocks, they often show up as a magnetic 'bull's eye' combined with a gravity low and ringed by a gravity high (http://explorationgeophysics.info/?p=318).
- The Mount Weld Carbonatite is characterised by a regional magnetic anomaly of 8150 nT[5] (see inset in Fig. 5.5) and ground gravity revealed a positive anomaly of about 6 mGal (Dentith et al., 1994). Variations in the magnetic signal reflect the heterogeneous distribution of magnetic minerals within both the primary intrusion and the regolith. Radiometric data did not detect the carbonatite due to the thicknesses of the overlying sedimentary rocks, and electrical methods were only partially

[5] nT: nanotesla is a unit of magnetic field.

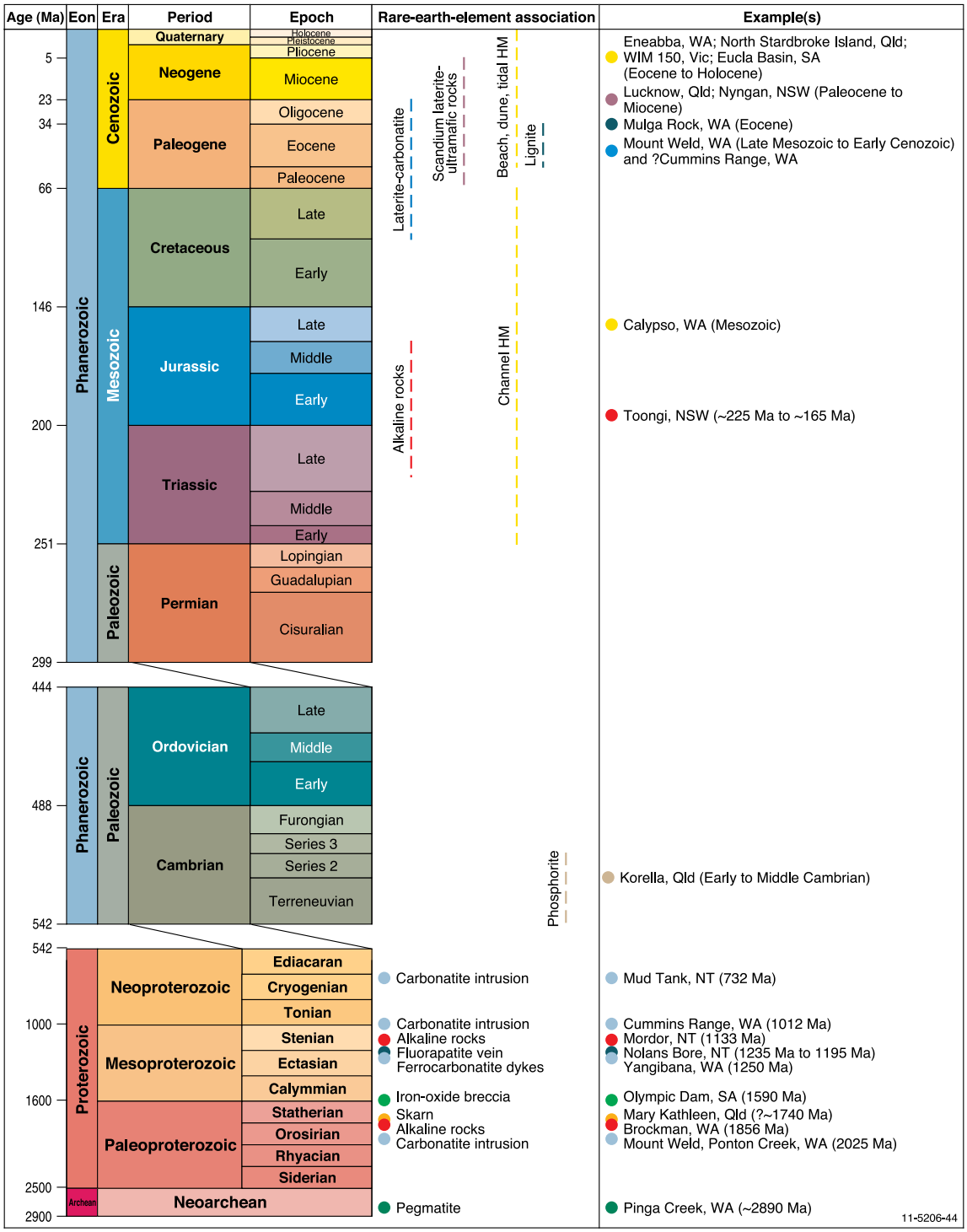

Figure 5.2. Geological time scale and formation of the major rare-earth-element deposits and prospects in Australia. The geological time lines of some of the major REE deposit types are chartered. The age data for the various deposits and prospects are from the type examples of major rare-earth-element deposits described in Section 3.3.1. The geological time scale is based on Gradstein et al. 2004). Ma = million years.

successful in mapping the regolith and water table. The Cummins Range Carbonatite is associated with a radiometric anomaly which is believed to be sourced from uranium in the regolith (Dentith et al., 1994).

- Mineralisation in carbonatite complexes, is often hosted by plugs, cone sheets, flows, dykes, and sills instead of large homogeneous plutons. This feature requires more detailed local-scale exploration methods, such as detailed airborne gravity, magnetic, electromagnetic, and geochemical surveys.
- As the dominant carbonate minerals (calcite, dolomite) have greater relative densities than quartz and feldspar, carbonatites may generate positive gravity anomalies. However, this will largely depend on the densities of the country rocks.
- Airborne Visible/Infrared Imaging Spectrometer (AVIRIS) has been successfully used to map carbonatites in the Mountain Pass area of California (Kingston and Crowley, 1992).
- High-resolution airborne gravity and magnetic surveys were used by the Quantum Rare Earth Development Corporation to explore the Elk Creek Carbonatite, Nebraska, USA (http://explorationgeophysics.info/?tag=carbonatite).
- Geochemical methods (soil, whole-rock, water, overbank sediments) to identify (per)alkaline rock anomalous in indicator elements, such as LREE, Rb, Sr, Ba, U, Th, and F. Sadeghi and Steele (1989) describe a stream-sediment survey undertaken to explore for mineralised carbonatites in Arkansas, USA. They found a REE + Ti + F map very effective in mapping anomalous areas.
- Mapping of alteration zones using HyLogger can be very affective for local-scale targeting.
- Heavy-mineral indicator surveys (stream sediment and loam) as REE-bearing minerals, such as monazite are commonly resistant to weathering. Other heavy minerals, such as pyrochlore, perovskite, zirconolite, and apatite, are associated with carbonatites.
- In general, the best tools for the discovery of carbonatites in Australia have been aeromagnetics (Dentith et al., 1994), followed by closer-spaced magnetics, and then drilling and geochemistry of the REE-enriched regolith zone.

5.2.2. Scandium-bearing laterite associated with ultramafic-mafic rocks

- Host 'alpine-type' intrusions consist of Paleozoic ultramafic-mafic bodies that occur in ~north-trending serpentinite belts associated with crustal-scale fault systems in the Lachlan Orogen of eastern Australia. Intrusions extend from western Tasmania, through Victoria, New South Wales to southern Queensland**.** The fault-bounded 'alpine' bodies are sometimes spatially associated with other intrusions having 'ophiolite' and 'Alaskan-type' affinities. This association is a useful regional criterion for locating prospective intrusions under cover (e.g., Fifield region, NSW).
- Regional distribution of intrusions is strongly controlled by steeply dipping northwest- to northeast-trending fault systems; hence they form well-defined linear belts that have a high degree of predictability about their distribution.
- Scandium mineralisation in the laterite profile is commonly associated with low-grade nickel and cobalt abundances.
- The ultramafic-mafic source rocks of the scandium can host disseminated and massive podiform chromite that may be enriched in Os-Ir-Ru alloys, or hydrothermal PGE-bearing base-metal sulphides (western Tasmania). Placer deposits of Cr and PGEs are generally more attractive targets than hard-rock deposits. Chromite and PGE-bearing spinels can be used as indicator minerals in stream-sediment geochemical programs (Hoatson and Glaser, 1989). These PGE and chromite deposits can assist in the identification of ultramafic-mafic rocks that may be favourable source rocks for laterite-hosted scandium mineralisation.
- Aeromagnetics, soil-costean and stream-sediment geochemistry, and core drilling are the common exploration methods. Gravity has applications for the larger intrusions with considerable areal extent.
- Deposits are amenable to large-scale, low cost open-pit mining methods that can take advantage of by-product PGEs, nickel, and cobalt.
- Significant deposits of scandium associated with nickel-cobalt laterites are rare in Australia, and indeed in the world. The Sipilou South nickel-cobalt-scandium laterite deposit is located in western Côte d'Ivoire, Africa (http://www.marketwire.com/press-release/Sama-Resources-Intersects-137-Metres-Up-25-Nickel-Its-Nickel-Cobalt-Scandium-Laterite-TSX-VENTURE-SME-1419535.htm), and similar scandium-bearing laterite deposits (Lola Project) also occur in the Republic of Guinea, West Africa.

5.2.3. Heavy-mineral sands (including beach; high dune; offshore shallow marine; channel) with rare-earth-element-bearing monazite

Exploration strategies and area selection are influced by land-use issues. Areas with potential for heavy-mineral concentrations containing REE-bearing monazite and xenotime can be broadly classified as:

- **Onshore environments**
  - Present-day shorelines
    - Beach deposits
      - Known heavy-mineral deposits on current beaches along the current east coast of Australia and Western Australia have either been mined out or are inaccessible due to land-use issues;
      - Some exploration for heavy-mineral sands along the current coast is still being conducted along the west coast of Cape York Peninsula.
    - High-dune deposits close to the present-day shoreline
      - Most of the high-dune-type deposits are in conservation reserves and state/national parks.
    - Land issues
      - Major obstacle to access of heavy-mineral sand deposits along the current coast;
      - At least 20% of known heavy-mineral-sand resources containing monazite lie within various types of conservation zones and parks;
      - Coastal areas with potential for heavy-mineral sand deposits are being encroached by urban development
  - Inland-fossil shorelines
    - Beach deposits
      - Beach deposits containing heavy minerals are known to occur and are currently either mined or actively explored for along fossil shorelines in the Murray Basin, Perth Basin, and the emerging heavy-mineral province of the Eucla Basin. The Arckaringa Basin in South Australia may also host heavy-mineral deposits and there may be potential for heavy-mineral deposits in other younger onshore basins.
    - Offshore shallow marine deposits
      - Most of the known fossil offshore heavy-mineral deposits occur in the northwest of the Murray Basin in Victoria.
    - Channel deposits
      - The only known channel deposits of potential commercial importance are in the northern part of the Perth Basin, north of Perth, Western Australia.
- **Present-day offshore environments**
  - Heavy-mineral sand deposits occur offshore along the eastern Australian coastline (Wallis and Oakes, 1990), but their monazite and xenotime contents are not known.

Current exploration techniques for heavy-mineral sand deposits include the following (Belperio, 1999; Dickson, 1999; Roy et al., 2000; Ferris et al., 2003; Elsner, 2010).

- Research and reconstruction of regional and local geomorphologic processes that form heavy-mineral concentrations, either present-day or fossil shorelines, to identify target areas for exploration of heavy-mineral concentration, involving:
  - stratigraphic-sedimentological studies to enable genetic classification of sediment sequences;
  - use of satellite and aerial photographs to identify locations with diminishing transport energy;
  - evaluation of hydrographic–oceanographic data to identify coastal currents and sedimentation processes;
  - *Side-Looking Airborne Radar* (SLAR) to identify geomorphological structures underneath cover/vegetation.
- Research of properties of the heavy minerals that enable detection using geophysical prospecting methods.
- Geophysical techniques include ground- and low-level-airborne magnetic and radiometric surveys.
- Digital elevation models.
- Drilling at both reconnaissance and closed-spaced detailed scales.
- Trenching of identified heavy-mineral sand deposits for bulk-sampling heavy-mineral-separation studies.

According to Ferris et al. (2003) the challenge for future exploration lies in discovering not only dune/barrier sands beneath cover, but also beach, shore-face, dune, tidal inlet, and wash-over sediments beneath thin cover. The use of high-resolution digital elevation modelling, AEM/TEM and magnetics, induced polarisation, remotely sensed (e.g., NOAA and Landsat) night-time-thermal imagery, shallow seismic in the areas of shallow cover may define strandlines developed in the high-energy beach sedimentary facies. Future exploration should seek a greater understanding of the stratigraphic significance of the Cenozoic succession

and apply a greater emphasis to paleogeomorphic and paleogeographic factors.

Because of the cost of thorium disposal, monazite is currently dispersed back into the heavy-mineral mine sites. In general, the monazite resources are no longer determined in current assessments of heavy-mineral resources, and detailed analyses of REE in the monazite of heavy-mineral sands are no longer available.

If monazite is to be considered as a source of REE in the future, a systematic sampling of heavy-mineral deposits would be required to determine their monazite content. Analyses for REE, thorium, and uranium content in the monazite are needed to make an accurate assessment of REE resources and possibly identify heavy-mineral deposits with low thorium and uranium contents in the monazite.

The importance of monazite and xenotime in the heavy-mineral concentrate as potential sources of REE is discussed in Section 3.3.2.

5.2.4. Rare-earth elements associated with phosphorites

Although the genesis of phosphorites and appropriate exploration strategies for phosphorites are relatively well established, there is an apparent lack of information on the association of REE with phosphorites in Australia which requires:

- detailed review of all existing analyses for REE in phosphorite supported by systematic sampling of known phosphorite deposits for REE analyses;
- possible application of isotope studies for likely sources of REE basement rocks to obtain a better understanding of the potential for economic concentrations of REE in Australian phosphorite deposits; and
- literature search to determine if potentially commercially viable metallurgical processes have been identified for extraction of REE from phosphorite under current economic conditions.

REE contents of phosphorites worldwide, as reported by Orris and Grauch (2002), do not appear to exceed 0.5%. The recovery of europium as a by-product of phosphate mining has been reported for the Schevchenko deposit in Kazakhstan (Orris and Grauch, 2002) and Li et al. (2007) have investigated the feasibility of extracting REE as a by-product of phosphate mining from the Zhijin phosphorite deposit in China.

Total phosphate resources in the Georgina Basin are considered to be of the order of 4 billion tonnes (Lottermoser, 1991), but total REE contents in the phosphorites are generally much less than 1000 ppm.

The Korella deposit south of Duchess, in northwest Queensland, appears to be the only REE-bearing phosphorite deposit with a published REE resource, but other REE-rich phosphorites may be present.

Altschuler et al. (1967) concluded in a detailed study of the geochemistry of REE in phosphorites in the United States that apart from exploration and discovery of REE in phosphorites, the successful exploitation of known REE resources from phosphorites is subject to the development of a viable extraction process that can be used in conjunction with phosphorite production.

5.2.5. Rare-earth elements associated with lignite

Exploration strategies for REE-bearing lignite deposits in Australia are not well documented with the Mulga Rock deposit (see Deposit Type 3.8) in Western Australia being the only known example of this deposit type in Australia. The economic viability for the extraction of scandium from the Mulga Rock deposit is also yet to be assessed. A literature search for global occurrences of REE in lignite and coal together with sample geochemistry are required to understand the distribution and potential of REE in lignite and coal in Australia.

The following investigations are required to address the apparent lack of readily available data on the distribution of potentially commercially viable REE in coals:

- comprehensive literature search for available geochemical data on the content and distribution of REE in peat, lignite, brown coal, and black coal to determine if potentially commercially viable REE concentrations are known in lignite and coal;
- literature search to determine if potentially commercially viable metallurgical processes have been identified for extraction of REE from lignite, coal, and coal ash;
- develop an understanding of the geochemical distribution of REE in coals, and use results to formulate geological environments favourable for deposition of REE in lignite/coal;
- conduct geochemical sampling of existing samples of lignite and coal in Australia to develop geological concepts for the identification of potential exploration targets;
- drilling and geochemical sampling to test exploration targets; and

- examine the possible application of isotope studies for possible sources of REE in regions where lignite and coal deposits occur in vicinity of Archean/ Proterozoic basement rocks with lamproite and carbonatite intrusions.

5.2.6. Rare-earth-element deposits associated with alkaline rocks

- Mapping of deep crustal (lithospheric) structures using gravity, aeromagnetic, seismic, and magneto-telluric surveys.
- Identification of regions with thickened lithosphere can provide first-order regional control on the distribution of alkaline and associated carbonatite rocks. Lithospheric mapping using Nd and Hf isotopes can be useful because they show the nature of lithospheric material from which melts are sourced.
- Radiometric surveys can identify alkaline (outcropping or shallow under-cover) rocks because they contain anomalous concentrations of uranium and thorium.
- Alkaline rocks are often characterised by negative magnetic anomalies (Richardson and Birkett, 1995c).
- Geochemical orientation surveys using different mediums (soil, whole-rock, water, overbank sediments) can identify alkaline rocks anomalous in indicator elements, such as LREE, Rb, Sr, Ba, U, Th, Nb, F, and P (Chalmers, 1990; Taylor et al. (1995a,b)).
- Stream sediment and loam sampling of heavy minerals to identify indicator minerals more resistant to weathering ('resistate' minerals), such as REE-bearing monazite and other associated minerals like Nb-rutile and zircon.
- Detailed exploration geophysical techniques (magnetic, radiometric, gravity, and aeromagnetic) can locate density, magnetic, and conductivity contrasts generated by fluid flow.
- Mapping of alteration zones by HyLogger can be effective for local-scale targeting.

5.2.7. Rare-earth-element-bearing pegmatites

- Pegmatite dykes generally occur along regional-scale faults in metamorphic terranes. Geophysical techniques (magnetic, gravity) which can map regional structures and structural corridors can be useful.
- REE-baring NYF-type pegmatites are subaluminous to metaluminous (rarely subalkaline). Major element geochemistry of pegmatite can distinguish pegmatites prospective for REE deposits.
- Most REE-bearing pegmatites are characterised by anomalous concentrations of uranium and thorium and thus create positive radiometric anomalies when the pegmatites either outcrop or buried under shallow cover.
- Fertile pegmatites are also enriched in LREE, Nb, Ta, F, P, Zr, and Li. Geochemical surveys (soil, overbank, bedrock, stream sediments and water, and ground water) can be effective to map prospective areas.

5.2.8. Rare-earth-element-bearing skarn

Skarns are generally associated with REE-enriched (per)alkaline, carbonatite, and metaluminous to subaluminous felsic melts which intrude calcareous (meta)sediments. Regional-scale targeting of these deposits can be undertaken by the techniques outlined in preceding sections. Once a REE-enriched magmatic source has been identified more detailed targeting can be undertaken by:

- geophysical techniques (magnetic, gravity) which can map regional-scale and lower-order faults that could have functioned as fluid conduits;
- radiometric survey to map positive anomalies caused by anomalous concentrations of uranium and thorium in these deposits;
- most skarn deposits are often enriched in iron-oxides (magnetite and hematite) and commonly have positive magnetic and gravity anomalies; and
- geochemical survey (bedrock, soil, and water) to map halo of dispersed elements (REE, P, F, U, Th).

5.2.9. Apatite and/or fluorite veins

REE-bearing apatite and/or fluorite veins can be genetically related to either carbonatitic, (per)alkaline, and/or pegmatitic systems. Exploration methods that are listed in this section for these three systems can also apply to the regional-scale targeting of REE-bearing apatite and/or fluorite veins.

- Veins enriched in uranium and thorium can generate positive radiometric anomalies.
- Geochemical halos of F, P, and REE can also be mapped by geochemical surveys (bedrock, soil, water).

5.2.10. Iron-oxide breccia complexes

- Major deposits of this type are controlled by large regional-scale structures and lineaments, which can be mapped by geophysical techniques (gravity, magnetic, seismic, magnetotelluric).
- Most Olympic Dam-style deposits of this type are associated with A-type uranium-rich melts. Major

and minor element geochemistry of felsic rocks can identify prospective intrusive-volcanic complexes.

- The presence of iron-rich (meta)sedimentary rocks are a common feature of many mineralised districts. Mapping of such rocks using geophysical techniques (magnetic and gravity) can delineate regional-scale prospective targets.
- Mineral deposits of this type are known to have coincident, but off-set gravity and magnetic anomalies, which are widely used as drilling targets in the Gawler Craton and Mount Isa Inlier.
- Hydrothermal-mineralised systems associated with deposits are known to form extensive alteration haloes, which can be effectively detected by HyLogger, PIMA, and other remote-sensing techniques (ASTER).
- As deposits of this type are often enriched in uranium and thorium, they form positive radiometric anomalies.
- A relatively large size of hydrothermal systems creates haloes of dispersed elements around these deposits. The haloes can be mapped by geochemical (bedrock, soil, stream sediments, stream, and ground water) surveys.
- Nd-isotope data for the Olympic Dam deposit show that REE could have been derived from the mantle. Nd- and Hf-isotope mapping can be useful to define fertile intrusive-volcanic complexes.

Table 5.1. Summary of exploration methods used for rare-earth-element deposits in Australia.

Deposit type	Deposit	Discovered	Aero-magnetics, ground magnetics	Gravity	Radiometrics	Drilling	Mapping, rock geochemistry, digital elevation model	Stream-sediment geochemistry
Carbonatite-associated	Mount Weld, WA	~1967	M; D	M		M	M	
	Ponton Creek, WA	1986	M		M	M; D	m	
	Cummins Range, WA	1978	M; D			M	m	
	Yangibana, WA	1986–1988				M; D	M	
Heavy-mineral sands:								
(1) Beach	Murray Basin; Eucla Basin	Initially late 1970s, but main deposits 1995 onwards	M			M, D	M	
(2) Offshore shallow marine	WIM 150	1984	M			M, D	M	
(3) Channel	Calypso		M			M, D	M	
Phosphorite	Korella	2011				M, D	M	
Lignite	Mulga Rock	1979 (U) 2005 (REE)			?M	M, D	M	
Ultramafic-mafic rock-associated	Greenvale (Lucknow) Qld	1957 (Ni-Co) 2009 (Sc)				M	M; D	
	Gilgai, NSW		M			M	M; D	
	Thuddungra, NSW		M; D			M	M; D	
Unconformity-related	Killi Killi Hills, WA	1969 (REE)			M; ?D	M	M	
(Per)alkaline rocks	Brockman, WA	1973			M; D	M	M	M; D
Pegmatite	Cooglegong, WA	~1913					M; ?D	?m
Skarn	Mary Kathleen, Qld	1954			M	M	M; D	
Fluorapatite veins	Nolans Bore, NT	1995			M; D	M	M; D	

M = Major application; m = Minor application; D = Discovery method.

5.3. NEW PRODUCTS FROM GEOSCIENCE AUSTRALIA: POTENTIAL APPLICATIONS FOR RARE-EARTH-ELEMENT EXPLORATION IN AUSTRALIA

5.3.1. Radiometric map of Australia

The **'Radiometric Map of Australia'** dataset comprises levelled and merged composite grids of potassium (K), uranium (U), and thorium (Th). The 2nd edition (August, 2010) National radiometric map described at the www link below displays a ternary image of the three radioelements K–red, U–blue, and Th–green (Fig. 5.3). The map shows the surface concentrations of K, U, and Th across the continent. Areas low in all three radioelements appear as dark hues (e.g., ultramafic and mafic igneous rocks: dunite, gabbro, basalt; sedimentary rocks: sandstone, quartzite; and quartz-rich soils) and areas high in all three radioelements appear as white hues (felsic igneous rocks: rhyolite, granite, trachyte, carbonatite).

Applications to rare-earth-element exploration

The National radiometric map datasets are relevant to REE exploration as many of the minerals that host REE also contain uranium and thorium with exposed source rocks having positive radiometric signatures. Airborne radiometric data only records gamma-rays emanating from only the upper 30 centimetres of the Earth's surface. Thus in areas of thick surficial cover the radiometric method will not reveal a K-U-Th-bearing source or REE-bearing rocks at depth. The radiometric data potentially have direct major applications in defining outcropping and sub-outcropping REE-bearing felsic and alkaline igneous rocks and their weathering products, such as potentially mineralised laterites above carbonatite bodies. Several alkaline complexes in Canada have been mapped by positive radiometric anomalies (Richardson and Birkett,

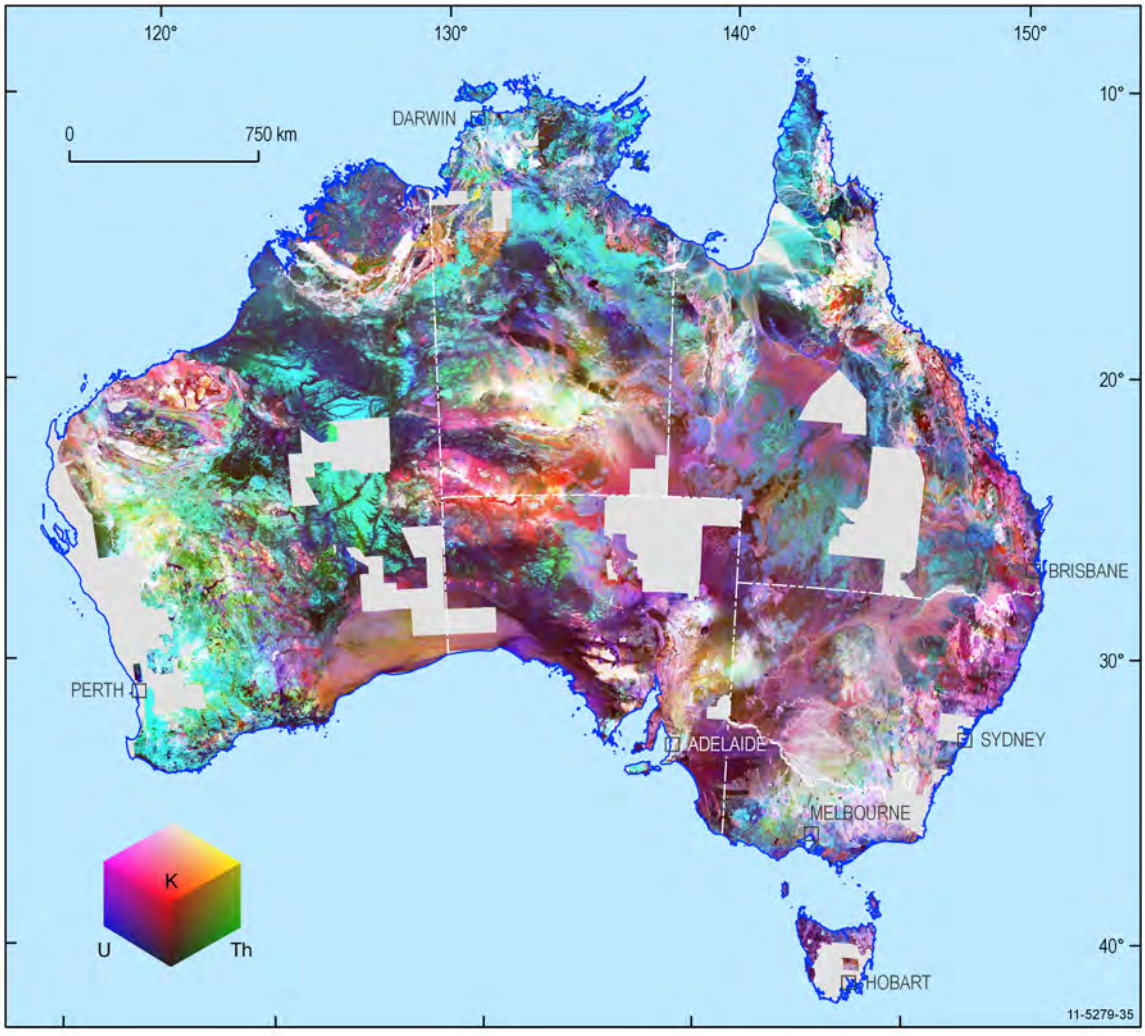

Figure 5.3. Radiometric image of Australia showing composite uranium (U), potassium (K), and thorium (Th) channels.

1995c). Similarly, heavy-mineral sands which are also commonly enriched in thorium and uranium can be mapped by radiometric surveys. The main utility of the radiometric datasets is that consistent and coherent regional compilations over large areas can now be made where previously these analyses would have been restricted to separate surveys.

Useful www links

Radiometric Map of Australia:
https://www.ga.gov.au/products/servlet/controller?event=GEOCAT_DETAILS&catno=70791

Overview and Movie describing how the 'Radiometric Map of Australia' was made and its applications:
http://www.ga.gov.au/energy/projects/awags.html

World Wind 3D Data Viewer:
http://www.ga.gov.au/products-services/maps/interactive-3d-models/world-wind-3d-data-viewer.html

Digital Data from the Geophysical Archive Data Delivery System–GADDS):
http://www.geoscience.gov.au/gadds

AusGeo News article (March 2009, Number 93, 29–31) describing the release of the First Edition of the 'Radiometric Map of Australia' in February 2009:
http://www.ga.gov.au/ausgeonews/ausgeonews200903/productnews.jsp#product1

AusGeo News article (September 2010, Number 99, 23–24) describing the release of updated datasets for the 'Radiometric Map of Australia' in July 2010:
http://www.ga.gov.au/ausgeonews/ausgeonews201009/productnews.jsp#product3

Contacts:

Brian Minty: Brian.Minty@ga.gov.au; 02 6249 9228
Murray Richardson: Murray.Richardson@ga.gov.au; 02 6249 9229

5.3.2. Gravity 'worms' map of Australia

The Earth consists of many rock types which have different physical characteristics, one of which is density. Earth's mass creates a gravity field which attracts everything to the Earth. However, this gravity field is not uniform, with denser rocks producing a stronger gravity field and less dense rocks producing a weaker gravity field. These differences are very small but can be measured using a very precise and sensitive instrument called a gravimeter. The ability to measure small changes in gravity due to changes in the density of rocks provides a method to remotely map the distribution of different rock types and the structure of the rocks, from near surface to deep within the Earth. Geoscience Australia maintains the Australian National Gravity Database, which contains data from gravity surveys conducted throughout the Australian region, and sourced from within Geoscience Australia, State and Territory governments, exploration companies, universities, and overseas organisations. These data are used to make images of the gravity variations across the region.

Applications to rare-earth-element exploration

Of particular importance to regional mineral exploration are regions where the gravity displays rapid changes, or gradients (Fig. 5.4). These gradients can be mapped as lines or 'worms', which provide useful information about the boundaries between different rock types, particularly fault zones, and the depths at which they occur (Milligan et al., 2003). This information may be used for the delineation of fluid pathways and structural traps that are important for the formation of such mineral deposits as structurally controlled hydrothermal REE ± U deposits. In addition, deep crustal (lithospheric?) structures appear to control the distribution of carbonatites and other alkaline intrusions in many geological provinces of Australia (Jaques, 2008; Fig. 5.4). Gravity 'worm' datasets can therefore facilitate the recognition of major crustal structures and potential REE-bearing alkaline igneous complexes, including those under shallow cover.

As carbonate minerals, which constitute more than 50 to 60% of carbonatite complexes, have relatively higher densities than quartz and feldspar it is possible that carbonatites in some regions may have positive gravity anomalies. However, the gravity signature would be dependent on the composition of the country rocks. In relatively denser greenstone sequences, carbonatites may not be traceable by gravity.

Useful www links and references

An example of the utility of 'worms' for analysis of diamondiferous alkaline intrusions in Australia can be found in Jaques and Milligan (2004). Further information can also be accessed at:

http://www.ga.gov.au/minerals/mineral-resources/diamonds.html

http://www.ga.gov.au/minerals/disciplines/geophysics/gravity.html

- Jaques A.L., 2008. Australian carbonatites: their resources and geodynamic setting. 9th International Kimberlite Conference, Extended Abstracts, 91KC–A–00347 (with poster produced by Geoscience Australia, Canberra).
- Jaques, A.L. and Milligan, P.R., 2004. Patterns and

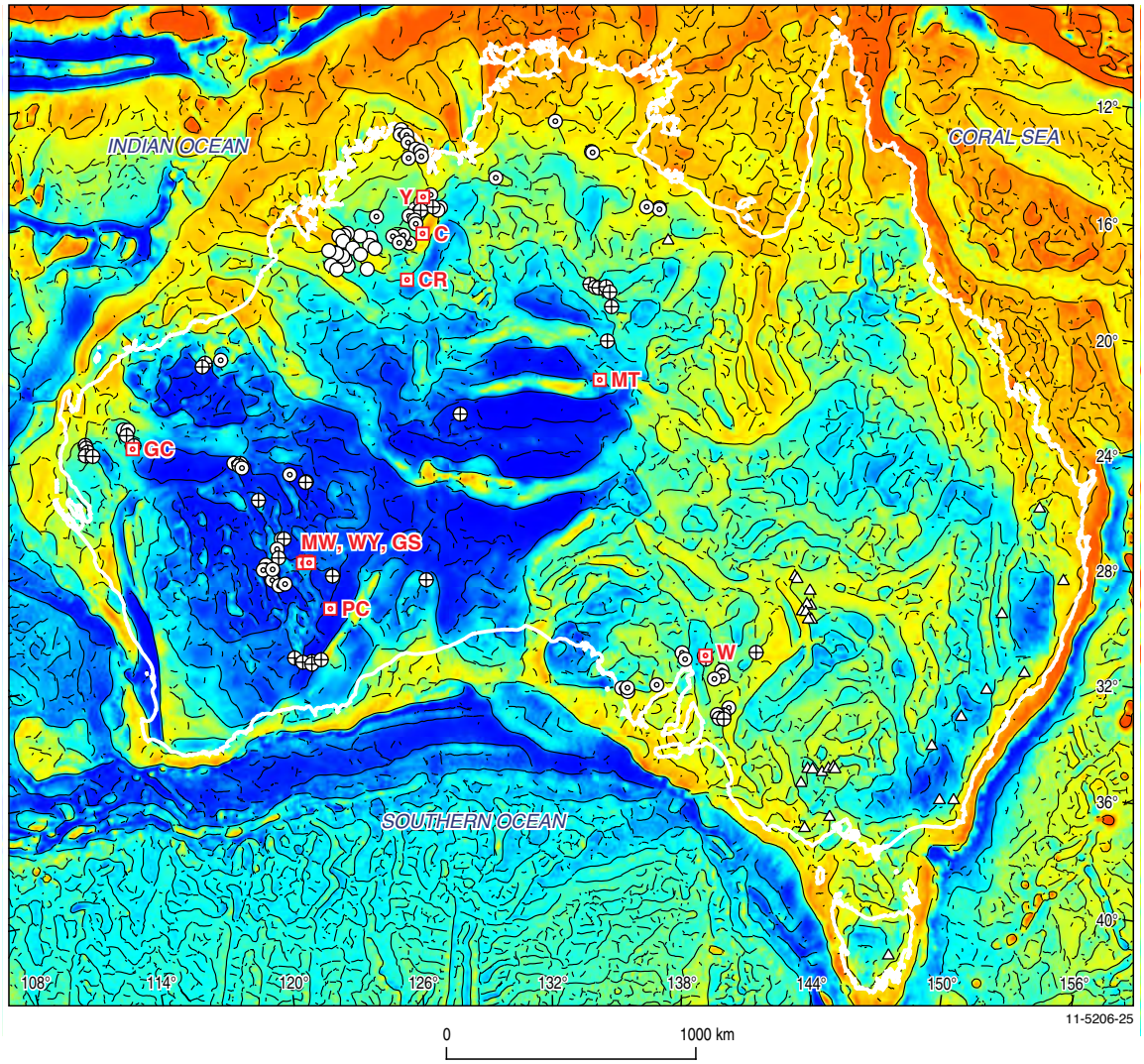

Figure 5.4. Distribution of carbonatites, kimberlites, lamprophyres, and other alkaline igneous rocks on a Bouguer gravity anomaly 'worms' image of Australia. This image shows locations of horizontal gradient maxima of the gridded data upward continued to 20 km plotted as dots. The horizontal gradients define domains and structures within the Bouguer gravity anomaly data. Carbonatites shown are: Copperhead (**C**), Cummins Range (**CR**), Gifford Creek (**GC**), Granny Smith (**GS**), Mud Tank (**MT**), Mount Weld (**MW**), Ponton Creek (**PC**), Wallaby (**WY**), Walloway (**W**), and Yungul (**Y**). From Jaques (2008).

controls on the distribution of diamondiferous intrusions in Australia. Lithos, 77, 783–802.

- Milligan, P.R., Lyons, P. and Direen, N., 2003. Spatial and directional analysis of potential field gradients—new methods to help solve and display three-dimensional crustal architecture. Extended Abstracts. ASEG 16th Geophysical Conference and Exhibition, February 2003, Adelaide.

Contact

Peter Milligan: Peter.Milligan@ga.gov.au; 02 6249 9224

5.3.3. Magnetic anomaly map of Australia

The **'Magnetic Anomaly Map of Australia'** (5th Edition, 1:5 million scale, 2010) was compiled from Total Magnetic Intensity survey data held in the National Airborne Geophysical Database by GA (Fig. 5.5). The image is a composite of data acquired from surveys flown by GA and surveys flown under contract to GA, the State and Territory geological surveys in either separate or joint projects and the private sector. The data from these surveys were acquired at a range of line spacings, flying heights, and measurement accuracies. 795 individual survey grids were matched and merged into the composite grid used to produce the image and it is estimated that 27 million line-kilometres of survey data were acquired to produce the grid data. The image was generated from the natural colour palette (magenta high, blue low).

Applications to rare-earth-element exploration

Aeromagnetics have been instrumental in delineating REE deposits that are associated with carbonatite and alkaline igneous rocks. Aeromagnetics are particularly useful as a regional tool for identifying those alkaline complexes that have deeply weathered profiles and occur under shallow cover. The world-class Mount Weld deposit in the eastern Yilgarn Craton and Cummins Range Carbonatite in the Halls Creek Orogen were both discovered during regional aeromagnetic surveys. High-amplitude circular magnetic anomalies reflect the steeply plunging cylindrical forms of the carbonatite bodies. The Mount Weld Carbonatite was found during a regional aeromagnetic survey carried out by the Bureau of Mineral Resources in 1966 (see inset A in Fig. 5.5). Magnetite at Mount Weld occurs as a minor primary igneous phase in the supergene zone of the laterite where it oxidises to maghemite, hematite, and ultimately goethite (Lottermoser, 1990). The Cummins Range body was found during the drilling of a 4900 nT aeromagnetic anomaly that extends over ~1.8 km. Ground surveys in 1978 located coarse-grained magnetite and exfoliating mica at the surface (Andrew, 1990).

The aeromagnetic data can be useful to map alkaline rocks. Many alkaline complexes in Canada are characterised by negative aeromagnetic and positive radiometric anomalies (Richardson and Birkett, 1995c).

Useful www links and references

Download map (A0 size: pdf and jpg formats)
https://www.ga.gov.au/image_cache/GA18004.pdf
https://www.ga.gov.au/image_cache/GA18005.jpg

Download map (A3 size: pdf and jpg formats)
http://www.ga.gov.au/image_cache/GA18012.pdf
http://www.ga.gov.au/image_cache/GA18013.jpg

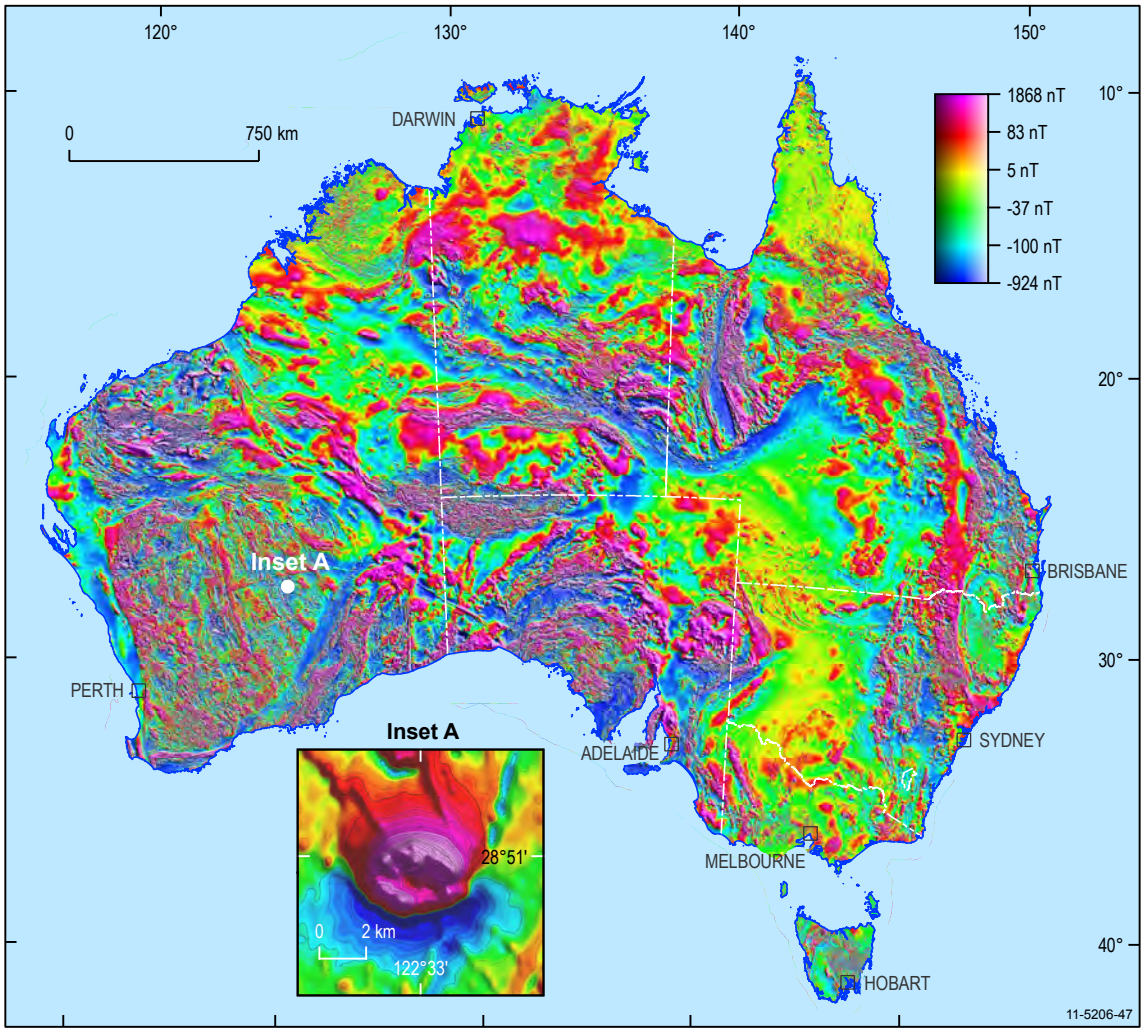

Figure 5.5. Magnetic anomaly image of Australia. The inset shows the total magnetic intensity anomaly over the Mount Weld Caronatite, Western Australia. Width of view is about 10 kilometres.

Digital Data from the Geophysical Archive Data Delivery System–GADDS):
http://www.geoscience.gov.au/gadds

World Wind 3D Data Viewer:
http://www.ga.gov.au/products-services/maps/interactive-3d-models/world-wind-3d-data-viewer.html

Milligan, P.R., Franklin, R., Minty, B.R.S., Richardson, M. and Percival, P.J., 2010. Magnetic Anomaly Map of Australia (Fifth Edition), 1:5 000 000 scale, Geoscience Australia, Canberra.

Milligan, P.R., Minty, B.R.S., Richardson, M. and Franklin, R., 2009. The Australia-wide Airborne Geophysical Survey-accurate continental magnetic coverage. Preview, 138, 70.

Minty, B.R.S., Milligan, P.R., Luyendyk, T. and Mackey, T., 2003. Merging airborne magnetic surveys into continental-scale compilations. Geophysics, 63, 1986–1996.

Contacts

Peter Milligan: Peter.Milligan@ga.gov.au; 02 6249 9224
Murray Richardson: Murray.Richardson@ga.gov.au; 02 6249 9229

5.3.4. Surface geology of Australia

The **'Surface Geology of Australia'** (1:1 million scale) dataset is the most detailed seamless national geological map of Australia (Fig. 5.6). The digital map dataset depicts rock materials and geological structures at or near the Earth's surface. It was compiled by standardising and joining over 400 individual detailed geological maps produced over 50 years of geological mapping in Australia. The dataset shows the age and compositions of bedrock units, and the character of surficial materials, such as sand dunes or river sediments, which may cover the underlying bedrock.

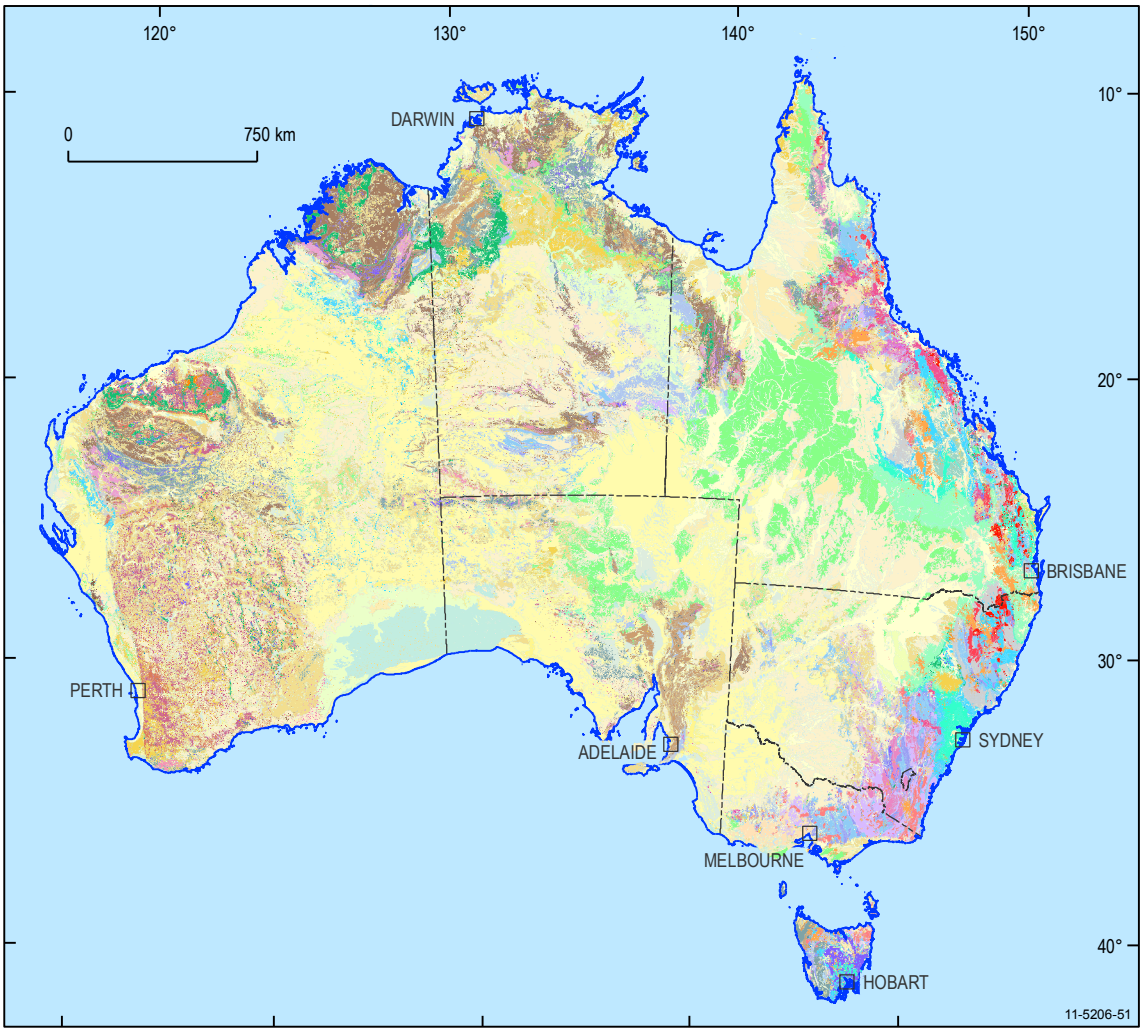

Figure 5.6. Surface geology image of Australia.

Applications to rare-earth-element exploration

By analysing the dataset using Geographical Information Systems (GIS) software, scientists can quickly identify areas underlain by a particular age or composition of bedrock across the whole of the continent. For instance, explorers looking for REE can highlight igneous rocks of alkaline composition and further refine their search for rock units of a particular age as well; for instance 'Mesozoic' igneous rocks, which are known to contain REE. By combining other geological, geophysical, and geochemical datasets with the national geological map in a GIS, explorers can perform intelligent analysis to identify areas prospective for REE prior to exploration fieldwork.

Useful www links

National Geological Maps and Standards Project and Surface Geology of Australia map:
http://www.ga.gov.au/minerals/projects/current-projects/geological-maps-standards.html

View, query, and download the national digital geology dataset on the GA website:
http://www.ga.gov.au/mapconnect/

AusGeo News article (March 2009, Number 93, 11–13) describing the release of the First Edition dataset in 2008:
http://www.ga.gov.au/image_cache/GA13583.pdf

Contact

Oliver Raymond: Oliver.Raymond@ga.gov.au;
02 6249 9575

5.3.5. National geochemical survey of Australia

The **'National Geochemical Survey of Australia'** (NGSA) aims to provide pre-competitive data and knowledge to support exploration for energy resources in Australia. In particular, it will improve the existing knowledge of the concentrations and distributions of energy-related elements such as uranium and thorium at the national scale (Fig. 5.7). In addition, NGSA will provide data and knowledge to support exploration for other mineral commodities and also natural resources management. The project is based on the chemical analysis of transported regolith samples collected at 1315 sites in 1186 large catchments covering nearly all the continent. Samples from the surface and a deeper sediment layer were collected, and both samples were sieved to a coarse- and a fine-grain size fraction. Chemical analyses will yield data relating to the total element content, as well as aqua regia soluble and Mobile Metal Ion concentrations. This information will help understand processes including the formation of chemical footprints in cover material over ore deposits and their preservation potential through time.

Applications to rare-earth-element exploration

The NGSA geochemical dataset includes all 15 lanthanide elements in addition to scandium and yttrium. This dataset and associated maps are relevant to REE exploration as they directly show where elevated concentrations of these elements can be found on the continent. In addition, the concentrations and distributions of uranium and thorium are also relevant as many of REE-hosting minerals also contain elevated uranium and thorium. As REE-hosting minerals tend to be fairly resistant to weathering, they are likely to be transported down the catchments and to be present in the sampled sediment, giving a direct indication of areas with higher prospectivity. A favourable characteristic of the NGSA data is that it is internally consistent because it targeted the same sampling material across Australia, which was prepared and analysed in the same laboratories following the same protocols.

Most REE deposits and associated alkaline, carbonatitic and felsic rocks form geochemical halos of LREE, Ba, Sr, Ti, Zr, Th, U, Be, F, P, Nb, and Ta. Geochemical surveys of overbank sediments in catchments can be used to identify prospective catchments. A low-density (1 sample/30 km^2) with multi-element analysis in combination with conductivity measurements of stream water was able to delineate several carbonatites in western Greenland (Richardson and Birkett, 1995a,b).

Useful www links

National Geochemical Survey of Australia Project:
http://www.ga.gov.au/ngsa

Maps and dataset 'Preliminary Soil pH Map of Australia':
https://www.ga.gov.au/products/servlet/controller?event=GEOCAT_DETAILS&catno=70105

GA Record 'National Geochemical Survey of Australia: Sample Preparation Manual':
https://www.ga.gov.au/products/servlet/controller?event=GEOCAT_DETAILS&catno=68657

GA Record 'National Geochemical Survey of Australia: Analytical Methods Manual':
https://www.ga.gov.au/products/servlet/controller?event=GEOCAT_DETAILS&catno=70369

Explore article (December 2008, Number 141, 1–11), 'New national geoscience datasets in Australia: geology, geophysics and geochemistry', The Association of Applied Geochemists:
https://www.ga.gov.au/products/servlet/controller?event=GEOCAT_DETAILS&catno=71112

Contact

Patrice de Caritat: Patrice.deCaritat@ga.gov.au;
02 6249 9378

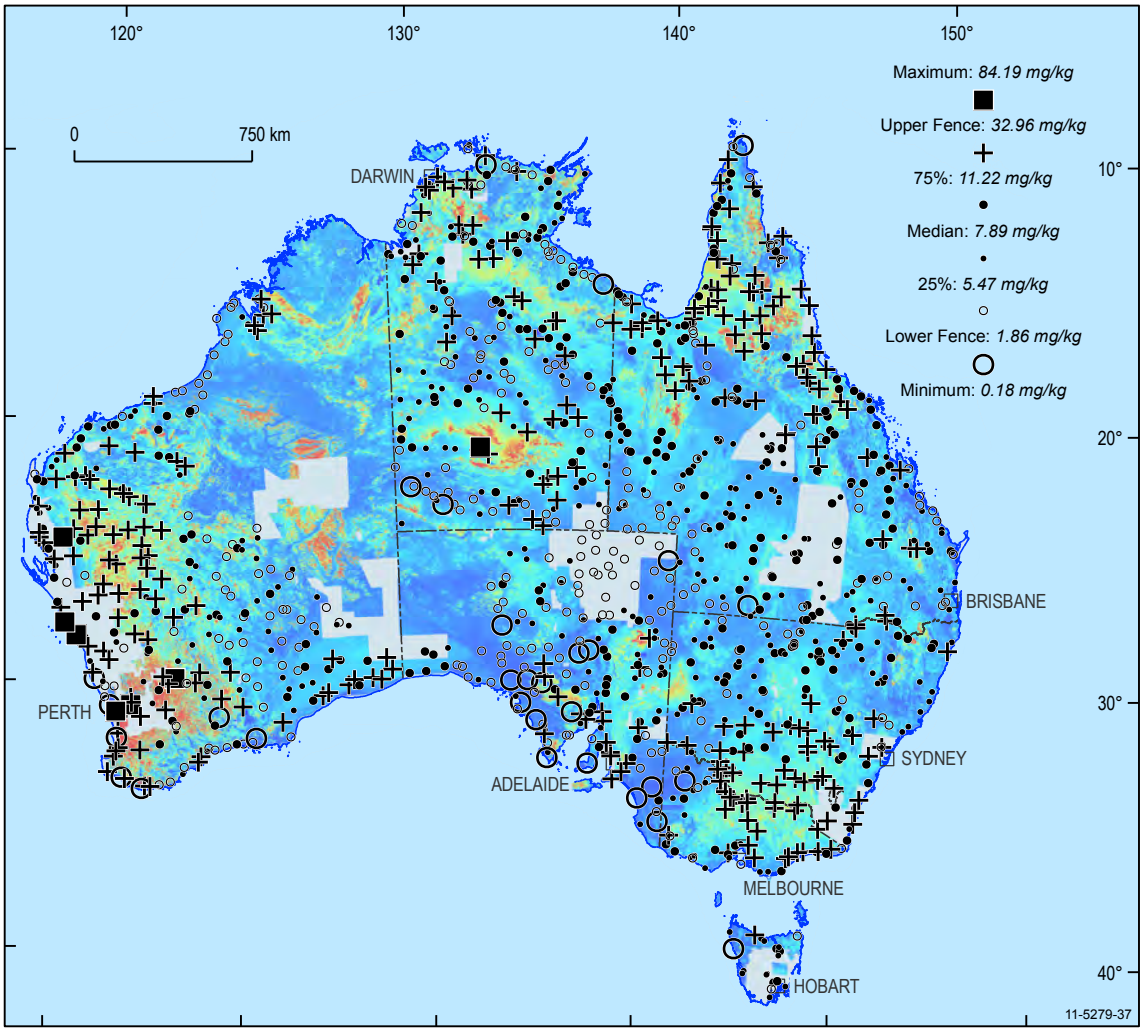

Figure 5.7. National geochemical image shows the distribution and concentration of thorium from surface samples collected by hand auger. Background layer is the airborne radiometrics thorium channel.

5.3.6. Australia's diamond deposits, kimberlite, and related-rocks map

The **'Australia's Diamond Deposits, Kimberlites and Related-Rocks'** map (April 2008) shows the distribution of kimberlites, lamproites, lamprophyres, carbonatites, and other alkaline rocks of deeper mantle origin by age in relation to continental structure as shown by the total magnetic intensity image of Australia. The map shows that these alkaline rocks are commonly clustered in fields or provinces at or near major crustal (and lithospheric) boundaries. The relationship between carbonatites and other mantle-derived rocks is examined in more detail by Jaques (2008) and for potentially diamond-bearing rocks by Jaques and Milligan (2004), who showed that kimberlites, lamproites and lamprophyres were commonly aligned either singly or in clusters, along or near discontinuities and/or gradients evident in regional- scale potential field data, especially the total horizontal gradients of gravity data continued upward tens to hundreds of kilometres.

Applications to rare-earth-element exploration

A compilation and review of the alkaline rocks of Australia (Jaques et al., 1985) showed that occurrences of alkaline rocks were sparsely distributed and of limited extent and, with the exception of the Cenozoic alkali basalts of the Tasman Orogen of Eastern Australia, are volumetrically insignificant compared with the volume of subalkaline rocks observed in each province. The alkaline rocks range in age from late Archean to Holocene. Where reliable isotopic dates are available the intrusive ages mostly appear to be broadly synchronous with, or closely postdate ages of, cratonisation for each of the provinces. The emplacement of many of the pre-Cenozoic rocks, particularly the mafic-ultramafic suites, appears to be influenced by, and in some cases clearly controlled by, initiation or reactivation of deep-crustal fractures. The distribution of many of the Cenozoic, and more recently some of the Mesozoic igneous rocks of eastern Australia has been ascribed to northward movement of the Australian continent over hot-spots, and is associated with regional uplift. The alkaline rocks of Australia include carbonatites and a spectrum of silicate rocks belonging to one of three series: an ultra-potassic ($K_2O/Na_2O > 3$) series of dominantly ultramafic to mafic rocks, which include kimberlite, lamprophyre, and lamproite (some of which are diamondiferous); a series of potassic ($K_2O/Na_2O = 1–3$), dominantly mafic to intermediate rocks (shoshonite association), including monzonite, latite, and lamprophyre; a sodic series ($Na_2O > K_2O$) of dominantly alkali basalt composition, but ranging from mafic (e.g., olivine nephelinite) to more fractionated felsic compositions, such as syenite, phonolite, and trachyte. The more fractionated felsic alkaline igneous rocks are commonly enriched in REE and other incompatible elements, such as Zr, Hf, Nb, and Ta.

Useful www link and reference

Download map:
https://www.ga.gov.au/products/servlet/controller?event=GEOCAT_DETAILS&catno=68455

Jaques A.L., Creaser R.A., Ferguson J. and Smith C.B., 1985. A review of the alkaline rocks of Australia. *Transactions of the Geological Society of South Africa,* 88, 311–334.

Contact

Keith Porritt: Keith.Porritt@ga.gov.au; 02 6249 9479

5.3.7. Felsic and intermediate igneous rocks of Australia project

The **'Felsic and Intermediate Igneous Rocks of Australia Project'** investigated the link between specific granite characteristics, such as oxidation state, degree of evolution, and tectonic setting, and granite-related metallogenesis. It was chiefly aimed at using syntheses of publicly available data sets to assess the metallogenic potential of Paleozoic and early Mesozoic granites in the Tasmanides of eastern Australia. A significant proportion of the mineral endowment of eastern Australia is associated with Phanerozoic granites and considerable scientific research and data gathering over the past 15 years has been focused on these magmatic systems. Much of this data is in the public domain, e.g., datasets such as Geoscience Australia's OZCHEM geochemical data, and the seamless Surface Geology of Australia. Improved usage of such datasets are considered as key ingredients for the better definition and targeting of potential granite-related mineralisation in brownfield and greenfield areas of eastern Australia, particularly when combined with regional geophysical and mineralisation data.

Useful www links

Felsic and Intermediate Igneous Rocks of Australia Project:
http://www.ga.gov.au/minerals/projects/concluded-projects/felsic-igneous-rocks.html
http://www.ga.gov.au/minerals/projects/concluded-projects/phanerozoic.html

GA Record 2010/20—Potential for magmatic-related uranium mineral systems in Australia, by A. Schofield:
http://www.ga.gov.au/image_cache/GA19084.pdf

OZCHEM:
https://www.ga.gov.au/products/servlet/controller?event=GEOCAT_DETAILS&catno=65464

Surface geology of Australia:
http://www.ga.gov.au/minerals/projects/current-projects/geological-maps-standards.html

Applications to rare-earth-element exploration

Skarn-related REE mineralisation hosted by calc-silicate rocks is formed from fluids derived from predominantly felsic magmas, which also form the granite complexes that intrude the calcareous rocks. The characterisation of Paleozoic and early Mesozoic granitic rocks in eastern Australia may have implications for REE-bearing skarn-type deposits similar to the Proterozoic granite-associated skarn deposits in the Mary Kathleen region of Queensland and the Olary and Mount Painter districts of South Australia. Other high-grade REE deposits in the USA occur in breccia pipes related to granites (Walters et al., 2010) and in pegmatite dykes. Schofield (2010) discusses the potential for magmatic-related uranium (and briefly REE) mineral systems in Australia. There is also a potential role for placer styles of REE mineralisation, such as beach sands. It is evident that REE-bearing accessory minerals, such as monazite, are often restricted to certain compositions of granite (e.g., S-type: Chappell and White, 1974). Areas of such granites, which occur in the New England and northeastern Queensland regions, may therefore be favourable source regions for such deposits.

Contact

David Champion: David.Champion@ga.gov.au; 02 6249 9215

5.3.8. Airborne electromagnetics

Airborne Electromagnetics (AEM) is applied world-wide in the search for minerals including REE in conjunction with other airborne and ground-based geophysical methods, such as magnetics and gravity, where the unique electrical, magnetic, and density properties of the materials, and the contrasts between them, may point towards potential mineralisation.

Geoscience Australia has flown three regional-scale AEM surveys in the highly prospective Paterson (WA), Pine Creek (NT), and Frome (SA) regions at line spacings ranging from 6 km to 200 m. The survey results are freely available to the public as geolocated images, digital data, and reports (see list below).

Applications to rare-earth-element exploration

At present, the AEM method is being used for REE exploration in North America, particularly in Canada and Alaska, and has been applied extensively in Australia, for uranium, where it may occur in association with REE. The AEM method is especially suitable for detecting the presence of near-surface (typically 200–800 m depth) environments where particular styles of REE mineralisation (mineral systems) may occur.

Useful www links and references

The Geoscience Australia AEM data sets may be downloaded free of charge at:
http://www.ga.gov.au/energy/projects/airborne-electromagnetics.html

A number of reports have been written about Geoscience Australia's AEM program, including:

- Costelloe, M.T., Whitaker, A., Brodie, R., Fisher, A. and Sorensen, C., 2007. Paterson airborne electromagnetic survey, onshore energy and minerals, Geoscience Australia. *In:* ASEG Extended Abstracts, http://www.publish.csiro.au/?act=view_file&file_id=ASEG2007ab183.pdf
- Costelloe, M.T. and Brodie, R.C., 2011. Kombolgie AEM survey images to 2 km. Preview, February 2011, 150, 29–32.
- Costelloe, M.T., Brodie, R. and Maher, J., 2011. Onshore Energy Security Program update—Kombolgie airborne electromagnetic survey goes deeper. AusGeo News 101, 22–23.
- Costelloe, M.T., Roach, I.C. and Hutchinson, D.K., 2010. Paterson AEM survey directly detects major unconformity near Kintyre, WA. Preview, April 2010, 145, 40–41.
- Craig, M.A., Costelloe, M.T., Liu, S.F., Whitaker, A.J., Hutchinson, D.K. and Roach, I.C., 2010. Data acquisition, processing, interpretation and data delivery from the Pine Creek airborne electromagnetic survey, Northern Territory. *In:* Australian Earth Sciences Convention, Canberra, Geological Society of Australia, 377–378.
- English, P.M., Nyquest, D., Kozikowski, M., Roach, I.C., Liu, S.F., Hutchinson, D.K., Costelloe, M.T., Whitaker, A.J., Brodie, R.C. and Williams, N., 2010. Application of airborne electromagnetic (AEM) data for mapping buried palaeovalleys in the Great Sandy Desert, Western Australia. *In:* Groundwater 2010, Canberra, International Association of Hydrogeologists and Geological Society of Australia, 4 pp.
- Hutchinson, D. K., Roach, I. C. and Costelloe, M. T., 2010. AEM Go-Map for the Paterson Region, WA and Pine Creek, NT. *In:* ASEG Conference, Sydney, Extended Abstracts, http://www.publish.csiro.au/?act=view_file&file_id=ASEG2010ab071.pdf

- Hutchinson, D.K., Roach, I.C. and Costelloe, M.T., 2010. Depth of Investigation Grid for Regional Airborne Electromagnetic Surveys. Preview, April 2010, 145, 38–39.
- Roach, I.C., 2009. A drill hole database for the Paterson airborne electromagnetic (AEM) survey, Western Australia. Geoscience Australia, Canberra. Record 2009/31, 16 pp.
- Roach, I.C. (editor), 2010. Geological and energy implications of the Paterson Province airborne electromagnetic (AEM) survey, Western Australia. Geoscience Australia Record 2010/12, 318 pp.
- Roach, I.C., Whitaker, A.J., Costelloe, M.T., Hutchinson, D.K., Liu, S.F. and Craig, M., 2010. The Paterson AEM Survey, Western Australia: Enhancing prospectivity using regional AEM data to image Paleozoic–Mesozoic palaeotopography. *In:* Australian Earth Sciences Convention, Canberra, Geological Society of Australia, 229–240.
- Sorensen, C., Fisher, A. and Costelloe, M.T, 2009. Airborne electromagnetic survey results from the Paterson Province, WA. *In:* ASEG Extended Abstracts, http://www.publish.csiro.au/paper/ASEG2009ab069.htm
- Stolz, E., 2010. Onshore Energy Security Program maintains momentum: Delivering data and improved scientific understanding. AusGeo News 97, 5–14.

Contacts

Ian Roach: Ian.Roach@ga.gov.au; 02 6249 9683
Marina Costelloe: Marina.Costelloe@ga.gov.au; 02 6249 9347

REFERENCES

Agangi, A., Kamenetsky, V.S. and McPhie, J., 2010. The role of fluorine in the concentration and transport of lithophile trace elements in felsic magmas; insights from the Gawler Range Volcanics, South Australia. Chemical Geology, 273, 314–325.

Alkane Resources Limited, 2007. Dubbo Zirconia Project, New South Wales Mineral Exploration and Investment Conference, Sydney, 24 August 2007, 36 pp, (http://www.alkane.com.au/presentations/pdf/20070824.pdf).

Alkane Resources Limited, 2011. Dubbo Zirconia Project, New South Wales, Presentation, 30 pp, (http://www.alkane.com.au/presentations/pdf/20110412.pdf).

Altschuler, Z.S., Berman, S. and Cuttitta, F., 1967. Rare earths in phosphorites—geochemistry and potential recovery. *In:* Geological Survey Research 1967. Chapter B. Geological Survey Professional Paper 575–B, B1–B9.

Alvin, M.P., Dunphy, J.M. and Groves, D.I., 2004. Nature and genesis of a carbonatite-associated fluorite deposit at Speewah, East Kimberley region, Western Australia. Mineralogy and Petrology, 80, 127–153.

Andrew, R.L., 1990. Cummins Range Carbonatite. *In:* Hughes, F.E. (editor), Geology of mineral deposits of Australia and Papua New Guinea. Australasian Institute of Mining & Metallurgy, Melbourne, Monograph 14, 711–713.

Arafura Resources Limited, 2007. Investor briefing Mining 2007 Resources Conference, 1 November 2007, Brisbane, 27 pp, (http://www.arafuraresources.com.au/documents/ArafuraMining2007presentation_ASX_release.pdf).

Arnold, G.O. and Rubenach, M.J., 1976. Mafic-ultramafic complexes of the Greenvale area, north Queensland: Devonian intrusions or Precambrian metamorphics? Australian Journal of Earth Sciences, 23, 119–139.

Astron Limited, 2010. ASX Release 27 April 2010: Donald mineral sands resource update, 4 pp.

Astron Limited, 2010. ASX Release 27 July 2010: Donald project reserve estimate July 2010, 3 pp.

Atkinson, W.J., Smith, C.B., Danchin, R.V. and Janse, A.J.A., 1990. Diamond deposits of Australia. *In:* Hughes, F.E. (editor), Geology of mineral deposits of Australia and Papua New Guinea. Australasian Institute of Mining & Metallurgy, Melbourne, Monograph 14, 69–76.

Australian Bureau of Statistics, 2009. International trade, Cat. No.5465.0, Australian Bureau of Statistics, Canberra, Australia.

Aztec Resources, 2003. Annual Report 2003, Aztec Resources Limited. Report to the Australian Securities Exchange, 30 September 2003, 45 pp (unpublished).

Bai, T.B. and Koster Van Groos, A.F., 1999. The distribution of Na, K, Rb, Sr, Al, Ge, Cu, W, Mo, La, and Ce between granitic melts and coexisting aqueous fluids. Geochimica et Cosmochimica Acta, 63, 1117–1131.

Bailey, D.K., 1970. Volatile flux, heat-focusing and the generation of magma. Geological Journal (London), Special Issue 2, 177–186.

Bain, J.H.C. and Draper, J.J., 1997. North Queensland Geology. Australian Geological Survey Bulletin 240, and Queensland Department of Mines and Energy Queensland Geology 9, 600 pp.

Bamborough, I., 2011. Quantum step in discovery: From uranium to rare earths. AGES 2011, Northern Territory Geological Survey Record 2011-003, Annual Geoscience Exploration Seminar, 21–23 March 2011, Alice Springs, Northern Territory, 51.

Banks, D.A., Yardley, B.W.D., Campbell, A.R. and Jarvis, K.E., 1994. REE composition of an aqueous magmatic fluid: a fluid inclusion study from the Capitan Pluton, New Mexico, USA. Chemical Geology, 113, 259–272.

Barnes, R., Jaireth, S., Miezitis, Y. and Suppel, D., 1999. Regional mineral potential assessments for land use planning; GIS-based examples from eastern Australia: Publication Series. Australasian Institute of Mining and Metallurgy, 4-99, 601–605.

Barnes, S.J., Anderson, A.C. and Smith, T.R., 2008. The Mordor alkaline igneous complex, Central Australia: PGE-enriched disseminated sulfide layers in cumulates from a lamprophyric magma. Mineralium Deposita, 43, 641–662.

Barrie, J., 1965. Rare Earths, *In:* McLeod, I.R. (editor), Australian Mineral Industry: The Mineral Deposits. Bureau of Mineral Resources, Australia, Bulletin 72, 515–521.

Bastrakov, E.N., Skirrow, R.G. and Davidson, G.J., 2007. Fluid evolution and origins of iron oxide Cu-Au prospects in the Olympic Dam district, Gawler Craton, South Australia. Economic Geology, 102, 1415–1440.

Bau, M., 1991. Rare-earth element mobility during hydrothermal and metamorphic fluid-rock interaction and the significance of the oxidation state of europium. Chemical Geology, 93, 219–230.

Baxter, J.L., 1977. Heavy mineral sand deposits of Western Australia. Geological Survey of Western Australia. Mineral Resources Bulletin 10, 148 pp.

Belperio, A.P., 1999. Geographic and tectonic controls on heavy mineral sand exploration targets in the Murray Basin. *In:* Stuart, R. (editor), Murray Basin Mineral Sands Conference. Extended Abstracts, 15–20.

Bennett, V.C., Heinrich, D.H. and Karl, K.T., 2003. Compositional Evolution of the Mantle, Treatise on Geochemistry, Oxford, Pergamon, 493–519.

Berger, V.I., Singer, D.A. and Orris, G.J., 2009. Carbonatites of the world; explored deposits of Nb and REE—databases and grade and tonnage models. United States Geological Survey Scientific Investigations Open-File Report 2009–1139, 17 pp.

Bierlein, F.P., Black, L.P., Hergt, J. and Mark, G., 2008. Evolution of pre-1.8 Ga basement rocks in the western Mt Isa Inlier, northeastern Australia; insights from SHRIMP U/Pb dating and in situ Lu-Hf analysis of zircons. Precambrian Research, 163, 159–173.

Black, L.P. and Gulson, B.L., 1978. The age of the Mud Tank carbonatite, Strangways Range, Northern Territory. Bureau of Mineral Resources, Australia, Journal of Australian Geology and Geophysics 3, 227–232.

Black, L.P., Bell, T.H., Rubenach, M.J. and Withnall, I.W., 1979. Geochronology of discrete structural–metamorphic events in a multiply deformed Precambrian terrain. Tectonophysics, 54, 103–137.

Blake, D.H., Hodgson, I.M. and Muhling, P.C., 1979. Geology of The Granites–Tanami region. Bureau of Mineral Resources, Australia, Bulletin 197, 91 pp.

Blake, D.H., Tyler, I.M., Griffin, T.J., Sheppard, S., Thorne, A.M. and Warren, R.G., 1999. Geology of the Halls Creek 1:100 000 Sheet area (4461), Western Australia. Australian Geological Survey Organisation, Canberra, 36 pp.

Bozau, E., Gottlicher, J. and Stark, H., 2008. Rare earth element fractionation during the precipitation and crystallisation of hydrous ferric oxides from anoxic lake water. Applied Geochemistry, 23, 3473–3486.

Bradshaw, M.T., Bradshaw, J., Weeden, R.J., Carter, P. and de Vries, D.F.H., 1998. Assessment - translating the future into numbers. APPEA Journal, 38, 528–551.

Braun, J.-J., Pagel, M., Herbillon, A. and Rosin, C., 1993. Mobilization and redistribution of REE and thorium in a syenitic lateritic profile; a mass balance study. Geochimica et Cosmochimica Acta, 57, 4419–4434.

Brookins, D.G., 1988. Eh-pH diagrams for geochemistry. Berlin, Springer-Verlag, 176 pp.

Brookins, D.G., 1989. Aqueous geochemistry of rare earth elements. Reviews in Mineralogy, 21, 201–225.

Brooks, J.H. and Shipway, C.H., 1960. Mica Creek pegmatites, Mount Isa, north-western Queensland. Queensland Government Mining Journal, October 20 1960. Department of Resource Industries, 511–522.

Bunting, J.A., van de Graff, W.J.E. and Jackson, M.J., 1974. Palaeodrainages and Cainozoic palaeogeography of the eastern Goldfields, Gibson Desert and Great Victoria Desert. Geological Survey of Western Australia, Annual Report 1973, 45–50.

Burger, P.A., 1982. The Greenvale lateritic nickel-cobalt deposit. *In:* Withnall, I.W. (editor), 1982 Field Conference Charters Towers–Greenvale area. Geological Society of Australia Incorporated, Queensland Division, Brisbane, 52–66.

Carew, J. and Craven, B., 2010. Mt Barrett and Mt Weld geophysical characteristics. Southern Geoscience Consultants Proprietary Limited Memorandum for DataMotion Asia Pacific Limited, SGC Report 2148, 25 January 2010, 25 pp (unpublished), http://www.datamotion.asia/.

Cassidy, K.F., Towner, R.R. and Ewers, G.R., 1997. Rare earth elements in Australia. Australian Geological Survey Organisation and Bureau of Resources Sciences, Canberra, Australia, Commercial-In-Confidence Report, November 1997, 47 pp.

Castor, S.B., 2008. Rare earth deposits of North America. Resource Geology, 58, 337–347.

Ceplecha, J., 1988. The Corkwood Yard xenotime prospect—EL80/696, East Kimberley, Western Australia, Bulk testing programme, October 1987. Geological Survey of Western Australia, Statutory exploration report, Item 4802 A24813 (unpublished).

Cerny, P., 1991a. Rare-element granitic pegmatites. Part I: anatomy and internal evolution of pegmatite deposits. Geoscience Canada, 18, 49–67.

Cerny, P., 1991b. Rare-element granitic pegmatites. Part II: regional to global environments and petrogenesis. Geoscience Canada, 18, 68–81.

Cetiner, Z.S., Wood, S.A. and Gammons, C.H., 2005. The aqueous geochemistry of the rare earth elements; Part XIV, The solubility of rare earth element phosphates from 23 to 150 degrees Celsius. Chemical Geology, 217, 147–169.

Chalmers, D.I., 1990. Brockman multi-metal and rare earth deposit. *In:* Hughes, F.E. (editor), Geology of the Mineral Deposits of Australia and Papua New Guinea. Australian Institute of Mining and Metallurgy, Monograph 14, 707–709.

Chalmers, I., 1999. Dubbo Zirconia Project. Minfo–New South Wales Mining and Exploration Quarterly, 62, 38–40.

Chappell, J. and Shackleton, N.J., 1986. Oxygen isotopes and sea level. Nature, 324, 3 November 1986, 137–140.

Chappell, B.W. and White, A.J.R., 1974. Two contrasting granite types. Pacific Geology, 8, 173–174.

Chesley, J., Righter, K. and Ruiz, J., 2004. Large-scale mantle metasomatism; a Re/Os perspective. Earth and Planetary Science Letters, 219, 49–60.

Chinalco-China Yunnan Copper Australia Limited, 2011. Further drilling extends rare earth-copper-cobalt discovery at Mount Dorothy, Mary Kathleen Joint Venture with Goldsearch Limited, ASX Release 22 March 2011, 8 pp, (http://www.cycal.com.au/IRM/Company/ShowPage.aspx?CPID=1456&EID=86904122&PageName=Drilling Extends Rare Earth-Copper-Cobalt Discovery).

Christie, T., Brathwaite, B. and Tulloch, A., 1998. Mineral commodities report 17 – rare earths and related elements. New Zealand Institute of Geological and Nuclear Sciences Limited, 13 pp.

Claoué-Long, J.C. and Hoatson, D.M., 2005. Proterozoic mafic-ultramafic intrusions in the Arunta Region, central Australia. Part 2: Event chronology and regional correlations. Precambrian Research, 142, 134–158.

Cook P.J., 1972. Petrology and geochemistry of the phosphate deposits of northwest Queensland, Australia. Economic Geology 67, 1193–1213.

Cooper, W., 1990. Queensland mineral commodity report. Queensland Government Mining Journal, September 1990. Department of Resource Industries, 383–389.

Cordier, D.J., 2011. Rare Earths. *In:* Mineral commodity summaries 2011: Rare Earths. United States Geological Survey, January 2011, 128–129.

Cox, D.P. and Singer, D.A. (editors), 1986. Mineral deposit models: Washington, United States Geological Survey, 379 pp.

Creaser, R.A. and Cooper, J.A., 1993. U-Pb geochronology of middle Proterozoic felsic magmatism surrounding the Olympic Dam Cu-U-Au-Ag and Moonta Cu-Au-Ag deposits, South Australia. Economic Geology, 88, 186–197.

Currie, K.L., Knutson, J. and Temby, P.A., 1992. The Mud Tank carbonatite complex, central Australia—an example of metasomatism at mid-crustal levels. Contributions to Mineralogy and Petrology, 109, 326–339.

Curtis, N., 2011. Rare earths, we touch them everyday. Investor Presentation, March 2011. Lynas Corporation Limited, http://www.lynascorp.com/content/upload/files/Presentations/Investor_Presentation_March_2011_950850.pdf (unpublished PowerPoint presentation).

Dai, S., Ren, D. and Li, S., 2006. Discovery of the superlarge gallium ore deposit in Jungar, Inner Mongolia, North China. Chinese Science Bulletin, 61, 2243–2252.

Davis, C., 2010. Mulga Rocks scoping study update. December 2010. Energy and Minerals Australia Limited, (unpublished).

Dayah, M., 1997. Dynamic Periodic Table (Ptable), 1 October 1997, (http://www.ptable.com/).

de Keyser, F. and Cook, P.J., 1972. Geology of the Middle Cambrian phosphorites and associated sediments of northwestern Queensland. Bureau of Mineral Resources, Australia, Bulletin 138, 79 pp.

Dentith, M.C., Frankcombe, K.F., Ho, S.E., Shepherd, J.M., Groves, D.I. and Trench, A. (editors), 1994. Geophysical Signatures of Western Australian Mineral Deposits. Geology & Geophysics Department (Key Centre) and UWA Extension Publication No.26, Australian Society of Exploration Geophysicists Special Publication 7, 454 pp.

Derrick, G.M., 1977. Metasomatic history and origin of uranium mineralization at Mary Kathleen, Northwest Queensland. BMR Journal of Australian Geology and Geophysics, 2, 123–130.

Dickson, T.W., 1999. A history of exploration for heavy minerals in the Victorian section of the Murray Basin. *In:* Stuart, R. (editor), Murray Basin Mineral Sands Conference. Extended Abstracts, 34–41.

Douglas McKenna and Partners Proprietary Limited, 2003. Final report on Exploration Licences 4964, 5185, 5135 Lake Innes, N.S.W. Nickel/cobalt/scandium laterite project. Report prepared for Jervois Mining Limited. Geological Survey of New South Wales, File GS2003/312 (unpublished).

Douglas, G.B., Butt, C.R. and Gray, D.J., 2011. Geology, geochemistry and mineralogy of the Ambassador uranium and multi-element deposit, Officer Basin, Western Australia. Mineralium Deposita, 41 pp (in prep/press).

Drew, L.J., Qingrun, M. and Weijun, S., 1990. The Bayan Obo iron-rare earth-niobium deposits, Inner Mongolia, China. Lithos, 26, 43–65.

Drexel, J.F. and Major, R.B., 1990. Mount Painter uranium-rare earth deposits. *In:* Hughes, F.E. (editor), Geology of the Mineral Deposits of Australia and Papua New Guinea. Australian Institute of Mining and Metallurgy, Monograph 14, 993–998.

Duncan, R.K., 1990. Tantalum, niobium and rare earth resources of the Mt Weld carbonatite, Western Australia: Tantalum–Niobium International Study Center, 31st General Assembly, Observation City, Perth, Western Australia. Proceedings.

Duncan, R.K. and Willett, G.C., 1990. Mount Weld Carbonatite. *In:* Hughes, F.E. (editor), Geology of mineral deposits of Australia and Papua New Guinea. Australasian Institute of Mining & Metallurgy, Melbourne, Monograph 14, 591–597.

Eckstrand, W.D., Sinclair, W.D. and Thorpe, R.I., 1995. Geology of Canadian Mineral Deposit Types. Geological Survey of Canada, 640 pp.

Einsele, G., 1992. Sedimentary basins: Evolution, facies, and sediment budget. Berlin, Springer-Verlag, 792 pp.

Elderfield, H. and Greaves, M.J., 1981. Negative cerium anomalies in the rare earth element patterns of oceanic ferromanganese nodules. Earth and Planetary Science Letters, 55, 163–170.

Elsner, H., 2010. Heavy minerals of economic importance. Assessment manual. Bundesanstalt für Geowissenschaften und Rohstoffe (BGR) (Federal Institute for Geosciences and Natural Resources), 218 pp.

EMC Metals Corporation of Canada in a press release on 8th February 2010, on the Toronto Stock Exchange.

Energy and Minerals Australia Limited, 2010a. Ambassador uranium deposit 25% increase in mineral resource. Announcement to the Australian Securities Exchange, 11 June 2010.

Energy and Minerals Australia Limited, 2010b. Mulga Rocks Ambassador deposit lignite uranium results and confirmation of polymetallic mineralisation. Announcement to the Australian Securities Exchange, 10 May 2010.

Energy and Minerals Australia Limited, 2010c. Annual general meeting presentation, 16th November 2010.

Eupene Exploration Enterprises Proprietary Limited, 1989. Rare earth element occurrences of the Northern Territory. Northern Territory Geological Survey, 10 pp.

Ewers, G.R. and Ryburn, R.J., 1997. OZMIN documentation: AGSO's national mineral deposits database. AGSO Record 1994/43 (second edition), 91 pp.

Fan, H.R., Xie, Y.H., Wang, K.Y. and Wilde, S.A., 2004. Methane-rich fluid inclusions in skarn near the giant REE-Nb-Fe deposit at Bayan Obo, northeast China. Ore Geology Reviews, 25, 301–309.

Ferguson, J. and Sheraton, J.W., 1979. Petrogenesis of kimberlitic rocks and associated xenoliths of Southeastern Australia. *In:* Boyd, F.R. and Meyer, H.O.A. (editors), Kimberlites, Diatremes and Diamonds: their Geology, Petrology, & Geochemistry, American Geophysical Union, Washington. D.C., 140–160.

Ferguson, K.M. and Ruddock, I., 2001. Mineral occurrences and exploration potential of the east Pilbara. Geological Survey of Western Australia, Report 81, 114 pp.

Fergusson, C.L., Henderson, R.A., Withnall, I.W. and Fanning, C.M., 2007. Structural history of the Greenvale Province, north Queensland: Early Palaeozoic extension and convergence on the Pacific margin of Gondwana. Australian Journal of Earth Sciences, 54, 573–595.

Ferris, G.M., Schwarz, M.S., Fairclough, M.C., Heithersay, P.H., Daly, S.J. and Morris, B.J., 2003. The mineral prospectivity of Yellabinna region, western Gawler Craton, South Australia Mineral Resources Group. Revised edition. Report Book 2003/18, 289 pp.

Fetherston, J.M., 2002. Industrial minerals in Western Australia: the situation in 2002. Geological Survey of Western Australia, Record 2002/12, 38 pp.

Fetherston, J.M., 2004. Tantalum in Western Australia. Geological Survey of Western Australia Mineral Resources Bulletin 22, 162 pp.

Fetherston, J.M., 2008. Industrial minerals in Western Australia: the situation in 2008. Geological Survey of Western Australia, Record 2008/16, 70 pp.

Fetherston, J.M. and Abeysinghe, P.B., 2000. Industrial minerals in Western Australia: the situation in 2000. Geological Survey of Western Australia, Record 2000/3, 60 pp.

Fetherston, J.M. and Searston, S.M., 2004. Industrial minerals in Western Australia: the situation in 2004. Geological Survey of Western Australia, Record 2004/21, 57 pp.

Fetherston, J.M., Abeysinghe, P.B. and Preston, W.A., 1997. Industrial minerals in Western Australia: the situation in 1997. Geological Survey of Western Australia, Record 1997/5, 55 pp.

Fisher, L. and Cleverley, J., 2010. Geochemical alteration and associated REE mobility of the Ranger 1, No 3 Mine, Northern Territory, Australia. Program Abstracts Volume, The AUSIMM International Uranium Conference 2010: The Decade for Development, 16–17 June 2010, Adelaide, South Australia, 57.

Fletcher, K. and Couper, J., 1975. Greenvale nickel laterite, north Queensland. *In:* Knight, C.L. (editor), Economic Geology of Australia and Papua New Guinea. 1. Metals. Australasian Institute of Mining & Metallurgy, Monograph 5, 995–1001.

Flynn, R.T. and Burnham, C.W., 1978. An experimental determination of rare earth partition coefficients between a chloride containing vapor phase and silicate melts. Geochimica et Cosmochimica Acta, 42, 685–702.

Frey, F.A., 1984. Rare earth element abundances in upper mantle rocks. *In:* Henderson, P. (editor), Rare Earth Element Geochemistry, 2. Amsterdam, Elsevier, 153–203.

Fulwood, K.E. and Barwick, R.E., 1990. Mulga Rock uranium deposits, Officer Basin. *In:* Hughes, F.E. (editor), Geology of Mineral Deposits of Australia and Papua New Guinea. Australasian Institute of Mining & Metallurgy, Melbourne, Monograph 14, 1621–1623.

Gammons, C.H., Wood, S.A. and Williams-Jones, A.E., 1996. The aqueous geochemistry of the rare earth elements and yttrium. VI. Stability of neodymium chloride complexes from 25 to 300C. Geochimica et Cosmochimica Acta, 60, 4615–4630.

Gardner, D.E., 1955. Beach sand heavy-mineral deposits of eastern Australia. Bureau of Mineral Resources Bulletin 28, 103 pp.

Gellatly, D.C., 1969. Probable carbonatites in the Strangways Range area, Alice Springs 1:250 000 sheet area SF53/14: petrography and geochemistry. Bureau of Mineral Resources and Geophysics, Australia, Record, 1969/77, 26 pp.

Gerasimovsky, V.I., 1974. Trace elements in selected groups of alkaline rocks [with comments]. *In:* Sorenson, H. (editor), The Alkaline Rocks. London, John Wiley & Sons, 402–411.

Gibson, G., Rubenach, M.J., Neumann, N.L., Southgate, P.N. and Hutton, L.J., 2008. Syn- and post-extensional tectonic activity in the Palaeoproterozoic sequences of Broken Hill and Mt Isa and bearing on reconstructions of Rodinia. Precambrian Research, 166, 350–369.

Giere, R., 1996. Formation of rare earth minerals in hydrothemal systems. *In:* Jones, A.P., Wall, F. and Williams, C.T. (editors), Rare Earth Minerals: Chemistry, origin and ore deposits. London, Chapman & Hall, 105–150.

Goleby, B.R., Huston, D.L., Lyons, P., Vandenberg, L., Bagas, L., Davies, B.M., Jones, L. E.A., Gebre-Mariam, M., Johnson, W., Smith, T. and English, L., 2009. The Tanami deep seismic reflection experiment; an insight into gold mineralization and Paleoproterozoic collision in the North Australian Craton. Tectonophysics, 472, 169–182.

Gradstein, F.M., Ogg, J. and Smith, A.G., 2004. A Geological Time Scale, 2004, Cambridge University Press, New York.

Graham, S., Lambert, D. and Shee, S., 2003. Geochemical and isotopic evidence of a kimberlite-melonite-carbonatite genetic link. 8th International Kimberlite Conference, Long Abstract, Victoria, British Columbia, Canada, June 22–27, 2003, 5 pp.

Graham, S., Lambert, D. and Shee, S., 2004. The petrogenesis of carbonatite, melonite and kimberlite from the Eastern Goldfield Province, Yilgarn Craton. Lithos, 76, 519–533.

Green, D.H., 1958. Geology and petrology of Gray Creek area, Queensland. Bureau of Mineral Resources, Australia, Record 1958/110, 59 pp.

Gunn, P.J. and Dentith, M.C., 1997. Magnetic responses associated with mineral deposits. AGSO Journal 17(2), Australian Geological Survey Organisation, Canberra, 145–158.

Gupta, C.K. and Krishnamurthy, N., 2005. Extractive metallurgy of the rare earths. CRC Press, 508 pp.

Gwalani, L.G., Rogers, K.A., Demény, A., Groves, D.I., Ramsay, R., Beard, A., Downes, P.J. and Eves, A., 2010. The Yungul carbonatite dykes associated with epithermal fluorite deposit at Speewah, Kimberley, Australia: carbon and oxygen isotope constraints on their origin. Mineralogy and Petrology, 98, 123–141.

Habashi, F., 1994. The discovery and industrialization of the rare earths—Part 1. The Canadian Institute of Mining and Metallurgy Bulletin, 87, 976, 80–86.

Hagemann, S.G. and Cassidy, K.F., 2000. Archean orogenic lode gold deposits. Reviews in Economic Geology, 13, 9–68.

Harben, P.W. and Kužvart, M., 1996. Industrial minerals: a global geology. Metal Bulletin. Industrial Minerals Information Limited, Surrey, London, United Kingdom, 330–340.

Hawkins, B.W., 1975. Mary Kathleen uranium deposit. *In:* Knight, C.L. (editor), Economic Geology of Australia and Papua New Guinea. 1. Metals. Australasian Institute of Mining & Metallurgy, Monograph 5, 398–402.

Haxel, G.B., Hedrick, J.B. and Orris, G.J., 2005. Rare earth element—Critical resources for high technology. United States Geological Survey Fact Sheet 087–02, http://pubs.usgs.gov/fs/2002/fs087-02/

Haynes, D.W., Cross, K.C., Bills, R.T. and Reed, M.H., 1995. Olympic Dam ore genesis: a fluid-mixing model. Economic Geology, 90, 281–307.

Hedrick, J.B., 2000. Rare earths. United States Geological Survey. Minerals Yearbook Reston, VA, 17 pp.

Henderson, P., 1984. General geochemical properties and abundances of the rare earth elements, *In:* Henderson, P. (editor), Rare Earth Element Geochemistry, 2, Amsterdam, Elsevier 1–32.

Henderson, P., 1996. The rare earth elements; introduction and review. The Mineralogical Society Series, 7, 1–19.

Henderson, R.A., Innes, B.M., Fergusson, C.L., Crawford, A.J. and Withnall, I.W., 2011. Collisional accretion of a late Ordovician oceanic island arc, northern Tasman Orogenic Zone, Australia. Australian Journal of Earth Sciences, 58, 1–19.

Hoatson, D.M. and Blake, D., 2000 (editors). Geology and economic potential of the Palaeoproterozoic layered mafic-ultramafic intrusions in the East Kimberley, Western Australia. Australian Geological Survey Organisation Bulletin 246, 476 pp.

Hoatson, D.M. and Glaser, L.M., 1989. Geology and economics of platinum-group metals in Australia. Bureau of Mineral Resources, Australia, Resource Report 5, 81 pp.

Hoatson, D.M., Sun, S-s. and Claoué-Long, J.C., 2005. Proterozoic mafic-ultramafic intrusions in the Arunta Region, central Australia. Part 1: Geological setting and mineral potential. Precambrian Research, 142, 93–133.

Holden, N.E., 2004. History of the origin of the chemical elements and their discoverers. 41st International Union of Pure and Applied Chemistry (IUPAC) General Assembly in Brisbane, Australia, June 29th–July 8th 2001, 14 pp, http://www.nndc.bnl.gov/content/elements.html., (from National Nuclear Data Centre (NNDC), Brookhaven National Laboratory, New York, USA, Report BNL-NCS-68350-01/10-Rev; last updated March 12, 2004.

Hornig-Kjarsgaard, I., 1998. Rare earth elements in sovitic carbonatites and their mineral phases. Journal of Petrology, 39, 2105–2121.

Hou, B., 2005. Heavy mineral sands potential of the Eucla Basin in South Australia – a world-class palaeo-beach-placer province. MESA Journal, 37, 4–12.

Howard, P.F., 1986. Proterozoic and Cambrian phosphorites – regional review: Australia. *In:* Cook, P.J. and Shergold, J.H. (editors), Phosphate Deposits of the World. Volume 1. Proterozoic and Cambrian phosphorites. Cambridge University Press, Cambridge, 20–41.

Howard, P.F. and Hough, M.J., 1979. On the geochemistry and origin of the D Tree, Wonarah, and Sherin Creek phosphorites of the Georgina Basin, northern Australia. Economic Geology, 74. 260–284.

Hussein, A.A.A. and El Sharkawi, M.A., 1990. Chapter 26. Mineral deposits. *In:* Said, Rushdi (editor), The Geology of Egypt: Rotterdam, A.A. Balkema, 511–566.

Hussey, K.J., 2003. Rare earth element mineralisation in the eastern Arunta Region: Darwin, Northern Territory Geological Survey Record 2003–004, 20 pp.

Hussey, K.J, Huston, D.L. and Goulevitch, J., 2008. Constraints on the genesis of the Nolans Bore REE-P-U-Th deposit, Northern Territory, Australia. Abstracts. Geological Society of Australia, 89, 142.

Huston, D.L., Wyborn, L. and Muhling, P., 1997. The changing nature of zinc–lead–silver deposits through time in Australia. Proceedings of the National Lead, Zinc and Silver Symposium, March 1998, Institute for International Research (IIR) Conferences, Sydney, Brisbane, 1997 (unpublished).

Huston, D.L., Maas, R. and Hussey, K.J., in press. The Nolans Bore rare earth element-phosphorous-uranium-thorium deposit: geology and origin. Proceedings of SGA 2011, Antofagasta, Chile.

Iluka Resources Limited, 2008. Annual Report 2008, 108 pp.

Image Resources Limited, 2007a. Quarterly report for the Quarter ended 31 December 2006. ASX Release 30 January 2007, 15 pp.

Image Resources Limited, 2007b. Quarterly report for the quarter ended 31 March 2007. ASX Release 30 April 2007, 17 pp.

Image Resources Limited, 2008. Maiden resource of 6.4 million tonnes of heavy minerals. ASX Release 8 May 2008, 18 pp.

Image Resources Limited, 2010. Measured resources estimate at Atlas begins. New drilling at Gingin and Chandala, ASX Release 8 April 2010, 10 pp.

Jackson, W.D. and Christiansen, G., 1993. International strategic minerals inventory summary report-rare-earth oxides. United States Geological Survey Circular 930–N, 68 pp.

Jackson, M.J., Scott, D.L. and Rawlings, D.J., 2000. Stratigraphic framework for the Leichhardt and Calvert superbasins: Review and correlations of the pre-1700 Ma successions between Mt Isa and McArthur River. Australian Journal of Earth Sciences, 47, 381–403.

Jagodzinski, E.A., 2005. Compilation of SHRIMP U-Pb geochronological data, Olympic Domain, Gawler Craton, South Australia, 2001–2003, Geoscience Australia, Canberra, 220 pp.

Jaques A.L., 2008. Australian carbonatites: their resources and geodynamic setting. 9th International Kimberlite Conference, Extended Abstracts, 91KC–A–00347 (with poster produced by Geoscience Australia, Canberra).

Jaques, A.L., Creaser, R.A., Ferguson, J. and Smith, C.B., 1985. A review of the alkaline rocks of Australia. Transactions of the Geological Society of South Africa, 88, 311–334.

Jaques, A.L., Jaireth, S. and Walshe, J.L., 2002. Mineral systems of Australia; an overview of resources, settings and processes. Australian Journal of Earth Sciences, 49, 623–660.

Jaques, A.L., Lewis, J.D. and Smith, C.B., 1986. The kimberlites and lamproites of Western Australia. Geological Survey of Western Australia Bulletin 132, 268 pp.

Jefferson, C.W., Thomas, J.D., Gandhi, S.S., Ramaekers, P., Delaney, G., Brisban, D., Cutts, C., Quirt, D., Portella, P. and Olson, R.A., 2007. Unconformity-associated uranium deposits of the Athabasca basin, Saskatchewan and Alberta. *In:* Goodfellow, D. (editor), Mineral Deposits of Canada: A Synthesis of Major Deposit Types, District Metallogeny, the Evolution of Geological Provinces, and Exploration Methods: Newfoundland, Geological Association of Canada, 273–306.

Johnson, J.P. and Cross, K.C., 1995. U-Pb geochronological constraints on the genesis of the Olympic Dam Cu-U-Au-Ag deposit, South Australia. Economic Geology, 90, 1046–1063.

Johnson, J.P. and McCulloch, M.T., 1995. Sources of mineralising fluids for the Olympic Dam Deposit (South Australia); Sm-Nd isotopic constraints. Chemical Geology, 121, 177–199.

Kennedy, B.A., 1990. Surface Mining, Second Edition. Society for Mining, Metallurgy, and Exploration, Incorporated. Port City Press Incorporated, Baltimore, Maryland, United States of America, 1197 pp.

Kingsnorth, D.J., 2010a. The challenges of meeting 'Energy' rare earths demand. IEA Standing Committee on Long-Term Co-operation, 17th May 2010, Paris, France.

Kingsnorth, D.J., 2010b. Rare earths: facing new challenges in the new decade, SME Annual Meeting 2010, Phoenix, Arizona, USA. Industrial Minerals Company of Australia Proprietary Limited, 25 pp (http://www.smenet.org/rareearthsproject/SME_2010_Kingsnorth.pdf).

Kingston, M.J. and Crowley, J.K., 1992. AVIRIS as a tool for carbonatite exploration; comparison of SPAM and Mbandmap data analysis methods. JPL Publication, 116–118.

Knox-Robinson, C.M. and Wyborn, L.A.I., 1997. Towards a holistic exploration strategy; using geographic information systems as a tool to enhanced exploration. Australian Journal of Earth Sciences, 44, 453–463.

Knutson, J. and Currie, K., 1990. The Mud Tank carbonatite, Northern Territory: an example of metasomatism at mid-crustal levels. BMR Research Newsletter 12, 11–12.

Korsch, R., Henson, P., Huston, D., Whitaker, A., Carson, C., Maas, R. and Hussey, K., 2009. Geoscience Australia's onshore energy security program in the Northern Territory: current results and future directions. Annual Geoscience Exploration Seminar (AGES) 2009, Alice Springs, 2009, 11–15.

Krapez, B. and Eisenlohr, B., 1998. Tectonic settings of Archean (3325-2775 Ma) crustal-supracrustal belts in the West Pilbara Block. Precambrian Research, 88, 173–205.

Krauskopf, K.B., 1979. Introduction to geochemistry. New York, N.Y., McGraw-Hill, 617 pp.

Krucible Metals Limited, 2010. ASX announcement, 8th April 2010. Positive scoping study results for Korella phosphate deposit. Announcement to the Australian Securities Exchange, 8 April 2010, 8 pp.

Krucible Metals Limited, 2011. ASX announcement, 5th April 2011. Maiden yttrium rare earth inferred resource at Krucible's Korella phosphate deposit, Mt. Isa District, Queensland. Announcement to the Australian Securities Exchange, 5 April 2011, 11 pp.

Kreuzer, O.P., Markwitz, V., Porwal, A.K. and McCuaig, T.C., 2010. A continent-wide study of Australia's uranium potential. Part I: GIS-assisted manual prospectivity analysis. Ore Geology Reviews, 38, 334–366.

Langworthy, A.P. and Black, L.P., 1978. The Mordor complex: a highly differentiated potassic intrusion with kimberlitic affinities in central Australia. Contributions to Mineralogy and Petrology, 67, 51–62.

Lawrence, B., 2006. Lynas sets itself up as long-term player in rare earths. Gold and Minerals Gazette, July 2006, 66.

Lawrence, M.G, Jupiter, S.D. and Kamber, B.S., 2006. Aquatic geochemistry of the rare earth elements and yttrium in the Pioneer River catchment, Australia. CSIRO Publishing, Marine and Freshwater Research, 57, 725–736.

Lees, B., 2006. Timing and formation of coastal dunes in northern and eastern Australia. Journal of Coastal Research, 2, 78–89.

Lewis, J.D., 1990. Chapter 5: Diatremes. *In:* Geology and mineral resources of Western Australia: Western Australia Geological Survey, Memoir 3, 565–589.

Li, J., Jin, H., Chen, Y. and Mao, X., 2007. Rare earth elements in Zhijin phosphorite and distribution in two-stage floatation process. Journal of Rare Earths, 25, Special Issue December 2007, 85–90.

Lissiman, J.C. and Oxenford, R.J., 1975. Eneabba rutile-zircon-ilmenite sand deposit, WA. *In:* Knight, C.L. (editor), Economic Geology of Australia and Papua New Guinea. Australian Institute of Mining and Metallurgy, Volume 1 Metals, 1062–1069.

Lockyer, G. and Brescianini, R., 2007. Investor Briefing Mining 2007 Resources Convention, 1 November 2007, Brisbane Australia (http://www.arafuraresources.com.au/documents/ArafuraMining2007presentation_ASX_release.pdf).

Long, K.R., Van Gosen, B.S., Foley, N.K. and Cordier, D., 2010. The principal rare earth deposits of the United States—A summary of domestic deposits and a global perspective. United States Geological Survey Scientific Investigations Report 2010–5220, 96 pp.

Lottermoser, B.G., 1990. Rare-earth element mineralisation within the Mt. Weld carbonatite laterite, Western Australia. Lithos, 24, 151–167.

Lottermoser, B.G., 1991. Rare earth element resources and exploration in Australia. The Australasian Institute of Mining and Metallurgy, Proceedings 296, Number 2, November 1991, 49–56.

Lottermoser, B.G., 1992. Rare earth elements and hydrothermal ore processes. Ore Geology Reviews, 7, 25–41.

Lottermoser, B.G., 1994. Carbonatites and ore deposits. The Australasian Institute of Mining and Metallurgy, Proceedings 299, Number 2, December 1994, 35–41.

Lottermoser, B.G. and England, B.M., 1988. Compositional variation in pyrochlores from the Mt Weld carbonatite laterite, Western Australia. Mineralogy and Petrology, 38, 37–51.

Lukanin, O.A. and Dernov-Pegarev, V.F., 2010. Partitoning of rare earth elements between an aqueous chloride fluid phase and melt during the decompression-driven degassing of granite magmas. Geochemistry International, 48, 961–978.

Lynas Corporation Limited, 2011. Rare earths, we touch them everyday. Investor presentation, February 2011, 36 pp, (http://www.lynascorp.com/content/upload/files/Presentations/Investor_Presentation_February_2011.pdf).

Maas, R., McCulloch, M.T., Campbell, I.H. and Page, R.W., 1987. Sm-Nd isotope systematics in uranium rare-earth element mineralization at the Mary Kathleen uranium mine, Queensland. Economic Geology, 82, 1805–1826.

Mandarino, J.A., 1999. Fleischer's Glossary of Mineral Species 1999. The Mineralogical Record Incorporated, Tucson, USA, 225 pp.

Mason, T., 1999. Exploration to mining—RZM at Wemen. *In:* Murray Basin Mineral Sands Conference. April 21–23, 1999. Mildura, Victoria, Australia. Australian Institute of Geoscientists Bulletin 26, 70–77.

Mason, A.J., Teakle, M. and Blampain, P.A., 1998. Heavy-mineral sand deposits, central Murray Basin. *In:* Berkman, D.A., Mackenzie, D.H. (editors), Geology of Australian and Papua New Guinean Mineral Deposits. Australasian Institute of Mining and Metallurgy, Melbourne, Monograph 22, 647–650.

Matheson, R.S. and Searl, R.A., 1956. Mary Kathleen uranium deposit, Mt Isa–Cloncurry district, Queensland, Australia. Economic Geology, 51. 528–540.

McDonough, W.F. and Sun, S.S., 1995. The composition of the Earth. Chemical Geology, 120, 223–253.

McDonough, W.F., Sun, S.S., Ringwood, A.E., Jagoutz, E. and Hofmann, A.W., 1992. Potassium, rubidium, and cesium in the Earth and Moon and the evolution of the mantle of the Earth. Geochimica et Cosmochimica Acta, 56, 1001–1012.

McKellar, J.B., 1975. The eastern Australian rutile province. *In:* Knight, C.L. (editor), Economic Geology of Australia and Papua New Guinea. Australian Institute of Mining and Metallurgy, Volume 1 Metals, 1055–1062.

Meinert, L.D., 1993. Skarns and skarn deposits. Geoscience Canada Reprint Series, 6, 117–134.

Mernagh, T.P. and Miezitis, Y., 2008. A review of the geochemical processes controlling the distribution of thorium in the Earth's crust and Australia's thorium resources. Geoscience Australia Record 2008/05, 48 pp.

Metallica Minerals Limited, 2010. Metallica Minerals Limited, Company Announcement to the Australian Securities Exchange, 20th August 2010, 10 pp (http://www.metallicaminerals.com.au/sites/default/files/Maiden%20Scandium%20Resource%20for%20Lucknow.pdf).

Metallica Minerals Limited, 2011. Metallica Minerals Limited, Company Announcement to the Australian Securities Exchange, 19th January 2011, 15 pp (http://www.metallicaminerals.com.au/sites/default/files/MLM_Greenvale_Resource_Update.pdf).

Metallica Minerals Limited, 2010. Nornico Project drilling update: Lucknow nickel-cobalt (and scandium) deposit, ASX Release 10 May 2010, 19 pp (http://www.metallicaminerals.com.au/sites/default/files/2010.05.10%20Lucknow%20Ni-Co-Sc%20drilling.pdf).

Miezitis, Y., 2010. Rare Earths. *In:* Australia's Identified Mineral Resources 2010. Geoscience Australia, Canberra, 61–68.

Mueller, A.G., Hall, G.C., Nemchin, A.A., Stein, H.R., Creaser, R.A. and Mason, D.R., 2008. Archaean high-Mg monzodiorite-syenite, epidote skarn, and biotite-sericite gold lodes in the Granny Smith-Wallaby district, Australia: U-Pb and Re-Os chronometry of two intrusion-related hydrothermal systems. Mineralium Deposita, 43, 337–362.

Mukherjee, T.K., 2007. Thorium resources in India, its mining, separation and chemical processing. IAEA Technical meeting on 'Thorium based fuels and fuel cycle options for pressurized heavy water cooled reactors, light water reactors and high temperature gas-cooled reactors. 22 to 25 October, 2007. Istanbul, Turkey.

Mungall, J.E., 2007. Magmatic ore deposits. *In:* Rudnick, R. (editor), The Crust. Treatise on Geochemistry Volume 3, Chapter 21. Elsevier, 1-33.

Navigator Resources Limited, 2007. High grade rare earths confirmed at Cummins Range: Navigator Resources Limited, Report to Australian Securities Exchange, 18 September 2007, 5 pp.

Navigator Resources Limited, 2010. Gold and rare earths by David Hatch, October 2010, 20 pp (http://www.navigatorresources.com.au/files/files/742_Investor_Mining_2010_Brisbane_PPR_v1.pdf).

Neary, C.R. and Highley, D.E., 1984. Chapter 12. The economic importance of rare earth elements. *In:* Henderson, P. (editor), Rare Earth Element Geochemistry. Developments in Geochemistry 2, Elsevier, Amsterdam, 423–466.

Nelson, D.R., Chivas, A.R., Chappell, B.W. and McCulloch, M.T., 1988. Geochemical and isotopic systematics in carbonatites and implications for the evolution of ocean-island sources. Geochimica et Cosmochimica Acta, 52, 1–17.

Neuendorf, K.K.E., Mehl, J.P.Jr. and Jackson, J.A. (editors), 2005. Glossary of Geology, Fifth Edition. American Geological Institute, Alexandria, Virginia, 779 pp.

Neumann, N.L., 2007. Geochronological synthesis and time-space plots for Proterozoic Australia. *In:* Neumann, N.L. and Fraser, G.L. (editors), Geochronological Synthesis and Time-Space Plots for Proterozoic Australia. Geoscience Australia Record 2007/06, Canberra, Australia, 52–73.

Noble Resources, 1992. Annual Report 1992. Noble Resources NL, Report to Australian Securities Exchange, 31 July 1992, 48 pp.

Norman, D.I., Kyle, P.R. and Baron, C., 1989. Analysis of trace elements including rare earth elements in fluid inclusion liquids. Economic Geology, 84, 162–166.

O'Driscoll E.S.T., 1985. The application of lineament tectonics in the discovery of the Olympic Dam Cu-Au-U deposit at Roxby Downs, South Australia. Global Tectonics and Metallogeny, 3, 43–57.

O'Driscoll E.S.T., 1990. Lineament tectonics of Australian ore deposits. Monograph Series, Australasian Institute of Mining and Metallurgy 14, 33–41.

Oliver, N.H.S., Pearson, P.J., Holcombe, R.J. and Ord, A., 1999. Mary Kathleen metamorphic-hydrothermal uranium-rare-earth element deposit; ore genesis and numerical model of coupled deformation and fluid flow. Australian Journal of Earth Sciences, 46, 467–484.

Oreskes, N. and Einaudi, M.T., 1992. Origin of hydrothermal fluids at Olympic Dam: preliminary results from fluid inclusions and stable isotopes. Economic Geology, 87, 64–90.

Orris, G.J. and Grauch, R.I., 2002. Rare earth element mines, deposits, and occurrences. Open-File Report 02–189, United States Geological Survey, 174 pp.

Page, R.W., 1983. Timing of superposed volcanism in the Proterozoic Mount Isa Inlier, Australia. Precambrian Research, 21, 223–245.

Palme, H., O'Neill, H.S.C., Heinrich, D.H. and Karl, K.T., 2007. Cosmochemical Estimates of Mantle Composition, Treatise on Geochemistry. Oxford, Pergamon, 1–38.

Pearson, J.M, 1995. Geology of the Mesoproterozoic Gifford Creek alkaline igneous complex, Gascoyne Province, Western Australia. Short Course Notes, Key Centre for Strategic Mineral Deposits, Department of Geology and Geophysics, University of Western Australia, 12 pp.

Pearson J.M. and Taylor W.R., 1996. Mineralogy and geochemistry of fenitized alkaline ultrabasic sills of the Gifford Creek Complex, Gascoyne Province, Western Australia. Canadian Mineralogist, 34, 201–219.

Pearson, J.M., Taylor W.R. and Barley M.E., 1996. Geology of the alkaline Gifford Creek igneous complex, Gascoyne Province, Western Australia. Australian Journal of Earth Sciences, 43, 299–309.

Pearson, R.G., 1963. Hard and soft acids and bases. Journal of the American Chemical Society, 85, 3533–3539.

Phillips, G.N., Groves, D.I. and Kerrich, R., 1996. Factors in the formation of the giant Kalgoorlie gold deposit: Ore Geology Reviews, 10, 295–317.

Pidgeon, R.T., 1989. Archaean diamond xenocrysts in kimberlites; how definitive is the evidence? Special Publication - Geological Society of Australia, 14, 1006–1011.

Piper, D.Z., 1974. Rare earth elements in ferromanganese nodules and other marine phases. Geochimica et Cosmochimica Acta, 38, 1007–1022.

Qi, H., Hu, R. and Qi, Z., 2007. REE geochemistry of the Cretaceous lignite from Wulantuga germanium deposit, Inner Mongolia, northeastern China. International Journal of Coal Geology, 71, 329–344.

Ramsden, A.R., French, D.H. and Chalmers, D.I., 1993. Volcanic-hosted rare-metals deposit at Brockman, Western Australia: mineralogy and geochemistry of the Niobium Tuff. Mineralium Deposita, 28, 1–12.

Reed, M.J., Candela, P.A. and Piccoli, P.M., 2000. The distribution of rare earth elements between monzogranitic melt and the aqueous volatile phase in experimental investigations at 800 degrees Celsius and 200 Mpa. Contributions to Mineralogy and Petrology, 140, 251–262.

Reeve, J.S., Cross, K.C., Smith, R.N. and Oreskes, N., 1990. Olympic Dam copper-uranium-gold-silver deposit. Monograph Series. Australasian Institute of Mining and Metallurgy, 14, 1009–1035.

Reynolds, L.J., 2001. Geology of the Olympic Dam Cu-U-Au-Ag-REE deposit. MESA Journal, 23, 4–11.

Richardson, D.G. and Birkett, T.C., 1995a. Carbonatite-associated deposits. *In:* Ecstrand, O.R., Sinclair, W.D. and Thorpe, R.I. (editors), Geology of Canadian Mineral Deposit Types. Geological Survey of Canada, 8, 541–558.

Richardson, D.G. and Birkett, T.C., 1995b. Residual carbonatite-associated deposits. *In:* Ecstrand, O.R., Sinclair, W.D. and Thorpe, R.I. (editors), Geology of Canadian Mineral Deposit Types. Geological Survey of Canada, 8, 108–119.

Richardson, D.G. and Birkett, T.C., 1995c. Peralkaline rock-associated rare metals. *In:* Ecstrand, O.R., Sinclair, W.D. and Thorpe, R.I. (editors), Geology of Canadian Mineral Deposit Types. Geological Survey of Canada, 8, 523–540.

Righter, K., Drake, M.J., Heinrich, D.H. and Karl, K.T., 2003. Partition Coefficients at High Pressure and Temperature, Treatise on Geochemistry. Oxford, Pergamon, 425–449.

Roberts, D.E. and Hudson, G.R.T., 1983. The Olympic Dam copper-uranium-gold deposit, Roxby Downs, South Australia. Economic Geology, 78, 799–822.

Robjohns, N., 1990. Rare Earths. *In:* Metals and Minerals Annual Review 1990, Mining Journal, London, 78–80.

Roden, M.F. and Murthy, V.R., 1985. Mantle metasomatism. Annual Review of Earth and Planetary Sciences, 13, 269–296.

Rogers, K.A., 1998. Speewah fluorite deposit. *In:* Berkman, D.A. and Mackenzie, D.H. (editors), Geology of Australian and Papua New Guinean mineral deposits. The Australasian Institute of Mining and Metallurgy, Melbourne, Monograph 22, 387–392.

Rollinson, H.R., 1993. Using geochemical data; evaluation, presentation, interpretation. Harlow, Longman, England, 352 pp.

Roy, P.S., 1999. Heavy mineral beach placers in southeastern Australia: their nature and genesis. Economic Geology, 94, 567–588.

Roy, P.S. and Whitehouse, J., 1999. Origin of the Loxton-Parilla Sands in the Murray Basin. In Murray Basin Mineral Sands Conference. April 21–23, 1999. Mildura, Victoria, Australia. Australian Institute of Geoscientists Bulletin 26, 90–97.

Roy, P.S., Whitehouse, J., Cowell, P.J. and Oakes, G., 2000. Mineral sands occurrences in the Murray Basin, southeastern Australia. Economic Geology, 95, 1107–1128.

Rubenach, M.J., 1982. Metamorphosed mafic-ultramafic complexes of the Greenvale area. *In:* Withnall, I.W. (editor), 1982 Field Conference Charters Towers–Greenvale area. Geological Society of Australia Incorporated, Queensland Division, Brisbane, 47–51.

Rudnick, R.L., Gao, S., Heinrich, D.H. and Karl, K.T., 2003. Composition of the Continental Crust, Treatise on Geochemistry. Oxford, Pergamon, 1–64.

Rugless, C.S. and Pirajno, F., 1996. Geology and geochemistry of the Copperhead albitite 'carbonatite' complex, east Kimberley, Western Australia. Australian Journal of Earth Sciences, 43, 311–322.

Russell, T.J. and Trueman., N.A., 1971. The geology of the Duchess phosphate deposits, northwestern Queensland, Australia. Economic Ecology, 66, 1186–1214.

Sadeghi, A. and Steele, K.F., 1989. Use of stream sediment elemental enrichment factors in geochemical exploration for carbonatite and uranium, Arkansas, USA. Journal of Geochemical Exploration, 32, 279–286.

Sanders, T.S., 1999. Mineralization of the Halls Creek Orogen, east Kimberley region, Western Australia. Geological Survey of Western Australia, Report 66, 44 pp.

Scott, A.K. and Scott, A.G., 1985. Geology and genesis of uranium-rare earth deposits at Mary Kathleen northwest Queensland. Australian Institute of Mining and Metallurgy Bulletin and Proceedings, 290, 79–89.

Schofield, A., 2010. Potential for magmatic-related uranium mineral systems in Australia. Geoscience Australia Record 2010/20, 56 pp (http://www.ga.gov.au/image_cache/GA19084.pdf).

Seredin, V.V., 2005. Rare earth elements in germanium-bearing coal seams of the Spetsugli deposit (Primor'e Region, Russia). Geology of Ore Deposits, 47, 238–255.

Shannon, R.D., 1976. Revised effective ionic radii and systematic studies of interatomic distances in halides and chalcogenides Acta Crystallographica, Section A, 32, 751–767.

Shepherd, M.S., 1990. Eneabba heavy mineral sand placers. *In:* Hughes, F.E. (editor), Geology of Mineral Deposits of Australia and Papua New Guinea. Australasian Institute of Mining & Metallurgy, Melbourne, Monograph 14, 1591–1594.

Sheppard, S., Johnson, S.P., Wingate, M.T.D, Kirkland, C.L. and Pirajno, F., 2010. Explanatory Notes for the Gascoyne Province. Geological Survey of Western Australia, 336 pp.

Skirrow, R.G., Bastrakov, E.N., Barovich, K., Fraser, G.L., Creaser, R.A., Fanning, C.M., Raymond, O.L. and Davidson, G.J., 2007. Timing of iron oxide Cu-Au-(U) hydrothermal activity and Nd isotope constraints on metal sources in the Gawler craton, South Australia. Economic Geology, 102, 1441–1470.

Skirrow, R.G., Jaireth, S., Huston, D.L., Bastrakov, E.N., Schofield, A., van der Wielen, S.E. and Barnicoat, A.J., 2009. Uranium mineral systems; processes, exploration criteria and a new deposit framework. Geoscience Australia Record 2009/20, 44 pp.

Solomon, M. and Groves, D.I., 1994. The geology and origin of Australia's mineral deposits. Oxford Monographs on Geology and Geophysics 24, Clarendon Press, Oxford, 951 pp.

Spaggiari, C.V., Gray, D.R. and Foster, D.A., 2003. Tethyan- and cordilleran-type ophiolites in eastern Australia: implications for the evolution of the Tasmanides. *In:* Dilek, K. and Robinson, P.T. (editors), Ophiolites In Earth History. Geological Society of London, Special Publication 218, 517–539.

Steinitz, J., 2010. Rare Earth Elements: the seventeen metals crunch, http://www.proactiveinvestors.com.au/companies/news/10742/rare-earth-elements-the-seventeen-metals-crunch-10742.html

Stitt, P., 1999. Thoughts on the paragenesis of the Wim deposits. *In:* Murray Basin Mineral Sands Conference. April 21–23, 1999. Mildura, Victoria, Australia. Australian Institute of Geoscientists Bulletin 26, 93–98.

Strategic Minerals Corporation, 2004. Annual Report 2004. 43 pp.

Sweetapple, M.T., 2000. Characteristics of Sn-Ta-Be-Li-industrial mineral deposits of the Archaean Pilbara Craton, Western Australia. Australian Geological Survey Organisation Record 2000/44, 54 pp.

Sweetapple, M.T. and Collins, P.L.F., 2002. Genetic framework for the classification and distribution of Archean rare metal pegmatites in the North Pilbara Craton, Western Australia. Economic Geology, 97, 873–895.

Taylor, S.R. and McLennan, S.M., 1985. The Continental Crust: Its Composition and Evolution. Oxford, Blackwell Scientific Publications, 312 pp.

Taylor, S.R. and McLennan, S.M., 1995. The geochemical evolution of the continental crust. Reviews of Geophysics, 33, 241–265.

Taylor, W.R., Esslemont, G. and Sun, S.-S 1995a. Geology of the volcanic-hosted Brockman rare-metals deposit, Halls Creek Mobile Zone, northwest Australia, Part II—Geochemistry and petrogenesis of the Brockman volcanics. Mineralogy and Petrology, 52, 231–255.

Taylor, W.R., Page, R.W., Esslemont, G., Rock, N.M.S. and Chalmers, D.I., 1995b. Geology of the volcanic-hosted Brockman rare-metals deposit, Halls Creek Mobile Zone, northwest Australia, Part I—Volcanic environment, geochronology and petrography of the Brockman volcanics. Mineralogy and Petrology, 52, 209–230.

Thevissen, J., 1995. Napperby Annual Report EL8411, 1995 field season. PNC Exploration (Australia) Proprietary Limited report NTDME CR96/187 (unpublished).

Towner, R.R., Ewers, G.R. and Cassidy, K.F., 1996. Rare earths and mineral sands in Australia. Australian Geological Survey Organisation and Bureau of Resources Sciences, Canberra, Australia, Commercial-In-Confidence Report, November 1997, 45 pp.

Towner, R.R., McLeod, I.R. and Ward, J., 1987. Rare earths, Australia's resources. Materials Australasia, 19, number 4, 8–11.

Tucker, D.H. and Collerson, K.D., 1972. Lamprophyric intrusions of probable carbonatitic affinity from South Australia. Australian Journal of Earth Sciences, 19, 387–391.

Turekian, K.K. and Wedepohl, K.H., 1961. Distribution of the elements in some major units of the Earth's crust. Geological Society of America Bulletin 72, 175–191.

Vallini, D.A., Groves, D.I., McNaughton, N.J. and Fletcher, I.R., 2007. Uraniferous diagenetic xenotime in northern Australia and its relationship to unconformity-associated uranium mineralization. Mineralium Deposita, 42, 51–64.

Wallis, D.S. and Oakes, G.M., 1990. Heavy mineral sands in eastern Australia. *In:* Hughes, F.E. (editor), Geology of Mineral Deposits of Australia and Papua New Guinea. Australasian Institute of Mining & Metallurgy, Melbourne, Monograph 14, 1599–1608.

Walters, A., Lusty, P., Chetwyn, C. and Hill, A., 2010. Rare Earth Elements. Mineral Profile Series, British Geological Survey, United Kingdom, 45 pp (http://www.bgs.ac.uk/mineralsuk/whatsnew.html).

Warren, A.Y.E., Barron, L.M., Meakin, N.S., Morgan, E.J., Raymond, O.L., Cameron, R.G and Colquhoun, G.P., 1999. Mesozoic igneous rocks. *In:* Meakin, N.S. and Morgan, E.J. (compilers), Dubbo 1:250 000 Geological Sheet SI 55–4, Second Edition, Explanatory Notes, Geological Survey of New South Wales, Sydney, 504 pp.

Webster, E.A. and Holloway, J.R., 1980. The partitioning of REE's, Sc, Rb and Cs between a silicic melt and a Cl fluid. Eos, Transactions, American Geophysical Union, 61, 1152.

Wedepohl, K.H., 1970. Handbook of Geochemistry, Vol. II/2. Berlin, Springer-Verlag, Germany, 667 pp.

Will, R., Anderson, E. and Mori, S, 1995. Rare Earth minerals and products. Chemical Economics Handbook Marketing Research Report.

Williams, P.J., Barton, M.D., Johnson, D.A., Fontbote, L., de Haller, A., Mark, G., Oliver, N.H.S. and Marschik, R., 2005. Iron oxide copper-gold deposits; geology, space-time distribution, and possible modes of origin, 371–405.

Williams, V.A., 1990. WIM 150 detrital heavy mineral deposit. *In:* Hughes, F.E. (editor), Geology of mineral deposits of Australia and Papua New Guinea. Australasian Institute of Mining & Metallurgy, Melbourne, Monograph 14, 1609–1614.

Witt, W.K., 1990. Pegmatite metals. Geology and mineral resources of Western Australia, Memoir 3, Geological Survey of Western Australia, Perth, Western Australia, 709–715.

Wood, S.A., 1990a. The aqueous geochemistry of the rare earth elements and yttrium, 1. Review of available low temperature data for inorganic complexes and the inorganic REE speciation of natural water. Chemical Geology, 82, 159–186.

Wood, S.A., 1990b. The aqueous geochemistry of the rare earth elements and yttrium, 2. Theoretical predictions of speciation in hydrothermal solutions to 350°C at saturated water vapor pressure. Chemical Geology, 88, 99–125.

Wood, S.A. and William-Jones, A.E., 1994. The aqueous geochemistry of the rare-earth elements and yttrium 4. Monazite solubility and REE mobility in exhalative massive sulfide-depositing environments. Chemical Geology, 115, 47–60.

Wormald, R.J., Price, R.C. and Kemp, A.I.S., 2004. Geochemistry and Rb/Sr geochronology of the alkaline-peralkaline Narraburra Complex, central southern New South Wales; tectonic significance of Late Devonian granitic magmatism in the Lachlan Fold Belt. Australian Journal of Earth Sciences, 51, 369–384.

Wu, C., Yuan, Z. and Bai, G., 1996. Rare earth deposits in China. *In:* Jones, P.A., Wall, F. and Williams, C.T. (editors), Rare Earth Minerals: Chemistry, Origin and Ore Deposits. The Mineralogical Society Series 7. Chapman and Hall, London, 281–310.

Wyborn, L.A.I., Heinrich, C.A. and Jaques, A.L., 1994. Australian Proterozoic mineral systems; essential ingredients and mappable criteria: Publication Series - Australasian Institute of Mining and Metallurgy, 5/94, 109–115.

Zhao, Y., Bai, G. and Li, D., 2005. REE-Nb (Fe, U, Th)-bearing alkaline skarns of China: Proceedings of the Biennial SGA (Society for Geology Applied to Mineral Deposits) Meeting, 1, 507–509.

APPENDICES

APPENDIX 1. GLOSSARY

(modified from Cassidy et al., 1997; Neuendorf et al., 2005).

aeolian–sand sized material picked up, transported, and deposited by wind.

airborne geophysical data–geophysical information (e.g., gravity, gamma-ray spectrometric, and magnetic data) collected by instruments specially fitted to and being transported by an aircraft.

alkaline–said of an igneous rock that contains more sodium and/or potassium than is required to form feldspar with the available silica.

alkaline igneous complex–igneous body consisting of several alkaline rock types (e.g., phonolite, syenite, loparite, nepheline syenite, sövite, alkaline basalt).

alluvial sediments–sediments deposited, usually in stream channels, by flowing water.

aplite–a light-coloured igneous rock characterised by a fine-grained granular texture and consisting predominantly of quartz, potassium feldspar, and sodium-calcium feldspar.

Archean–the term, meaning ancient, has been generally applied to the oldest rocks of the Precambrian (older than 2500 million years).

base metal–generally referring to the elements, copper, lead, zinc and sometimes nickel.

basement–the lowest mappable rocks, generally with complex structure, that underlies other major rock sequences of a region.

breccia–a coarse-grained clastic rock, composed of angular broken rock fragments held together by a mineral cement or in a fine-grained matrix.

Cambrian–see Paleozoic.

carbonaceous–said of a rock or sediment that is rich in carbon or organic matter.

carbonatite–a carbonate rock of apparent magmatic origin, generally associated with kimberlites and alkaline rocks. Carbonatites may be calcitic (sövite) or dolomitic (rauhaugite).

Cenozoic–the era of geological time from 65.5 million years to present; divided into three Periods: Paleogene, Neogene, and Quaternary, which in turn are divided into seven Epochs: Paleocene, Eocene, Oligocene, Miocene, Pliocene, Pleistocene, and Holocene (present). See Figure 5.2 for details of the geological time scale.

concordant–structurally conformable; said of strata displaying parallelism of bedding or structure.

conglomerate–a coarse-grained clastic sedimentary rock, composed of rounded to subangular fragments larger than 2 mm in diameter set in a fine-grained matrix of sand or silt.

craton–a part of the Earth's crust that has attained stability and has been little deformed for a prolonged period, and generally restricted to continents.

discordant–structurally unconformable; said of strata lacking conformity or parallelism of bedding or structure.

dyke–a tabular igneous intrusion that cuts across the bedding or foliation of the country rock.

element–one of a class of substances which consist entirely of atoms of the same atomic number.

exploration–phase in which a company or organisation searches for mineral resources by carrying out geological and geophysical surveys, followed up where appropriate by drilling and other evaluation of the most prospective sites.

felsic–a descriptive term applied to the composition of an igneous rock containing abundant light coloured and few dark coloured minerals.

fenite–a quartzofeldspathic rock that has been altered by alkali metasomatism at the contact of a carbonatite intrusive complex. The process is called fenitisation.

gneiss–a foliated rock formed by regional metamorphism, in which bands or lenticles of granular minerals alternate with bands or lenticles in which minerals having flaky or elongate prismatic habits. Varieties include augen gneiss, granite gneiss, feldspar gneiss, and aplitic gneiss.

granite, granitic–broadly applied, any holocrystalline, quartz–bearing plutonic (intrusive) igneous rock.

greenstone–a field term applied to any compact dark-green altered or metamorphosed mafic igneous rock (e.g., basalt, gabbro, diorite) that owes its colour to the presence of chlorite, amphibole or epidote.

Heavy-Mineral (HM) sands–a concentration of heavy minerals (rutile, zircon, ilmenite, monazite) on a contemporary or ancient beach, or along a coastline.

Holocene–see Cenozoic.

holocrystalline–texture of an igneous rock composed entirely of crystals.

hydrothermal–of or pertaining to hot water, to the action of hot water or to the products of this action, such as a mineral deposit precipitated from a hot aqueous solution, with or without demonstrable association with igneous processes.

hydrothermal deposit–a mineral deposit formed by precipitation of ore and gangue minerals in fractures, faults, breccia openings, or other spaces, by replacement or open-space filling, from fluids generally ranging in temperature from 50 to 700 degrees Celsius and ranging in pressure from less than 4 kilobars.

igneous complex–an assemblage of intimately associated and roughly contemporaneous igneous rocks differing in form or in petrographic type; it may consist of plutonic rocks, volcanic rocks, or both.

igneous rocks–said of a rock or mineral that solidified from molten or partly molten material, i.e., from a magma; also, applied to processes leading to, related to, or resulting from, the formation of such rocks. Igneous rocks constitute one of the three main classes into which rocks are divided, the others being metamorphic and sedimentary.

inlier–an area or group of rocks surrounded by rocks of younger age.

intermediate–said of an igneous rock that is transitional between felsic and mafic, generally having a silica content of 54 to 65%.

JORC Code–The Australasian Code for Reporting of Exploration Results, Mineral Resources and Ore Reserves, prepared by the Joint Ore Reserves Committee. This is a principal-based code, which sets out recommended minimum standards and guidelines on classification and public reporting. Companies listed on the Australian Securities Exchange are required to report exploration outcomes, resources, and reserves in accordance with the JORC Code standards and guidelines.

lacustrine sediments–sediments that accumulated in a lake-like environment.

laterite–a term for a highly weathered red subsoil or material rich in secondary oxides of iron and/or aluminium. It develops in a tropical or forested warm to temperate climate, and is a residual product of weathering.

LCT–Lithium–Cesium–Tantalum-bearing pegmatite.

lignite–a brownish-black coal that is intermediate in qualification (maturity) between peat and subbituminous coal.

limonite–a general field term for a group of brown, amorphous, naturally occurring hydrous ferric oxides whose real identities are unknown. Common secondary material formed by oxidation (weathering) of iron or iron-bearing minerals.

Ma–million years.

mafic–a descriptive term applied to the composition of an igneous rock containing abundant dark coloured minerals, such as pyroxene and olivine.

magma–naturally occurring mobile 'rock' material, generated within the Earth and capable of intrusion and extrusion, from which igneous rocks are thought to have been derived through solidification and related processes.

Mesozoic–the era of geological time from the end of the Paleozoic (251 million years) to the beginning of the Cainozoic (65.5 million years). The Mesozoic is divided into the Triassic, Jurassic, and Cretaceous time Periods.

metamorphic grade–the intensity or rank of metamorphism, measured by the amount or degree of difference between the original parent rock and the metamorphic rock. It indicates in a general way the pressure-temperature environment or facies in which the metamorphism took place. For example, conversion of shale to slate or phyllite would be low-grade metamorphism, whereas continued transformation to a garnet-sillimanite schist would be very high-grade metamorphism.

metamorphic rocks–any rock derived from pre-existing rocks by mineralogical, chemical, and/or structural changes, essentially in the solid state, in response to marked changes in temperature, pressure, shear stress, and chemical environment, generally at depth in the Earth's crust.

metasomatic–pertaining to the process of metasomatism and to its results. The term is especially used in connection with the origin of ore deposits.

metasomatism–the processes by which one mineral is replaced by another of different chemical composition owing to reactions set up by the introduction of material from external sources.

migmatite–a composite rock composed of igneous or igneous–appearing and/or metamorphic materials, which are generally distinguishable megascopically.

Mt–million tonnes.

NYF–Niobium–Yttrium–Fluorine-bearing pegmatite.

Paleozoic–the era of geological time from the end of the Precambrian (542 million years) to the beginning of the Mesozoic (251 million years). The Paleozoic is divided into Cambrian, Ordovician, Silurian, Devonian, Carboniferous, and Permian time Periods.

paludal sediments–sediments that accumulated in a marsh-like environment.

pegmatite–an exceptionally coarse-grained igneous rock, with interlocking crystals, usually found as irregular dykes, lenses, or veins, especially at the margins of large granitic igneous bodies. Pegmatites have gross compositions generally similar to that of granite.

(per)alkaline–said of an igneous rock in which the molecular proportion of aluminium oxide is less than that of sodium and potassium oxides combined; a general chemical class of igneous rocks.

PGEs–platinum-group elements comprising the six metallic elements: platinum (Pt), palladium (Pd), rhodium (Rh), iridium (Ir), osmium (Os), and ruthenium (Ru).

phosphorite–a sedimentary rock with a high enough content of phosphate minerals to be of economic interest. Most commonly it is a bedded primary or reworked secondary marine rock composed of carbonate fluorapatite in the form of laminae, nodules, oolites, and shell and skeletal fragments.

placer–a surficial mineral deposit formed by mechanical concentration of mineral particles from weathered debris. The common types are beach placers and alluvial placers. The mineral concentrated is usually a heavy mineral, such as gold, cassiterite, magnetite, zircon, rutile, and monazite.

Pleistocene–see Cenozoic.

Pliocene–see Cenozoic.

Precambrian–all geological time, and its corresponding rocks, before the beginning of the Paleozoic; it is equivalent to about 90% of geological time and includes the Proterozoic and Archean Eons.

Precambrian basement–basement rocks belonging to the Precambrian.

production–the phase at which operations produce mined product.

prospect–a potential accumulation of minerals that is sufficiently well defined to represent a viable drilling target.

Proterozoic–the era of geological time from the end of the Archean (about 2500 million years) to the beginning of the Phanerozoic (542 million years).

pyroclastic–pertaining to clastic rock material formed by volcanic explosion or aerial expulsion from a volcanic vent; also, pertaining to rock texture of explosive origin.

Quaternary–see Cenozoic.

regolith–the unconsolidated material, both weathered in place and transported, which overlies consolidated rocks (bedrock).

resources–a concentration of naturally occurring solid, liquid, or gaseous materials in or on the Earth's crust in such form and amount that its economic exploitation is currently or potentially feasible.

rift, rift basins–a long, narrow continental trough that is bounded by normal faults; a graben of regional extent that marks a zone along which the entire thickness of the lithosphere has ruptured under extension.

sedimentary rocks–a rock resulting from the consolidation of loose sediment that has accumulated in layers; e.g., a clastic rock (such as conglomerate or sandstone) consisting of mechanically formed fragments of older rock transported from its source and deposited in water or from air or ice; or a chemical rock (such as rock salt or gypsum) formed by precipitation from solution; or an organic rock (such as certain limestones) consisting of the remains or secretions of plants and animals.

shale–a fine-grained detrital sedimentary rock, formed by the consolidation (especially by compression) of clay, silt, or mud. It is characterised by finely laminated structure, which imparts a fissility approximately parallel to the bedding, along which the rock breaks readily into thin layers and that is commonly most conspicuous on weathered surfaces.

sill–a tabular igneous intrusion that parallels the planar structure of the surrounding rock.

skarn–a general term for silicate gangue (amphibole, pyroxene, garnet, etc.) of certain iron–ore and sulphide deposits, particularly those that have replaced limestone and dolomite, and experienced introduction of large amounts of silicon, aluminium, iron, and magnesium by hydrothermal fluids.

slate–a compact, fine-grained metamorphic rock that possesses slaty cleavage and hence can be split into slabs and thin plates.

strandline–a former shoreline now elevated above the present water level.

supergene–said of a mineral deposit or enrichment formed near the surface, commonly by descending solutions.

tectonic–said of, or pertaining to, the rock structure and external forms resulting from the deformation of the Earth's crust; broad architecture of the outer part of the Earth.

tuff–a general term for all consolidated pyroclastic rocks associated with a volcano.

volcanic–pertaining to the activities, structures, or rock types of a volcano.

volcanic rocks–a generally finely crystalline or glassy igneous rock resulting from volcanic action at or near the Earth's surface, either ejected explosively or extruded as lava (e.g., basalt, andesite, dacite, rhyolite).

weathered rock–bedrock which has had its composition and appearance changed by weathering.

weathering–the destructive process or group of processes by which earthy and rocky materials on exposure to atmospheric agents at or near the Earth's surface are changed in colour, texture, composition, firmness, or form, with little or no transport of the loosened or altered material; specifically the physical disintegration and chemical decomposition of rock that produce an in situ mantle of waste and prepare sediments for transportation.

APPENDIX 2. ALPHABETICAL LISTING OF CHEMICAL ELEMENTS

Symbol	Element	Atomic Number
Ac	Actinium	89
Al	Aluminum	13
Am	Americium	95
Ar	Argon	18
As	Arsenic	33
At	Astatine	85
Ba	Barium	56
Bk	Berkelium	97
Be	Beryllium	4
Bi	Bismuth	83
Bh	Bohrium	107
B	Boron	5
Br	Bromine	35
Cd	Cadmium	48
Ca	Calcium	20
Cf	Californium	98
C	Carbon	6
Ce	Cerium	58
Cs	Cesium	55
Cl	Chlorine	17
Cr	Chromium	24
Co	Cobalt	27
Cn	Copernicium	112
Cu	Copper	29
Cm	Curium	96
Ds	Darmstadtium	110
Db	Dubnium	105
Dy	Dysprosium	66
Es	Einsteinium	99
Er	Erbium	68
Eu	Europium	63
Fm	Fermium	100
F	Fluorine	9
Fr	Francium	87
Gd	Gadolinium	64
Ga	Gallium	31
Ge	Germanium	32
Au	Gold	79
Hf	Hafnium	72
Hs	Hassium	108
He	Helium	2
Ho	Holmium	67
H	Hydrogen	1
In	Indium	49
I	Iodine	53
Ir	Iridium	77
Fe	Iron	26
Kr	Krypton	36
La	Lanthanum	57
Lr	Lawrencium	103
Pb	Lead	82
Li	Lithium	3
Lu	Lutetium	71
Mg	Magnesium	12
Mn	Manganese	25
Mt	Meitnerium	109

Symbol	Element	Atomic Number
Md	Mendelevium	101
Hg	Mercury	80
Mo	Molybdenum	42
Nd	Neodymium	60
Ne	Neon	10
Np	Neptunium	93
Ni	Nickel	28
Nb	Niobium	41
N	Nitrogen	7
No	Nobelium	102
Os	Osmium	76
O	Oxygen	8
Pd	Palladium	46
P	Phosphorus	15
Pt	Platinum	78
Pu	Plutonium	94
Po	Polonium	84
K	Potassium	19
Pr	Praseodymium	59
Pm	Promethium	61
Pa	Protactinium	91
Ra	Radium	88
Rn	Radon	86
Re	Rhenium	75
Rh	Rhodium	45
Rg	Roentgenium	111
Rb	Rubidium	37
Ru	Ruthenium	44
Rf	Rutherfordium	104
Sm	Samarium	62
Sc	Scandium	21
Sg	Seaborgium	106
Se	Selenium	34
Si	Silicon	14
Ag	Silver	47
Na	Sodium	11
Sr	Strontium	38
S	Sulfur	16
Ta	Tantalum	73
Tc	Technetium	43
Te	Tellurium	52
Tb	Terbium	65
Tl	Thallium	81
Th	Thorium	90
Tm	Thulium	69
Sn	Tin	50
Ti	Titanium	22
W	Tungsten	74
U	Uranium	92
V	Vanadium	23
Xe	Xenon	54
Yb	Ytterbium	70
Y	Yttrium	39
Zn	Zinc	30
Zr	Zirconium	40

Source: modified from http://periodic.lanl.gov/list.shtml. Rare-earth elements are shown in blue font.

APPENDIX 3. ESTIMATED MINE PRODUCTION OF RARE-EARTH ELEMENTS BY COUNTRY (TONNES OF REO EQUIVALENT)

Country	1990	1992	1994	1996	1998	2000	2002	2004	2006	2008	2010
Australia	6050	3300	3300	0	0	0	0	0	0	0	0
Brazil	911	396	400	200	1400	200	0	402	730	650	550
China	16 500	21 300	30 600	55 000	65 000	73 000	88 000	95 000	119 000	120 000	130 000
India	2500	2200	2500	2700	2700	2700	2700	2700	2700	2700	2700
Malaysia	1830	427	234	340	350	450	450	250	200	380	350
Republic of South Africa	724	400	400	0	0	0	0	0	0	0	0
USA	22 700	20 700	20 700	20 400	5000	5000	5000	0	0	0	0
Commonwealth of Independent States[1]	8500	8000	6000	6000	2000	2000	2000	2000	NA	NA	NA
Others	409	237	303	130	120	120	120	2200	NA	NA	NA
Total	60 124	56 960	64 437	84 770	76 570	83 470	98 270	102 552	122 630	123 730	134 000

[1] Former members of Soviet Union.

Source of data: United States Geological Survey Mineral Commodity Summaries for 1990 to 2011—Rare Earths (http://minerals.usgs.gov/minerals/pubs/commodity/rare_earths/).

Others = Other countries include Congo (Kinshasa), Madagascar, Sri Lanka, Thailand, and Zaire.

NA = Not Available.

APPENDIX 4. COMPOSITIONS[1] OF THE MAJOR RARE-EARTH-ELEMENT DEPOSITS IN THE WORLD

	Mount Weld Australia Monazite[2]	Nolans Bore Australia Apatite	Brockman Australia Bastnäsite	Bayan Obo China Bastnäsite	Guang-dong China Monazite	Guangdong China Ion-adsorption clays	Mountain Pass USA Bastnäsite	Lovozersky Russia Loparite
LREO								
Lanthanum	25.5	19.74	5.8	25	24	30.4	33.2	28
Cerium	46.74	47.53	16.8	50	42.7	1.9	49.1	57.5
Praseodymium	5.32	5.82	0.1	5.1	4.1	6.6	4.3	3.8
Neodymium	18.5	21.20	0.4	16.7	17	24.4	12	8.8
Samarium	2.27	2.37	0.03	1.2	3	5.2	0.8	0.96
HREO								
Europium	0.44	0.40	0	0.2	0.1	0.7	0.12	0.13
Gadolinium	Trace	1.00	0.4	0.7	2	4.8	0.17	0.21
Terbium	0.07	0.08	0.1	Trace	0.7	0.6	Trace	0.07
Dysprosium	0.12	0.33	10.4	Trace	0.8	3.6	Trace	0.09
Holmium	Trace	0.05	0.2	Trace	Trace	Trace	Trace	0.03
Erbium	0.03	0.09	7.7	Trace	0.3	1.8	Trace	0.07
Thulium	Trace	0.01	0.1	Trace	NA	Trace	Trace	Trace
Ytterbium	0.06	0.05	5.0	Trace	2.7	Trace	Trace	0.29
Lutetium	Trace	0.01	0.1	Trace	NA	Trace	Trace	0.05
Yttrium	0.35	1.32	52.4	0.2	2.4	20	2.6	Trace

Source of data: modified from Hastings Rare Metals Limited (2011: http://www.hastingsrareметals.com/userfiles/file/Hastings%20Investors%20Presentation.pdf), the United States Geological Survey, Arafura Resources Limited (http://www.arafuraresources.com.au/nol_reo_dist.html), and company reports.

[1] Percentage of total rare-earth oxides.

[2] Dominant mineralogy/style of deposit.

NA = Not Available.

APPENDIX 5. RESOURCE CLASSIFICATIONS AND DEFINITIONS

Mineral resource classification

Estimated resources of minerals and elements (e.g., the REE) are geologically-based and their classification is largely based on the McKelvey resource classification system.

The McKelvey resource classification system classifies known (identified) resources according to the certainty or degree of (geological) assurance of occurrence and the degree of economic feasibility of exploitation either now or in the future. The first takes account of information on the size and quality of the resource, whereas the economic feasibility considers the changing economic factors such as commodity prices, operating costs, capital costs, and discount rates.

The assessments of **Identified Resources**—resources for which the location, quantity, and quality are known from specific measurements or estimates from geological evidence—are based on and compiled from resource data reported for individual mineral deposits by companies. The Australian Securities Exchange mandates standards for the public reporting of mineral resources by Australian-listed companies. Listed exploration and mining companies must follow the Joint Ore Reserves Committee (JORC) Code. This is a principal-based code which sets out recommended minimum standards and guidelines on classification and public reporting in Australasia. Companies listed on the Australian Securities Exchange are required to report exploration outcomes, resources, and reserves in accordance with the JORC Code standards and guidelines.

Data from company reports on specific projects are aggregated into categories in the national classification scheme to provide estimates of the national resource base.

In the national system used by Geoscience Australia, **Demonstrated Resources** are resources that can be recovered from an identified resource and whose existence and quality have been established with a high degree of geological certainty, based on drilling, analysis, and other geological data and projections.

Economic Demonstrated Resources (EDR) are resources with the highest levels of geological and economic certainty. For petroleum these include remaining proved plus probable commercial reserves. For minerals, these include JORC Code proved and probable ore reserves and measured and indicated mineral resources. For these categories, profitable extraction or production has been established, analytically demonstrated or assumed with reasonable certainty using defined investment assumptions.

Sub-Economic Demonstrated Resources (SDR) are resources for which, at the time of determination, profitable extraction or production under defined investment assumptions has not been established, analytically demonstrated, or cannot be assumed with reasonable certainty (this includes contingent petroleum resources).

Inferred Resources (INF) are those with a lower level of confidence that have been inferred from more limited geological evidence and assumed but not

<table>
<tr><th colspan="4">DECREASING GEOLOGICAL ASSURANCE →</th></tr>
<tr><td rowspan="2">DECREASING ECONOMIC FEASIBILITY ↓</td><td colspan="2">Identified resources</td><td rowspan="2">Undiscovered resources</td></tr>
<tr><td colspan="2">Demonstrated resources</td><td>Inferred resources</td></tr>
<tr><td rowspan="4">Economic Demonstrated Resources</td><td>JORC mineral reserves</td><td rowspan="4">JORC inferred mineral resources

Possible petroleum resources</td><td rowspan="5">Quantitative mineral potential assessments

Undiscovered petroleum resource assessments</td></tr>
<tr><td>Proved petroleum reserves</td></tr>
<tr><td>Proved and probable petroleum reserves</td></tr>
<tr><td>JORC measured and indicated mineral resources</td></tr>
<tr><td rowspan="2">Subeconomic Resources</td><td>Subeconomic mineral resources</td><td rowspan="2">Contingent possible resources</td></tr>
<tr><td>Contingent proved and probable petroleum resources</td></tr>
</table>

Figure Appendix 5.1. Australia's national energy resources classification scheme (based on the McKelvery resource classification scheme). See text for explanation of terms.

Source: Geoscience Australia.

verified. Where probabilistic methods are used there should be at least a 10% probability that recovered quantities will equal or exceed the sum of proved, probable and possible reserves.

Undiscovered or potential resources are unspecified resources that may exist based on certain geological assumptions and models, and be discovered through future exploration. Undiscovered resource assessments have inbuilt uncertainties, and are dynamic and change as knowledge improves and uncertainties are resolved.

Uranium resources (including REE in some deposits) at the national level are commonly reported under the Nuclear Energy Agency/International Atomic Energy Agency (IAEA) uranium resources classification system. Economic Demonstrated Resources correlate with **Reasonably Assured Resources** recoverable at <US$80/kg U, and Inferred Resources are the same in both systems.

APPENDIX 6. AUSTRALIAN PRODUCTION (TONNES) OF MONAZITE, 1980 TO 1995

Year	New South Wales	Queensland	Western Australia	Total
1980	261	457	12 357	13 075
1981	639	-	12 643	13 282
1982	198	-	9364	9562
1983	36	14	14 629	14 679
1984	668	-	15 592	16 260
1985	980	-	17 755	18 735
1986	75	-	14 747	14 822
1987	688	189	11 250	12 127
1988 (e)	<500	<200	11 000	<12 000
1989 (e)	0	<500	11 000	<11 000
1990 (e)	NA	0	7900	7900
1991 (e)	NA	0	6700	6700
1992 (e)	0	0	5600	5600
1993 (e)	0	0	6500	6500
1994 (e)	0	0	2300	2300
1995 (e)	0	0	200	200
Approximate total	<4045	<1360	159 537	<164 942

Source of data: Cassidy et al. (1997).
(e) – estimated annual production.
NA = Not Available.

APPENDIX 7. EXPLORATION HISTORY OF RARE-EARTH ELEMENTS IN AUSTRALIA

The following description (see summary in Section 1.6) of REE exploration in Australia is largely from Barrie (1965), Cassidy et al. (1997), Miezitis (2010), various REE reviews relating to Western Australia (Fetherston et al., 1997; Fetherston and Abeysinghe, 2000; Fetherston, 2002, 2008), Queensland (Cooper 1990), the Northern Territory (Eupene Exploration Enterprises Proprietary Limited, 1989; Hussey, 2003), and from mining company websites. This section is not a complete compilation of REE exploration activities in Australia, but it describes the major discoveries and events. For further details on these occurrences, and the most recent developments in the REE industry, it is recommended that the interactive online databases (e.g., DIGS, MINEDEX, STRIKE, TIGER) managed by the various State/Territory geological surveys are interrogated (http://www.geoscience.gov.au/), and such information can also be found in annual National mining compilations, such as the 2011/12 Register of Australian Mining (http://www.riu.com.au/Register/AustralianMining/).

The names of those deposits described in this appendix, or their general locations, are indicated in bold font for quick reference.

Exploration history

Pre-1950:

Precambrian[6] albite-rich pegmatites and veins in the Pilbara Craton of Western Australia have attracted considerable exploration interest since tin was first mined in the Pilbara in 1889. The Mount Cassiterite vein deposit was considered the most important deposit since it represented the largest underground tin mine in Western Australia. Other commodities, such as REE, tantalum, beryllium, niobium, together with non-metallic industrial minerals (mica, feldspar) have been produced from pegmatites, associated hydrothermal veins, and secondary alluvial/eluvial deposits (Sweetapple, 2000). The REE-bearing minerals manganotantalite, manganocolumbite, microlite, fergusonite, tanteuxenite, 'calciosamarskyite', and 'tapiolite' occur at **Cooglegong, Wodgina, Moolyella, and Mount Francisco**. Barrie (1965) reported that a pegmatite deposit at Cooglegong Crossing, ~55 km south-southwest of Marble Bar, was worked in 1913 and 1920 and yielded about 2 tonnes of gadolinite (yttrium iron beryllium silicate: $(Ce,La,Nd,Y)_2FeBe_2Si_2O_{10}$). An analysis of the Cooglegong gadolinite yielded 45.78% of Y_2O_3 and 4.81% of other REO (note that gadolinite does not contain more than trace amounts of gadolinium). Associated REE minerals in the concentrates include allanite, yttrotantalite, monazite, 'tantalopolycrase', and tanteuxenite (Barrie, 1965). Some of the concentrate samples contained more than 70% of REE minerals. Tantalite-bearing dykes in the Wodgina area, ~95 km south of Port Hedland, contain thorogummite, 'makintoshite', and manganotantalite (Barrie, 1965). Quantities of REE as rare-earth silicates, and complex Nb-Ta-bearing species, have been identified in alluvial deposits from Cooglegong, and the Shaw River–Pinga Creek tin fields.

Minerals documented from the **Shaw River** Tinfield (see references in Sweetapple, 2000) include:
Major minerals: cassiterite (SnO_2); columbite–tantalite mineral series $[(Fe,Mn)(Ta,Nb)_2O_6]$; yttrotantalite $[(Y,U,Fe)(Ta > Nb)O_4]$; tanteuxenite $[(Y,REE > U,Th)(Ta > Nb,Ti)_2O_6]$; monazite $[(Ce,La,Y,Th)(PO_4,SiO_4)]$; microlite $[(Na,Ca)_{2-m}(Ta+Nb > 2Ti)_2O_6(F,OH,O)_{1-n} \cdot pH_2O]$; xenotime ($YPO_4$, includes HREE); and zircon ($ZrSiO_4$).
Minor minerals: gadolinite $(Be_2Fe(Ce,Y,Nd,La)_2Si_2O_{10})$; thorite $[Th(SiO_4)]$; euxenite $[(Y,REE > U,Th)(Nb > Ta,Ti)_2O_6]$; fergusonite $[(REE,Fe)(Nb,Ta,Ti)O_4]$; cheralite $[(Ce,Ca,Th,U)(P,Si)O_4]$; samarskite $[(Y,Fe,U,REE)(Nb,Ta)O_4]$; and wodginite (probably $MnSnTa_2O_8$).

Minerals documented in the **Pinga Creek** Tinfield (including Abydos and Woodstock: see references in Sweetapple, 2000) include:
Major minerals: cassiterite (SnO_2); gadolinite $(Be_2Fe(Ce,Y,Nd,La)_2Si_2O_{10})$; 'tantaliferous polycrase' (probably tanteuxenite $[(Y,REE > U,Th)(Ta > Nb,Ti)_2O_6]$; and allanite $[(Ce,Ca,Y)(Al,Fe)_3(SiO_4)_3(OH)]$.
Minor minerals: monazite $[(Ce,La,Y,Th)(PO_4,SiO_4)]$; and manganocolumbite (ideally $MnNb_2O_6$).

Other REE occurrences in Western Australia (Barrie, 1965) found during exploration for mainly tin and uranium include: gadolinite near **Bullock Well**, ~130 km south-southeast of Port Hedland; yttrotantalite in tin-bearing gravels at **Eleys Well** on Split Rock station, ~40 km southwest of Marble Bar, and also with calciosamarskyite and cassiterite at **Hillside station**, ~70 km south-southwest of Marble Bar; and tanteuxenite in tin concentrate at **Francisco Well**,

[6] The geological timescale is shown in Figure 5.2, and the technical terms are explained in the Glossary (Appendix 1).

~150 km south of Port Hedland, and also with allanite in pegmatite on the western side of the **Yule River**, ~90 km southwest of Marble Bar; xenotime grains up to 5 mm in diameter from **Nullagine**, ~90 km southeast of Marble Bar; monazite in tin placers near Moolyella; euxenite from **Mount Dale**, ~45 km southeast of Perth; detrital thorogummite coated with hydrothorite at **Saunders Creek** in the East Kimberleys; and gadolinite from **Payne's Find**, ~140 km southeast of Yalgoo.

Proterozoic sedimentary units ~150 km southeast of Halls Creek in the Proterozoic Birrindudu Basin near the Western Australian–Northern Territory border have been explored for REE, uranium, and gold. Canadian Energy Resources (CER) discovered uranium mineralisation in the 1980s at the **Mount Mansbridge** prospect (http://www.qur.com.au/gardnerrange/). A significant uranium geochemical anomaly (up to 980 ppm U in pits) with a 300 m strike length was found from the testing of an airborne geophysical target. The only REE assayed by CER was yttrium. Follow-up sampling by Quantum Resources Limited (http://www.qur.com.au/CompanyAnnoucements/) indicated that the uranium had associated REE abundances of up to 7%, with the mineralisation described as a xenotime-rich alteration zone. Uraniferous xenotime and xenotime-rich in HREE have been discovered in several localities in the region. The uranium-REE mineralisation appears to be associated with the unconformity between the Paleoproterozoic Killi Killi Formation and the overlying Mesoproterozoic Gardner Sandstone. Orion Metals Limited has described HREE mineralisation in unconformity and basement rocks at the nearby **Killi Killi Hills** prospects (http://www.orionmetals.com.au/documents/MarchHK2011.pdf). These prospects were tested for uranium in 1969. No systematic analysis for the REE was conducted because of the focus for uranium. Two radiometric anomalies 1 km apart were tested in 1969, and results confirmed significant levels of HREE, including dysprosium, ytterbium, and erbium. Maximum yttrium and uranium abundances of 2.06% and 326 ppm, respectively, were recorded, and the average yttrium value for 45 samples was 1327 ppm. Anomalous strontium is also associated with the REE-uranium mineralisation. REE-bearing minerals xenotime and florencite of possible hydrothermal origin have been reported. Mineralisation is not hosted in veins, but it occurs pervasively throughout the conglomerate and sandstone units (http://www.mining-reporter.com/index.php/component/content/article/811-metallica-minerals/5146-high-grade-heavy-rare-earth-element-hree-uranium-and-gold-discovery).

Pegmatites in the Mount Isa–Cloncurry region of Queensland have been a source of REE-bearing monazite, mica, beryl, feldspar, tourmaline, tin, tantalite, and bismuth-bearing minerals (Cooper, 1990). Brooks and Shipway (1960) indicated that the **Mica Creek** pegmatites, ~20 km southwest of Mount Isa, crop out over 15 km along the eastern margin of the Sybella Granite. These pegmatites were discovered in 1914, with intermittent mining of mica and beryl occurring from 1922 to 1927 and after 1943. Monazite concentrations were found in four locations in the pegmatites, with Th contents ranging from 5.73 to 7.1%, but no REE abundances were reported. Barrie (1965) described REE occurrences associated with felsic dykes in the Mount Isa–Cloncurry region, including allanite at **Spear Creek**, **Elaine Dorothy**, **Hidden Valley**, and davidite [$(La,Ce,Ca)(Y,U)(Ti,Fe^{3+})_{20}O_{38}$]-like minerals at **Cameron River–Ballara**, **Six Kangaroos**, and 'absite' (thorium brannerite) at **west Cloncurry** and **Ballara**.

Several minor occurrences of REE associated with monazite have been documented from Tasmania. Monazite was reported in tin-tungsten-bismuth mines in the **Moina** district and with wolframite in the **Mount Bischoff** tin deposit of Tasmania. Monazite was also found with alluvial tin deposits north of **Zeehan** and on **King Island**. The only commercial production (~30 t of concentrates) of monazite from Tasmania was in 1943 from the **Endurance** alluvial tin mine near South Mount Cameron in the northeast of the state (Barrie, 1965).

1950 to 1980:

Australia exported large quantities of monazite from heavy-mineral sands mined in **Western Australia, New South Wales, and Queensland**, for the extraction of both REE and thorium. Much of the historical production in eastern Australia has been derived from North Stradbroke Island and the beaches from Southport south to the New South Wales border. The monazite content of the heavy-mineral fraction of the Queensland and New South Wales deposits ranges up to 2% (Barrie, 1965). Between 1952 and 1995, Australia exported 265 000 tonnes of monazite with an export value (in 2008 dollars) of $284 million (Australian Bureau of Statistics, 2009). However, since production ceased in 1995 it is believed no significant quantities of REE or thorium associated with the mineral sands have been imported or exported by Australia. Details of exploration activities related to monazite by-products of heavy-mineral sand mining in Australia can be found in Barrie (1965), Cooper (1990), Williams (1990), Towner et al. (1996), Cassidy et al. (1997), Mason et al. (1998), and Miezitis (2010).

In the 1950s, Zircon Rutile Limited at **Byron Bay**, New South Wales, processed a small quantity of monazite to produce Ce oxide for use in glass polishing.

Many deposits containing REE were discovered as a result of uranium prospecting in the Mount Isa–Cloncurry region of northwest Queensland. The presence of REO in the Proterozoic **Mary Kathleen** uranium deposit was recognised soon after its discovery in 1954 (Hawkins, 1975). Prospectors found boulders of radioactive rock in a creek draining from a hill on which the deposit occurs, and then tracked them back to their source. The Rio Tinto Group carried out regional and detailed geological mapping, radiometric prospecting, diamond drilling, and costeaning (Matheson and Searl, 1956). Mary Kathleen is a major hard-rock occurrence of uranium-REE in Queensland. Mining was carried out from 1956 to 1963, and from 1975 to 1982. The major occurrences of uranium-REE mineralisation in the Mary Kathleen orebody, the Rita-Rary and Elaine prospects are steeply dipping uraniferous lenses in garnet skarns. Mary Kathleen originally contained around 10 000 tonnes of uranium oxide at a grade of 1.2 kg/t and 200 000 tonnes of mixed REO. The ratio of REO to uranium is about 20:1 (Cooper, 1990). Some 9.5 million tonnes of ore with 4.5% rare earths were mined, processed, and retained in the tailings dam. The REE are hosted by allanite (orthite) and stillwellite (lanthanum boro-silicate), which are the main uranium-bearing components of the orebody. Local concentrations of REE also occur in fluorapatite and sulphides. Yttrium occurs within the garnet lattice and is largely unrecoverable. Allanite comprised about 35% of the ore at outcrop. The REE are broadly distributed with the uranium mineralisation, but the relationship between them is not clear. Isolated areas of non-uraniferous allanite are present in remobilised zones. Ceric and lanthanum oxides constitute approximately 85% of the REE. Hawkins (1975) noted that the TREO concentrations are: scandium oxide (0.006%), yttrium oxide (0.3%), lanthanum oxide (33.5%), ceric oxide (51.5%), praseodymium oxide (4.0%), neodymium oxide (9.1%), samarium oxide (1.1%), europium oxide (0.05%), gadolinium oxide (<0.06%), terbium oxide (<0.02%), dysprosium oxide (0.05%), holmium oxide (<0.02%), erbium oxide (0.06%), thulium oxide (<0.02%), ytterbium oxide (0.01%), and lutetium oxide (<0.01%). The LREE subgroup constitutes about 99% of the TREO content.

Several REE-bearing minerals, including 'absite', allanite, betafite, brannerite, davidite, euxenite, fergusonite, florencite, monazite, orthite, polycrase, samarskite, thorite, xenotime, and yttrocrastite have been documented in pegmatites, in fissure-fillings within granitic rocks, and in hematitic breccias in the Olary and Mount Painter districts of the Curnamona Province of South Australia (Cassidy et al., 1997). These minerals were found throughout the state during uranium and base-metal exploration, but no primary commercial production of the REE took place. The REE-bearing minerals are generally associated with uranium minerals, occurring in uraniferous titanium-rich minerals at **Radium Hill, Crockers Well,** and **Mount Victoria** (Barrie, 1965). Davidite is an important component of lodes in high-grade metamorphic rocks at Radium Hill, whereas the major uranium and REE mineral in the Crockers Well deposits is 'absite'. Samarskite and monazite are associated with hematite and brown feldspar in quartz veins at **Mount Painter**, monazite in rutile-bearing pegmatite veins near **Myponga**, and davidite-type minerals have been recorded at **Houghton**, near Adelaide (Barrie, 1965).

Davidite concentrates produced from the uranium tailings of the **Radium Hill** uranium mine were treated between 1954 and 1961 at Port Pirie. The tailings contained an estimated 1500 tonnes of REO comprising the oxides: scandium (3%); yttrium (16%); lanthanum (38%); cerium (24%); praseodymium (0.7%); neodymium (1.8%); samarium (0.2%); europium (0.07%); gadolinium (0.4%); terbium (0.5%); dysprosium (3.3%); holmium (0.7%); erbium (3.8%); thulium (0.7%); ytterbium (6.5%); and lutetium (0.6%). About 136 kg of high-purity scandium was produced as a by-product of the uranium mining at Radium Hill (Towner et al., 1987). In 1969, the Rare Earth Corporation of Australia Limited, operating at Port Pirie in South Australia, began producing Ce, La, Y, and Th compounds from locally produced monazite. However, the plant ceased operations in mid-1972 because of a lack of working capital and the difficulty of breaking into world markets for processed REE.

The first significant exploration of the **Brockman** multi-element prospect, 18 km southeast of Halls Creek in the Halls Creek Orogen of Western Australia, was carried out by Rio Tinto in 1954 when they detected anomalous radiation in the area during regional radiometric surveys. In the 1960s, the Geological Survey of Western Australia conducted regional geological mapping of the region as part of the Gordon Downs 1:250 000 Geological Sheet. In 1973, Trend Exploration Proprietary Limited recorded high levels of niobium in stream-sediment samples

during follow up of radiometric anomalies originally identified in regional surveys by the Bureau of Mineral Resources. Several sources of niobium mineralisation with anomalous yttrium, fluorine, zirconium, tantalum, and zinc values were associated with Paleoproterozoic alkaline volcanic rocks. In 1983–84, Union Oil Development Corporation completed detailed geological mapping, reconnaissance stream sediment, and soil and rock-chip geochemistry. Maximum REO abundances in rock chips were 2820 ppm Y_2O_3, 830 ppm La_2O_3, and 1040 ppm Ce_2O_3. Nineteen trenches across the mineralised formation, called the 'Niobium Tuff', returned grades of up to 0.45% Nb and 0.23% Ta. In 1985, the Union Oil Development Corporation commissioned mineralogical studies at the CSIRO which identified the fine-grained nature of the monazite-dominated mineralisation, with an average grain size of less than 10 microns. Major REE minerals include bastnäsite, calcian-bastnäsite, parisite, and synchysite (see Table 1.2). Drilling programs by West Coast Holdings in the mid-1980s confirmed the findings of earlier trench sampling with the target commodities confined to the 'Niobium Tuff'. In mid-2004, Brockman Minerals Proprietary Limited released a measured, indicated, and inferred resource totalling 50 million tonnes grading 0.09% REO, 1.04% ZrO_2, 0.44% Nb_2O_5, and 0.027% Ta_2O_5 (Aztec Resources, 2003). Metallurgical test work involving heavy liquid mineral separation commenced in late 2005. Initial development plans for the Brockman multi-element deposit involved the production of high purity oxides of zirconium, hafnium, yttrium, niobium, tantalum, aluminium, selected REO, beryllium, scandium, and gallium metal. In December 2010, Augustus Minerals Limited released a JORC-compliant resource for the Brockman (alternate name Hastings deposit) REE deposit as over 22 million tonnes (0.79% ZrO_2, 0.31% Nb_2O_5, 0.023% Ta_2O_5, and 0.10% Y_2O_3) comprising 8.83 million tonnes in the Indicated category and 13.25 million tonnes in the Inferred category. The REE (except Y) were not included in this resource, but the relative abundances of individual REE in the Brockman deposit are shown in Appendix 4. Historically, the exploitation of this resource was hindered by the fine-grained (<20 um), hydrous nature of the ore minerals, which requires a specialised chemical leaching process to achieve high degrees of recovery of rare metals (Ramsden et al., 1993; Taylor et al., 1995a,b). The Brockman deposit is described in detail in Section 3.3.1.

The nickeliferous laterites associated with ultramafic-mafic complexes in the **Greenvale** area of northern Queensland were discovered in 1957 during the regional mapping programs carried out by the Bureau of Mineral Resources and the Queensland Geological Survey (Fletcher and Couper, 1975). Limited sampling of the upper ferruginous zone of the Greenvale laterite defined nickel concentrations of over 1%. In 1966, Metals Exploration NL located a nickel-enriched silicate zone beneath the ferruginous cap with nickel concentrations in excess of 3%. Metals Exploration NL with Freeport Minerals Company undertook drilling programs and by 1969 a rsource of 40 million tonnes of ore averaging 1.57% Ni and 0.12% Co had been established. The two companies decided to proceed in December 1971 with a mining operation that would produce 25 000 tonnes of nickel and 1000 t of cobalt annually (Fletcher and Couper, 1975). The scandium credits of the laterites in the Greenvale region are currently being assessed by Metallica Minerals Limited (http://www.metallicaminerals.com.au/). Ni-Co-Sc resources have been determined at the Lucknow (comprising Red Fort, Grant's Gully, and Lady Agnes), Kokomo, and Greenvale (comprising Power Line, Powder Magazine, Moonscape, Area 15, Edge, and Edge South) deposits that are associated with the Boiler Gully and Gray Creek ultramafic complexes.

One of the most significant REE deposits in Australia is **Mount Weld**, 35 km south-southeast of Laverton in the Yilgarn Craton of Western Australia. This polymetallic deposit is associated with a Paleoproterozoic carbonatite pipe-like body that has REE grades ranging from 4 to 13.8%. It is one of the richest REE deposits in the world and one of the few commercial viable operations outside China. The deposit has been subjected to a number of operational changes since it was first drilled in the late 1960s. The mining operational phase is currently being managed by Lynas Corporation Limited, with the first ore planned for processing in the concentration plant in 2011. The Mount Weld deposit features on the cover of this publication. The presence of a prominent circular magnetic anomaly high (see Inset of Fig. 5.5) was highlighted from a regional aeromagnetic survey carried out by the Bureau of Mineral Resources in 1966. Interpretation of aeromagnetic data by Utah Development Company and modelling of gravity data collected by Union Oil Development Corporation indicated a vertical cylindrical body comprising a high-density core 3 to 4 km in diameter, surrounded by a 0.5 km-wide annulus of lower density rock. The presence of carbonatite was confirmed in 1967 by core drilling by the Utah Development Company (Duncan and Willett, 1990). The carbonatite pipe has no surface expression due to Quaternary alluvium cover. Drilling programs by Union Oil Development Corporation from 1981 to

1984 outlined polymetallic REE, niobium, tantalum, zirconium, and phosphorous mineralisation in the regolith above the carbonatite. A number of feasibility studies from 1980 to 2002 have investigated the potential of phosphate-rich mineralisation derived from apatite concentrations as a source for fertilizer. Lynas Corporation Limited undertook further REE resource assessments from October 2001 when it obtained 100% acquisition of the Mount Weld project from Anaconda Industries Limited. Feasibility studies completed in 2005 showed that the open-cut mine had 2.8 million tonnes of proved and probable reserves at 15.5% REO ore during the first 14 years of mine life. Inclusion of low-grade ores and further metallurgical tests will result in a mine life in excess of 20 years. Lynas Corporation Limited announced in December 2006 that a proposed $220 million plant to carry out final separation and product enhancement would be built at Gebeng on the east coast of Malaysia (Fetherston, 2008). In late 2007, mining operations had commenced and plans were in place to build a concentration plant at Mount Weld. By March 2008, over 2.0 Mm^3 of overburden had been removed from the open-pit, and 0.32 Mm^3 of ore had been mined, graded, and stockpiled. The mining initially focused on a central high-grade secondary monazite zone. In September 2010, Lynas Corporation Limited announced that the Central lanthanide deposit had a Measured, Indicated, and Inferred Resource of 9.88 million tonnes with total lanthanide rare-earth oxides (TLnREO) at 10.6% and 990 ppm Y_2O_3 (HREO), and the Duncan HREE deposit had a Measured, Indicated, and Inferred Resource totalling 7.62 Mt @ 4.5% TLnREO and 2570 ppm Y_2O_3. Forge Resources in March 2011 acquired the niobium-tantalum (Crown) and phosphate (Swan) resources from Lynas Corporation Limited. Further descriptions of the Mount Weld REE deposit are provided in Section 3.3.1.

Other prominent magnetic anomalies similar to the anomaly at Mount Weld have been explored for REE deposits in the eastern Yilgarn Craton. Preliminary geophysical modelling by Southern Geoscience Consultants (unpublished SGC Report 2148, 25-01-2010) suggests that the **Mount Barrett** magnetic anomaly, ~150 km northeast of Laverton, may be prospective for Mount Weld-style REE mineralisation. 3D inversion modelling of the undrilled Mount Barrett anomaly indicates a ~1.5 km-wide body with the depth to the top of the body ranging from 300 to 500 m (Carew and Craven, 2010).

Geophysical comparisons to Mount Weld have also been made for the coeval **Ponton Creek** (previously called Cundeelee) carbonatite plug near Cundeelee Mission, 180 km east-northeast of Kalgoorlie, Western Australia (Lewis, 1990). Exploration commenced in the Cundeelee Mission region in the 1970s targeting sandstone-hosted uranium mineralisation. In 1986, a hole drilled by Union Oil intersected serpentinised pyroxenite at 557 m. In 1994, aerial and ground magnetic and radiometric surveys undertaken by Herald Resources Limited outlined a strong radiometric anomaly in addition to several magnetic anomalies. Surface sampling and small pits dug over the radiometric anomaly in 1995 produced strongly anomalous results up to 23% REO (Cassidy et al., 1997). Galaxy Resources Limited reported in 2011 (http://www.galaxyresources.com.au/projects_ponton.shtml) that Herald Resources completed an air-core drilling program with the best drill intersections being: 16 m @ 14.48% REO (all lanthanide elements plus Y), and 28 m @ 10.50% REO, including 8 m @ 13.12% REO. Further drilling identified a 10 km-wide central core of alkaline ultramafic cumulates (mostly olivine pyroxenite). In contrast to the Mount Weld Carbonatite, there is no development of a paleo-regolith profile due to the scouring of the complex by Permian glaciation (Lewis, 1990).

Exploration in the Kimberley region of Western Australia has also defined several carbonatite bodies with associated REE mineralisation. The **Cummins Range Carbonatite** is a sub-vertical, zoned stock, located near the junction of the Halls Creek and King Leopold orogens (Andrew, 1990). CRA Exploration Proprietary Limited (CRAE) discovered the carbonatite complex in 1978 when they ground tested a 4900 nT (nT: nanotesla is a unit of magnetic field) aeromagnetic anomaly that extended over ~1.8 km. The carbonatite is also associated with a radiometric anomaly (Dentith et al., 1994). Uranium enrichment in the regolith is believed to be the source of this anomaly. Subsequent ground magnetics revealed internal curvilinear patterns which were to be confirmed by drilling to be concentric lithological zones within a roughly circular carbonatite complex. The carbonatite is deeply weathered and covered by a thin layer of aeolian soil. A central core of carbonatite is enclosed by carbonated, mica-rich pyroxenite, passing outwards into an outer zone of unaltered pyroxenite that constitutes about 60% of the intrusion. Coarse magnetite and exfoliating flakes of mica were found at surface, and a few small isolated outcrops of silicified breccia occurred near the centre of the intrusive. High cerium concentrations were recorded in a drill hole near the margin of the body, and the exploration program changed from the initial focus of kimberlites and diamonds to regolith-hosted

REE. From 1978 to 1984, CRAE explored the area drilling 3240 m of auger, rotary air blast, air core, and percussion drilling in 187 holes in addition to 804 m of diamond drilling in two holes. The widely spaced shallow drilling program confirmed the deposit consisted primarily of apatite and monazite, and it had a resource of 3 to 4 million tonnes grading 2 to 4% REO (Fetherston, 2008). Between 2002 and 2006, Navigator Resources Limited carried out surveying and reviewed all historical data. Navigator Resources in 2007 completed 464 m of air-core drilling in 21 holes and 9293 m of RC drilling in 93 holes within the central carbonatite zone. In September 2009, the company reported an Inferred Resource of 4.17 Mt @ 1.72% TREO, 11.0% P_2O_5, 187 ppm U_3O_8, and 41 ppm Th at a cut-off grade of 1% TREO. Economically important abundances of Nb, Ta, Zr, and Ti have also been reported. The deposit is similar to that at Mount Weld with an indicative mix of predominantly LREE from CeO_2 (47.5%), La_2O_3 (27.6%), Nd_2O_3 (16.2%), Pr_6O_{11} (5.0%), Sm_2O_3 (1.7%), to Gd_2O_3 (1.0%) (Navigator Resources, 2007). Figure 3.32 shows a schematic section of the mineralised regolith profile and significant drill-hole intersections at Cummins Range (http://www.navigatorresources.com.au/files/files/742_Investor_Mining_2010_Brisbane _PPR_v1.pdf).

The **Yungul** carbonatite dykes in the East Kimberley of Western Australia are massive calcite carbonatites that host very coarse, pegmatitic veins and pods of calcite (Gwalani et al., 2010). The dykes have carbonatised and fenitised the ~1790 Ma Hart Dolerite country rocks. The Yungul carbonatites are spatially associated with epithermal fluorite deposits that contain resources of 6.7 Mt @ 24.6% CaF_2. In contrast to other calcite-dominant carbonatites, the TREE contents of the Yungul carbonatite are low (174.0–492.8 ppm; La/Yb 2.28–10.74: Gwalani et al., 2010).

The **Mordor** Complex (Langworthy and Black, 1978; Barnes et al., 2008) in the eastern Arunta Region of the Northern Territory is a composite plug-like alkaline-ultramafic body that has been explored for REE, PGEs, Ni, Cu, Cr, diamonds, vermiculite-phlogopite, and uranium. The alkaline felsic rocks and discordant carbonate-rich dykes have been a focus for REE exploration over several decades. Barnes et al. (2008) reported maximum REE concentrations in alkaline syenite and apatite pyroxenite of 175.2 ppm La, 374.3 ppm Ce, 48.2 ppm Pr, 188.7 ppm Nd, 36.0 ppm Sm, and 25.5 ppm Gd. Stratabound PGE mineralisation (8 m @ 0.67 ppm Pt+Pd+Au) hosted by cyclic sequences of ultramafic rocks (Barnes et al., 2008), and base-precious mineralisation (1 m @ 1.4% Cu, 0.3% Ni, 0.4 ppm Pt+Pd, and 0.1 ppm Au) at the Braveheart ironstone on the southeast margin of the intrusion highlight the polymetallic character of the complex.

Other minor carbonatite bodies (Table 3.14) throughout the Precambrian Australian Shield have created various levels of exploration interest (Jaques, 2008). However, for most of these occurrences the carbonatite complexes are generally small in size, and TREE abundances are low or have not been reported. Such examples include the 1821 Ma Copperhead alkaline intrusion (Halls Creek Orogen, WA), **Walloway** suite of Jurassic dykes and plugs (Gawler Craton, SA), 732 Ma **Mud Tank Carbonatite** (Arunta Region, NT), and carbonatite veins from the **Granny Smith** and **Wallaby** gold mines (Yilgarn Craton, WA).

1980 to 1990:

In the 1980s, Lachlan Resources NL explored for PGE mineralisation in the **Gilgai intrusion**, 20 km west-southwest of Nyngan in central New South Wales. The Gilgai intrusion is one of several 'Alaskan'-type mafic-ultramafic bodies which intrude Cambrian-Ordovician metasedimentary rocks of the Girilambone Group. The intrusion is covered by up to 50 m of Cenozoic alluvial material. Airborne and ground magnetic surveys were used to delineate the poorly exposed intrusion and rotary-air blast (134 holes) and diamond (2 holes) drilling defined a range of 'alkaline' rock types including monzonite, hornblendite, pyroxenite, olivine pyroxenite, dunite, and peridotite. Jervois Mining Limited obtained the sample pulps from a drilling program undertaken for nickel in 1999–2001 and showed that there was significant enrichment of scandium in the laterite above the Gilgai intrusion. Jervois Mining Limited is currently targeting the scandium resources at the Nyngan Gilgai laterite deposit that was previously explored by Platsearch NL. The laterite zone is locally up to 40-m thick, layered, and comprises hematitic clay at the surface, followed downwards by limonitic clay, saprolitic clay, weathered bedrock, and finally fresh mafic-ultramafic rocks. Scandium is concentrated in the hematitic, limonitic, and saprolitic zones, with values attaining 350 ppm. Further drilling (69 holes) in 2006 determined a JORC-compliant resource (as of 2nd of August 2010), using a 100 ppm Sc cut-off, consisting of a: Measured Resource of 2.718 Mt @ 274 ppm Sc; Indicated Resource of 9.294 Mt @ 258 ppm Sc; and a Total Resource of 12.012 Mt @ 261 ppm Sc (http://www.resourceinvestor.com/News/2010/2/Pages/EMC-Metals-will-develop-Rare-Earth-Scandium-Deposit.aspx).

In similar geological settings to the Gilgai intrusion, high grades of scandium have been found in a number

of 'Alaskan'-type mafic-ultramafic bodies in the Nyngan–Fifield district. It was reported (Financial Review, 31st July 1998) that Uranium Australia found scandium grades ranging from 19.8 g/t to 370 g/t in the **Syerston** nickel-cobalt laterite project near Fifield. The project contains 76.8 Mt @ 0.73% Ni and 0.13% Co, with significant PGE credits. The laterite is developed over the Tout intrusion, an ultramafic-mafic complex comprising a serpentinised dunite core surrounded by pyroxenite, gabbro, and diorite. The laterite profile is best developed over the dunite core, where it averages 35 m in thickness. Laterite overlying the pyroxenite is thinner and has elevated cobalt, but relatively low nickel grades. Platina Resources Limited in late 2010 reported that the surficial laterite above the **Owendale intrusion**, 10 km north of Fifield, contains elevated cobalt, nickel, copper, and scandium. Best drill intersection in the laterite was 9 m @ 0.3% Co, 0.3% Ni, and 514 g/t Sc (http://new.platinaresources.com.au/projects/fifield/).

Four nickel-cobalt laterite deposits extending over a strike length of 30 km have been explored by Jervois Mining Limited at **Thuddungra**, about 25 km northwest of Young, New South Wales. Regionally the host serpentinite rocks extend from at least Grenfell in the north to Tumut in the south, a distance of ~150 km. Airborne and ground magnetics and local serpentinite outcrops led to the discovery of the laterites virtually concealed by alluvium. Since the underlying serpentinite source rocks are strongly magnetic, the exploration procedure was to locate the magnetic anomalies and pattern drill them. A combined resource for the deposits amounts to 168 Mt @ 0.72% Ni and 0.07% Co, with additional significant scandium credits (~40 g/t in representative mineralised bulk samples). The source of the Ni-Co-Sc mineralisation is the Cambrian Wambidgee Serpentinite. The serpentinites (harzburgite protoliths) have intruded the Jindalee Beds as north-trending elongated bodies associated with faulting. In the Young–Cootamundra area, the ultramafic rocks are flanked on the eastern side by the Silurian Young Granodiorite. This felsic body is interpreted to have played an important role in the formation of the mineralised laterites. Water run-off in the region is from east to west (away from the Great Dividing Range) and the acid-rich ground water chemically leached the mafic components of the serpentinites, removing silica, magnesium, and other soluble elements, and leaving a laterite enriched in iron, aluminium, nickel, cobalt, and scandium. The mineralised laterites formed from the weathering of the serpentinite during the Cenozoic. The laterite profile is zoned downwards from hematitic (pisolitic) clay at the surface, to limonitic clay, saprolite (smectitic clay), with weathered serpentinite at the base. Scandium is enriched in the upper parts of the profile, cobalt in the middle, and nickel in the weathered serpentinite and saprolite zones. (http://www.jervoismining.com.au/index.cfm?siteaction=tenement&tenementid=1 and http://www.dpi.nsw.gov.au/__data/assets/pdf_file/0011/316838/Nickel.pdf).

Exploration activities have defined nickel, cobalt, and scandium resources in laterites at **Lake Innes**, near Port Macquarie, New South Wales (Douglas McKenna and Partners Proprietary Limited, 2003). Serpentinite complexes occur in a Permian fault zone in Silurian–Devonian country rocks. Locally, over the serpentinite complexes, laterites containing weathered serpentinite, saprolite, limonitic clay, and hematitic clay, range in thickness from 10 m to 30 m. Scandium is enriched in the upper part of the lateritic profile, whereas cobalt and nickel are found in the middle and lower parts of the profile. The deposits contain 15.7 million tonnes of Ni at 1.46% Ni, 0.09% Co, and 41 ppm scandium (http://www.dpi.nsw.gov.au/__data/assets/pdf_file/0016/238201/RareEarth.pdf).

Between 1986 and 1988, twelve REE prospects were evaluated by reconnaissance drilling at **Yangibana**, 280 km east-northeast of Carnarvon, in the Gascoyne Complex of Western Australia (Fetherston, 2008). REE were associated with anomalous base-metal concentrations in a tightly folded ironstone-dyke sequence. The dykes crop out over an area of 500 km^2 and were later explored in the early 1990s by Grenfell Resources NL. The Yangibana prospect has a recorded resource of 3.5 Mt @ 1.7% REO. The REE are in coarse-grained monazite containing up to 20% Nd_2O_5 and 1600 ppm Eu_2O_3. Artemis Resources Limited reported in its December 2009 quarterly report that it had acquired the Yangibana REE prospect.

In January 1987, it was announced that the French chemical company Rhone-Poulenc would build a two-stage monazite processing plant at **Pinjarra** in Western Australia to produce REE from monazite, but the project was suspended. Deckhand Proprietary Limited, a wholly owned subsidiary of Currumbin Minerals, was blocked in 1988 on environmental grounds from establishing a REE processing plant at **Lismore**, New South Wales. SX Holdings Limited of South Australia was planning to establish a plant at **Port Pirie** to process monazite with a 2000 tonnes per annum cracking and separation plant but the project did not proceed.

The **John Galt** and adjacent **Corkwood Yard** REE deposits are located near the western end of the Osmond Range, about 120 km north-northeast of

Halls Creek in the East Kimberley. REE mineralisation at John Galt consists of disseminations of xenotime in lithic quartz sandstone of the Proterozoic Red Rock Formation. Inferred resources at the Corkwood Yard deposit, which is an alluvial occurrence, are 0.359 Mt @ 0.001% REO (Ceplecha, 1988). Limited exploration activities have occurred at these deposits since these resource estimates.

A review of REE in the Northern Territory by Eupene Exploration Enterprises Proprietary Limited in 1989 provides an insight into the search for REE prior to the discovery of the Nolans Bore REE-P-U-Th deposit in 1995. The company reported that no significant occurrences or deposits of REE (and Y) were identified in the Northern Territory. Elevated levels of REE were recorded in six geological provinces, namely the **Pine Creek Orogen, Davenport Province, Southern McArthur Basin–Murphy Inlier, Arunta Region, Birrindudu Basin**, and the **Musgrave Block**.

1990 to present:

The **Nolans Bore** REE-P-U-Th deposit in the Reynolds Range of the Arunta Region, Northern Territory, is one of Australia's most important and advanced REE developments. Mineralisation at Nolans Bore was discovered in 1995 when PNC Exploration (Australia) Proprietary Limited followed up an airborne radiometric anomaly as part of a uranium exploration program (Thevissen, 1995). A literature review in 1999 of exploration results in the area highlighted the polymetallic potential of the prospect. Surface sampling by Arafura Resources Limited indicated high REE abundances (averaging about 7% TREE) were associated with massive fluorapatite, which occurs as veins and forms 53–93% of the rock (Hussey, 2003). A ground radiometric response coincided with the apatite that cropped out sporadically over an area of ~800 by 1700 m. Drilling in 2001 outlined an Inferred Resource of REE-bearing fluorapatite mineralisation of 3.8 million tonnes at a grade of 3.8% acid-soluble REE within 100 m of the surface. Arafura Resources Limited is conducting a definitive feasibility study on the Nolans Bore project and, in July 2010, reported that it is on track to commence production in 2013.

The development of the Nolans Bore REE-P-U-Th deposit in the Northern Territory has stimulated recent exploration interest in the REE prospectivity of the central Australia region. Uranium explorers found numerous pegmatite, breccia, vein, and alteration-hosted REE occurrences in the **Harts Range** and **Plenty River** mica fields and over large areas near Arltunga. Hussey (2003) describes the different styles of REE mineralisation and the potential of the Arunta Region to host major REE deposits. Some of the more important REE occurrences he describes include: **Blueys Folley, Origin Hill,** and **Entia** pegmatite group (pegmatite-related); **Mount Finniss** (leucosome or metasomatic pod); **Hosteins** and **Mary River** (hydrothermal veins); and **Quartz Hill** (metasomatic). Most of the several hundred occurrences of REE compiled by Hussey (2003) for the eastern Arunta Region appear to be small and uneconomic, however, only a few of them have been fully evaluated.

Capital Mining Limited have undertaken geological mapping, surface sampling, ground radiometric surveying, bulk sampling, and metallurgical analysis at the **Narraburra** REE deposit near Temora in central New South Wales. In 2006, RC drill testing of a deeply weathered granitic intrusive with relatively high Zr, Hf, Nb, Th, and REE in a 1500 m by 800 m zone generated interest. Follow up air-core drilling in 2008 closed off the main mineralised zone. An Inferred JORC compliant oxide resource of 55 Mt @ 1500 g/t Zr, Y, Nb, Th, Li, and REO, containing 55 000 tonnes zirconium oxide and 16 000 tonnes REO has been estimated as of 18 January 2011 (http://www.capitalmining.com.au/narraburra.html; http://www.capitalmining.com.au/Announcements/CMY_145_Notice_18Jan2011.pdf).

Resampling of historical drill core by Alligator Energy Limited (AGE) defined a REE-bearing alteration halo peripheral to the uranium mineralisation at the **Caramel** uranium prospect, 20 km south of the Nabarlek uranium deposit in the Pine Creek Orogen, Northern Territory. The uranium potential of the region was initially highlighted by regional rock geochemical programs undertaken by Uranerz in the mid-1980s. Best drill-hole intersections reported by AGE were 4 m @ 5094 ppm TREE and 5 m @ 7351 ppm TREE, including 2 m @ 1.16% TREE. The mineralisation is dominated by the LREE La, Ce, and Nd. In 1987, Uranerz also defined TREE abundances of 2.48%, 3.27%, 2.08%, and 1.59% from 2 km east of the Two Rocks prospect. Mineralisation is dominantly La, Ce, Nd, and Pr, with lesser Y, Gd, and Sm (http://www.asx.com.au/asxpdf/20110309/pdf/41xb5z56bnxm3k.pdf).

Crossland Uranium Mines Limited has obtained anomalous REE concentrations in a stream sediment and drilling program at their **Charley Creek** Project near Mount Chapple in the Arunta Region, Northern Territory. Stream-sediment concentrates from the Cattle Creek prospect consisted of 3 samples >32% TREO (maximum value of 38.4% TREO); 12 samples >16% TREO; 25 samples >8% TREO, 45 samples >4% TREO, and 74 samples exceeded 2% TREO. Re-assaying of unweathered bedrock in drill core returned a 5 m intersection of 1.03% TREO and 0.103% Y_2O_3,

with the HREO representing 8.3% of the TREO (http://www.crosslanduranium.com.au/LinkClick.aspx?fileticket=AemQBpNli3I%3d&tabid=3280&mid=5687).

The Territory Uranium Company (TUC) has recently identified fluorite- and sulphide-bearing shales enriched in REE at the **Quantum** uranium-REE prospect south of the Rum Jungle uranium field in the Pine Creek Orogen of the Northern Territory (http://www.territoryuranium.com.au/images/stories/PDFs/tuc_asx_110321_qtm%20second%20phase%20results.pdf). The following description of this uranium-REE prospect is mostly from Bamborough (2011). Interest in the area was initiated in early 2010, when a review of historical company data and an interpretation of open-file aeromagnetic and radiometric data by TUC identified several potential exploration targets. The prospective stratigraphy of the region comprises the Paleoproterozoic Finniss River Group and older Proterozoic sedimentary rocks of the Mount Partridge Group. Both groups are known to host unconformity-related vein-type uranium ± gold mineralisation. Historic mines in the area have produced 19.7 tonnes of U_3O_8. The mineralisation is associated with gossanous outcrops and faults within folded sedimentary rocks. Gamma-ray spectrometer examination of historic drill core in the Northern Territory Geological Survey core library by TUC led to the identification of several zones of uranium mineralisation. Geochemical analysis of the core returned an intersection of 0.5 m @ 4224 ppm U_3O_8. Zinc-bismuth mineralisation was also identified, with an intersection of 3.4 m @ 4.84% Zn, including 0.9 m @ 15.6% Zn and 1.4 m @ 0.07% Bi. The historic drilling confirmed the presence of fertile rocks under 40 to 120 m of Cambrian basinal sedimentary rocks. The first hole of a drill program in September 2010 tested a weak, 4.5 km-long, airborne radiometric anomaly near the historic mineralised hole and intersected 50 m of quartz/fluorite veining and sulphide mineralisation in a black carbonaceous shale unit, correlated with the Gerowie Tuff. The co-existence of fluorite, pegmatite vein systems, low-level radioactive anomalies, and unusual sulphide mineral assemblages refocused the exploration programs towards REE. A high-grade zone of 9.2 m @ 3.78% TREO was intersected within a 21.9 m-wide zone assaying 2.55% TREO. Average proportions of 11% neodymium, 4%, praseodymium, and 0.2% dysprosium plus europium, collectively totalled about 15%. The REE-bearing mineral allanite, hosts the secondary REE-bearing minerals bastnäsite and synchysite, which occur within veins and fissures, or as rims to allanite crystals in a hydrothermal vein and alteration system. These minerals have been documented in other well-known REE deposits, such as Mountain Pass, USA, and Hoidas Lake, Canada. Gold, uranium, zinc, silver, and bismuth are also associated with the REE highlighting the potential of the Quantum region for polymetallic hydrothermal mineralisation. Mineralogical studies suggest a granitic association for the mineralising fluids with gravity gradient data under the Daly Basin indicating a possible deep-seated ?Archean granite beneath the Quantum prospect. (http://www.territoryuranium.com.au/images/stories/PDFs/quarterly%20report%20tuc%20dec%202010_final.pdf).

In late 2009, TUC also discovered the **Energy** prospect, ~70 km south of the Quantum uranium-REE prospect, Northern Territory. A significant zone of yttrium mineralisation was found to be associated with uranium and minor REE in a shallow dipping weathered sandstone unit. A best intersection of 7 m @ 1% Y + TREO (72% Y) was reported for this sandstone-hosted uranium-REE occurrence (http://www.territoryuranium.com.au/images/stories/PDFs/quarterly%20report%20tuc%20dec%202010_final.pdf).

The Northern Territory Geological Survey discovered in 2006 a group of dykes hosting anomalous REE in the **Hale River** region in the southeastern corner of the Northern Territory. The Hale River area is underlain by the Casey Inlier, which is composed of Proterozoic mafic and felsic gneiss, and deformed ultramafic and mafic rocks. A rock sampling program (~174 samples) by Kidman Resources identified 8 zones of REE mineralisation, with 16 samples exceeding 0.32% TREE + Y_2O_3, and the maximum value attaining 1.66% REE + Y_2O_3. Secondary copper mineralisation (up to 27% Cu) occurs in 1 to 3 m-wide carbonate-rich veins at the Arthur Popes prospect (http://www.kidmanresources.com.au/hale_river.html).

Xenotime (REE-Y-bearing phosphate mineral) was first identified in the western Brown Range Dome in the Northern Territory in the1980s by the Japanese nuclear energy organisation PNC Exploration while exploring for uranium. The **Browns Range** Project is located in the Tanami region on the Western Australia–Northern Territory border, 150 km southeast of Halls Creek in Western Australia. The Paleoproterozoic dome consists of a granitic core intruding the Archean–Paleoproterozoic Browns Range Metamorphics (meta-arkose, feldspathic metasandstone, and schist). The dome and its aureole of metamorphics are surrounded by the Mesoproterozoic Gardiner Sandstone of the Victoria–Birrindudu Basin. Xenotime mineralisation (up to 16% Y, 0.2% U, 0.5% LREE, and 12% HREE) at the Area 5 Prospect is hosted by 10 to 30 cm-wide,

15 m-long quartz veins. Unusually high concentrations of HREE have recently been reported by Northern Minerals, 4 km to the north-northeast of the Area 5 prospect. Xenotime concentrations up to 4% occur in a hydrothermal quartz stockwork mineralising system. Hymap hyperspectral airborne mapping and airborne radiometrics the quartz stockworks and associated alteration clay signature. Based on anomalous uranium radiometrics have identified the REE target zone is open in several directions and extends over some 9 km (http://www.northernuranium.com.au/index.php/rare_earths/browns-range).

A group of prospects (**Green Valley, Florence Bore, Sterling, QMH**) managed by ActivEx Limited, located about 55 km southeast of the Mary Kathleen REE prospects, Queensland (described above), have elevated concentrations of HREO/TREO. Highest concentrations of TREO in rock samples occur in the Green Valley and Sterling prospects, and the highest proportion of HREO occur at Florence Bore. Rock samples from Florence Bore North returned 4538 g/t TREO with a 64% HREO/TREO ratio. The HREO are associated with copper-gold-cobalt mineralisation, with hydrothermal fluids possibly transporting the HREO by the formation of halide (chloride and fluoride) and hydroxide complexes (http://www.activex.com.au/reports/2010-11/AIV_20110301_ASX_Announ_Cloncurry_REO.pdf).

Callabonna Uranium Limited located anomalous REO in rock chips at the **Gilbert River** REE prospect in the Georgetown Inlier of northern Queensland. Reconnaissance follow up of radiometric anomalies found the radiometric response was due to heavy-mineral concentrates in basal Jurassic sandstones. Samples of these often ferruginous sandstones returned high TREO (1.93%) with moderate uranium values up to 311 ppm U_3O_8 (http://www.callabonna.com.au/?LinkServID=BCF6EC46-D481-6E25-5828A4FA6343647D&showMeta=0).

Spectrometer surveys by Jervois Mining Limited over **Lake Barlee** in southwest Western Australia indicate the area is anomalous in uranium, potassium, and thorium, and iron-rich laterites (48% Fe) were identified. The Geological Survey of Western Australia reported that a ferruginous sample from the Lake Barlee region, as part of a regional laterite geochemical survey over the western Yilgarn Craton, obtained 2640 ppm Ce, with anomalous europium, lanthanum, thallium, lead, barium, and cobalt. Consequently, Jervois Mining Limited has recently changed their exploration focus to include REE, iron, and base metals (http://www.jervoismining.com.au/uploaditems/reports/20110131%20Quarterly%20Report%20to%2031%20December%202010.pdf).

Ground truthing of prospective areas with high uranium signatures identified in ground spectrometer surveys in the northern Gawler Craton, South Australia, has defined elevated REE abundances associated with other metals. Mineralised ferruginised mafic dykes, quartz veins, and zones of silicification traverse Early Proterozoic metamorphic rocks that are overlain by Late Proterozoic (Adelaidean) rocks. Reedy Lagoon Corporation Limited has located weathered rocks with up to 3.92% TREE + Y at the **Victory** uranium-REE prospect near Edward Creek, northern Gawler Craton. The samples are enriched in uranium (up to 412 ppm) and are described as fine-grained, intensely weathered kaolinised rocks. The presence of mineralisation (0.56% TREE + Y, 1320 ppm Cu, 60.3 ppm U, 1250 ppm Co, 361 ppm Zn, 7.87% Mn) in weathered metamorphic rocks at the Victory prospect, which represents secondary enrichment near the surface due to weathering effects, may indicate a primary mineralised source at depth http://www.reedylagoon.com.au/downloads/ASX_10-10-12_Edward%20Creek.pdf.

The **Carrapateena** copper-gold project is located 100 km southeast of the world-class Olympic Dam deposit on the eastern margin of the Gawler Craton, South Australia (http://www.ozminerals.com/Media/docs/ASX_20110309_OZAcquiresCCP-b7c5f474-aba2-4272-a397-619d68a286de-0.pdf). This iron-oxide copper-gold deposit has many geological similarities to the Olympic Dam and Prominent Hill deposits. Carrapateena was discovered in 2005 by Rudy Gomez (RMG Services), whose exploration program was funded in collaboration with the South Australian Government's 'Plan for Accelerating Exploration' (PACE) incentive program. Geophysical (gravity and aeromagnetics) and structural lineament studies played important roles in the discovery of these deposits. Carrapateena is hosted in a Proterozoic brecciated sequence comprising conglomeratic sediments with clasts and fragments of granite, gneiss and vein quartz, and altered dolerite and felsic dykes. Copper is mostly chalcopyrite in veins and as blebs and bornite forms a discrete high-grade zone. Mineralisation has been intersected over a vertical height of approximately 1000 m, the deposit is roughly cylindrical and its top is located 470 m below barren sedimentary rock. Copper, gold, silver are the dominant metals, with significant quantities of uranium, iron (hematite), and REE. The mineralisation is interpreted to be controlled by the intersection of north-northwest–south-southeast-trending structures and east-west-trending structures.

One of the early drill-hole intersections that created much interest was 905 m @ 2.17% Cu, 0.9 g/t Au, 11.5 g/t Ag, 255 ppm U and 38.8% Fe, including 82 m @ 4.78% Cu and 1.1 g/t Au. LREE abundances in DDH CAR002 are 178.2 m @ 0.21% Ce and 0.13% La, with the major components being 1.83% Cu and 0.64 g/t Au. An inferred resource (calculated from 33 drill holes totalling 45 504 m on the southern part of the deposit), stands at 203 Mt @ 1.31% Cu, 0.56 g/t Au, 270 ppm U_3O_8, and 6 g/t Ag, for a contained 2.7 million tonnes of Cu, 3.7 Moz Au, 120.9 million pounds of U_3O_8, and 39.2 Moz of Ag, based on a 0.7% copper cut-off grade (http://www.ozminerals.com/Media/docs/ASX_20110414_March2011_Quarterly-Report-9ef5527d-ae2d-4486-9c02-a1acac16f1f2-0.pdf).

APPENDIX 8. RARE-EARTH-ELEMENT DEPOSITS AND PROSPECTS IN AUSTRALIA (SOURCE OF DATA OZMIN[1])

Name	State	Operating status	Longitude	Latitude	Commodities	Mineral-system association	Mineral system group	Deposit type
Alice Springs	NT	Mineral deposit	133.8679383	-23.695682	Rare-earth oxides	Magmatic	Magmatic-hydrothermal	Apatite and/or fluorite vein
Ambergate	WA	Mineral deposit	115.340088	-33.701553	Rare-earth elements	Basinal	Placer	Heavy-mineral sands (Beach)
Angourie	NSW	Unknown	153.268	-29.815	Ilmenite, rutile, zircon, (monazite)	Basinal	Placer	Heavy-mineral sands (Beach)
Atlas	NSW	Mineral deposit	143.35	-33.883333	Rutile, zircon, ilmenite, leucoxene, uranium	Basinal	Placer	Heavy-mineral sands (Beach)
Avonbank	VIC	Mineral deposit	142.32	-36.62	Zircon, rutile, ilmenite, (leucoxene)	Basinal	Placer	Heavy-mineral sands (Offshore shallow marine)
Barda	NSW	Mineral deposit	142.836	-33.54	Rutile, zircon, ilmenite, leucoxene	Basinal	Placer	Heavy-mineral sands (Beach)
Beenup	WA	Historic mine	115.2643219	-34.235112	Ilmenite, zircon, leucoxene	Basinal	Placer	Heavy-mineral sands (Offshore shallow marine?)
Benbow	NSW	Mineral deposit	142.7342827	-33.829501	Rutile, zircon, ilmenite, leucoxene	Basinal	Placer	Heavy-mineral sands (Beach)
Bidaminna	WA	Mineral deposit	115.6033936	-31.100482	Ilmenite, leucoxene, rutile, zircon	Basinal	Placer	Heavy-mineral sands (Beach)
Birthday Gift	NSW	Mineral deposit	142.9166899	-33.480284	Zircon, rutile, ilmenite, mineral sands, leucoxene	Basinal	Placer	Heavy-mineral sands (Beach)
Blind Pew	NSW	Mineral deposit	142.67565	-33.711064	Zircon, ilmenite, rutile, leucoxene	Basinal	Placer	Heavy-mineral sands (Beach)
Boambee	NSW	Unknown	153.11553	-30.3341	Ilmenite, rutile, zircon, (monazite)	Basinal	Placer	Heavy-mineral sands (Beach)
Bribie Island N.P.	QLD	Mineral deposit	153.1699798	-27.04681	Rutile, zircon, ilmenite, monazite, mineral sands	Basinal	Placer	Heavy-mineral sands (High dune)
Brigantine	NSW	Mineral deposit	142.8	-33.65	Rutile, zircon, ilmenite, leucoxene	Basinal	Placer	Heavy-mineral sands (Beach)
Broadwater N.P.	NSW	Unknown	153.432392	-29.024825	Ilmenite, rutile, zircon, magnetite, (monazite)	Basinal	Placer	Heavy-mineral sands (High dune)

Name	State	Operating status	Longitude	Latitude	Commodities	Mineral-system association	Mineral system group	Deposit type
Brockman	WA	Mineral deposit	127.7820325	-18.319196	Rare-earth oxides	Magmatic	Orthomagmatic	(Per)alkaline rocks
Brooks Bore	SA	Mineral deposit	140.75	-32.9	Ilmenite, rutile, zircon, xenotime	Basinal	Placer	Heavy-mineral sands (Beach)
Bullant–Karridale	WA	Mineral deposit	115.148163	-34.150181	Ilmenite, zircon, rutile	Basinal	Placer	Heavy-mineral sands (Beach)
Bundjalung N.P.	NSW	Unknown	153.322287	-29.428164	Ilmenite, rutile, zircon, (monazite)	Basinal	Placer	Heavy-mineral sands (High dune)
Bunker Bay	WA	Mineral deposit	115.043976	-33.545716	Ilmenite, zircon, (leucoxene)	Basinal	Placer	Heavy-mineral sands (Beach)
Byfield	QLD	Mineral deposit	150.6999876	-22.796865	Rutile, zircon, ilmenite, monazite, mineral sands	Basinal	Placer	Heavy-mineral sands (High dune)
Byrnes Tank	NSW	Mineral deposit	142.8	-33.64	Zircon, rutile, ilmenite, leucoxene	Basinal	Placer	Heavy-mineral sands (Beach)
Calypso	WA	Mineral deposit	115.3423167	-30.550886	Rare-earth elements	Basinal	Placer	Heavy-mineral sands (Channel)
Campaspe	NSW	Mineral deposit	143.34	-33.79	Zircon, rutile, ilmenite	Basinal	Placer	Heavy-mineral sands (Beach)
Capel North	WA	Mineral deposit	115.585724	-33.520386	Ilmenite, zircon, (rutile, leucoxene)	Basinal	Placer	Heavy-mineral sands (Beach)
Cavalier	NSW	Mineral deposit	142.72	-33.83	Zircon, rutile, ilmenite, leucoxene	Basinal	Placer	Heavy-mineral sands (Beach)
Coburn	WA	Mineral deposit	114.126953	-26.70377	Ilmenite, zircon, rutile, leucoxene	Basinal	Placer	Heavy-mineral sands (Beach)
Coliban	NSW	Mineral deposit	143.08	-33.93	Zircon, rutile, ilmenite, leucoxene	Basinal	Placer	Heavy-mineral sands (Beach)
Cooglegong	WA	Mineral deposit	119.4167	-21.5834	Ti, Nb, rare-earth elements	Magmatic	Orthomagmatic	Pegmatite
Cooljarloo	WA	Operating mine	115.413696	-30.625429	Ilmenite, zircon, rutile, leucoxene, mineral sands	Basinal	Placer	Heavy-mineral sands (Beach)

Name	State	Operating status	Longitude	Latitude	Commodities	Mineral-system association	Mineral system group	Deposit type
Cooljarloo JV (Atlas, Telesto, Titan)	WA	Mineral deposit	115.42978	-30.62985	Zircon, ilmenite, rutile, (leucoxene)	Basinal	Placer	Heavy-mineral sands (Beach)
Cooljarloo North	WA	Mineral deposit	115.2333333	-30.533333	Rare-earth elements	Basinal	Placer	Heavy-mineral sands (Beach)
Cooloola N.P.	QLD	Mineral deposit	152.9999814	-26.126816	Rutile, zircon, ilmenite, monazite, mineral sands	Basinal	Placer	Heavy-mineral sands (High dune)
Coolup	WA	Mineral deposit	115.93924	-32.769043	Rare-earth elements	Basinal	Placer	Heavy-mineral sands (Beach)
Coombah 1	NSW	Mineral deposit	141.7499891	-32.907005	Zircon, ilmenite, rutile, leucoxene	Basinal	Placer	Heavy-mineral sands (Beach)
Crayfish	NSW	Mineral deposit	142.3299771	-33.397007	Rutile, zircon, ilmenite, leucoxene	Basinal	Placer	Heavy-mineral sands (Beach)
Crowdy Bay N.P.	NSW	Unknown	152.711	-31.838866	Ilmenite, rutile, zircon, (monazite)	Basinal	Placer	Heavy-mineral sands (High dune?)
Cummins Range	WA	Mineral deposit	127.1760141	-19.285821	Rare-earth oxides, uranium, (thorium, phosphorous oxide, rare-earth elements, uranium oxide)	Magmatic	Orthomagmatic	Carbonatite
Cyclone	WA	Mineral deposit	128.1	-28.4333	Zircon, rutile, (ilmenite, leucoxene)	Basinal	Placer	Heavy-mineral sands (Beach)
Cylinder	NSW	Unknown	143.067	-34.15	Zircon, rutile, ilmenite, leucoxene	Basinal	Placer	Heavy-mineral sands (Beach)
Dardanup	WA	Mineral deposit	115.789497	-33.43029	Ilmenite, zircon, leucoxene, rutile, (monazite, rare-earth oxides, thorium)	Basinal	Placer	Heavy-mineral sands (Beach)
Dardanup (Doral)	WA	Operating mine	115.805012	-33.353732	Ilmenite, zircon, leucoxene, rutile, (monazite, rare-earth oxides, thorium)	Basinal	Placer	Heavy-mineral sands (Beach)
Dongara Project	WA	Mineral deposit	115.1665914	-29.459703	Ilmenite, zircon, rutile, leucoxene	Basinal	Placer	Heavy-mineral sands (Beach)

Name	State	Operating status	Longitude	Latitude	Commodities	Mineral-system association	Mineral system group	Deposit type
Doubloon North	NSW	Mineral deposit	142.693932	-33.746904	Rutile, zircon, ilmenite, leucoxene	Basinal	Placer	Heavy-mineral sands (Beach)
Douglas (Iluka Murray Basin)	VIC	Operating mine	141.77835	-37.104525	Zircon, rutile, ilmenite, mineral sands	Basinal	Placer	Heavy-mineral sands (Beach)
Elaine Dorothy	QLD	Mineral deposit	140.0166667	-20.8	Rare-earth oxides, uranium, uranium oxide	Magmatic	Magmatic hydrothermal	Skarn
Eneabba area (Iluka Mid West)	WA	Historic mine	115.3017944	-29.835537	Ilmenite, zircon, rutile	Basinal	Placer	Heavy-mineral sands (Beach)
Fingal-Box Beach	NSW	Unknown	152.182473	-32.738664	Ilmenite, rutile, zircon, (monazite)	Basinal	Placer	Heavy-mineral sands (Beach)
Finigans Tank	NSW	Unknown	143.067	-34.15	Zircon, rutile, ilmenite, leucoxene	Basinal	Placer	Heavy-mineral sands (Beach)
Fouracres	WA	Mineral deposit	115.577	-34.309696	Zircon, ilmenite, rutile, leucoxene	Basinal	Placer	Heavy-mineral sands (Beach)
Fraser Island N.P.	QLD	Mineral deposit	152.9999841	-25.516816	Rutile, zircon, ilmenite, monazite, Mineral sands	Basinal	Placer	Heavy-mineral sands (High dune)
Frasers REE	WA	Mineral deposit	116.3119	-23.95093	Rare-earth oxides, thorium, rare-earth elements	Magmatic	Orthomagmatic	Carbonatite
Galileo	VIC	Mineral deposit	142.4125	-34.9575	Rutile, zircon, ilmenite, (leucoxene)	Basinal	Placer	Heavy-mineral sands (Beach)
Gallipoli	NSW	Mineral deposit	142.3299779	-33.457007	Zircon, rutile, ilmenite, leucoxene	Basinal	Placer	Heavy-mineral sands (Beach)
Ginkgo	NSW	Operating mine	142.2159283	-33.371548	Zircon, rutile, ilmenite, (leucoxene)	Basinal	Placer	Heavy-mineral sands (Beach)
Gladstone–Eurimbula	QLD	Mineral deposit	151.2676818	-23.845292	Rutile, zircon, ilmenite	Basinal	Placer	Heavy-mineral sands (Unknown)
Goliath	NSW	Mineral deposit	142.97	-34.27	Rutile, zircon, ilmenite, leucoxene	Basinal	Placer	Heavy-mineral sands (Beach)
Gordon Inlet	WA	Mineral deposit	119.500366	-34.295395	Ilmenite, zircon, rutile	Basinal	Placer	Heavy-mineral sands (Beach)

Name	State	Operating status	Longitude	Latitude	Commodities	Mineral-system association	Mineral system group	Deposit type
Gray Bridge	VIC	Mineral deposit	142.962	-36.612	Zircon, rutile, ilmenite, (leucoxene)	Basinal	Placer	Heavy-mineral sands (Offshore shallow marine)
Gwindinup North	WA	Operating mine	115.725235	-33.543156	Zircon, ilmenite, (leucoxene, rutile)	Basinal	Placer	Heavy-mineral sands (Beach)
Gwindinup South	WA	Mineral deposit	115.692871	-33.562393	Ilmenite, zircon, (leucoxene, rutile)	Basinal	Placer	Heavy-mineral sands (Beach)
Happy Valley North	WA	Mineral deposit	115.716217	-33.549896	Zircon, ilmenite, (leucoxene, rutile)	Basinal	Placer	Heavy-mineral sands (Beach)
Happy Valley South	WA	Mineral deposit	115.582321	-33.697113	Zircon, ilmenite, (leucoxene, rutile)	Basinal	Placer	Heavy-mineral sands (Beach)
Hassell Beach	WA	Mineral deposit	118.396225	-34.835159	Zircon, ilmenite, rutile	Basinal	Placer	Heavy-mineral sands (Beach)
Hat Head N.P.	NSW	Unknown	153.047296	-31.055851	Ilmenite, rutile, zircon, (monazite)	Basinal	Placer	Heavy-mineral sands (High dune)
Hopelands	WA	Mineral deposit	115.906189	-32.396255	Zircon, ilmenite, rutile, leucoxene	Basinal	Placer	Heavy-mineral sands (Beach)
Inskip Point	QLD	Mineral deposit	152.9999867	-25.816815	Rutile, zircon, ilmenite, monazite, Mineral sands	Basinal	Placer	Heavy-mineral sands (Beach)
Israelite Bay	WA	Mineral deposit	123.869217	-33.600922	Ilmenite, zircon, leucoxene	Basinal	Placer	Heavy-mineral sands (Beach)
Jacinth–Ambrosia	SA	Operating mine	132.228669	-30.861125	Zircon, (rutile, ilmenite)	Basinal	Placer	Heavy-mineral sands (Beach)
Jacks Tank (Spring Hill)	NSW	Mineral deposit	143.2999796	-33.15528	Zircon, rutile, ilmenite, mineral sands, leucoxene	Basinal	Placer	Heavy-mineral sands (Beach)
Jangardup	WA	Historic mine	115.6287362	-34.359577	Ilmenite, zircon, rutile, leucoxene, Mineral sands	Basinal	Placer	Heavy-mineral sands (Beach)
Jangardup South	WA	Mineral deposit	115.656784	-34.400177	Ilmenite, rutile, zircon, leucoxene	Basinal	Placer	Heavy-mineral sands (Beach)
John Galt	WA	Mineral deposit	128.2012906	-17.345804	Rare-earth oxides	Magmatic	Magmatic-hydrothermal	Apatite and/or fluorite vein

Name	State	Operating status	Longitude	Latitude	Commodities	Mineral-system association	Mineral system group	Deposit type
Jurien	WA	Historic mine	115.0811824	-30.271872	Ilmenite, zircon, rutile, leucoxene	Basinal	Placer	Heavy-mineral sands (Beach)
Karra	NSW	Mineral deposit	143.067	-34.15	Zircon, rutile, ilmenite, leucoxene	Basinal	Placer	Heavy-mineral sands (Beach)
Kemerton	WA	Mineral deposit	115.7441	-33.1781	Ilmenite, zircon, rutile	Basinal	Placer	Heavy-mineral sands (Beach)
Keysbrook	WA	Mineral deposit	115.926491	-32.431545	Ilmenite, zircon, leucoxene, rutile	Basinal	Placer	Heavy-mineral sands (Beach)
Killi Killi Hills No.1	WA	Mineral deposit	128.9741218	-19.774964	Uranium, rare-earth elements	Basinal	Diagenetic hydrothermal	Unconformity-related
Killi Killi Hills No.2	WA	Mineral deposit	128.8750222	-19.728015	Uranium, rare-earth elements	Basinal	Diagenetic hydrothermal	Unconformity-related
King Sound–Fitzroy River	WA	Mineral deposit	123.5513	-17.45626	Rare-earth elements	Basinal	Placer	Heavy-mineral sands (Offshore shallow marine)
Kokomo	QLD	Mineral deposit	145.171214	-18.552506	Nickel, cobalt, (scandium, platinum)	Regolith	Residual lateritic	Ultramafic/mafic–associated
Korella	QLD	Mineral deposit	139.9667	-21.95	Y_2O_3, P_2O_5	Basinal	Sedimentary	Phosphorite
Kulwin	VIC	Mineral deposit	142.5697	-34.9886	Zircon, rutile, ilmenite, leucoxene	Basinal	Placer	Heavy-mineral sands (Beach)
Laburnum	NSW	Mineral deposit	142.2799769	-33.337007	Rutile, zircon, ilmenite, leucoxene	Basinal	Placer	Heavy-mineral sands (Beach)
Lake Innes	NSW	Mineral deposit	152.8708758	-31.476212	Nickel, scandium, chromium, iron, cobalt, talc	Regolith	Residual lateritic	Ultramafic/mafic associated
Limeburners Creek N.P.	NSW	Unknown	152.972724	-31.317698	Ilmenite, rutile, zircon, (monazite)	Basinal	Placer	Heavy-mineral sands (Unknown)
Lucknow	QLD	Mineral deposit	144.9554727	-19.025366	Nickel, cobalt, scandium	Regolith	Residual lateritic	Ultramafic/mafic–associated
Magic	NSW	Mineral deposit	141.35	-32.883333	Zircon, ilmenite, leucoxene	Basinal	Placer	Heavy-mineral sands (Beach)

Name	State	Operating status	Longitude	Latitude	Commodities	Mineral-system association	Mineral system group	Deposit type
Mary Kathleen	QLD	Historic mine	140.0130208	-20.746033	Rare-earth oxides, uranium, uranium oxide	Magmatic	Magmatic hydrothermal	Skarn
Mercury	VIC	Mineral deposit	142.3522222	-34.898889	Rutile, zircon, ilmenite, leucoxene	Basinal	Placer	Heavy-mineral sands (Beach)
Mindarie	SA	Historic mine	140.2075	-34.795	Zircon, rutile, ilmenite, leucoxene	Basinal	Placer	Heavy-mineral sands (Beach)
Mindarra Springs	WA	Mineral deposit	115.970398	-31.08153	Ilmenite, zircon, (rutile, monazite, leucoxene)	Basinal	Placer	Heavy-mineral sands (Beach)
Minervah	NSW	Mineral deposit	142.12	-33.39	Zircon, rutile, ilmenite, leucoxene	Basinal	Placer	Heavy-mineral sands (Beach)
Moreton Island N.P.	QLD	Mineral deposit	153.3999761	-27.076808	Rutile, zircon, ilmenite, monazite, mineral sands	Basinal	Placer	Heavy-mineral sands (High dune)
Mount Gee	SA	Mineral deposit	139.3391	-30.2224	Uranium, uranium oxide, rare-earth oxides, rare-earth elements	Magmatic	Magmatic-hydrothermal	Iron-oxide breccia complex
Mount Painter	SA	Historic mine	139.3699731	-30.227049	Uranium, uranium oxide, rare-earth elements	Magmatic	Magmatic-hydrothermal	Iron-oxide breccia complex
Mount Weld	WA	Operating mine	122.5475227	-28.859949	Rare-earth oxides, (many components: yttrium oxide, thorium, tantalum pentoxide, zirconia, niobium pentoxide, phosphate, phosphorous, niobium, tantalum, rare-earth elements, phosphorous oxide)	Regolith	Residual lateritic	Carbonatite-associated
Mulga Rock	WA	Mineral deposit	123.592004	-29.904345	Uranium, rare-earth elements	Basinal	Sedimentary	Lignite
Myall Lakes N.P.	NSW	Historic mine	152.392487	-32.459314	Ilmenite, corundum - ruby, zircon, rutile	Basinal	Placer	Heavy-mineral sands (Beach)

Name	State	Operating status	Longitude	Latitude	Commodities	Mineral-system association	Mineral system group	Deposit type
Narraburra	NSW	Mineral deposit	147.5667	-34.325	Rare-earth oxides, (thorium, zirconia, yttrium oxide, hafnium, niobium)	Magmatic	Orthomagmatic	(Per)alkaline rocks
Nepean HMS	NSW	Mineral deposit	143.36	-34.07	Zircon, rutile, ilmenite	Basinal	Placer	Heavy-mineral sands (Beach)
Nolans Bore	NT	Mineral deposit	133.238557	-22.59385	Rare-earth oxides, (uranium, phosphate, phosphorous oxide, uranium oxide, rare-earth elements, thorium)	Magmatic	Magmatic-hydrothermal	Apatite and/or fluorite vein
North Dandalup	WA	Mineral deposit	115.948945	-32.583286	Ilmenite, zircon, rutile, (leucoxene)	Basinal	Placer	Heavy-mineral sands (Beach)
North Entrance	NSW	Unknown	151.518538	-33.320618	Ilmenite, rutile, zircon	Basinal	Placer	Heavy-mineral sands (Beach)
North Stradbroke Island	QLD	Operating mine	153.4435	-27.476791	Zircon, rutile, ilmenite	Basinal	Placer	Heavy-mineral sands (High dune)
Nyngan	NSW	Mineral deposit	146.983333	-31.633333	Scandium, nickel, cobalt, (platinum, gold)	Regolith	Residual lateritic	Ultramafic/mafic–associated
Olympic Dam	SA	Operating mine	136.889293	-30.437444	Copper, uranium, gold, (silver)	Magmatic	Magmatic hydrothermal	Iron-oxidised breccia complex
Phoenix	NSW	Mineral deposit	143.3072839	-34.468497	Zircon, ilmenite, rutile, leucoxene	Basinal	Placer	Heavy-mineral sands (Beach)
Pinga Creek	WA	Mineral deposit	119.00008	-21.75	Sn, Nb, rare-earth elements	Magmatic	Orthomagmatic	Pegmatite
Port Gregory	WA	Operating mine	114.281448	-28.178205	Garnet, ilmenite	Basinal	Placer	Heavy-mineral sands (Beach)
Puwanapi	NT	Mineral deposit	130.065651	-11.72027	Rare-earth elements	Basinal	Placer	Heavy-mineral sands (Beach)
Rocky Point	QLD	Mineral deposit	151.9499792	-24.276837	Rutile, zircon, ilmenite, monazite	Basinal	Placer	Heavy-mineral sands (Unknown)
Rodds Peninsula N.P.	QLD	Mineral deposit	151.6999813	-24.02684	Rutile, zircon, ilmenite, monazite	Basinal	Placer	Heavy-mineral sands (Unknown)
Round Hill Head–Deepwater	QLD	Mineral deposit	151.891464	-24.183744	Rutile, zircon, ilmenite, monazite	Basinal	Placer	Heavy-mineral sands (Unknown)

Name	State	Operating status	Longitude	Latitude	Commodities	Mineral-system association	Mineral system group	Deposit type
Rover Range–Glenarty Creek	WA	Mineral deposit	115.186218	-34.199345	Ilmenite, (leucoxene, rutile, zircon)	Basinal	Placer	Heavy-mineral sands (Beach)
Scott River	WA	Mineral deposit	115.3332222	-34.260112	Ilmenite, zircon, rutile, leucoxene, mineral sands	Basinal	Placer	Heavy-mineral sands (Beach)
Shamrock	NSW	Mineral deposit	142.52	-33.51	Rutile, zircon, (ilmenite, leucoxene)	Basinal	Placer	Heavy-mineral sands (Beach)
Shoalwater Bay Training Area	QLD	Mineral deposit	150.802439	-22.67014	Rutile, zircon, ilmenite, monazite	Basinal	Placer	Heavy-mineral sands (Beach)
Snapper	NSW	Mineral deposit	142.11998	-33.397009	Rutile, zircon, ilmenite, (leucoxene)	Basinal	Placer	Heavy-mineral sands (Beach)
Somme	NSW	Mineral deposit	142.32	-33.35	Rutile, zircon, ilmenite, leucoxene	Basinal	Placer	Heavy-mineral sands (Beach)
Sunshine Coast N.P.	QLD	Mineral deposit	153.101331	-26.416506	Rutile, zircon, ilmenite, monazite	Basinal	Placer	Heavy-mineral sands (Unknown)
Swan Lake	WA	Mineral deposit	115.178482	-34.305012	Ilmenite, zircon, rutile, leucoxene, monazite	Basinal	Placer	Heavy-mineral sands (Unknown)
Tarawi North	NSW	Mineral deposit	141.16804	-33.42866	Zircon, ilmenite, rutile, (leucoxene, Thorium)	Basinal	Placer	Heavy-mineral sands (Beach)
Tarawi South	NSW	Mineral deposit	141.18427	-33.473733	Zircon, rutile, ilmenite, (leucoxene)	Basinal	Placer	Heavy-mineral sands (Beach)
The Loop	WA	Mineral deposit	115.941566	-32.656712	Zircon, leucoxene, ilmenite, rutile	Basinal	Placer	Heavy-mineral sands (Beach)
Titan	VIC	Mineral deposit	142.4130556	-34.968889	Rutile, zircon, ilmenite, leucoxene	Basinal	Placer	Heavy-mineral sands (Beach)
Tiwi	NT	Operating mine	131.026301	-11.36257	Zircon, rutile, leucoxene, ilmenite	Basinal	Placer	Heavy-mineral sands (Beach)

Name	State	Operating status	Longitude	Latitude	Commodities	Mineral-system association	Mineral system group	Deposit type
Toongi	NSW	Mineral deposit	148.6181783	-32.445319	Rare-earth oxides, uranium, (zirconia, niobium pentoxide, tantalum pentoxide, yttrium oxide, uranium oxide, niobium, tantalum, yttrium)	Magmatic	Orthomagmatic	(Per)alkaline rocks
Trelawney	NSW	Mineral deposit	142.71	-33.65	Zircon, rutile, ilmenite, leucoxene	Basinal	Placer	Heavy-mineral sands (Beach)
Triangle	NSW	Mineral deposit	142.92	-33.46	Zircon, rutile, ilmenite, leucoxene	Basinal	Placer	Heavy-mineral sands (Beach)
Tutunup	WA	Mineral deposit	115.5647222	-33.681111	Ilmenite, rutile, zircon, leucoxene	Basinal	Placer	Heavy-mineral sands (Beach)
Tyrrell Ridge	VIC	Mineral deposit	142.7533333	-35.735556	Rutile, ilmenite, zircon	Basinal	Placer	Heavy-mineral sands (Beach)
Urquhart	QLD	Mineral deposit	141.8	-12.75	Ilmenite, rutile, leucoxene, zircon	Basinal	Placer	Heavy-mineral sands (Beach)
Wakool	NSW	Mineral deposit	143.2	-33.93	Zircon, rutile, ilmenite, leucoxene	Basinal	Placer	Heavy-mineral sands (Beach)
Warner Glen	WA	Mineral deposit	115.213165	-34.180729	Ilmenite, zircon, leucoxene	Basinal	Placer	Heavy-mineral sands (Beach)
Watchem ‘A’ Strand	VIC	Mineral deposit	142.8955556	-36.071111	Rutile, ilmenite, zircon, leucoxene	Basinal	Placer	Heavy-mineral sands (Beach)
Watchem ‘B’ Strand	VIC	Mineral deposit	142.8955556	-36.071111	Rutile, ilmenite, zircon, leucoxene	Basinal	Placer	Heavy-mineral sands (Beach)
Wedderburn	VIC	Mineral deposit	143.2666667	-36.616667	Zircon, rutile, ilmenite, (leucoxene)	Basinal	Placer	Heavy-mineral sands (Offshore shallow marine)
Wemen	VIC	Historic mine	142.7000132	-34.813696	Rutile, zircon, ilmenite, mineral sands	Basinal	Placer	Heavy-mineral sands (Beach)
Western Strands	NSW	Mineral deposit	142.85	-33.49	Zircon, rutile, ilmenite, (leucoxene)	Basinal	Placer	Heavy-mineral sands (Unknown)

Name	State	Operating status	Longitude	Latitude	Commodities	Mineral-system association	Mineral system group	Deposit type
Whicher Scarp	WA	Mineral deposit	115.49828	-33.74525	Zircon, ilmenite, rutile	Basinal	Placer	Heavy-mineral sands (Beach)
Wild Cattle Island	QLD	Mineral deposit	151.3999727	-23.976851	Rutile, zircon, ilmenite, monazite, mineral sands	Basinal	Placer	Heavy-mineral sands (Unknown)
WIM 50	VIC	Mineral deposit	141.8846887	-37.062241	Ilmenite, rutile, zircon, xenotime, leucoxene, (monazite)	Basinal	Placer	Heavy-mineral sands (Offshore shallow marine)
WIM 100	VIC	Mineral deposit	141.6013771	-36.96224	Ilmenite, rutile, zircon, leucoxene, xenotime, (monazite)	Basinal	Placer	Heavy-mineral sands (Offshore shallow marine)
WIM 150	VIC	Mineral deposit	142.3400494	-36.806155	Leucoxene, rutile, zircon, xenotime, ilmenite, (mineral sands)	Basinal	Placer	Heavy-mineral sands (Offshore shallow marine)
WIM 200 (Jackson)	VIC	Mineral deposit	142.6346869	-36.678866	Rare-earth elements	Basinal	Placer	Heavy-mineral sands (Offshore shallow marine)
WIM 250 (Donald)	VIC	Mineral deposit	142.768011	-36.512196	Ilmenite, rutile, zircon, leucoxene	Basinal	Placer	Heavy-mineral sands (Offshore shallow marine)
Winchester	NSW	Mineral deposit	142.31	-33.34	Rutile, ilmenite, zircon, leucoxene	Basinal	Placer	Heavy-mineral sands (Beach)
Witchcliffe	WA	Mineral deposit	115.128998	-34.027115	Ilmenite, zircon, (garnet, leucoxene, rutile)	Basinal	Placer	Heavy-mineral sands (Beach)
Wonnerup	WA	Mineral deposit	115.4506	-33.653782	Zircon, ilmenite, (leucoxene, rutile)	Basinal	Placer	Heavy-mineral sands (Beach)
Yabbie	NSW	Mineral deposit	142.5	-33.52	Rutile, zircon, ilmenite, leucoxene	Basinal	Placer	Heavy-mineral sands (Beach)
Yalyalup	WA	Mineral deposit	115.472298	-33.689709	Rare-earth elements	Basinal	Placer	Heavy-mineral sands (Beach)
Yangibana	WA	Mineral deposit	116.1972149	-23.890331	Rare-earth oxides	Magmatic	Orthomagmatic	Carbonatite
Yuraygir N.P.	NSW	Mineral deposit	153.2690624	-29.813401	Ilmenite, rutile, zircon	Basinal	Placer	Heavy-mineral sands (Unknown)

[1] The REE resource data used in this review for Australia's deposits and prospects are from OZMIN (2011: Ewers and Ryburn, 1977)—Geoscience Australia's national database of Mineral deposits andf resources.

N.P.= National Parks and other reserves.

APPENDIX 9. SUMMARY OF AUSTRALIAN GOVERNMENT AND RARE-EARTH-ELEMENT MINING INDUSTRY DEVELOPMENTS

Australian Government developments

Geoscience Australia (www.ga.gov.au)

Very few reviews on the distribution and geology of REE deposits in Australia have been published by the Australian Government. Two exceptions include reports ('Commercial-In-Confidence' at the time of release) by Towner et al. (1996) and Cassidy et al. (1997) of the Australian Geological Survey Organisation (predecessor to Geoscience Australia). The report by Towner et al. (1996) focuses on resources, exploration, and processing of mineral-sand deposits, whereas the latter report by Cassidy et al. (1997) discusses the geology and potential of primary hard-rock and mineral-sand deposits. This particular publication represents the first national review that describes the geological setting and exploration of REE since Cassidy et al. (1997). Other digital map and database products with potential applications for REE exploration produced by Geoscience Australia since 2008 are summarised in Section 5.3 and Appendix 10.

Commonwealth Scientific and Industrial Research Organisation
(http://www.csiro.au/csiro/channel/_ca_dch2t.html)

The Minerals Down Under National Research Flagship (http://www.csiro.au/org/MDU-Overview--ci_pageNo-1.html) is a collaborative program between the Commonwealth Scientific and Industrial Research Organisation (CSIRO), the minerals industry, and various government organisations to create new knowledge and transform technologies for the mineral sector. Within this and previous research frameworks, the CSIRO has carried out a number of scientific projects involving the REE. The wide variety of research projects highlights the diverse applications of these strategically important elements. Such projects include:

- mineralogical and metallurgical investigations of REE deposits (e.g., Cummins Range Carbonatite-hosted deposit in the East Kimberley, WA: Andrew, 1990) and scandium-bearing Ni-Co laterites (Gilgai intrusion, Nyngan project, NSW: http://www.jervoismining.com.au/uploaditems/reports/20110211%20Nyngan%20Scandium%20Report%20from%20CSIRO.pdf);
- aquatic geochemistry of REE in geological materials associated with river catchments (e.g., Pioneer River, central Qld: Lawrence et al., 2006); and
- CSIRO has applied advanced techniques in design incorporating the use of REE permanent magnets to develop high-efficiency electric motors.

Australian Nuclear Science and Technology Organisation Minerals
(http://www.ansto.gov.au/home)

ANSTO Minerals is a business unit of the Australian Nuclear Science and Technology Organisation, located at Lucas Heights near Sydney.

The focus of ANSTO Minerals is on the processing of ores containing naturally occurring radioactivity, specifically ores containing uranium and thorium, which are often associated with the REE. ANSTO Minerals undertake innovative process development for the mining industry, from evaluation of drill-hole samples through to operation of pilot plants and demonstration plants at our own facilities, or if required, at the clients mine site.

Since 1990, ANSTO Minerals have been involved in commercial process development projects targeting the recovery of rare earths from Australian ores and concentrates and have gained expertise in areas specific to rare-earth processing including caustic conversion of rare-earth phosphate type minerals, sulphuric acid bake/water leach processes and purification of rare earths by solvent extraction techniques which requires operation of multiple circuits containing many mixer-settler units.

An example of this recovery-processing service involves the Toongi deposit (Dubbo Zirconia Project), New South Wales, that is managed by Alkane Resources Limited. ANSTO Minerals has used a demonstration pilot plant to process an initial 100 tonnes of ore from the deposit and has recovered 1300 kg of zirconium chemicals and nearly 300 kg of saleable niobium concentrate containing approximately 70% Nb_2O_5. The demonstration plant also has produced zirconia concentrate and yttrium-REE concentrate from the deposit.

Rare-earth-element mining industry developments in Australia

Lynas Corporation Limited: The Mount Weld deposit in Western Australia occurs in the lateritic profile over an alkaline carbonatite complex. In September 2010, Lynas announced resource figures for the Central lanthanide deposit of Measured, Indicated and Inferred Resources of 9.88 million tonnes with total lanthanide oxides (TLnO) at 10.6% and 990 ppm Y_2O_3 ('heavy' REO) and the newly named 'Duncan'

'heavy' REO deposit with Measured, Indicated and Inferred resources totalling 7.62 Mt @ 4.5% TLnO (4.8% TREO) and 2570 ppm Y_2O_3. In another part of the carbonatite complex called the Crown Polymetallic deposit, there are Indicated (1.5 Mt) and Inferred (36.2 Mt) Resources totalling 37.7 million tonnes, which include total lanthanides at 1.16% and 0.09% Y_2O_3. The company completed the first stage of mining activities in 2008 and commenced construction of a concentration plant at Mount Weld and an advanced materials plant in Malaysia. Both of these activities were suspended in the first quarter of 2009 because of uncertainty concerning the financing arrangements for the project. In September 2009, Lynas announced a fully underwritten share issue in Lynas to raise $450 million, which will be used to complete phase 1 of the Lynas REE project. Lynas reported in its 2009 annual report that it had signed long-term contracts with four customers to supply REE and signed letters of intent with another two customers. Lynas Corporation Limited has announced that it plans to commence production of rare-earth mineral concentrate, followed by further processing to rare-earth concentrates and separated products in Malaysia, in 2011. This is a milestone for the REE industry as most of the new production capacity in the last 15 years has been in China. ANSTO Minerals has been associated with this project through various companies owning the deposit, Carr Boyd Minerals, Ashton Mining, and Lynas Corporation. The ANSTO facilities in Sydney tested a caustic conversion route in the early 1990s and later carried out test work on an acid bake processing route. Test work included operation of continuous solvent extraction mini-plant to achieve separation of middle, light, and rare-earth fractions as well as production of separated rare-earth products, mainly cerium and neodymium. As part of these studies, ANSTO Minerals has developed a solvent extraction process specifically for cerium based on extraction from sulphate liquor.

Arafura Resources Limited: Nolans Bore REE-phosphate-uranium-thorium deposit is located 135 km northwest of Alice Springs in the Northern Territory. It has Measured, Indicated and Inferred Resources totalling 30.3 million tonnes to a depth of 130 m with grades at 2.8% REO, 12.9% P_2O_5, 0.44 pounds per tonne U_3O_8, and 0.27% Th. According to Arafura, the distribution of the LREE currently being considered for extraction, (La, Ce, Pr, and Nd) amount to 95%, whereas other REE (Sm, Eu, Gd, Tb, Dy) amount to 4.23%. Since 2006, ANSTO has been involved in the development of a process route for the recovery of rare earths from this deposit, with phosphoric acid and uranium as by-products. ANSTO Minerals has tested various stages of the process to pilot scale and a demonstration plant is currently being planned. The test work has also included the application of solvent extraction technology for further purification of a mixed rare-earth solution into separate rare-earth products. In February 2009, Arafura announced it had executed a letter of intent with the Jiangsu Eastern China Non-Ferrous Metals Investment Holding Co Limited (JEC) a subsidiary of the East China Mineral Exploration and Development Bureau (ECE) for ECE to acquire up to 25% for the issued capital of Arafura through two share placements. The proposal was approved by the Foreign Investment Review Board in May 2009 and accepted by the shareholders in September 2009. The company is conducting a definitive feasibility study on the Nolans Bore project and, in July 2010, reported that it is on track to commence production in 2013 (http://www.arafuraresources.com.au/documents/July2010AdvertorialFINAL.PDF accessed September 2010).

Alkane Resources Limited: A Demonstration Pilot Plant (DPP) was constructed and commissioned in May 2008 at (ANSTO). Alkane reported that the DPP completed two trial runs in 2008 and one more in the first quarter of 2009, producing high quality zirconium and niobium products. In November 2009, Alkane reported that the plant had produced the first LREE and Y-HREE products and stressed the importance of the rare earths as a revenue earner, particularly the HREE. The current plans are to make a decision on development during the second half of 2010 with production to commence in 2011–12 if development goes ahead.

Navigator Resources Limited: The company's Cummins Range Carbonatite deposit occurs in the Kimberley region of Western Australia. In September 2009, it reported Inferred Resources of 4.17 Mt @ 1.72% TREO, 11.0% P_2O_5, 187 ppm U_3O_8 and 41 ppm Th, at a cut-off grade of 1% TREO. The TREO was subdivided into 95.6% LREE (La, Ce, Pr, Nd), 4.1% MREE (Sm, Eu, Gd, Tb, Dy) and 0.3% HREE (Ho, Er, Tm, Yb, Lu). A mineralogical investigation of the Cummins Range deposit by the CSIRO Minerals Down Under Flagship was completed during the March 2010 quarter with the principal REE-bearing minerals being primary apatite and monazite and only subordinate amounts of secondary REE-bearing minerals are present.

Capital Mining Limited: Similarly, the (per)alkaline granitic intrusions of the Narraburra complex, near Temora in central New South Wales, contain anomalous amounts of zirconium, REO, and low

concentrations of thorium. The ThO_2 content amounts to 2750 tonnes (2420 tonnes Th). In the March Quarterly Report in 2010, the owners of the project, Capital Mining Limited reported that it was conducting metallurgical tests to recover Hf, Th, Ta, Nb, Nd, and Ce.

During the last couple of years **scandium-bearing lateritic nickel-cobalt deposits** have attracted increasing attention in response to anticipated global rise in demand for scandium. Scandium-stabilised zirconia rather than yttrium-stabilised zirconia as an electrolyte for Solid Oxide Fuel Cells (SOFC) reduces the operating temperature of the fuel cell significantly, thereby providing a much longer life. SOFCs are expected to play a major role in the developing battery powered electric transportation industry (cars, trucks, trains, etc) as well as in stationary applications, using SOFCs as electricity generators in substitution of coal fired power plants or directly in the home (EMC Metals Corporation of Canada, 2010).

Metallica Minerals Limited: During 2010 Metallica announced scandium resources located within their Kokomo and Lucknow lateritic nickel-cobalt deposits in northern Queensland. At the Kokomo deposit, about 175 km northwest of Townsville, the company used a cut-off of 70 g/t Sc to delineate a scandium-rich Measured, Indicated and Inferred Resource of 9.0 Mt @ 109 g/t Sc, 0.24% Ni, and 0.03% Co, which is located within a larger lateritic nickel-cobalt deposit of 16.3 Mt @ 0.67% Ni, 0.12% Co, and 36 g/t Sc.

Jervois Mining Limited: A scandium-rich portion of Nyngan lateritic nickel-cobalt-scandium-platinum deposit in central New South Wales was updated in June 2009 as Measured Resources of 2.718 Mt @ 274 ppm Sc and Indicated Resources of 9.294 Mt @ 258 ppm Sc. Jervois in a joint venture agreement with EMC Metals Corporation of Canada are currently engaged in scoping studies to provide data for a prefeasibility study of the Nyngan scandium joint venture project in 2011.

APPENDIX 10. USEFUL WWW LINKS FOR INFORMATION ABOUT RARE-EARTH ELEMENTS

Australian information, maps, and statistical data relating to rare-earth elements from Geoscience Australia:

Australia's Identified Mineral Resources 2010:
https://www.ga.gov.au/products/servlet/controller?event=GEOCAT_DETAILS&catno=71584

Australian Mineral Exploration a review of exploration for the year 2010:
https://www.ga.gov.au/products/servlet/controller?event=GEOCAT_DETAILS&catno=71503

Rare-Earth Elements:
http://www.ga.gov.au/minerals/mineral-resources/rare-earth-elements.html

Australian Mines Atlas:
http://www.australianminesatlas.gov.au/index.jsp

General issues and international statistical data of rare-earth elements:

Wikipedia, the free encyclopedia about rare-earth elements:
http://en.wikipedia.org/wiki/Rare_earth_element

United States Geological Survey
Annual rare-earth-element statistics and information:
http://minerals.er.usgs.gov/minerals/pubs/commodity/rare_earths/

United States Geological Survey
Scientific Investigations Report 2010–5220:
http://pubs.usgs.gov/sir/2010/5220/

British Geological Survey
Rare-earth elements: a beginner's guide from the BGS:
http://www.bgs.ac.uk/research/highlights/rare_earth_elements.html

British Geological Survey
Map of rare-earth-element deposits in the world:
http://www.bgs.ac.uk/research/highlights/documents/Global_REE_Deposits.pdf

About.com Chemistry
Multiple articles about the rare-earth elements:
http://chemistry.about.com/lr/rare_earths/239403/2/

Baotou National Rare-Earth Hi-Tech Industrial Development Zone
Overview of China's rare-earth element industry:
http://www.rev.cn/en/int.htm

Australian Shares: Database of Australian mining and energy shares. Searchable by what they mine or explore for, how much of any given resource they have:
http://www.australian-shares.com

AustralianRareEarths.com:
http://www.australianrareearths.com/current-issues.html

National Nuclear Data Centre, Brookhaven, USA:
http://www.nndc.bnl.gov/

International Union of Pure and Applied Chemistry (IUPAC):
http://old.iupac.org/dhtml_home.html

Thomas Jefferson National Accelerator Facility: Periodic Table of Elements:
http://education.jlab.org/itselemental/

Elementymology & Elements Multidict:
http://elements.vanderkrogt.net/index.php

Tasman Metals Limited:
http://www.tasmanmetals.com/s/Home.asp

Naming rare-earth elements and rare-earth-element-bearing minerals:

http://www.nndc.bnl.gov/nndc/history/origindc.pdf

http://elements.vanderkrogt.net/rareearths.php

http://www.tasmanmetals.com/s/OresMinerals.asp

http://www.mindat.org/index.php

http://www.angelo.edu/faculty/kboudrea/periodic/trans_lanthanides.htm

Government organisations involved with research into rare-earth elements:

Geoscience Australia (GA):
www.ga.gov.au

Commonwealth Scientific and Industrial Research Organisation (CSIRO):
http://www.csiro.au/csiro/channel/_ca_dch2t.html

Australian Nuclear Science and Technology Organisation Minerals (ANSTO):
http://www.ansto.gov.au/home

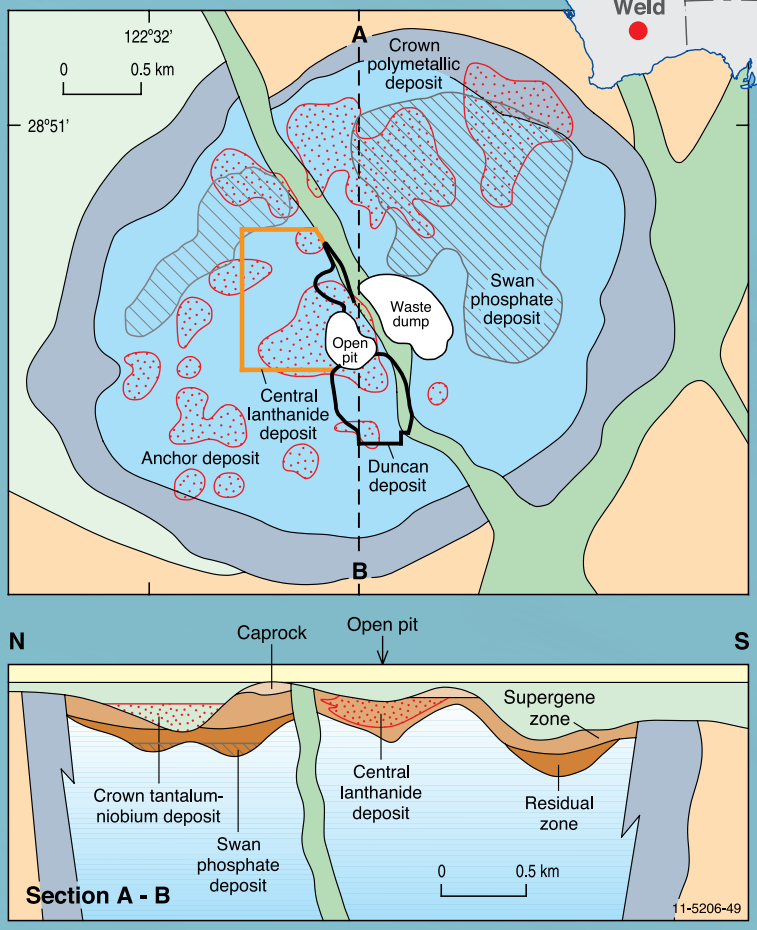

Rare-earth elements (REE: lanthanum, cerium, praseodymium, neodymium, promethium, samarium, europium, gadolinium, terbium, dysprosium, holmium, erbium, thulium, ytterbium, lutetium, scandium, and yttrium) have unique chemical, magnetic, and luminescent properties that make them critical to several high-technology industries. Their applications in many emerging technologies associated with the transport, information, environment, energy, defence, nuclear, and aerospace industries have gained rapid momentum in recent years. This, together with a narrow global supply base, has led to price increases for the REE, and so they are becoming an increasingly attractive commodity for the minerals industry.

This report produced by Geoscience Australia describes the distribution, geological characteristics, and resources of Australia's major REE deposits as a stimulus for further research into their geological characteristics. The information and main messages presented are intended to inform the public, students, and professionals.